ERDC/EL SR-01-3

Environmental Laboratory

US Army Corps
of Engineers®
Engineer Research and
Development Center

Water Quality Modeling of Allatoona and West Point Reservoirs Using CE-QUAL-W2

Thomas M. Cole and Dorothy H. Tillman

July 2001

ERDC/EL SR-01-3
July 2001

Water Quality Modeling of Allatoona and West Point Reservoirs Using CE-QUAL-W2

by Thomas M. Cole, Dorothy H. Tillman

Environmental Laboratory
U.S. Army Engineer Research and Development Center
3909 Halls Ferry Road
Vicksburg, MS 39180-6199

Final report

Prepared for U.S. Army Engineer District, Mobile
Mobile, AL 36628-0001

and Georgia Department of Environmental Resources
Atlanta, GA 30334

Contents

List of Figures

Preface

This report presents results of a CE-QUAL-W2 water quality modeling study for Allatoona and West Point Reservoirs. This report was prepared in the Environmental Laboratory (EL), U.S. Army Engineer Research and Development Center, Vicksburg, MS. The study was sponsored by the State of Georgia through the U.S. Army Engineer District, Mobile, and was funded under the Military Interdepartmental Purchase Request No. E86960041 dated 20 March 1996 for $245K.

The Principal Investigators of this study were Mr. Thomas M. Cole and Ms. Dorothy H. Tillman of the Water Quality and Contaminant Modeling Branch (WQCMB), Environmental Processes and Effects Division (EPED), EL. This report was prepared by Mr. Cole and Ms. Tillman under the direct supervision of Dr. Mark Dortch, Chief, WQCMB, and under the general supervision of Dr. Richard Price, Chief, EPED, and Dr. Edwin A. Theriot, Acting Director, EL. Technical review by Dr. Barry W. Bunch and Ms. Lillian T. Schneider are gratefully acknowledged. Mr. Fred Herrmann is gratefully acknowledged for the generation of many of the figures used in this report.

At the time of publication of this report, Dr. James R. Houston was Director of ERDC. COL John W. Morris III, EN, was Commander.

This report should be cited as follows:

> Cole, T. M., and Tillman, D. H. (2001). "Water quality model of Allatoona and West Point Reservoirs Using CE-QUAL-W2," ERDC/EL SR-01-3, U.S. Army Engineer Research and Development Center, Vicksburg, MS.

1 Introduction

Background

The Georgia Environmental Protection Division (GEPD) is concerned about the effects of increased nutrient loadings into Allatoona and West Point Lakes from point and nonpoint sources due to projected population growth in the region. West Point Lake is located in the Chattahoochee River basin and receives loads from Atlanta, a large metropolitan area, in addition to agricultural runoff from the watershed (Kennedy 1995). Allatoona Lake is located in the Coosa River basin and, although not as developed as the Atlanta area, the watershed has undergone significant development associated with the growth of Atlanta to the north.

A number of government- and private-sponsored water quality investigations have been conducted studying the effects of point and nonpoint source pollution on water quality in both reservoirs (Georgia Department of Natural Resources 1993). Water demand and nutrient loading will most likely increase in the future. The ability to predict the effects of increased nutrient loading in West Point and Allatoona would allow GEPD to set waste load allocations and better manage the reservoirs for water quality in the future. To meet this goal, the GEPD has requested the assistance of the Water Quality and Contaminant Modeling Branch at the U.S. Army Engineer Research and Development Center to develop a water quality model for Allatoona and West Point Lakes.

Objective

The objective of this study is to provide a calibrated water quality model for Allatoona and West Point Lakes capable of predicting future water quality conditions resulting from changes in water allocations, point/nonpoint nutrient loadings, and reservoir operations.

Approach

CE-QUAL-W2, a two-dimensional, longitudinal and vertical hydrodynamic and water quality model, was chosen for the study. The model is recognized as the state-of-the-art reservoir hydrodynamic and water quality model and has been successfully applied to over 100 different systems in the United States and throughout the world. It is the reservoir model of choice for Tennessee Valley Authority, U.S. Bureau of Reclamation, U.S. Geological Survey, U.S. Army Corps of Engineers (USACE), and U.S. Environmental Protection Agency (USEPA).

The model consists of a hydrodynamic module that predicts water surface elevations, horizontal/vertical velocities, and temperature. The hydrodynamics are influenced by variable water density resulting from variations in temperature, total dissolved solids, and suspended solids. Seventeen water quality state variables and their kinetic interactions are included in the water quality module. They are:

(1) Conservative tracer.

(2) Coliform bacteria.

(3) Total dissolved solids or salinity.

(4) Inorganic suspended solids.

(5) Labile dissolved organic matter (LDOM).

(6) Refractory dissolved organic matter (RDOM).

(7) Detritus.

(8) Phytoplankton.

(9) Phosphate phosphorus.

(10) Ammonia nitrogen.

(11) Nitrate + nitrite nitrogen.

(12) Dissolved oxygen (DO).

(13) Organic sediments.

(14) Total inorganic carbon.

(15) Alkalinity.

(16) Total iron.

(17) Biochemical oxygen demand (BOD).

Any combination of the above state variables can be included in a simulation, but care must be taken to ensure that all relevant variables are included. The state variables included for this study were variables 5 through 13. These included all relevant variables for computing algal/nutrient/DO interactions and their effects on water quality within the reservoirs.

Site Description

Allatoona

Allatoona Lake is located in northwest Georgia approximately 72 km upstream of Atlanta, GA (Figure 1). The damsite is 78 km north of Rome, GA, and 8 km due east of Cartersville, GA. The drainage area above the dam is 2,845 km^2 and is composed of 12 distinct sub-watersheds. Construction was completed in late 1949, and filling was completed by May 1950. The U.S. Army Engineer District, Mobile, operates the project for purposes of flood control, hydropower, and recreation.

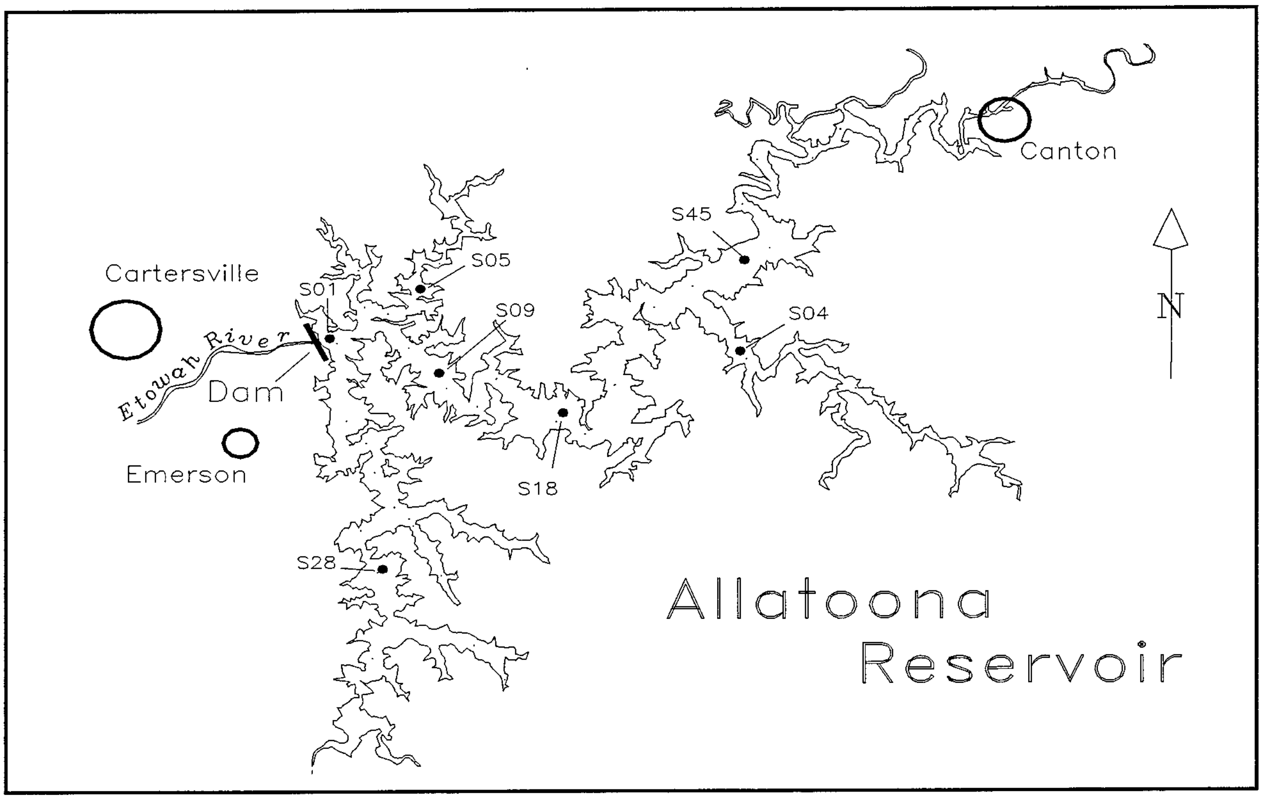

Figure 1. Allatoona Reservoir with location of sampling stations

The dam is a concrete gravity-type dam and is one of the oldest Corps of Engineers multipurpose projects in the southeast. It has a total length of 311 m and a maximum height of 58 m. The spillway is controlled by 11 tainter gates, 9 of which are 12.2 m by 7.9 m (width by height, respectively) and 2 of which are 6 by 7.9 m. There are two main generating units that have a capacity of 36,000 kilowatts (kW) each and one small generating unit that has a capacity of 2,000 kW within the intake structure. The openings for the main units and small unit are at elevations 244.5 m and 225.6 m (as referenced to the National Geodetic Vertical Datum (NGVD)). Power generation can cause water surface elevations to vary as much as 1 m/day because of the small size of the lake.

West Point

West Point Reservoir is located in west-central Georgia approximately 112 km downstream of Atlanta, GA (Figure 2). The damsite is 5 km north of West Point, GA, and 44.8 km downstream from Buford Dam. The drainage area above the dam is 8,754 km^2 and represents about 40 percent of the Chattahoochee River Basin. The construction of West Point Reservoir was authorized by the Flood Control Act of October 23, 1962. Construction began in 1965 and was completed in February 1965. The Mobile District operates the project that provides for flood control, hydropower, recreation, fish and wildlife enhancement, and streamflow regulation for downstream navigation.

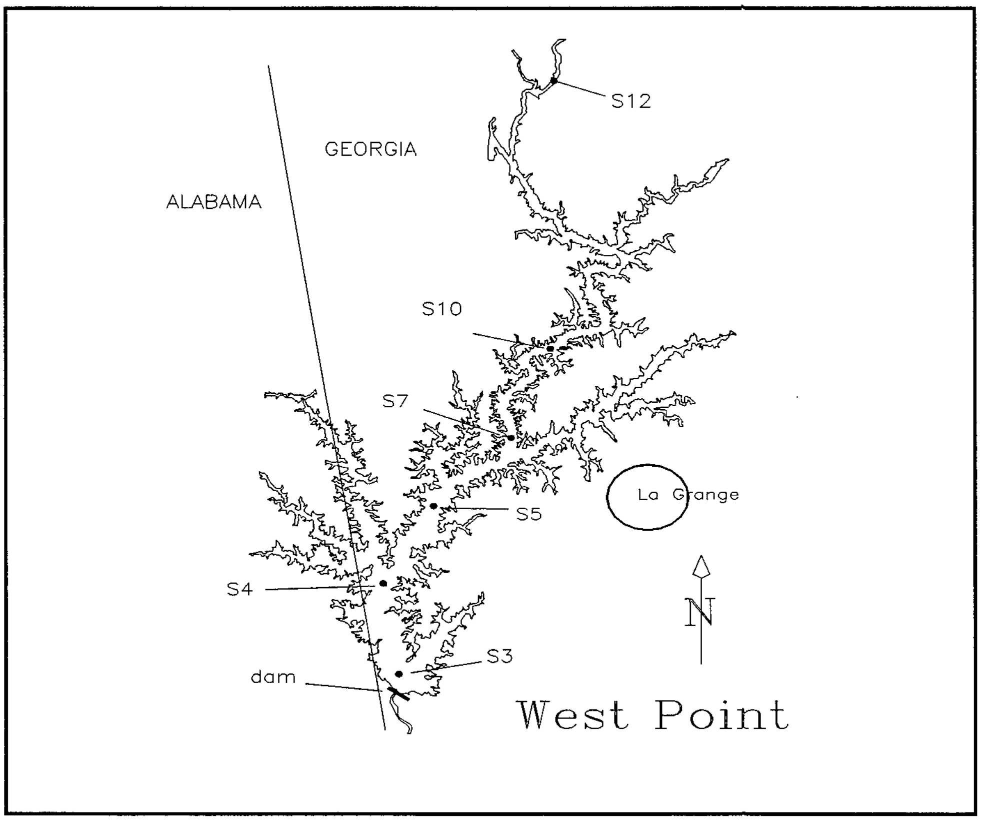

Figure 2. West Point Reservoir with location of sampling stations

The dam is a gravity-type dam with a total length of 2,211 m and a maximum height of 29.6 m. The dam consists of an intake powerhouse structure, a nonoverflow section, a gated spillway located on the main river channel, and a left embankment retaining wall that supports an earth embankment on the east abutment. There are two main generating units and one small generating unit within the intake structure. The openings for the main units are at elevations 184.5 m and 170.1 m (NGVD), and the opening for the small unit is at 193.5 m and 184.4 m (NGVD). The small unit has the capability to take water from the upper 4 to 5 m of the lake to maintain a minimum flow with higher DO concentrations when the main units are not operating.

2 Input Data

The following data are required for an application of CE-QUAL-W2:

a. Initial conditions.

- Bathymetry
- Water surface elevation.
- Temperature.
- Water quality constituents.

b. Boundary conditions.

- Inflow/outflow.
- Temperature.
- Water quality.
- Meteorology.

These data are used to set initial conditions at the start of a model run and to provide time-varying inputs that drive the model during the course of a simulation. Additional data such as outlet descriptions, tributary and withdrawal locations are also required to complete the physical description of the prototype. In-pool data including water surface elevations, temperatures, and constituent concentrations are also required during model calibration in order to assess the performance of the model.

A clear distinction needs to be made regarding initial and boundary conditions and in-pool data. In-pool data have no effect on model performance – they are used only to assess model performance. Initial and boundary conditions are of greater importance because they directly affect model performance. Unfortunately, boundary conditions are rarely determined with a frequency that most modelers deem sufficient to accurately describe the forcing functions that are responsible for observed temperature and water quality conditions. Such is the case for both Allatoona and West Point as will be discussed below.

Bathymetry

CE-QUAL-W2 requires that the reservoir be discretized into longitudinal segments and vertical layers that may vary in length and height. An average width must then be defined for each active cell where an active cell is defined as potentially containing water. Segment layer heights for West Point and Allatoona were constant while segment lengths varied. Once the segment lengths and layer heights were finalized for each reservoir, average widths were determined for each cell from sediment range data provided by the Mobile District.

Allatoona

The Allatoona grid is shown in Figure 3. The grid consists of five branches comprising 39 active segments and a maximum of 22 layers. Segment lengths varied from 0.8 to 3.2 km. The main branch represents the Etowah River. The remaining branches represent Little River, Stamp Creek, Rowland Creek, and Little Allatoona River, respectively. A comparison of computed volume-elevation curve and Mobile District data is presented in Figure 4. The computed volume-elevation curve closely matches the Mobile District data.

West Point

The West Point grid is shown in Figure 5. The grid consists of six branches with a total of 29 active segments and a maximum of 11 layers. Segment lengths

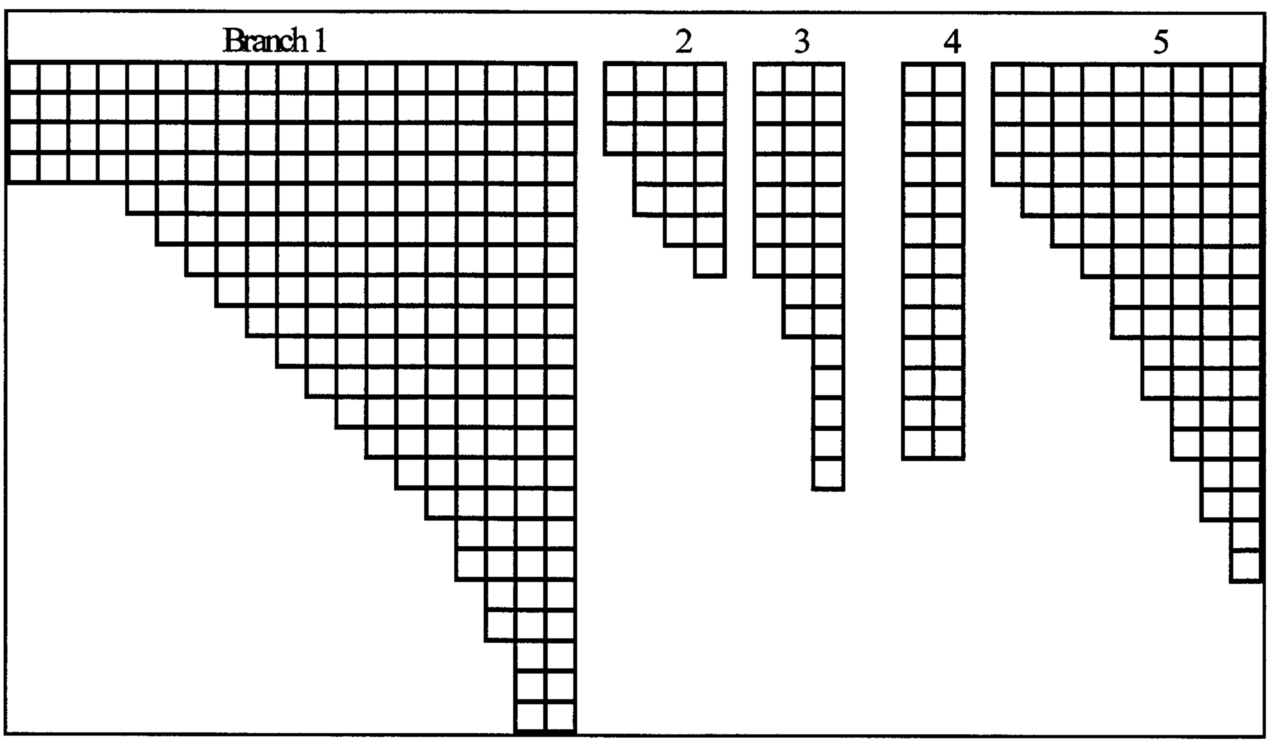

Figure 3. Allatoona computational grid

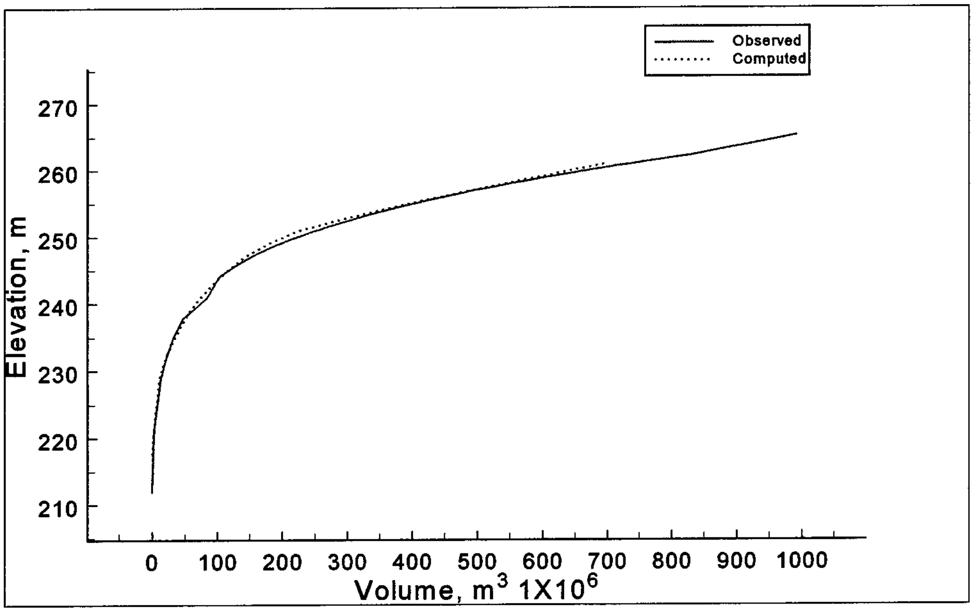

Figure 4. Allatoona volume-elevation curve

varied from approximately 1 to 6 km and layer thicknesses were set to 2 m. The main branch represents the Chattahoochee River. The remaining branches represent Yellowjacket, Whitewater, Wehadkee, Stroud, and Maple Creeks, respectively. A comparison of computed volume-elevation curve and USACE data is presented in Figure 6. The computed volume-elevation curve closely matches the USACE data.

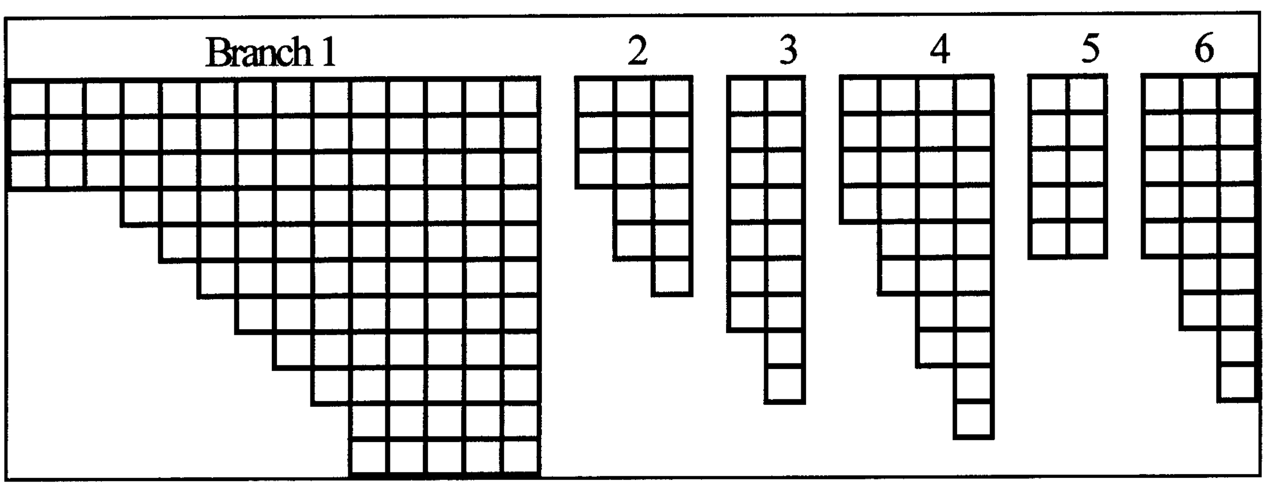

Figure 5. West Point computational grid

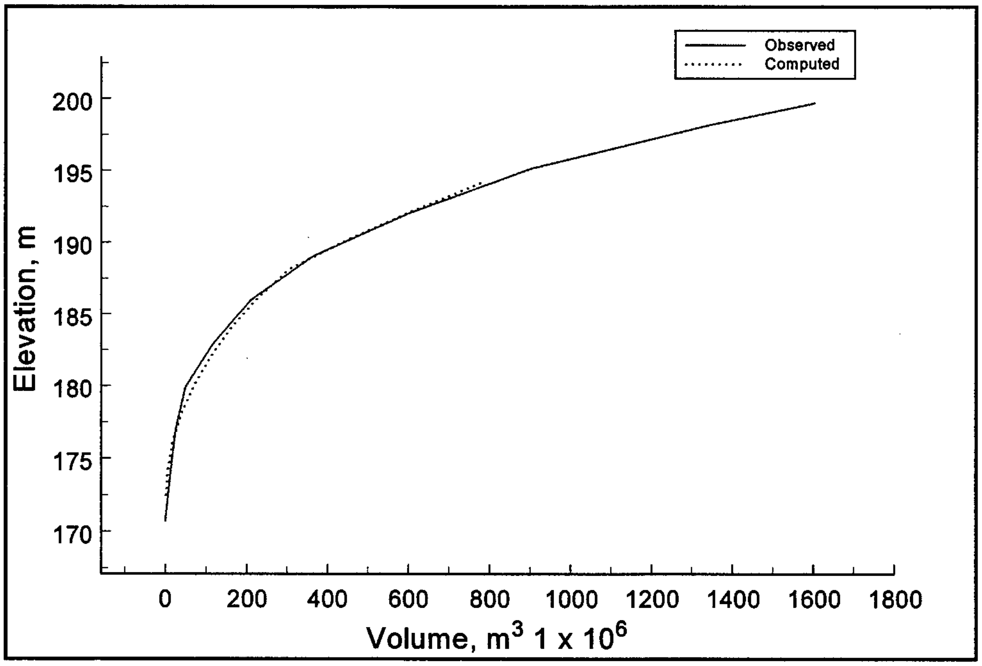

Figure 6. West Point volume-elevation curve

In-Pool Data

Allatoona

In-pool data for Allatoona were received from the A. L. Burruss Institute at Kennesaw State College and GEPD. Observed data received from Kennesaw State College were collected as part of the USEPA Clean Lakes Program and were collected monthly in 1992-1994. During the Clean Lakes study, temperature and DO were the only constituents collected as profiles. All other constituents were collected as photic zone averages. Data received from the GEPD were collected as a supplement to the Clean Lakes Program Study and to provide an expanded data base for developing a water quality model. These data were collected monthly in 1996 in addition to Clean Lakes data.

West Point

West Point Lake in-pool profile data were obtained from a report prepared by Radtke, Buell, and Perlman (1984) for 1979. Data were also received from GEPD for 1996 and 1997.

Initial Conditions

The following options are available for setting initial conditions in the model:

(1) Initialize all cells in the grid to a single value.

(2) Initialize all cells in the grid based on vertical variations.

(3) Initialize all cells in the grid based on vertical and longitudinal variations.

For all calibration years, simulation start date and initial conditions at each reservoir were set to the first date that data were collected. For all years, initial conditions for phosphorus, ammonium, nitrate-nitrite, algae, LDOM, RDOM, labile particulate organic matter (LPOM), and refractory particulate organic matter (RPOM) were set using option 1 since there was little variation in concentrations throughout the reservoirs.

For the 1993 Allatoona calibration, the starting date of the simulation was January 26 when conditions were essentially isothermal. Therefore, option 1 was used to set initial conditions for temperature and DO. For 1996, the starting date was April 25 when the lake was more stratified, so initial conditions of temperature and DO were set with option 2. In 1979, West Point Lake initial conditions for temperature and DO for all years (except DO in 1994) were set using option 2 because of the vertical variation in temperature and DO. For the 1996 calibration at West Point, initial conditions for temperature and DO were set using option 2.

Boundary Conditions

Meteorology

Hourly meteorology was obtained from the U.S. Air Force Environmental Technical Applications Center in Asheville, NC, for Columbus and Atlanta, GA. Data required by CE-QUAL-W2 for surface heat exchange were air temperature, dew point temperature, wind speed and direction, and cloud cover.

Inflows

Mobile District provided calculated daily average inflows measured every hour for the years 1979, 1996, and 1997 for West Point and 1992, 1993, 1996, and 1997 for Allatoona. Inflows were calculated based on daily average outflows and changes in water surface elevations. During calibration, discrepancies in the computed and observed water surface elevations were reconciled by adding or subtracting the appropriate amount of flow using the distributed tributary option.

Outflows

Mobile District provided daily average outflows for all calibration years for Allatoona and 1979 and 1997 for West Point. Outflows for 1996 in West Point were furnished on an hourly basis. Lack of more frequent outflow data for 1979 and 1997 could have impacted the calibration of the model to both reservoirs.

Inflow temperatures

Only monthly inflow temperature data were available for the main branch of West Point and Allatoona. Missing data were filled in using a program that uses meteorological data and depth of the stream to calculate water temperatures. Temperatures were then adjusted to match the values at the most upstream lake station since they were most affected by the upstream inflow temperatures.

Inflow constituent concentrations

Water quality inflow concentrations for other constituents of the main branch for West Point and Allatoona Lake were also very limited. When observed constituent concentrations were not available at the boundary of the grid for each reservoir, data at the most upstream station were used. These were then adjusted to match the observed profiles at the most upstream lake station.

Although inflow concentrations of labile and refractory dissolved and particulate organic matter (LDOM, RDOM, and LPOM) were not monitored at West Point Lake or Allatoona Lake, their boundary concentrations were estimated from total organic carbon (TOC). The assumption was made that the majority of the TOC was refractory. To remove the uncertainty of these assumptions, data would have to be collected for the different forms. Listed below are the equations used in estimating these constituents from TOC.

$$\text{LDOM} = [(\text{TOC} - \text{algae}) * 0.75] * 0.30 \tag{1}$$

$$\text{RDOM} = [(\text{TOC} - \text{algae}) * 0.75] * 0.70 \tag{2}$$

$$\text{LPOM} = (\text{TOC} - \text{algae}) * 0.5 \tag{3}$$

Inflow algal concentrations were estimated from chlorophyll *a* (chl*a*) data. CE-QUAL-W2 requires algal concentrations in units of grams of organic matter (OM) per cubic meter. Measured chl*a* concentrations were in units of micrograms of chl*a* per liter (μ*g* chl*a*/l) and were converted to gm OM/m^3 using the conversion factor 65 as recommended by the QUAL2E and CE-QUAL-W2 user manuals (Brown and Barnwell 1987, Cole and Buchak 1995).

The conversion equation is written as:

$$\frac{\mu\text{g chla}}{\text{l}} * \frac{\text{mg}}{10^3\mu\text{g}} * \frac{\text{gm}}{10^3\text{mg}} * \frac{10^3\text{l}}{\text{m}^3} * 65\frac{\text{gm OM}}{\text{gm chla}} = \frac{0.065\text{ gmOM}}{\text{m}^3} \tag{4}$$

It was assumed that the chl*a* measurements were corrected for pheophytin according to procedures in Standard Methods (American Public Health Association, American Water Works Association, and Water Pollution Control Federation 1985).

3 Calibration

The concept of calibration/verification of a model has changed in recent years. Previously, calibration was performed for a chosen year with coefficients being adjusted to give the best comparison between computed and observed data. Verification involved applying the model to another year without changing coefficients. In reality, if the results for the verification year were inadequate, both years were revisited and coefficients adjusted until an adequate fit of both years was achieved, essentially making both data sets calibration years. Including additional years for calibration further obscures the distinction between calibration and verification data sets.

Additionally, although not done in this application, there is no reason to expect that all water quality calibration parameters should remain constant from year to year. For example, sediment oxygen demand (SOD) and nutrient fluxes can and do change over time; otherwise, there would be no purpose in using a model to determine a system's response to changes in loadings. There is no reason to expect that SOD in 1979 would be the same as SOD in 1997 in Allatoona Reservoir. The only way to account for these changes would be to model all the years from 1979 to 1997 and hope that whatever changes in SOD and nutrient fluxes that occurred over the years would be captured by the model. Indeed, this would be the best way to gain confidence in a model's predictive ability. Clearly, however, this is not feasible as the data do not exist to drive the model for this period.

Successful model application requires calibrating the model to observed in-pool water quality. If at all possible, two or more years should be modeled with widely varying hydrology and/or water quality if corresponding water quality data are available. For West Point, 1979, 1996, and 1997 were used for calibration. For Allatoona, 1992, 1993, 1996, and 1997 were used for calibration. The more years included for calibration, the more confidence one can have in model predictions under future conditions.

Graphical and statistical comparisons of computed versus observed data were made to evaluate model performance. When interpreting temperature and water quality predictions from CE-QUAL-W2, several points need to be kept in mind. First, temperature and water quality predictions are averaged over the length, height, and width of a cell, whereas observed data represent values at a specific point in the reservoir. Second, meteorological data were obtained from a station located approximately 80.5 km (50 miles) from the reservoir. Third, exact times observed data were taken were not available, so model output was taken at 12 noon for comparison. Fourth, inflow temperatures were estimated from meteorological data. Fifth, measurement errors also exist with regards to measured depths, temperatures, and water quality. As a consequence, expecting the model to exactly match measured observations is unrealistic.

Two statistics were used to compare computed and observed in-pool observations. The absolute mean error (AME) indicates how far, on the average, computed values are from observed values and is computed according to the following equation:

$$AME = \frac{\Sigma \mid \text{Predicted - Observed} \mid}{\text{Number of Observations}} \tag{5}$$

An AME of 0.5 °C means that the computed temperatures are, on the average, within ± 0.5 °C of the observed temperatures.

The root mean square error (RMS) indicates the spread of how far the computed values deviate from the observed data and is given by the following equation:

$$RMS = \sqrt{\frac{\Sigma\,(\text{Predicted - Observed})^2}{\text{Number of Observations}}} \tag{6}$$

An RMS error of 0.5 °C means that 67 percent of the computed temperatures are within 0.5 °C of the observed temperatures.

Table 1 gives the values for all hydraulic and water quality parameters available for adjustment in the model. It may seem like there are a large number of coefficients available for water quality calibration. However, of the 46 coefficients available for adjustment, 20 involve the temperature rate multiplier function used in the algal and nutrient compartments. Of the remaining 26, seven involve stoichiometric relationships that are basically fixed, leaving 19 coefficients for calibration. Experience has shown that the model provides good results with the default values for algal rates and half saturation coefficients. For nutrient calibration, the only coefficients adjusted are typically the sediment release rates for ammonium and phosphorus. For DO, the only coefficients usually adjusted are the zero-order SOD rates and possibly the organic matter decay rates. As a result, the amount of "curve fitting" has been kept to a minimum. Values in bold face represent parameters that are different between reservoirs.

Table 1
Water Quality Coefficient Calibration Values

Coefficient	Variable	Allatoona	West Point
Hydraulic			
Horizontal eddy viscosity	AX	1.0 $m^2 s^{-1}$	1.0 $m^2 s^{-1}$
Horizontal eddy diffusivity	DX	1.0 $m^2 s^{-1}$	1.0 $m^2 s^{-1}$
Chezy bottom friction factor	CHEZY	70 $m^{½} s^{-1}$	70 $m^{½} s^{-1}$
Wind-sheltering	WINDSH	**0.7**	**0.85**
Fraction solar radiation absorbed at water surface	BETA	0.45	0.45
Light extinction for pure water	GAMMA	0.25 m^{-1}	0.25 m^{-1}
Coefficient of bottom heat exchange	CBHE	7.0 * 10^{-8} °C $m^{-1} s^{-1}$	7.0 * 10^{-8} °C $m^{-1} s^{-1}$
Water Quality			
Algae			
Growth rate	AG	2 day^{-1}	2 day^{-1}
Mortality rate	AM	0.1 day^{-1}	0.1 day^{-1}
Excretion rate	AE	0.04 day^{-1}	0.04 day^{-1}
Respiration rate	AR	0.04 day^{-1}	0.04 day^{-1}
Settling rate	AS	0.1 m s^{-1}	0.1 m s^{-1}
Phosphorus half-saturation for algal growth	AHSP	0.003 g m^{-3}	0.003 g m^{-3}
Nitrogen half-saturation for algal growth	AHSN	0.014 g m^{-3}	0.014 g m^{-3}
Light saturation intensity	ASAT	75 W m^{-2}	75 W m^{-2}
Fraction of algae to POM	APOM	0.8	0.8
Lower temperature for minimum algal rates	AT1	10 °C	10 °C
Lower temperature for maximum algal rates	AT2	30 °C	30 °C
Upper temperature for maximum algal rates	AT3	35 °C	35 °C
Upper temperature for minimum algal rates	AT4	40 °C	40 °C
Lower temperature rate multiplier for minimum algal rates	AK1	0.1	0.1
Upper temperature rate multiplier for minimum algal rates	AK2	0.99	0.99
Lower temperature rate multiplier for maximum algal rates	AK3	0.99	0.99
Upper temperature rate multiplier for maximum algal rates	AK4	0.1	0.1
Phosphorus to biomass ratio	BIOP	0.005	0.005
Nitrogen to biomass ratio	BION	0.08	0.08
Carbon to biomass ratio	BIOC	0.45	0.45
Phosphorus			
Sediment release rate (fraction of SOD)	PO4R	**0.002 day^{-1}**	**0.005 day^{-1}**
Ammonium			
Ammonium decay rate	NH4DK	0.12 day^{-1}	0.12 day^{-1}
Sediment release rate (fraction of SOD)	NH4R	**0.05**	**0.125**
Lower temperature for ammonium decay	NH4T1	5 °C	5 °C
Upper temperature for ammonium decay	NH4T2	25 °C	25 °C
Lower temperature rate multiplier for ammonium decay	NH4K1	0.1	0.1
Upper temperature rate multiplier for ammonium decay	NH4K2	0.99	0.99
Nitrate			
Nitrate decay rate	NO3DK	**0.03 day^{-1}**	**0.05 day^{-1}**
Lower temperature for nitrate decay	NO3T1	5 °C	5 °C
Upper temperature for nitrate decay	NO3T2	25 °C	25 °C
Lower temperature rate multiplier for nitrate decay	NO3K1	0.1	0.1
Upper temperature rate multiplier for nitrate decay	NO3K2	0.99	0.99
Organic matter			
Labile DOM decay rate	LDOMDK	0.12 day^{-1}	0.12 day^{-1}
Refractory DOM decay rate	RDOMDK	0.001 day^{-1}	0.001 day^{-1}
Labile to refractory DOM decay rate	LRDK	0.01 day^{-1}	0.01 day^{-1}
Labile POM decay rate	LPOMDK	0.08 day^{-1}	0.08 day^{-1}
POM settling rate	POMS	0.5 m s^{-1}	0.5 m s^{-1}
Lower temperature for organic matter decay	OMT1	5 °C	5 °C
Upper temperature for organic matter decay	OMT2	25 °C	25 °C
Lower temperature rate multiplier for organic matter decay	OMK1	0.1	0.1
Upper temperature rate multiplier for organic matter decay	OMK2	0.99	0.99
Sediment decay rate	SDK	0.08	0.08
Oxygen			
Stoichiometry for ammonium decay	O2NH4	4.57	4.57
Stoichiometry for organic matter decay	O2OM	1.4	1.4
Stoichiometry for algal respiration decay	O2AR	1.1	1.1
Stoichiometry for algal growth decay	O2AG	1.4	1.4

Allatoona

Water surface elevations

Water surface elevations are predicted by the model based on the interactions between inflows, outflows, evaporation, and precipitation. Since the inflows provided include the effects of evaporation and precipitation, these options were not used during calibration. Any discrepancies between computed and observed elevations were eliminated by including either positive or negative inflows in the distributed tributary inflow file. Distributed tributary inflows enter the surface layer of all segments in a branch and are apportioned according to the surface area of each segment. As shown in Figure 7, predicted elevations closely matched observed elevations.

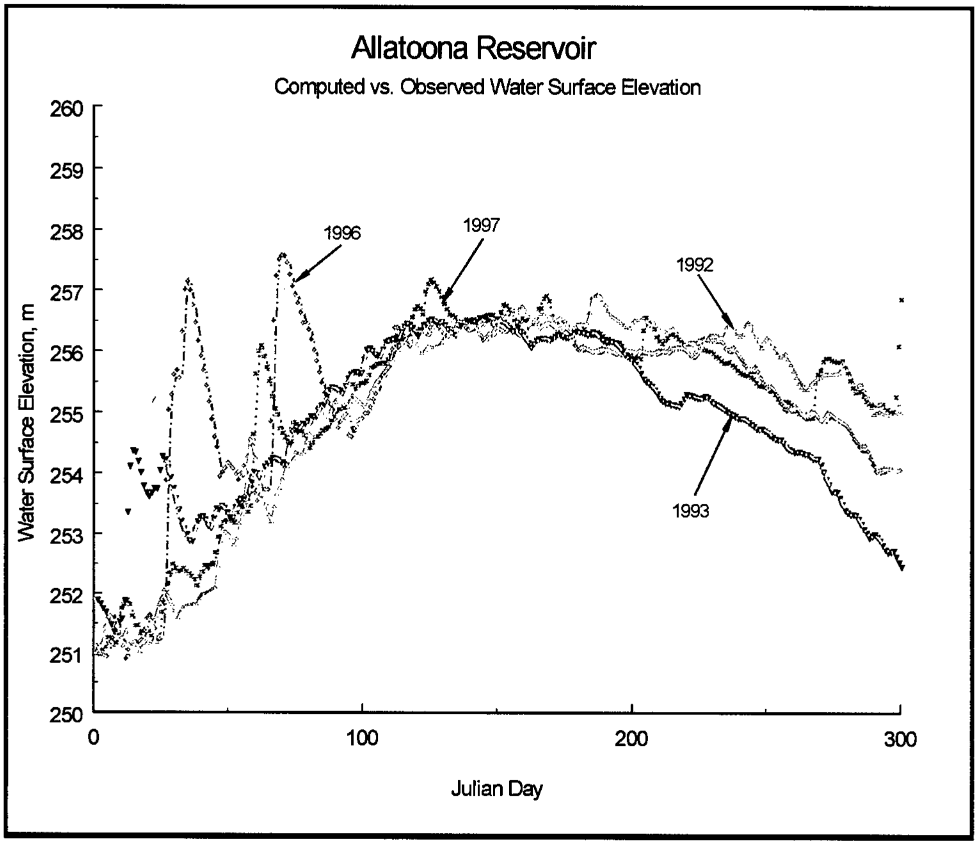

Figure 7. Computed (lines) vs. observed (symbols) water surface elevations

Temperature

Results for temperature calibration at station 01, the station closest to the dam, are given in Figures 8-11. Results for the other stations are given in Appendix A. Overall, the model is reproducing the observed temperature profiles accurately. Most of the discrepancies between predicted and observed temperatures occur in the epilimnion. Epilimnetic temperatures are influenced primarily by surface heat exchange that is in turn a function of the accuracy of the meteorological data.

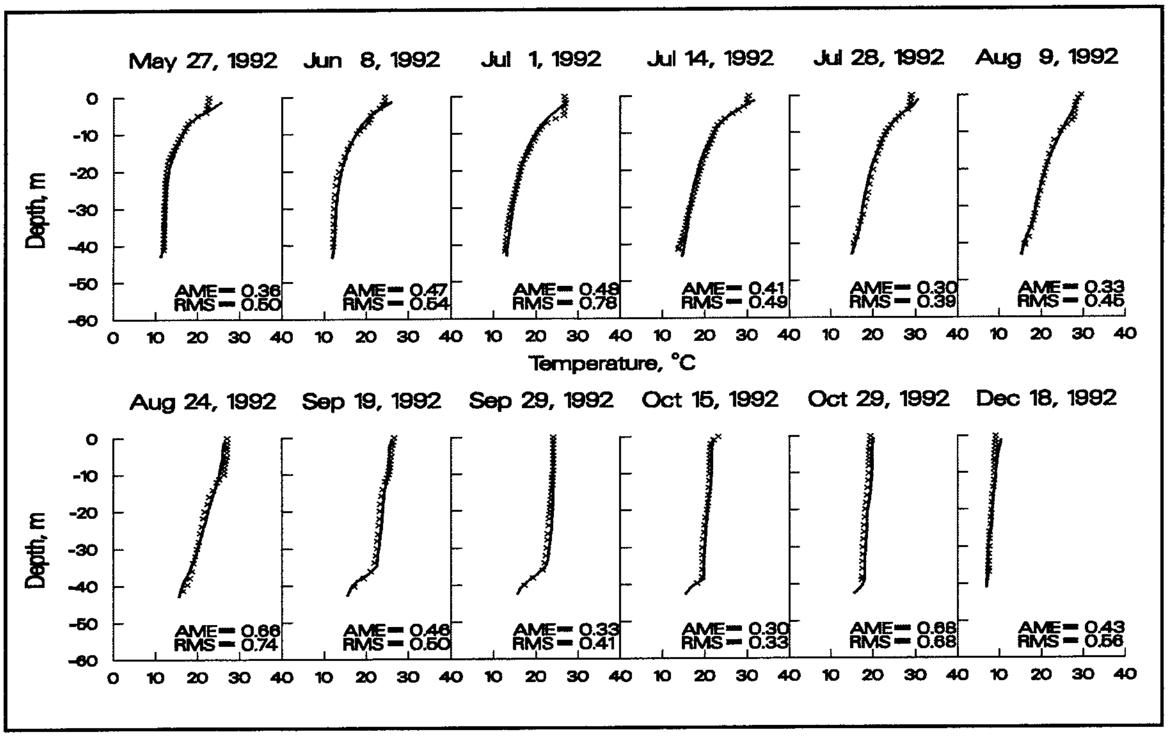

Figure 8. 1992 computed (...) vs. observed (x) temperatures at station 01

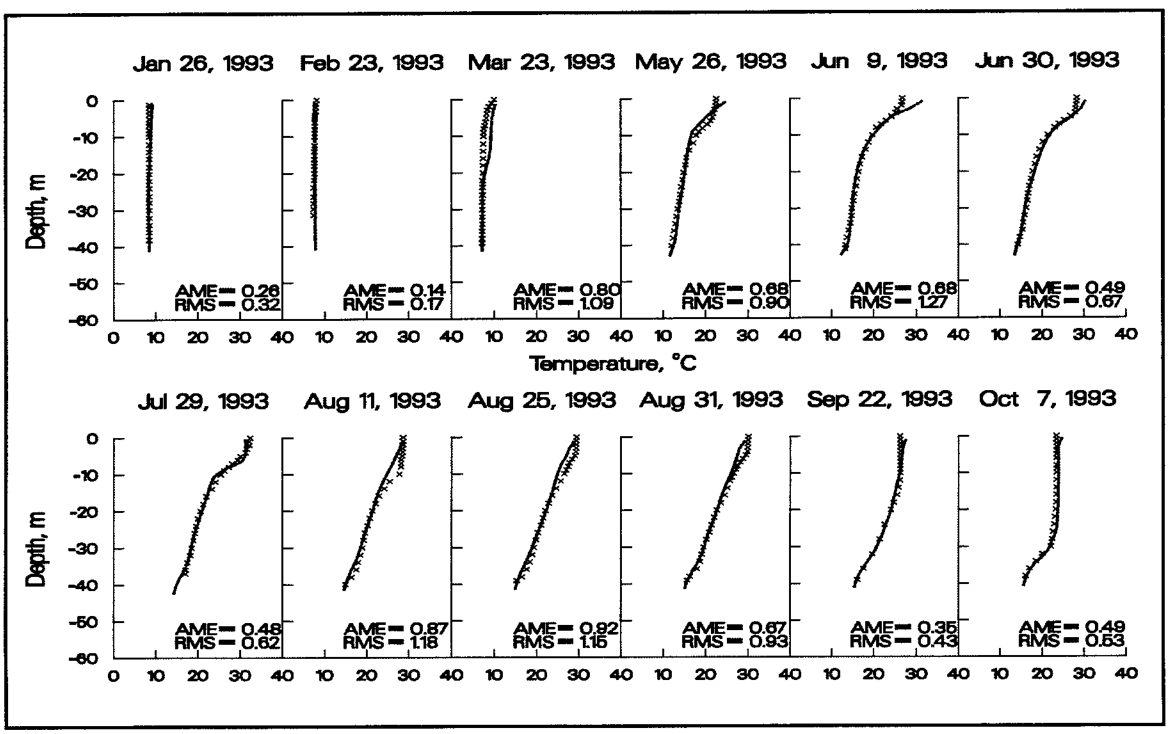

Figure 9. 1993 computed (...) vs. observed (x) temperatures at station 01

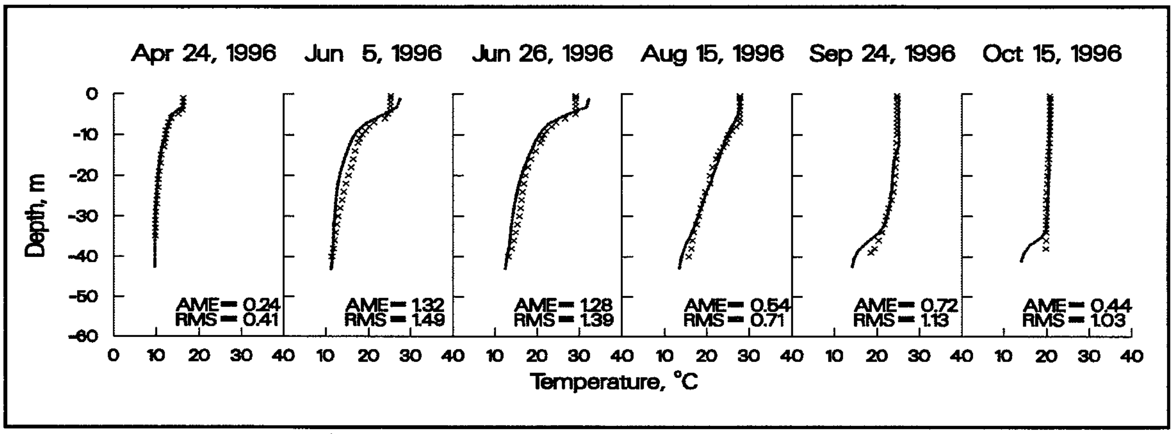

Figure 10. 1996 computed (...) vs. observed (x) temperatures at station 01

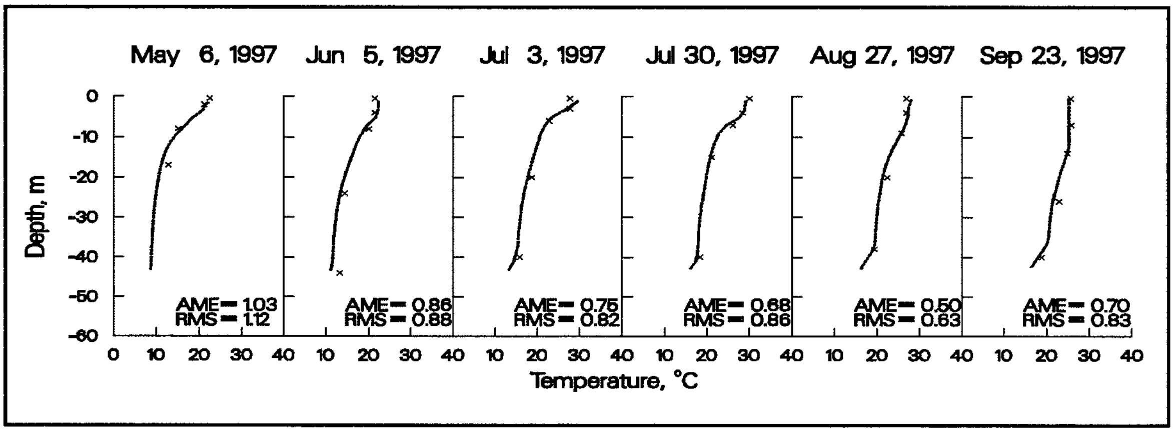

Figure 11. 1997 computed (...) vs. observed (x) temperatures at station 01

Also, epilimnetic temperatures are influenced by the time of day the data were taken and can change several degrees over the course of a day. The time at which the profiles were taken was not available for this study.

An important aspect in any model application to different calibration sets is that the model capture the differences in temperature between calibration years. For example, the temperature profile on September 19, 1992, is different than on September 22, 1993, and the model is capturing this difference, indicating that the model is accurately reproducing the response to different forcings. This gives increased confidence in the model's ability to accurately respond to different forcings for management scenarios.

Dissolved oxygen

Calibration results at station 01 are given in Figures 12-15. Results for the other stations are given in Appendix A. Overall, the model is doing a good job of reproducing the observed spatial and temporal patterns of DO depletion in Allatoona. The model is capturing the timing of the onset of oxygen depletion in

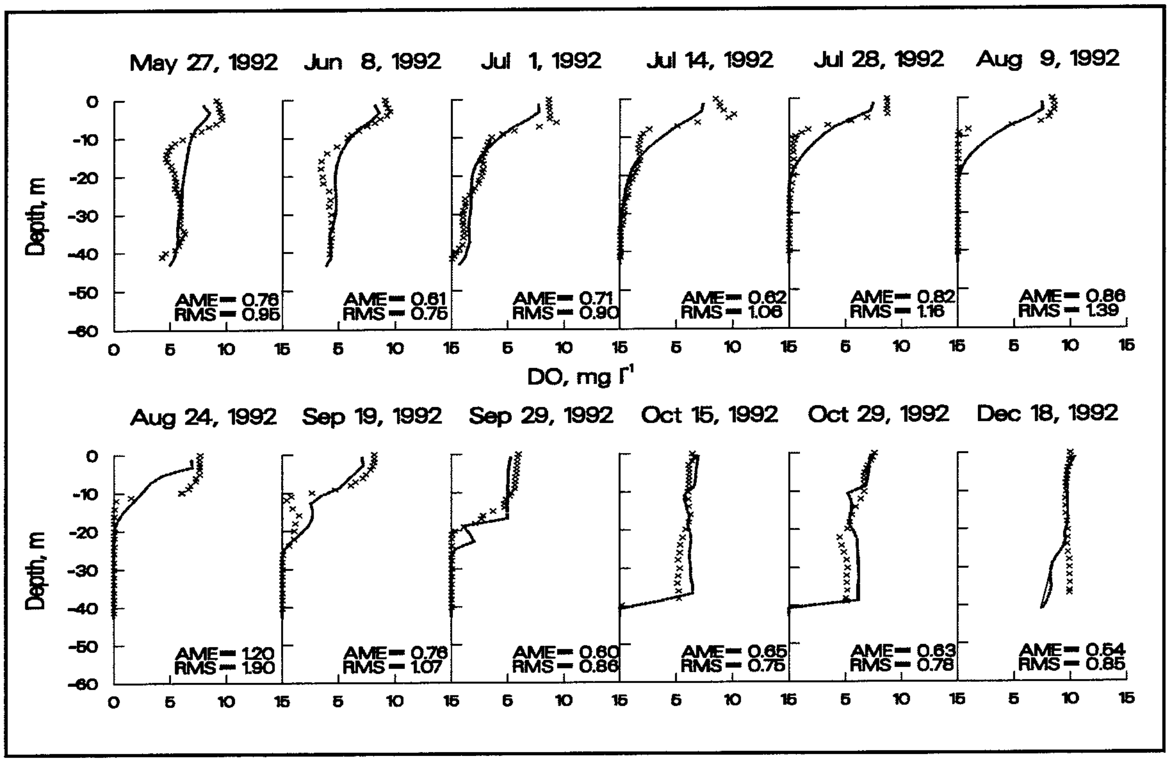

Figure 12. 1992 computed (...) vs. observed (x) DO at station 01

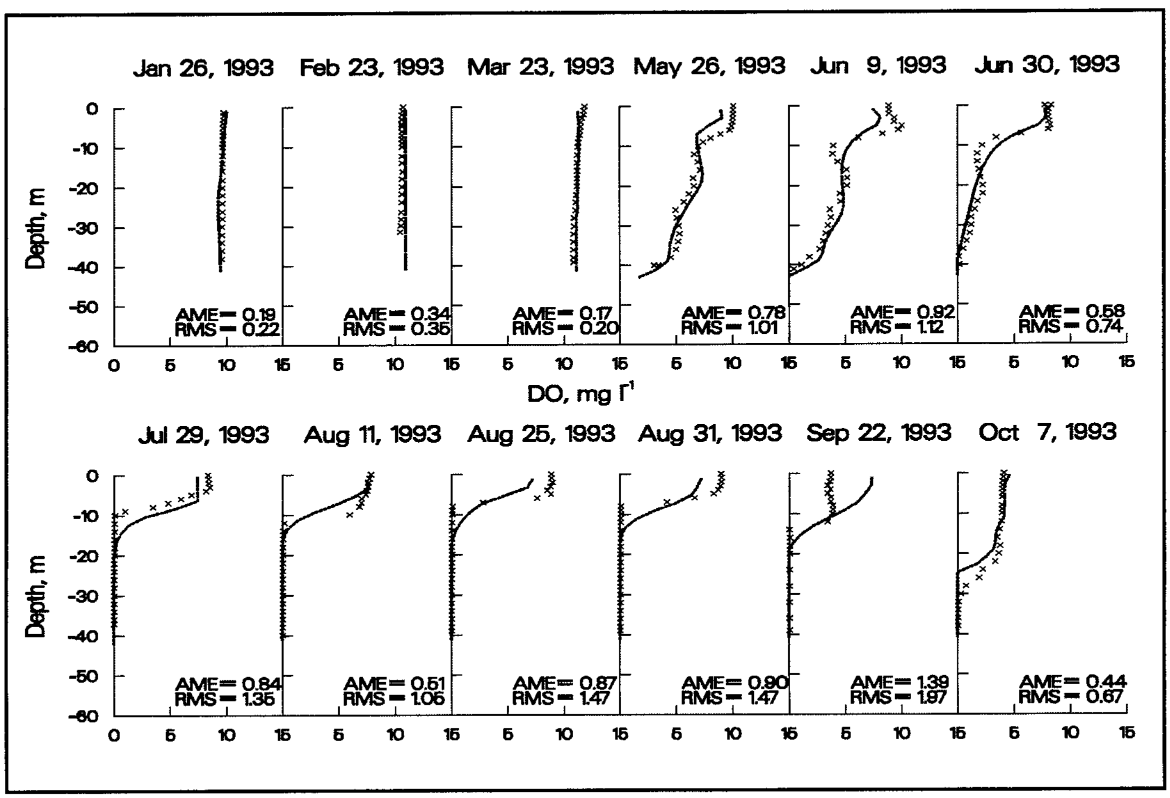

Figure 13. 1993 computed (...) vs. observed (x) DO at station 01

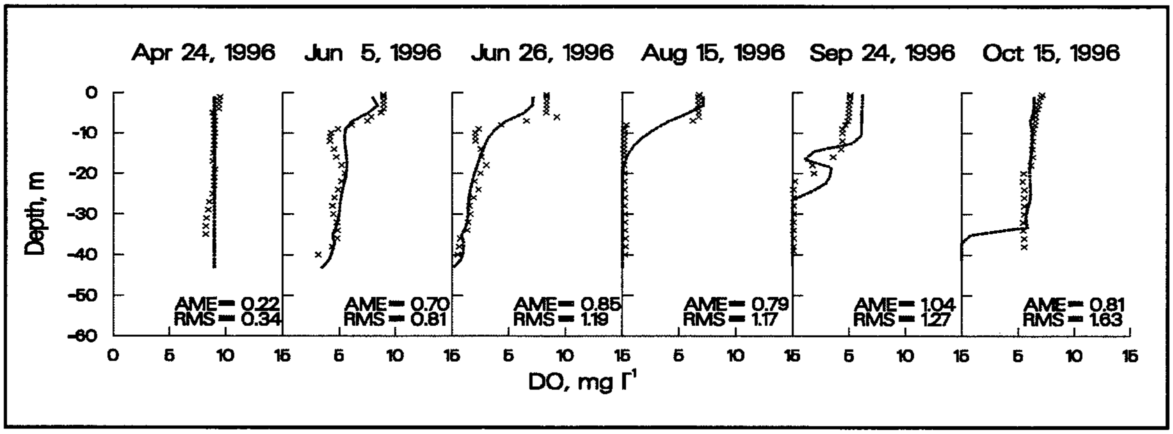

Figure 14. 1996 computed (...) vs. observed DO (x) at station 01

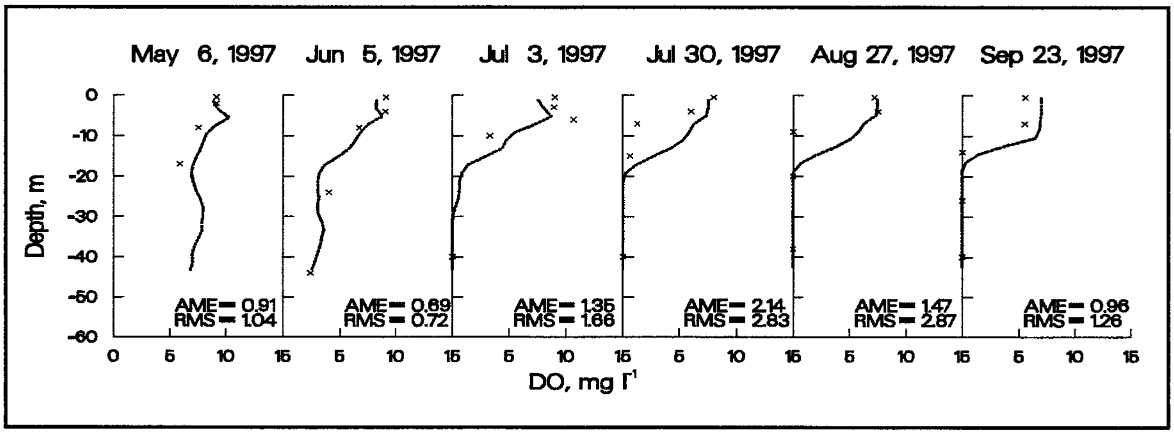

Figure 15. 1997 computed (...) vs. observed DO (x) at station 01

the springtime, the development of hypolimnetic anoxia in summer, and the increase in DO with depth during fall overturn. It should be pointed out that the only kinetic rate parameters manipulated during calibration were the SOD and sediment nutrient fluxes. This is appropriate and necessary since a mechanistic description of carbon diagenesis and subsequent SOD and nutrient fluxes is not included in the current version of the model. All other kinetic coefficients relating to algal/nutrient/DO interactions were set to their default values.

Discrepancies between computed and observed DO occur mainly in the epilimnion and metalimnion. The model tends to underpredict surface DO and overpredict DO at the bottom of the thermocline during the summer months. These trends have been seen on a number of other reservoirs and are thought to be due to the inability of the model to exactly describe algal dynamics in these zones. This in turn is thought to be due to the inability to properly model nutrient dynamics in the photic zone. If dissolved inorganic phosphorus concentrations are accurately reproduced (typically at detection levels), then there is usually insufficient phosphorus available in the model to sustain high algal productivity levels required to generate supersaturated DO levels in the epilimnion. Much research needs to be done in this area in order to accurately determine nutrient recycling rates in the photic zone that impact algal production. It should be stressed that this is a short-coming common to eutrophication models and is not unique to CE-QUAL-W2.

Discrepancies are also observed during overturn when the model is computing greater epilimnetic DO concentrations. This is most likely due to not including the effects of chemical oxygen demand induced by reduced iron, manganese, and sulfide. These were not included in the model because of a lack of observed data.

While it is important to point out the shortcomings of model predictions, it is also important to emphasize model capabilities. For Allatoona, the model is capturing complex DO profiles on July 1, 1992, and May 26 and June 9, 1993. The model also accurately represents the depth of the oxycline during fall overturn. The AME for station 01 is less than 0.7 mg/l for all the calibration years, indicating that model predictions are, on the average throughout the water column, accurate to within ±0.7 mg/l of the observed data.

It should be pointed out that a point-to-point comparison of model predictions with observed data is the most rigorous means of evaluating model output. Many modelers will compare computed versus observed contour plots or average model output and observed data over space and/or over time in order to determine if the model is capturing general trends in the observed data. Although appropriate for determining the proper temporal and spatial scales of resolution suitable for a given model, these methods of presentation also obscure a model's shortcomings. The point to be made is that the method of presenting model results in this report is intended to show the model's shortcomings as well as strengths in order to provide more information as to the model's capabilities and limitations when used as a management tool.

Nutrients

Results for ammonium, nitrate-nitrite, and dissolved inorganic phosphorus calibration are given in Figures 16–33. Where mixed samples over the photic zone were taken, the figures include all the sampling stations located along the length of the mainstem. The 1992 and 1993 data are mixed samples taken over the depth of the photic zone. Vertical profile data were available only for 1996 and 1997. For 1992 and 1993, the model generally captures the spatial trends in ammonium from the upstream to downstream stations. For 1996 and 1997, the model reproduces the increases in hypolimnetic ammonium and phosphorus during the summer stratification period and their decreases during fall overturn for the station at the dam.

When interpreting model predictions, it is also important to examine the observed data to determine what is occurring in the system and whether or not the spatial and temporal changes in the observed data can be reproduced by the mechanisms represented in the model. For example, the large increase in ammonium concentrations throughout the reservoir from June 8 to June 30, decrease from June 30 to July 14, increase from July 14 to July 28, and decrease from July 28 to August 10 must have some physical or chemical explanation for the rapid change in the observed data in order to ensure that the model can reproduce the observed

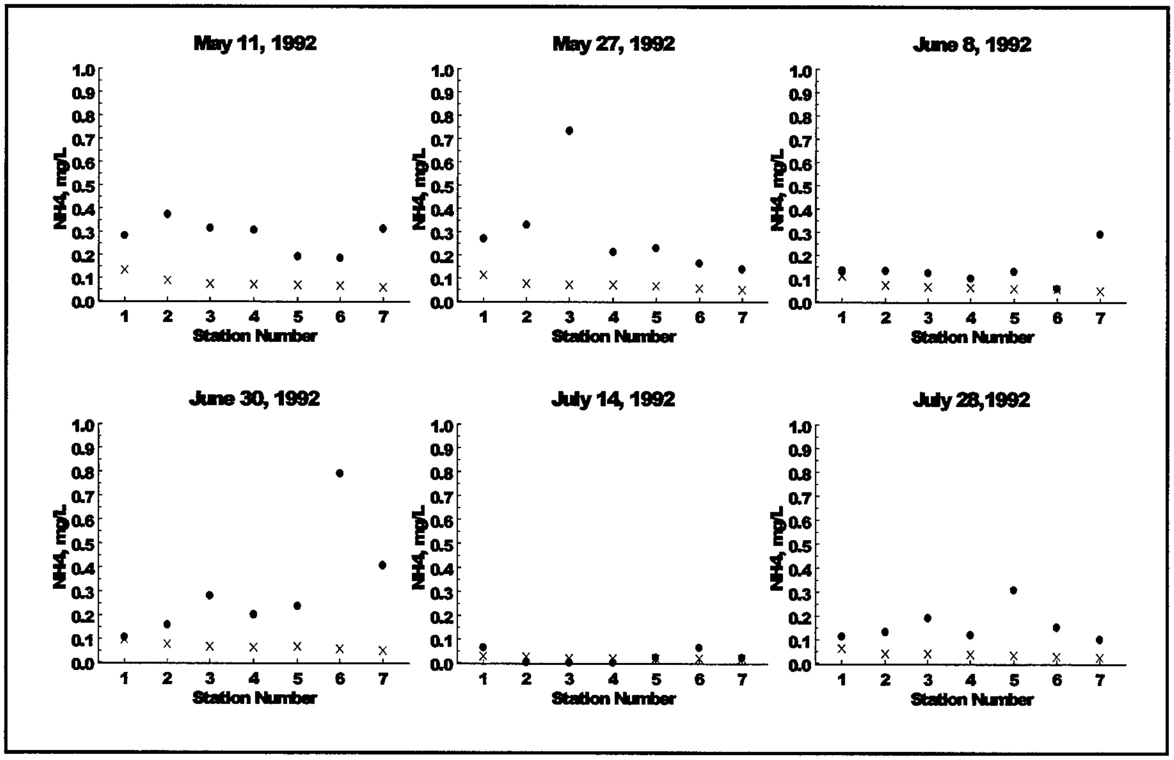

Figure 16. 1992 computed (x) versus observed (•) ammonium mixed over the photic zone depth for the mainstem stations (continued)

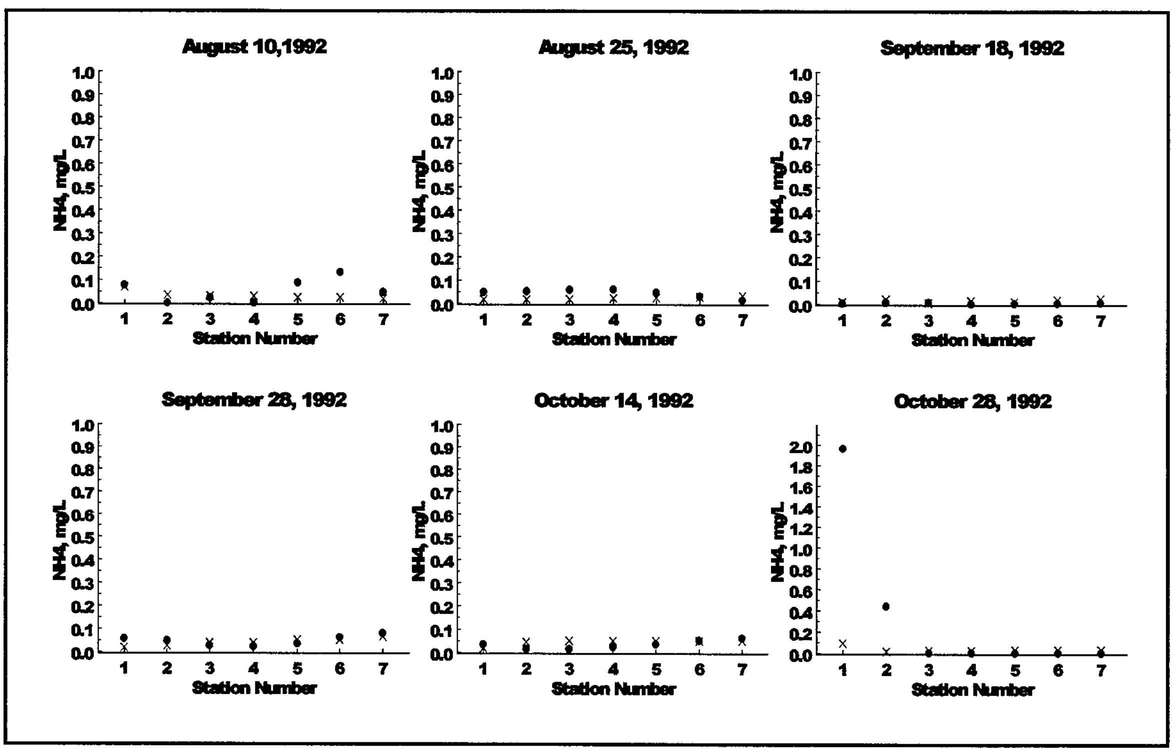

Figure 17. 1992 computed (x) versus observed (•) ammonium mixed over the photic zone depth for the mainstem stations(concluded)

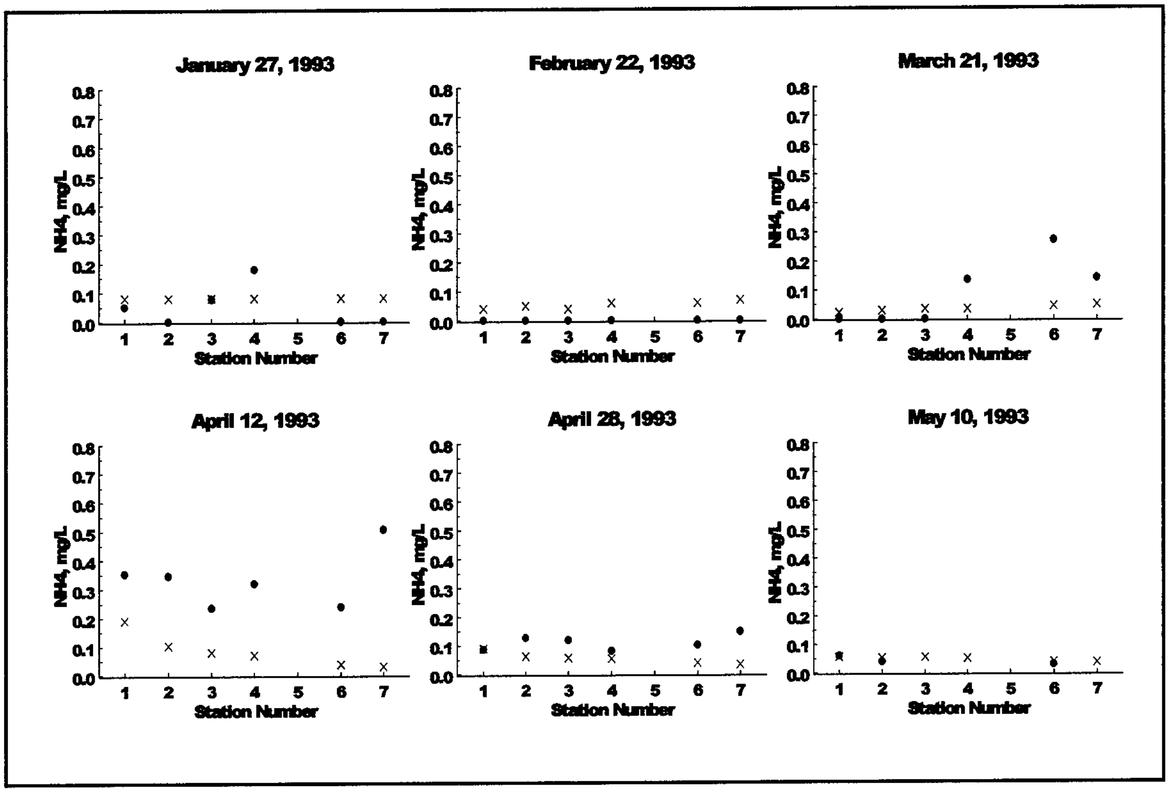

Figure 18. 1992 computed (x) versus observed (•) ammonium mixed over the photic zone depth for the mainstem stations, January 27 – May 10

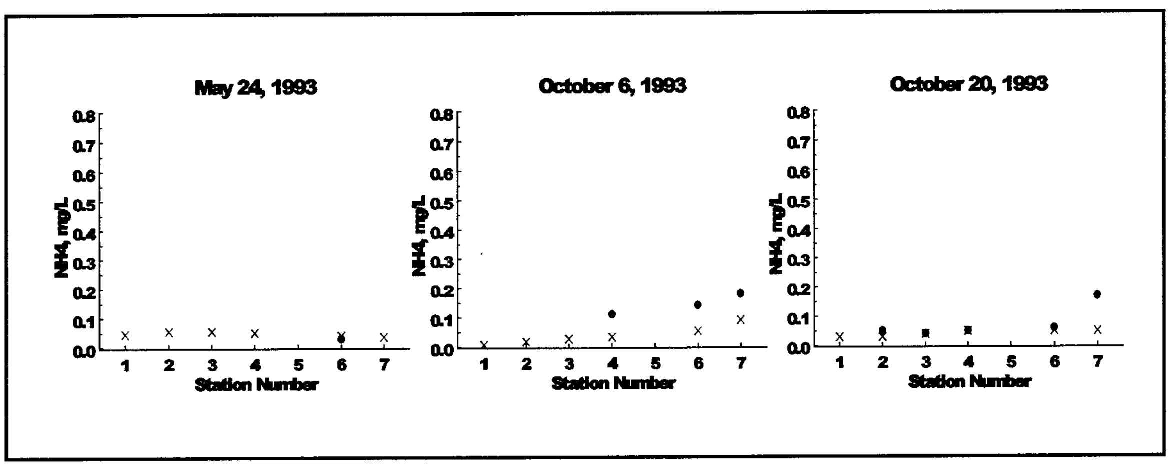

Figure 19. 1992 computed (x) versus observed (•) ammonium mixed over the photic zone depth for the mainstem stations, May 24 – October 20

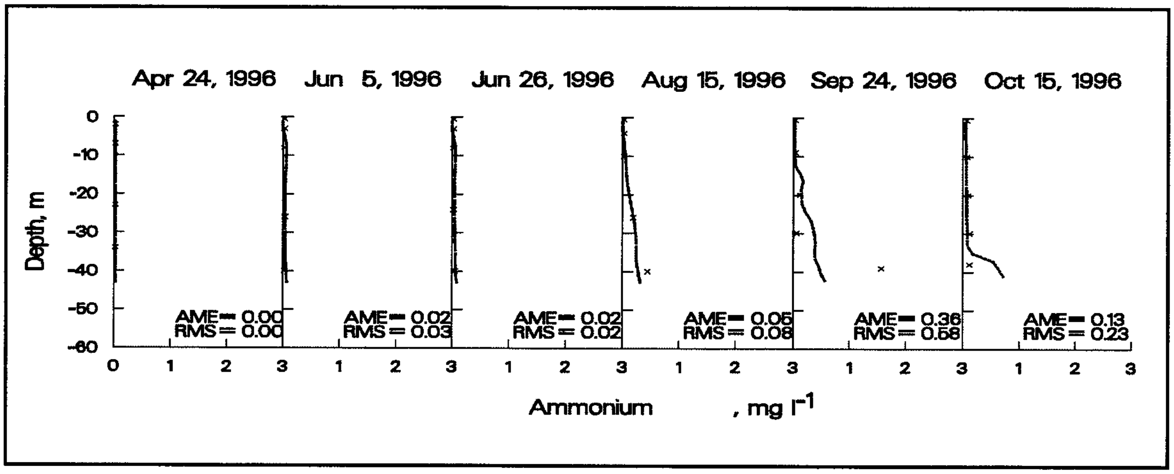

Figure 20. 1996 computed (...) vs. observed (x) ammonium at station 01

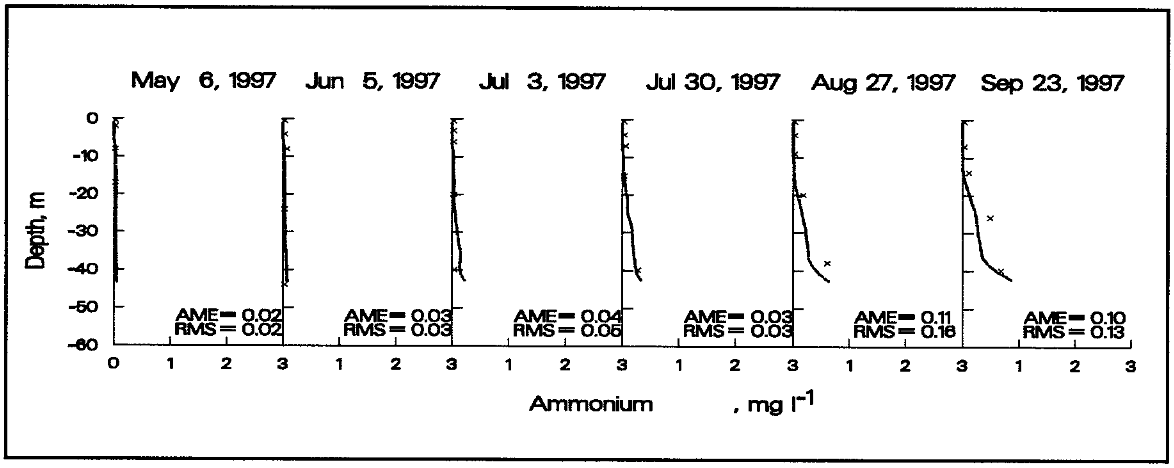

Figure 21. 1997 computed (...) vs. observed (x) ammonium at station 01

data. Residence time during this period is too great for the advection of varying boundary conditions to be responsible for the observed pattern, leaving internal kinetic interactions as the only possible explanation.

The only possible kinetic reactions that could be responsible for the observed pattern of increasing and decreasing ammonium concentrations from June 8 to June 30 to July 14 are decay of autochthonously produced organic matter to ammonium and subsequent nitrification or uptake by algae. This would require a large algal bloom with a resulting production of particulate and/or dissolved organic matter through excretion and/or die-off of the algae. The resulting organic matter decay would result in the production of ammonium. Nitrification or algal uptake would then have to take place in order to decrease the ammonium concentrations from June 30 to July 14. The process would have to be repeated from July 14 to July 28 to August 10. The observed algal and nitrate-nitrite data do not provide strong support that the above mechanism was occurring. The nitrate-nitrite profiles as well as their differences between years are also well represented.

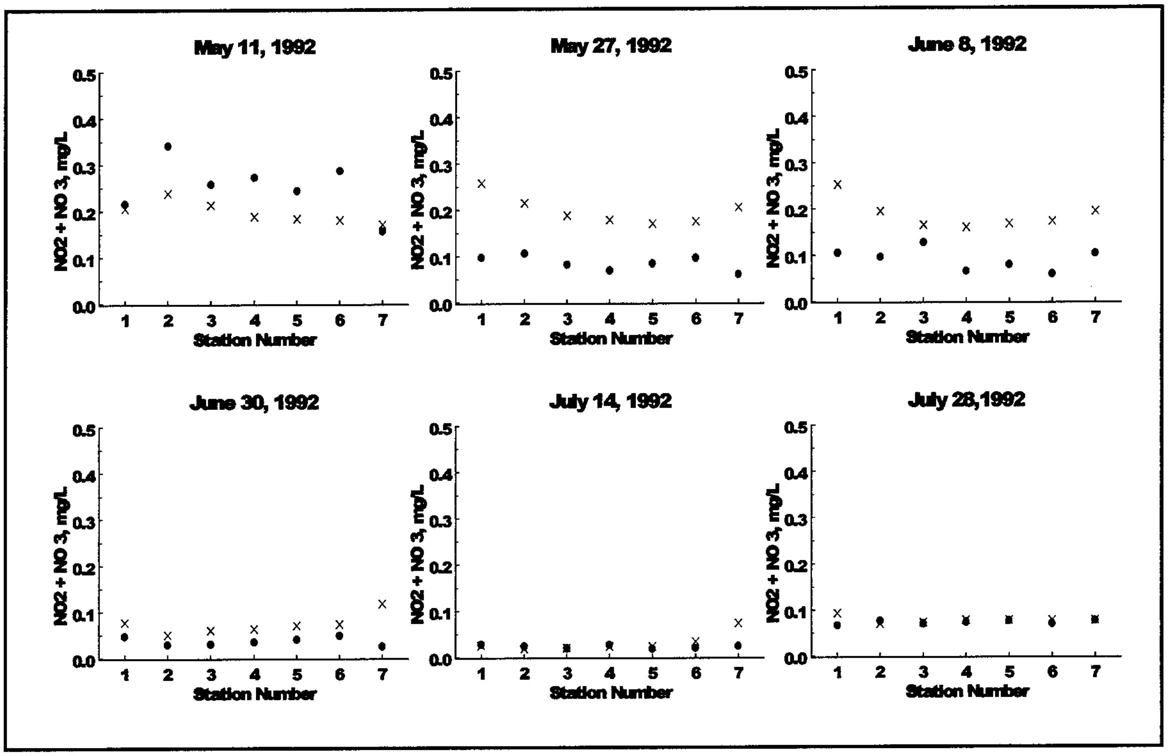

Figure 22. 1992 computed (x) versus observed (•) nitrate-nitrite mixed over the photic zone for mainstem stations (May – July)

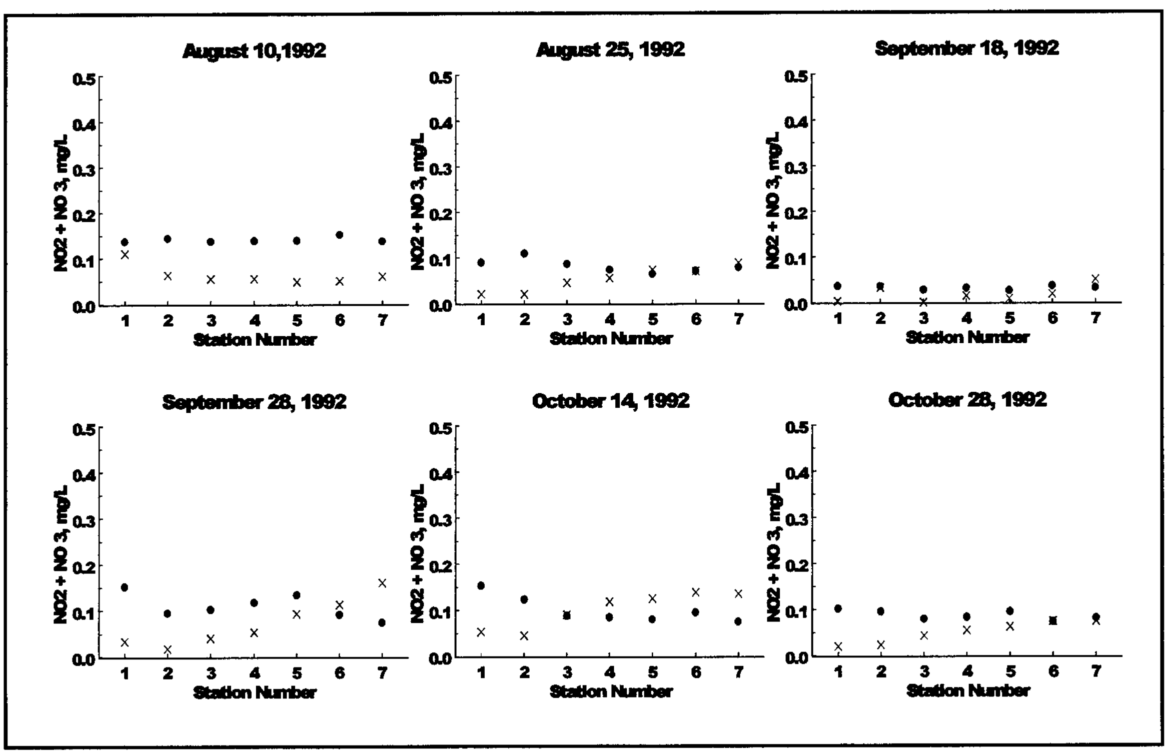

Figure 23. 1992 computed (x) versus observed (•) nitrate-nitrite mixed over the photic zone for mainstem stations (August - October)

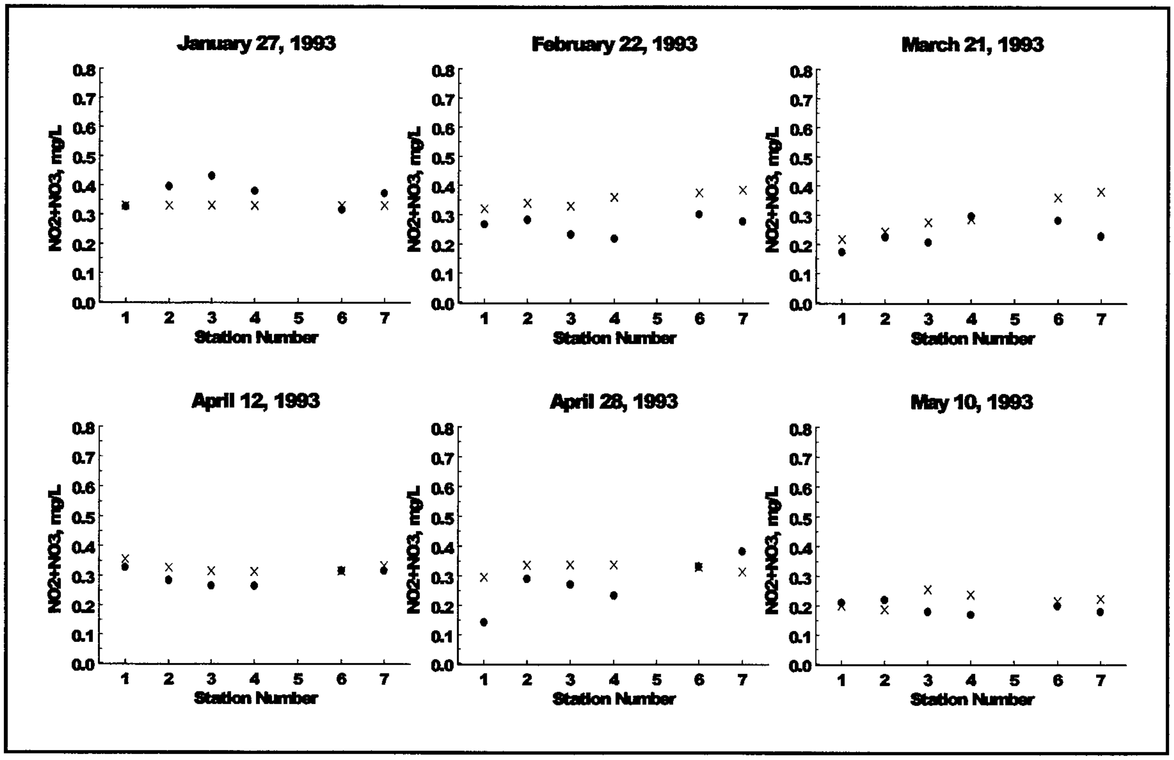

Figure 24. 1993 computed (x) versus observed (•) nitrate-nitrite mixed over the photic zone for mainstem stations (January 27 – May 10)

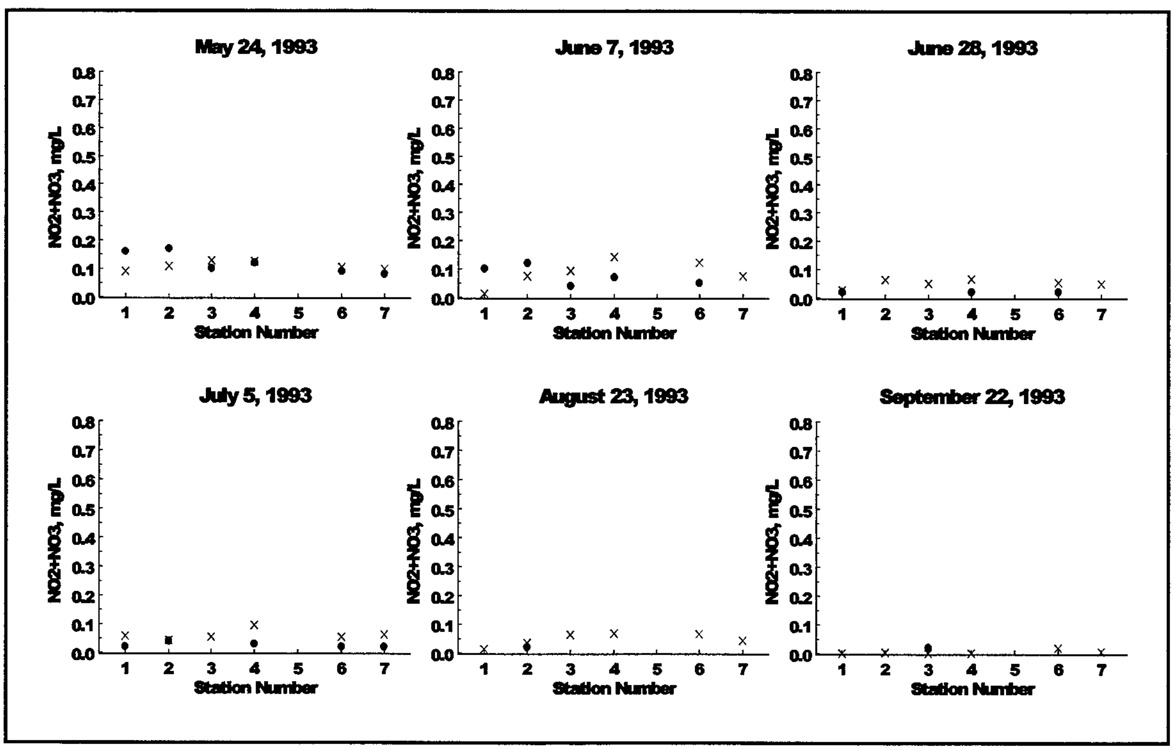

Figure 25. 1993 computed (x) versus observed (•) nitrate-nitrite mixed over the photic zone for mainstem stations (May 24 – September 22)

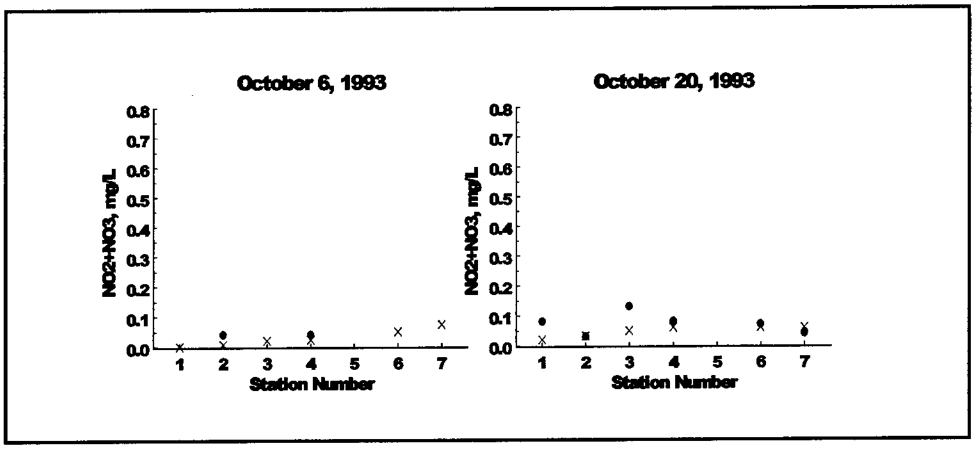

Figure 26. 1993 computed (x) versus observed (•) nitrate-nitrite mixed over the photic zone for mainstem stations (October)

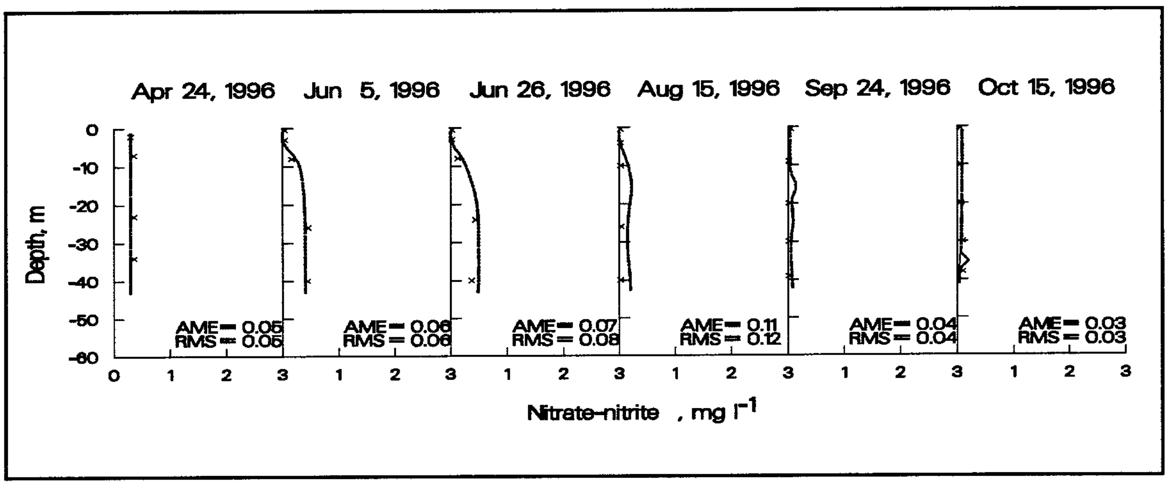

Figure 27. 1996 computed (...) vs. observed (x) nitrate-nitrite at station 01

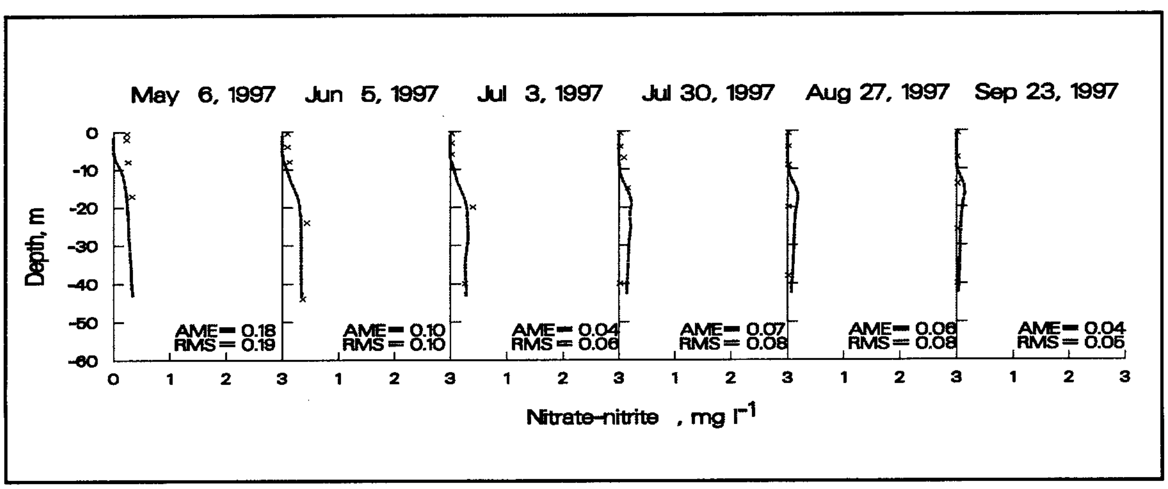

Figure 28. 1997 computed (...) vs. observed (x) nitrate-nitrite at station 01

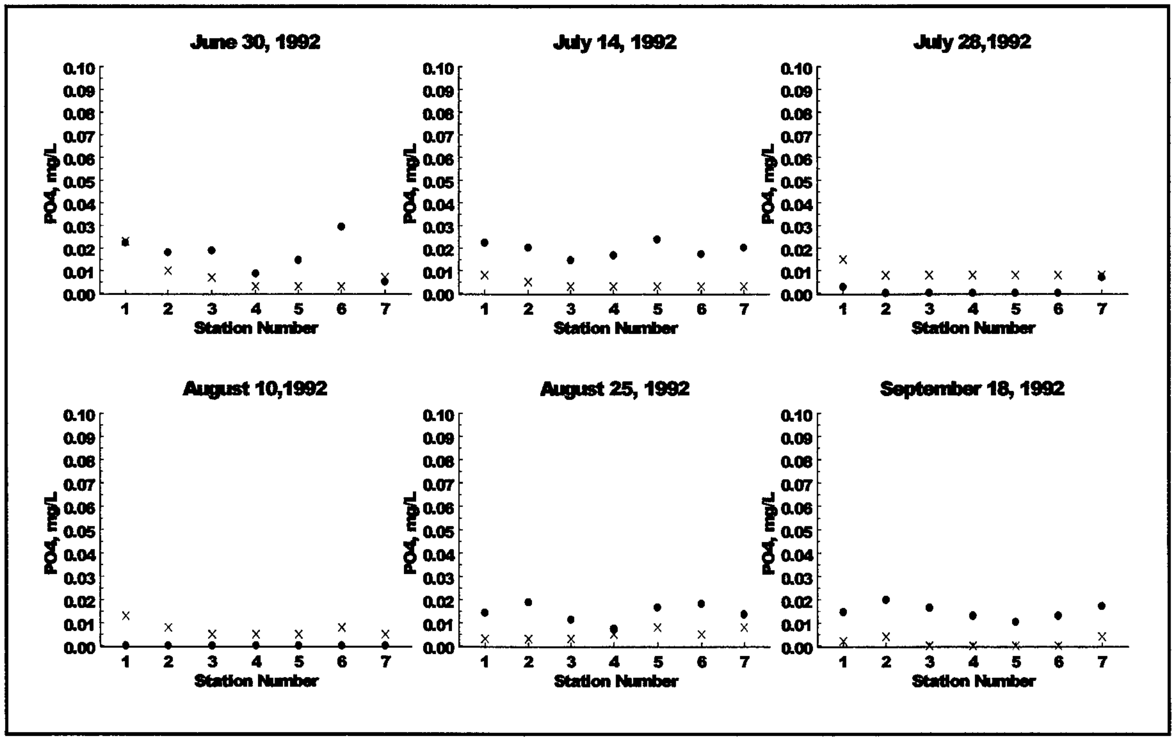

Figure 29. 1992 computed (x) versus observed (•) phosphorus mixed over the photic zone for mainstem stations (June 30 – September 18)

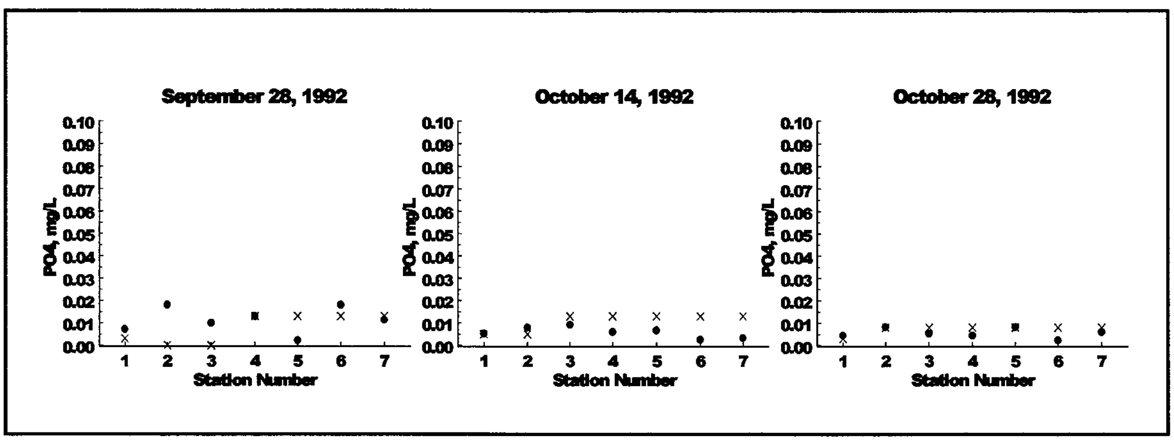

Figure 30. 1992 computed (x) versus observed (•) phosphorus mixed over the photic zone for mainstem stations (September 28 – October 28)

Algae

Predicting algal biomass is probably the most difficult task for any water quality model. Algal biomass in the model is represented as grams organic matter (dry weight)/cubic meter and measurements are represented as micrograms of chl*a* per liter. In order to compare the two, model output (or measured chl*a* concentrations) must be converted into the same units requiring a conversion factor between organic matter and chl*a*. This information was not measured for either Allatoona

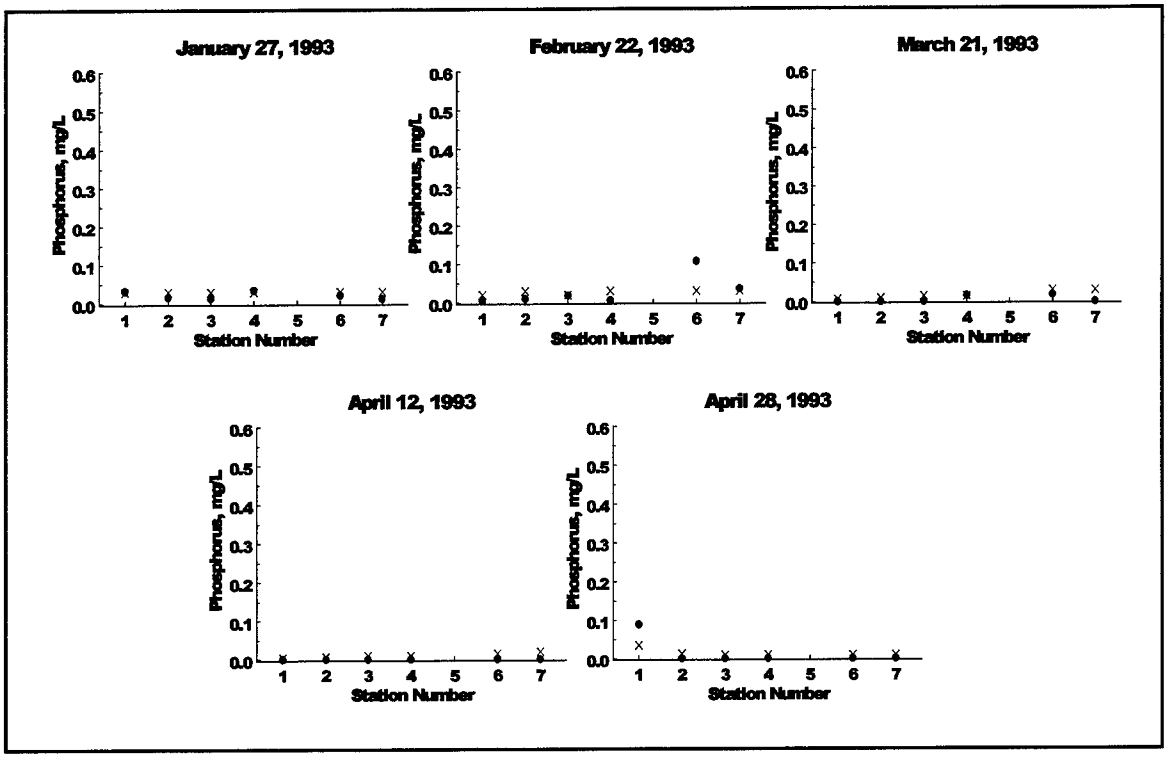

Figure 31. 1993 computed (x) versus observed (•) phosphorus mixed over the photic zone for mainstem stations

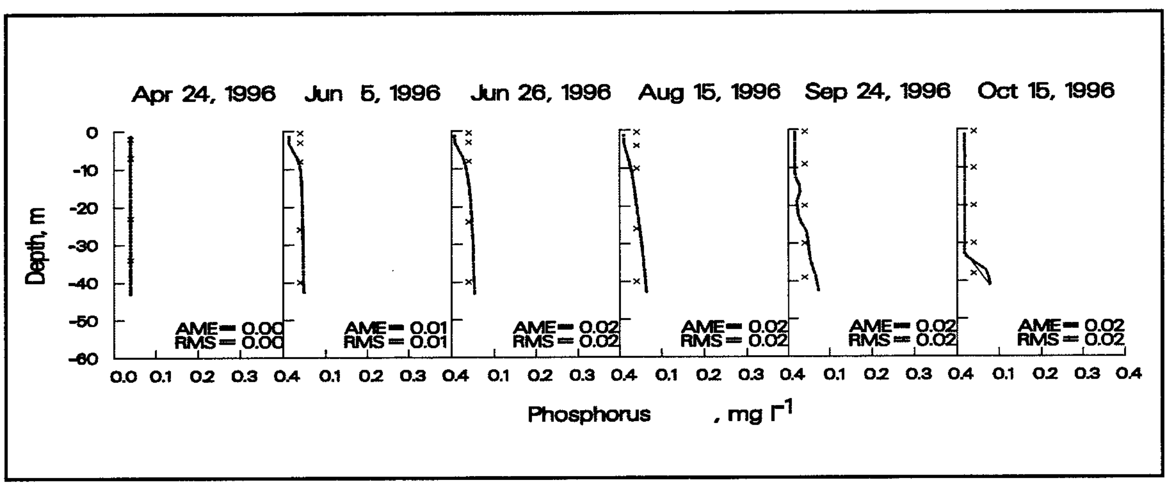

Figure 32. 1996 computed (...) vs. observed (x) phosphorus at station 01

or West Point, and, therefore, the default value of 65 for the conversion of chl*a* to OM was used. Additionally, the model represents only a single algal assemblage, whereas the prototype usually has different dominant algal types with different organic matter (OM) to chl*a* ratios depending upon the time of year. Further complicating model predictions is that the samples for 1992 and 1993 represent a mixed sample of chl*a* over the photic zone depth requiring that the output from the model be mixed over the best estimate of the photic zone depth.

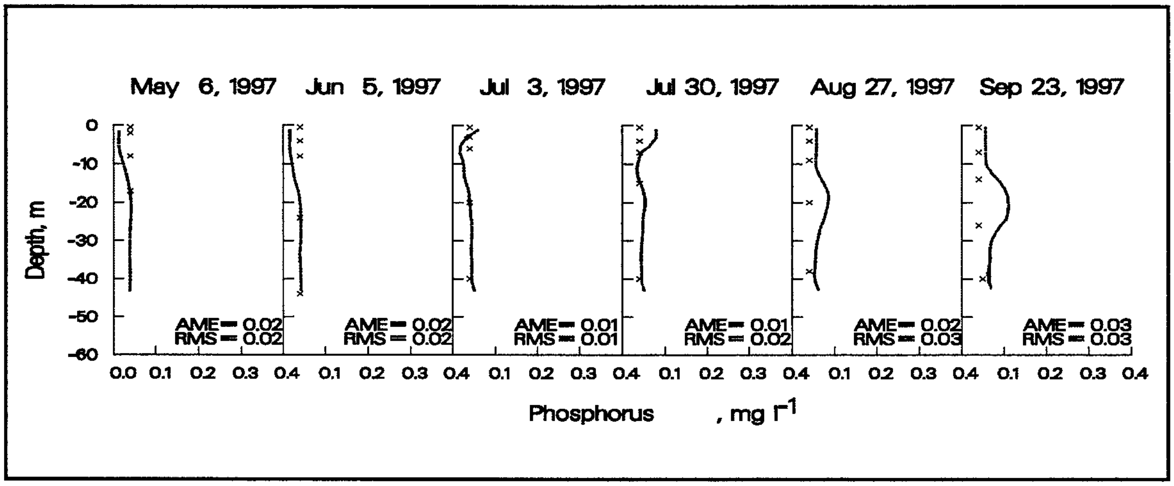

Figure 33. 1997 computed (...) vs. observed (x) phosphorus at station 01

The model also represents the algal assemblage using only one growth rate, settling rate, excretion rate, mortality rate, temperature dependency on kinetic rates, etc., whereas in the prototype these values change depending upon the dominant algal group. Variable algal types could be represented in the model, but rarely is there sufficient information to distinguish between the dominant algal groups depending upon the time of year, thus making it hard to justify modeling more than one algal group. Adding to this the sparsity of (or more commonly the complete lack of) algal and nutrient loadings at the upstream boundary, then the ability of the model to even be on the same page as the observed data is a major accomplishment.

In spite of all these difficulties, the model can still be a useful management tool if the model captures the trends in algal biomass spatially and temporally regardless of whether the model accurately computes the "actual" biomass concentrations. For example, the model consistently overpredicts the algal biomass in spring (based on an OM to chl*a* ratio of 65) and early summer for 1992 (Figures 35–35) but does capture the trend in decreasing biomass from the upstream to the downstream stations. In July and August, the model is capturing not only the spatial trends but is also closely simulating the biomass concentrations. In late summer and early fall, the model again overpredicts the algal biomass but captures the spatial trend of decreasing biomass from the upstream to the downstream stations. The model could be made to more accurately represent the actual concentrations in the spring and fall by using different OM to chl*a* ratios. However, without measured data to support the different ratios, varying the OM to chl*a* ratios is not justified and becomes simply an exercise in curve-fitting.

Similar results were obtained for 1993 (Figures 36-38). The model captured the onset of the spring bloom from April 12 to April 28, but the biomass was overpredicted using the OM to chl*a* ratio of 65. The model captured the spatial trends in algal biomass throughout the simulation period and also captured the differences between 1992 and 1993 during late summer. Results for 1996 contained some vertical resolution. The model again overpredicted biomass in the spring and fall (Figure 39).

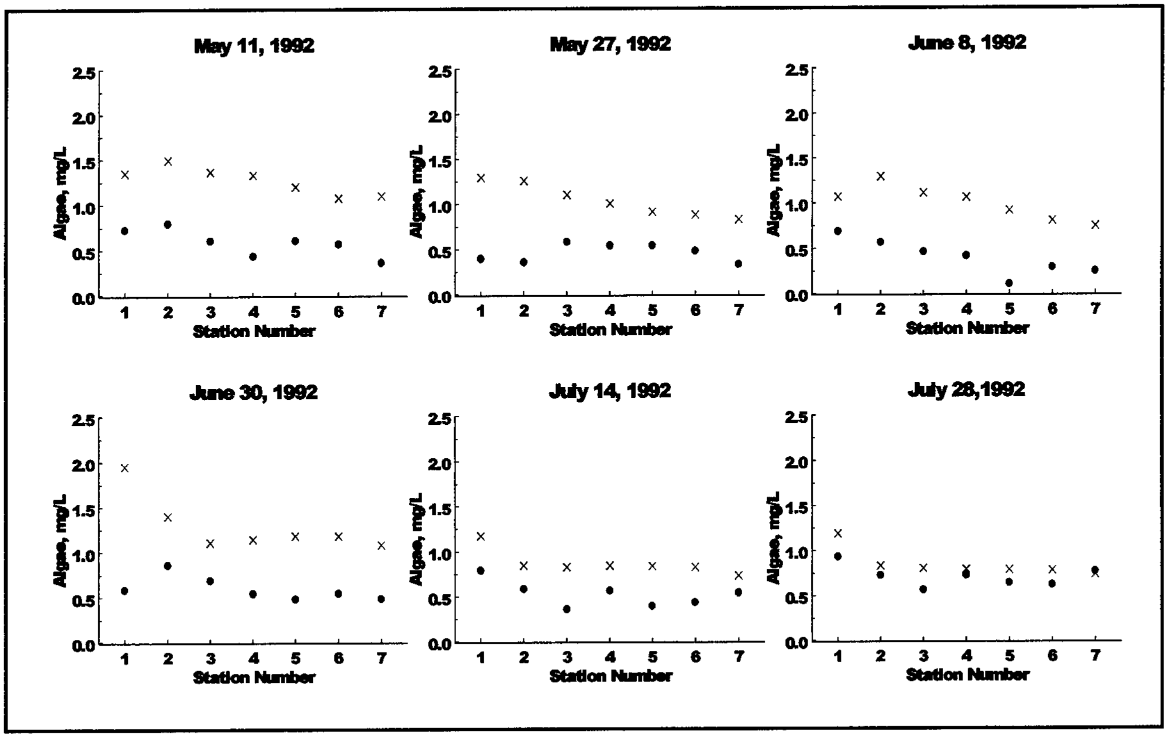

Figure 34. 1992 computed (x) versus observed (•) algal biomass (May – July)

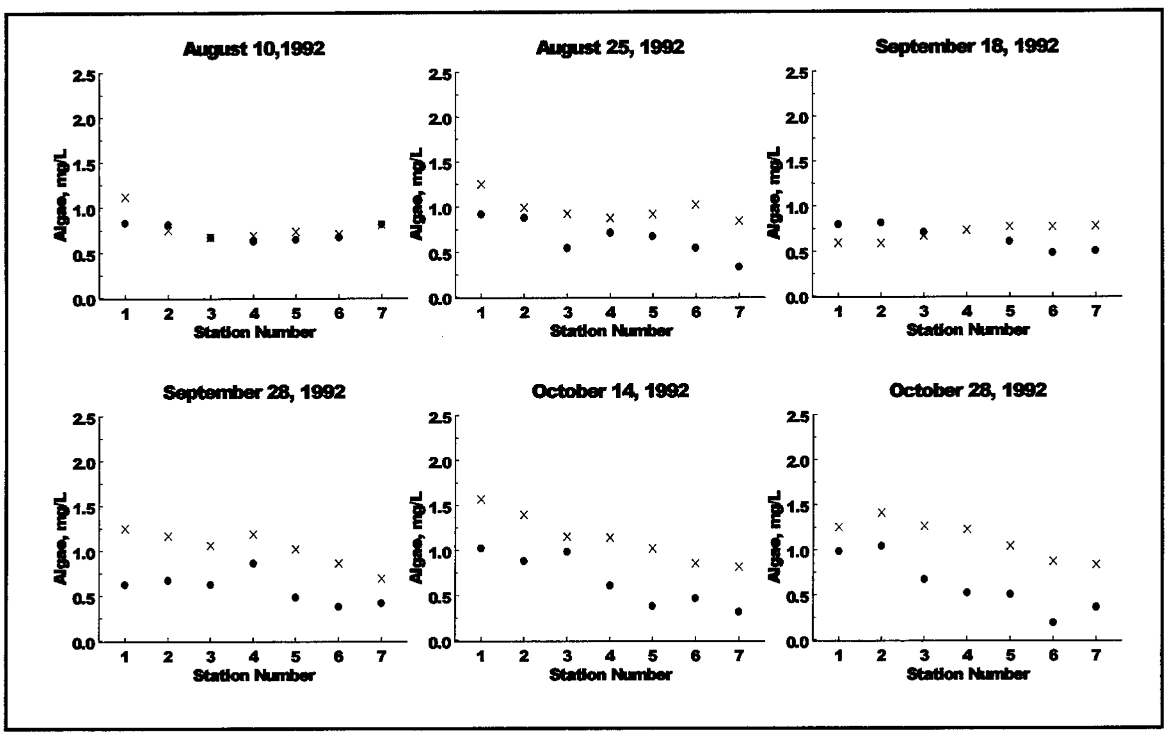

Figure 35. 1992 computed (x) versus observed (•) algal biomass (August – October)

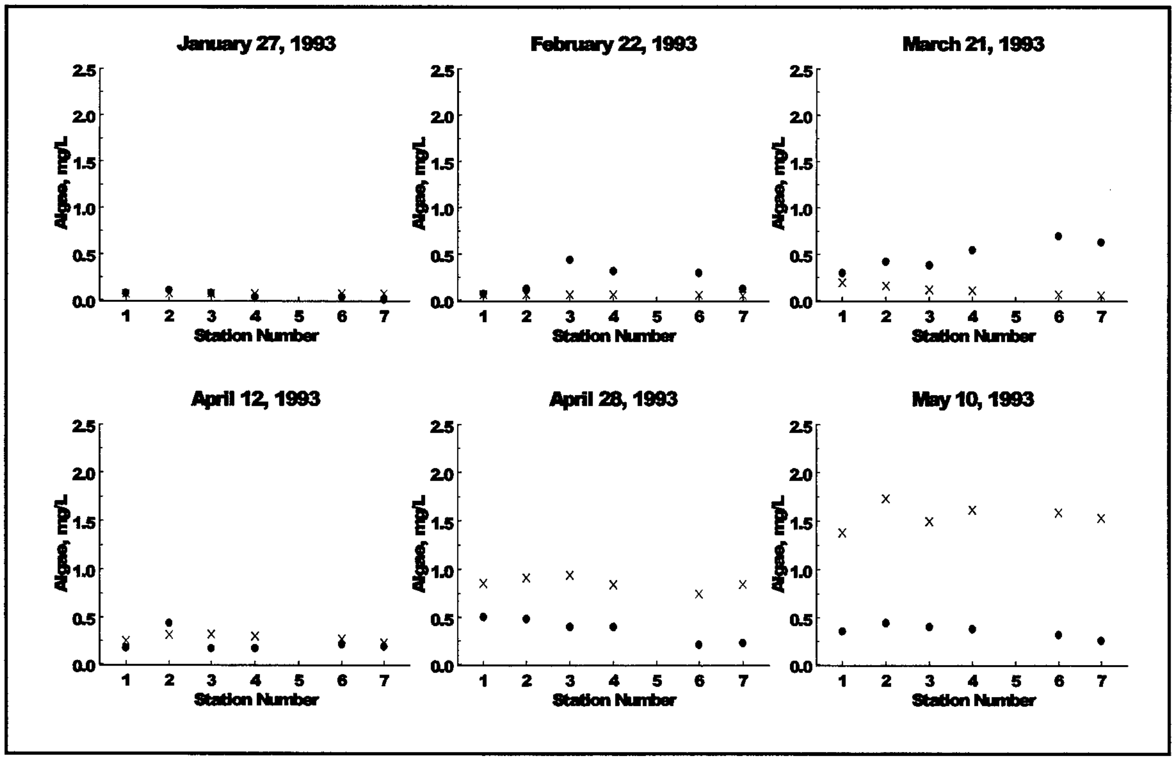

Figure 36. 1993 computed (x) versus observed (•) algal biomass (January 27 – May 10)

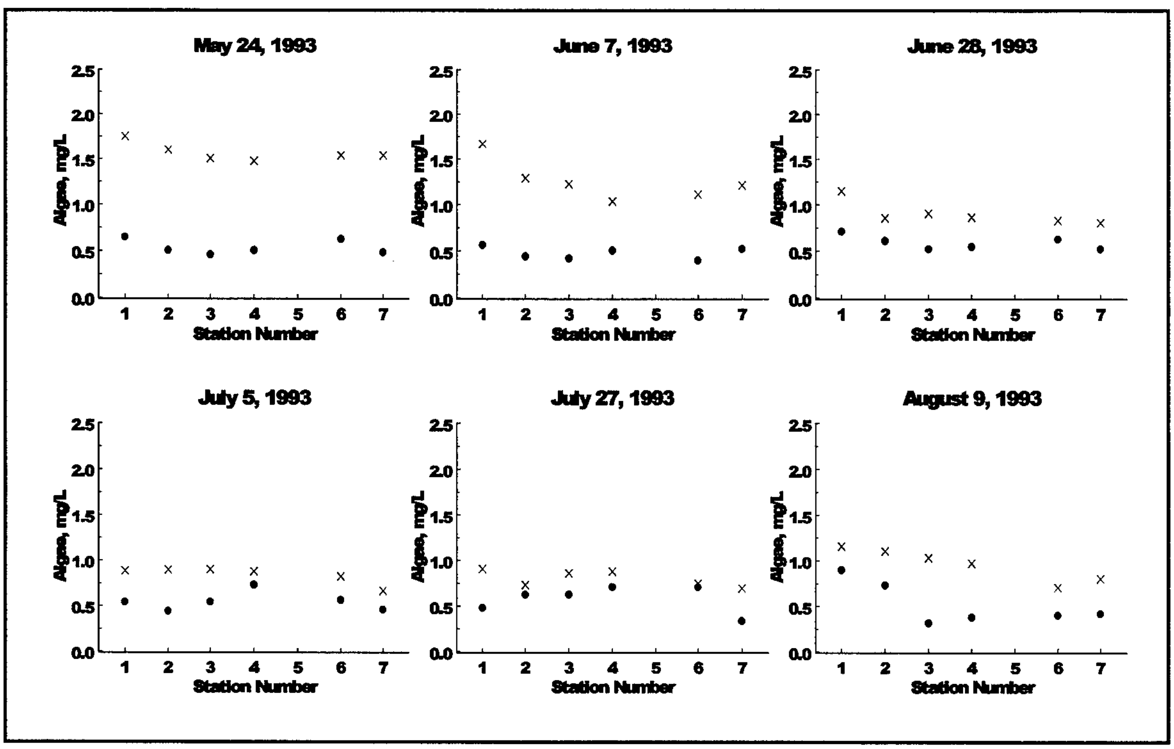

Figure 37. 1993 computed (x) versus observed (•) algal biomass (May 24 – August 9)

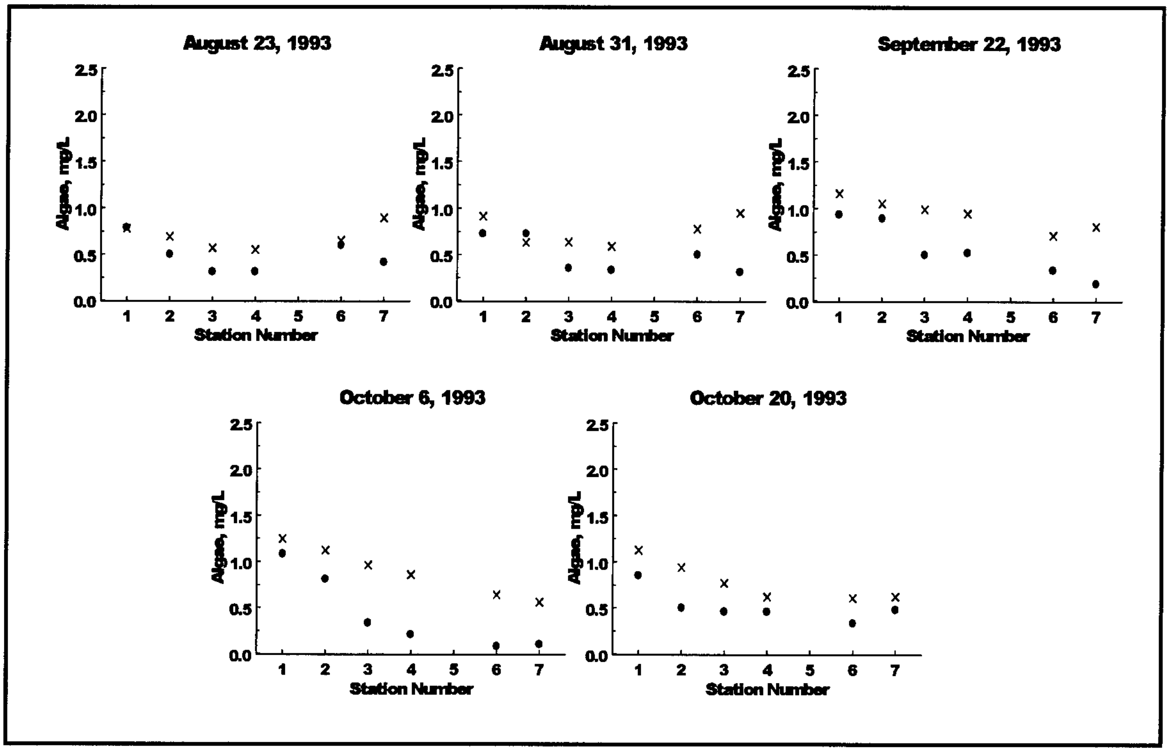

Figure 38. 1993 computed (x) versus observed (•) algal biomass (August 23 – October)

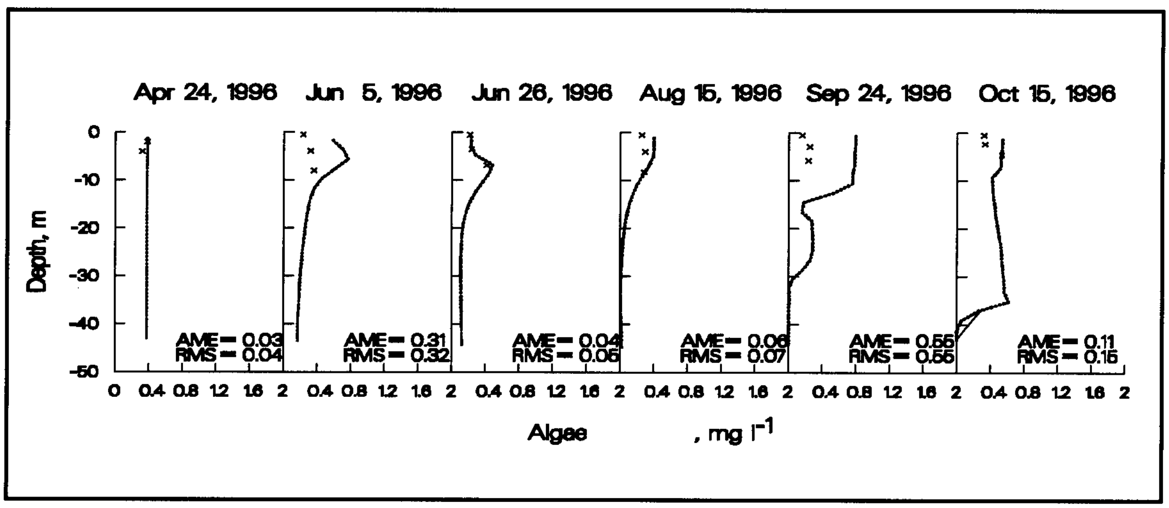

Figure 39. 1996 computed (…) versus observed (x) algal biomass

West Point

Water surface elevations

As shown in Figure 40, predicted elevations closely match observed elevations.

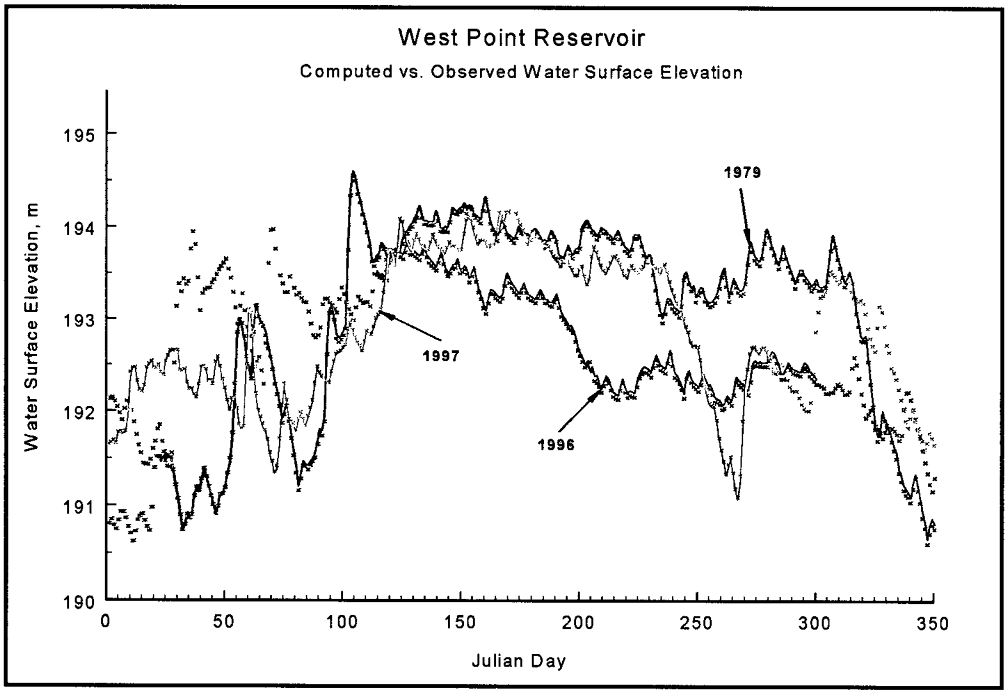

Figure 40. Computed (lines) versus observed (symbols) water surface elevations

Temperature

Results for temperature calibration at station 03, the station closest to the dam, are given in Figures 41-43. Results for the other stations are given in Appendix A. As in the Allatoona calibration, the AME is less than 1 °C for all dates for all calibration years, although the results are not as accurate as the Allatoona calibration. The model accurately represents the differences in the thermal regimes between Allatoona and West Point with no adjustment of hydraulic calibration parameters except for wind-sheltering. As can be seen from the results, the model captures the less pronounced changes in temperature over depth in West Point when compared to Allatoona.

Discrepancies between computed and observed temperatures are believed to be due primarily to the lack of accurate inflow temperatures. Inflow temperatures for both Allatoona and West Point were generated from meteorological data since observed data were either insufficient or lacking for the inflow temperature boundary condition. Since West Point has a much shorter residence time than Allatoona, any errors in inflow temperatures will be more apparent in West Point than in Allatoona.

Dissolved oxygen

Results for DO calibration at station 03 are given in Figures 44-46. Results for the other stations are given in Appendix A. With the exceptions of SOD and nutrient release rates, all kinetic coefficients were the same for Allatoona and West Point. For 1979, the model quite accurately predicts the DO regime in

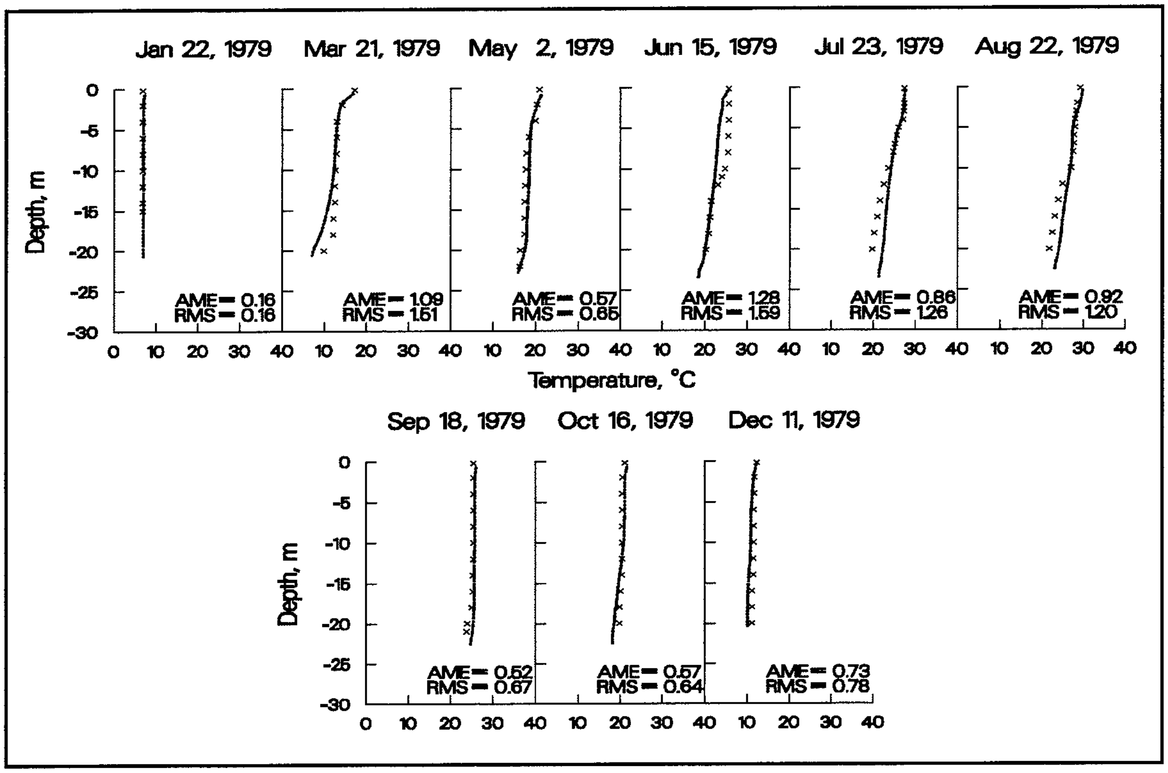

Figure 41. 1979 computed (...) vs. observed (x) temperatures at station 03

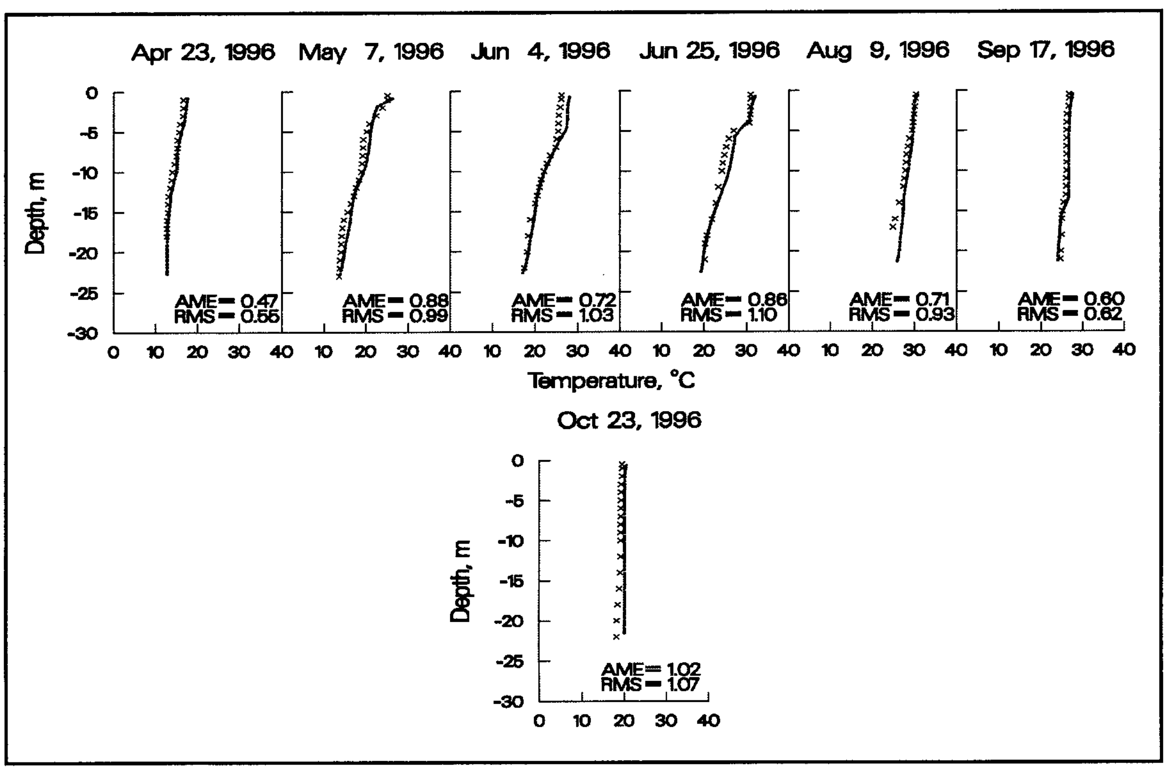

Figure 42. 1996 computed (...) vs. observed (x) temperatures at station 03

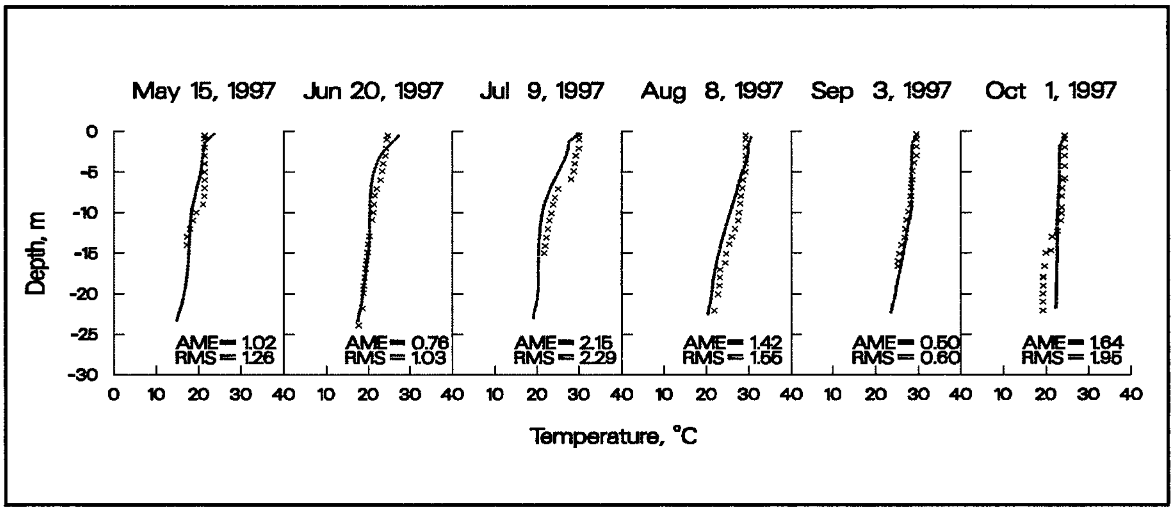

Figure 43. 1997 computed (...) vs. observed (x) temperatures at station 03

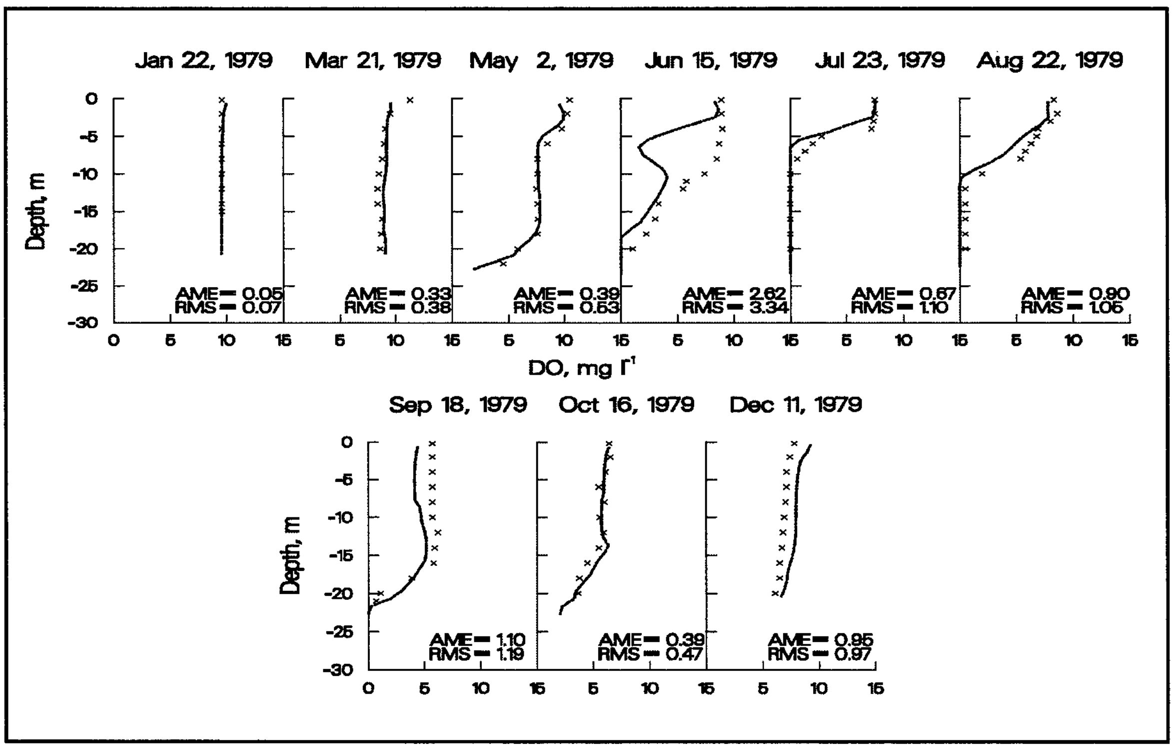

Figure 44. 1979 computed (...) vs. observed (x) DO at station 03

West Point with the glaring exception of June 15. As was noted in the discussion for temperature, West Point is more sensitive to any errors in boundary conditions due to the shorter residence time, and it is believed that the discrepancy between computed and observed DO on June 15 is due primarily to inaccurate water quality boundary conditions. In contrast to Allatoona, the model has less of a tendency to overpredict DO at the bottom of the chemocline.

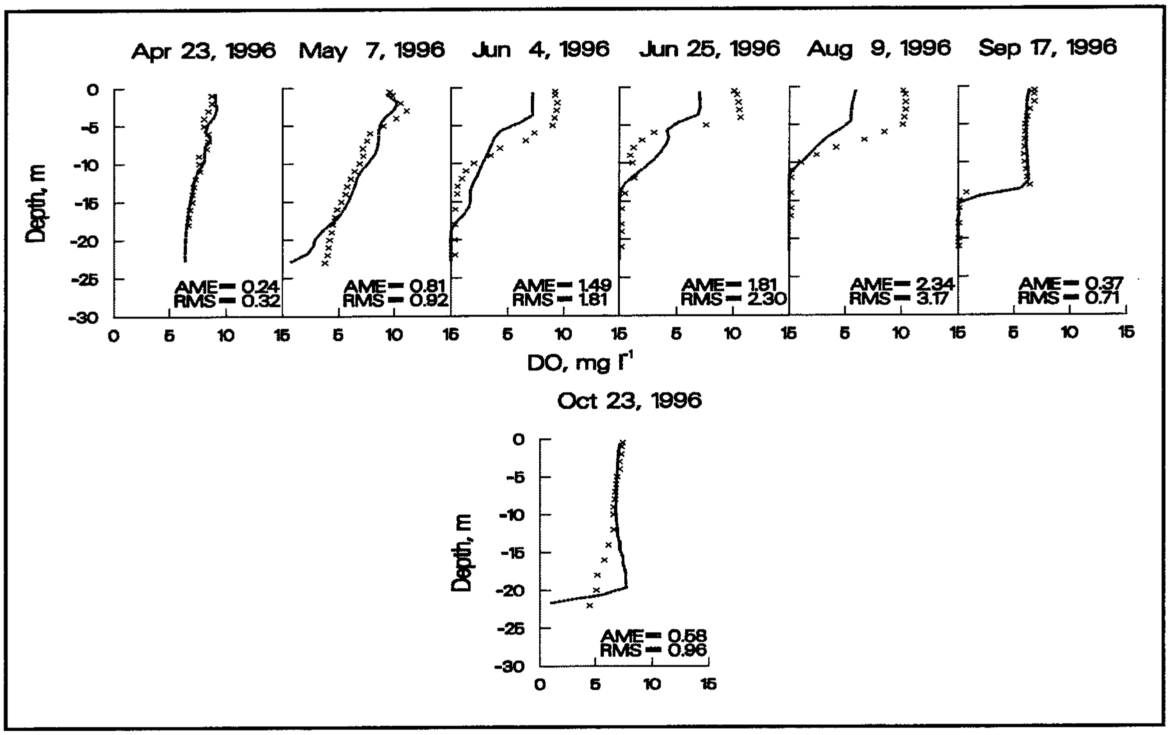

Figure 45. 1996 computed (...) vs. observed (x) DO at station 03

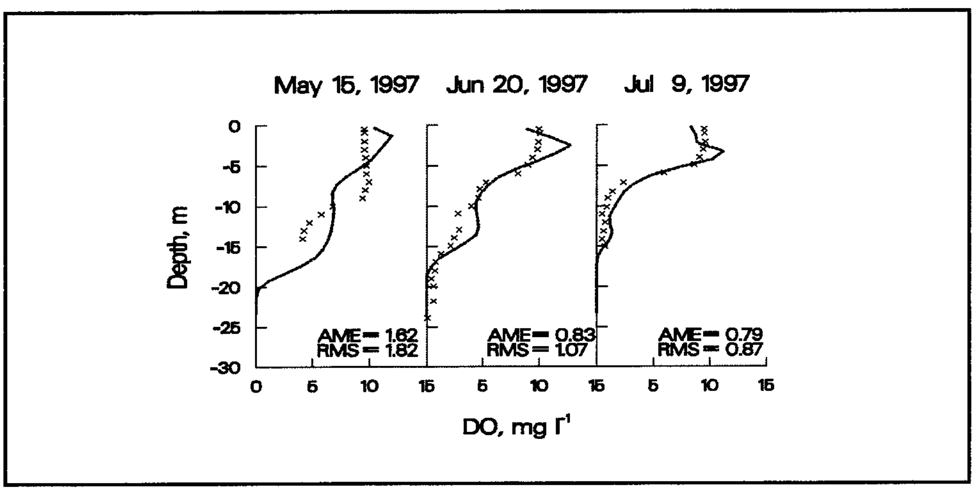

Figure 46. 1997 computed (...) vs. observed (x) DO at station 03

DO predictions for 1996 considerably underestimate epilimnetic concentrations while in 1997 epilimnetic concentrations are overpredicted. Clearly, this is not a problem with the model formulations as there is no consistent bias towards overprediction or underprediction of epilimnetic DO concentrations. The model accurately reproduces epilimnetic DO in 1979, underpredicts it in 1996, and overpredicts it in 1997. Again, this is most likely due to inaccuracies in inflow water quality loadings and their resultant effects on algal production. It should also be pointed out that it is evident from the different epilimnetic DO concentrations for the various calibration years that the model is quite sensitive to differences in loadings between the years.

The model also accurately represents much of the differences in the DO regime between years. The profiles for May and September in 1979 and 1996 are good examples. Differences in the DO regimes between Allatoona and West Point are also well represented.

Nutrients

Results for ammonium, nitrate-nitrite, and dissolved inorganic phosphorus calibration at station 03 are given in Figures 47-55. Results for the other stations are given in Appendix A. As in the Allatoona calibration, the model accurately captures the increase in hypolimnetic ammonium and phosphorus concentrations during summer anoxic conditions and their decrease during fall overturn. With the exception of a few dates, the model is also capturing the trends in nitrate-nitrite. Again, this is thought to be due to the sparseness of boundary condition loadings. However, the model is clearly capturing some of the differences between years (August and September for 1996 and 1997).

Algae

Algal data for West Point were only available for 1979 and 1996. Results are given in Figures 56-77 for stations 10, 07, 05, and 03. Keeping in mind all the problems associated with predicting algal biomass discussed previously for

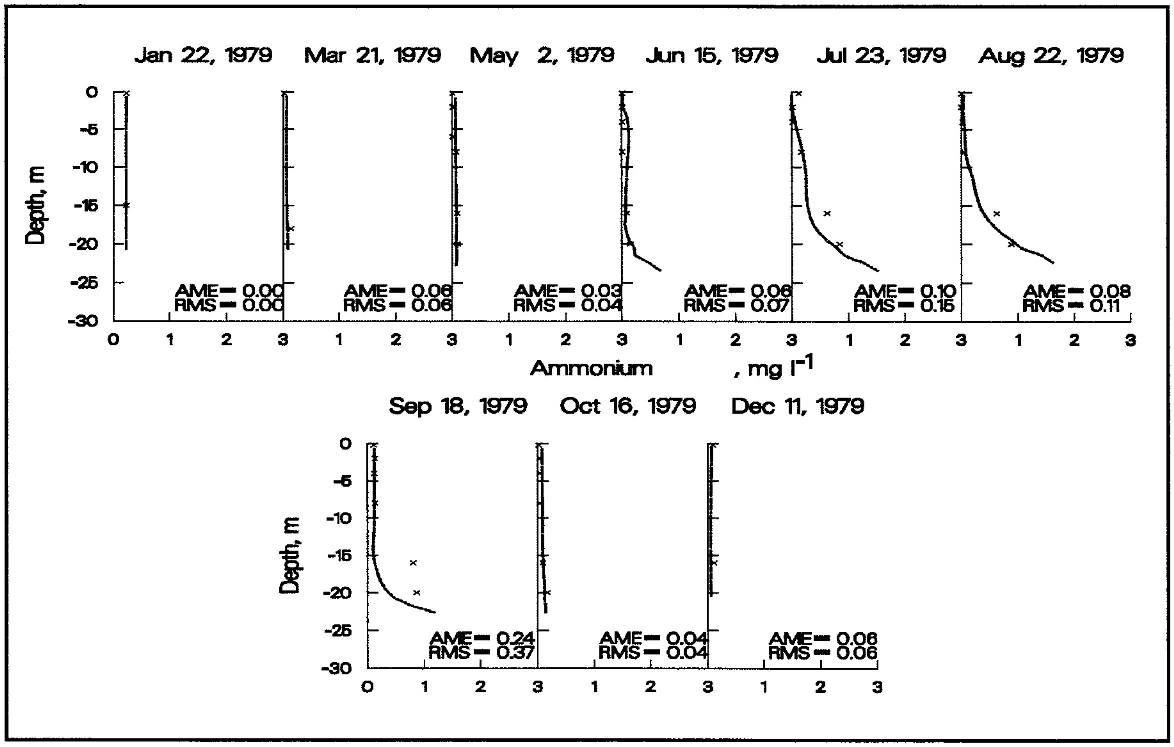

Figure 47. 1979 computed (...) vs. observed (x) ammonium at station 03

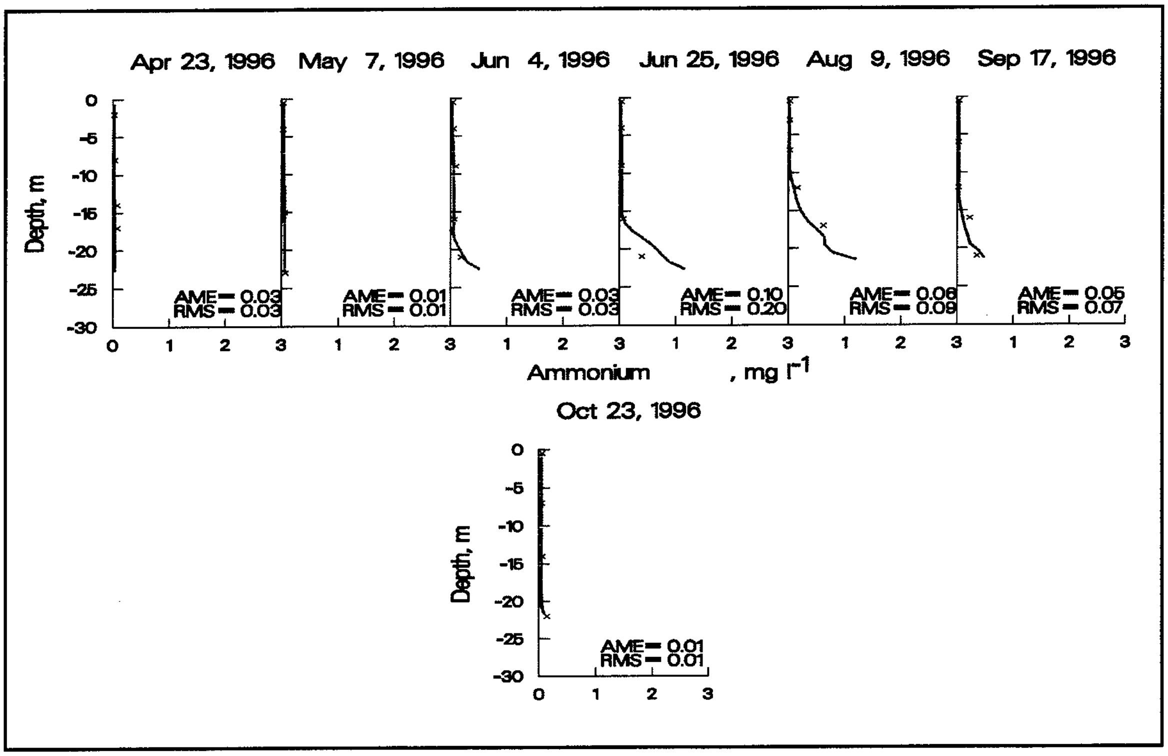

Figure 48. 1996 computed (...) vs. observed (x) ammonium at station 03

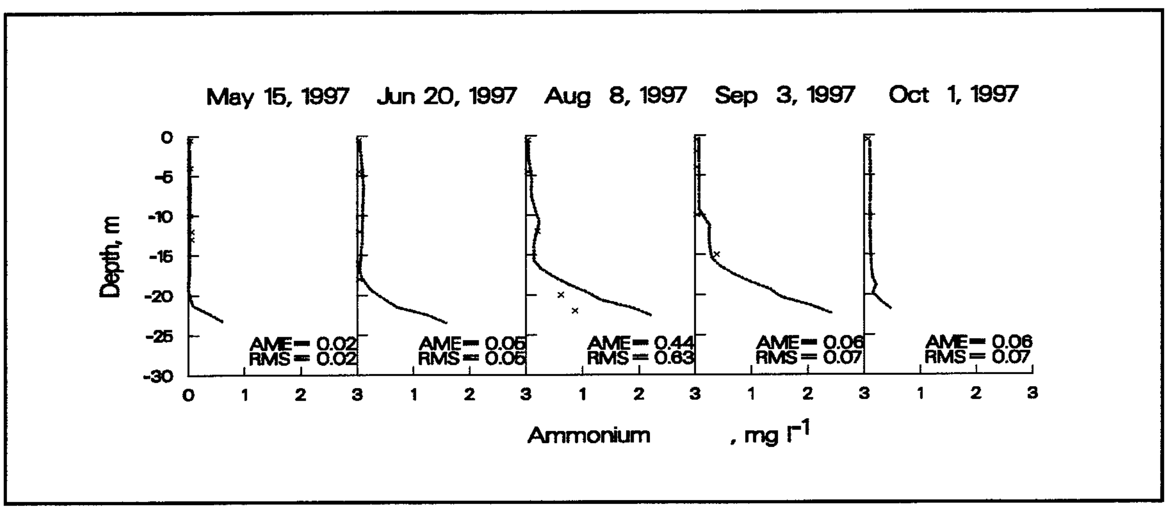

Figure 49. 1997 computed (...) vs. observed (x) ammonium at station 03

Allatoona, the model predictions are at least on the same page as the observed data. Further complicating West Point predictions is the shorter residence time compared to Allatoona. The shorter residence time means that inflow concentrations for algae and nutrients need to be measured more frequently if they are to be accurately reproduced.

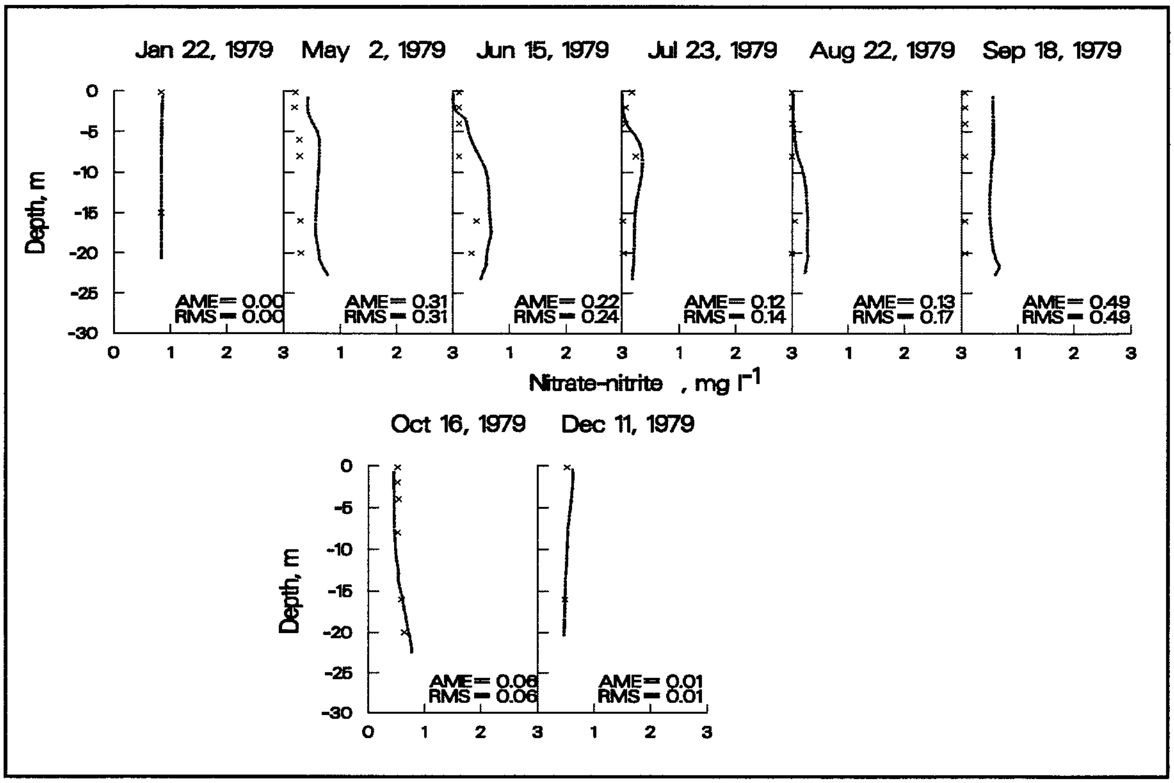

Figure 50. 1979 computed (...) vs. observed (x) nitrate-nitrite at station 03

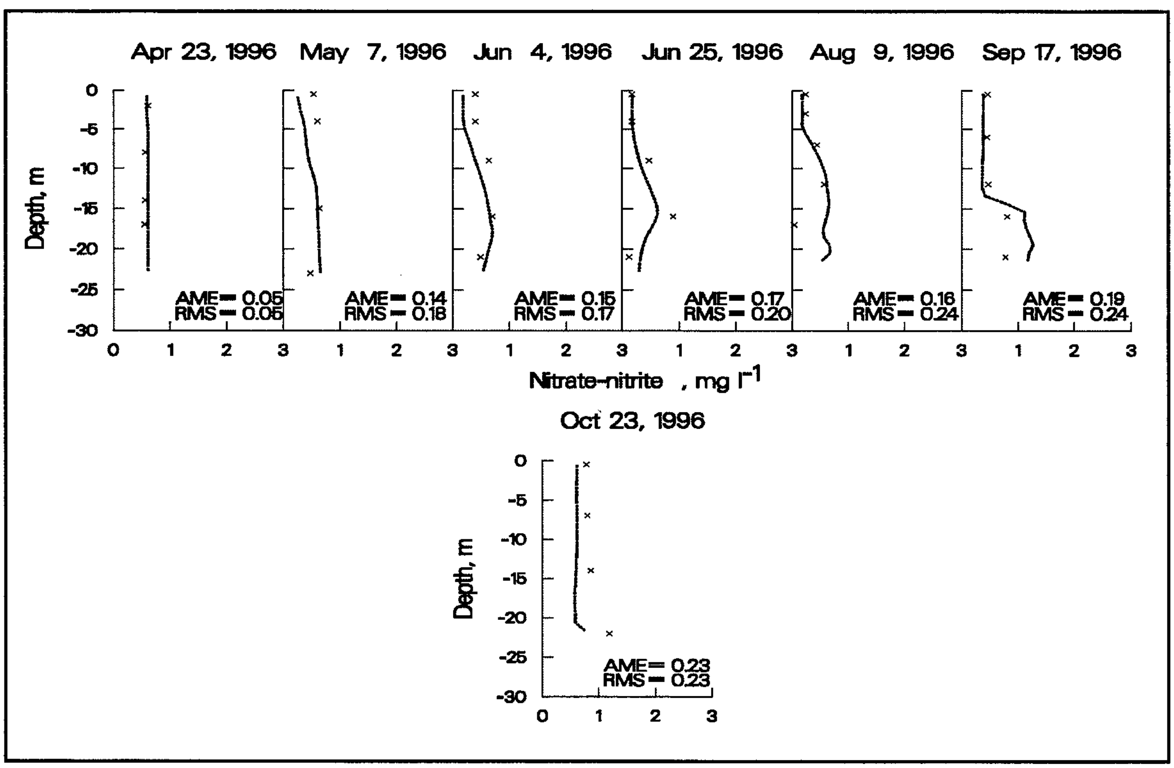

Figure 51. 1996 computed (...) vs. observed (x) nitrate-nitrite at station 03

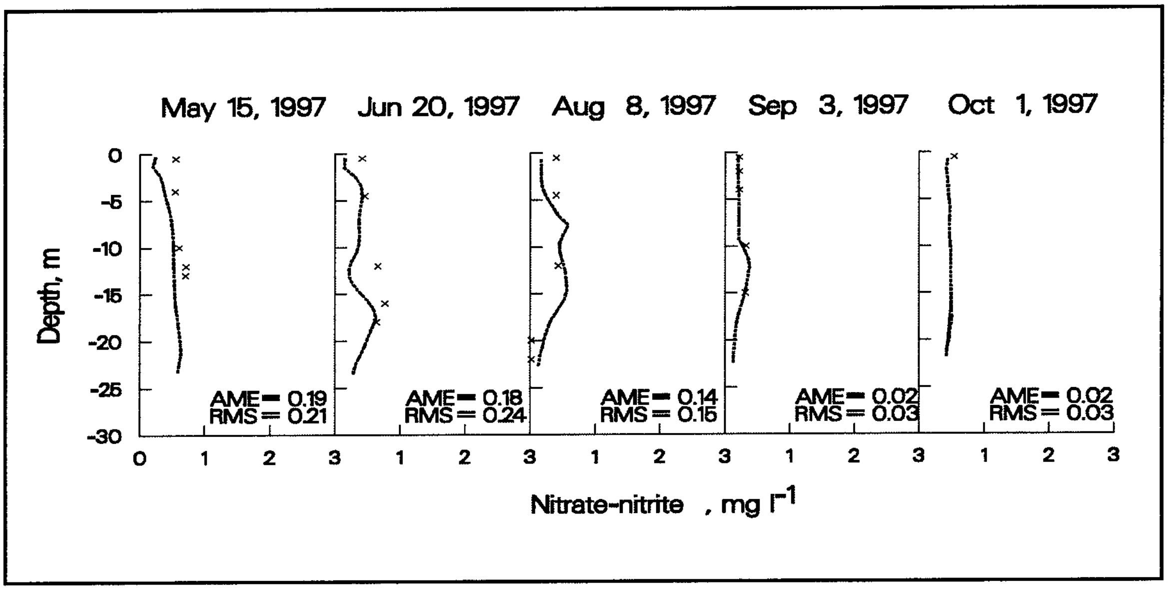

Figure 52. 1997 computed (...) vs. observed (x) nitrate-nitrite at station 03

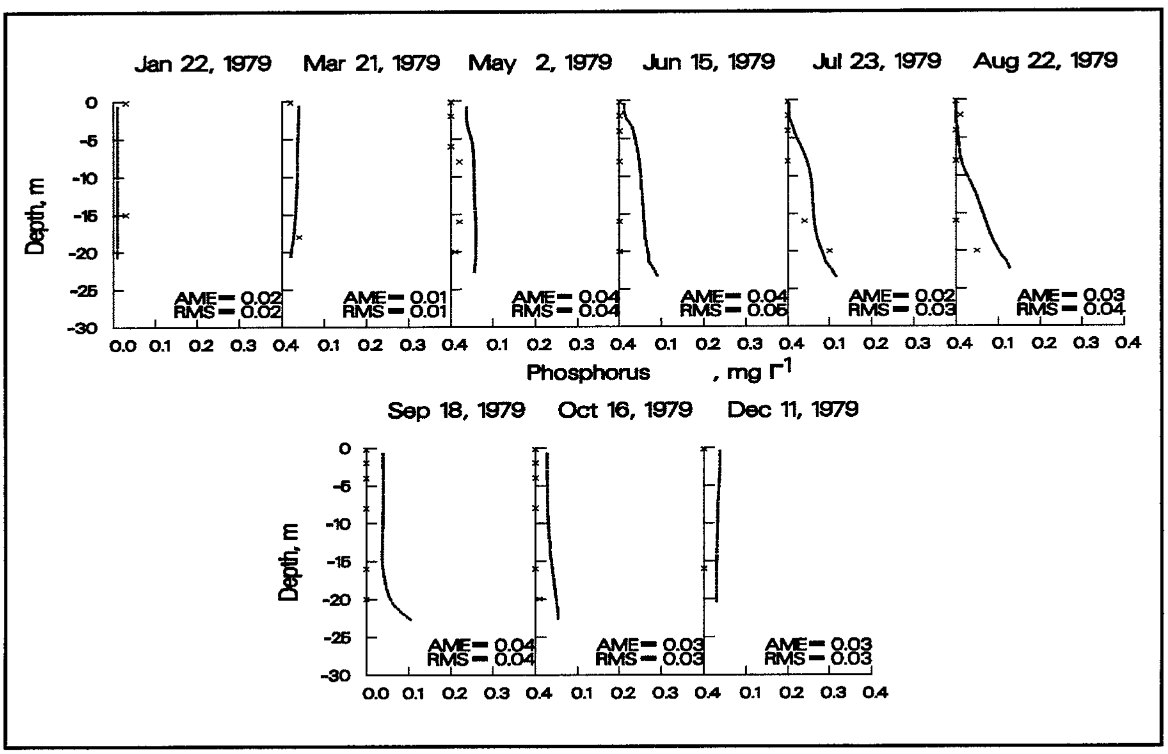

Figure 53. 1979 computed (...) vs. observed (x) phosphorus at station 03

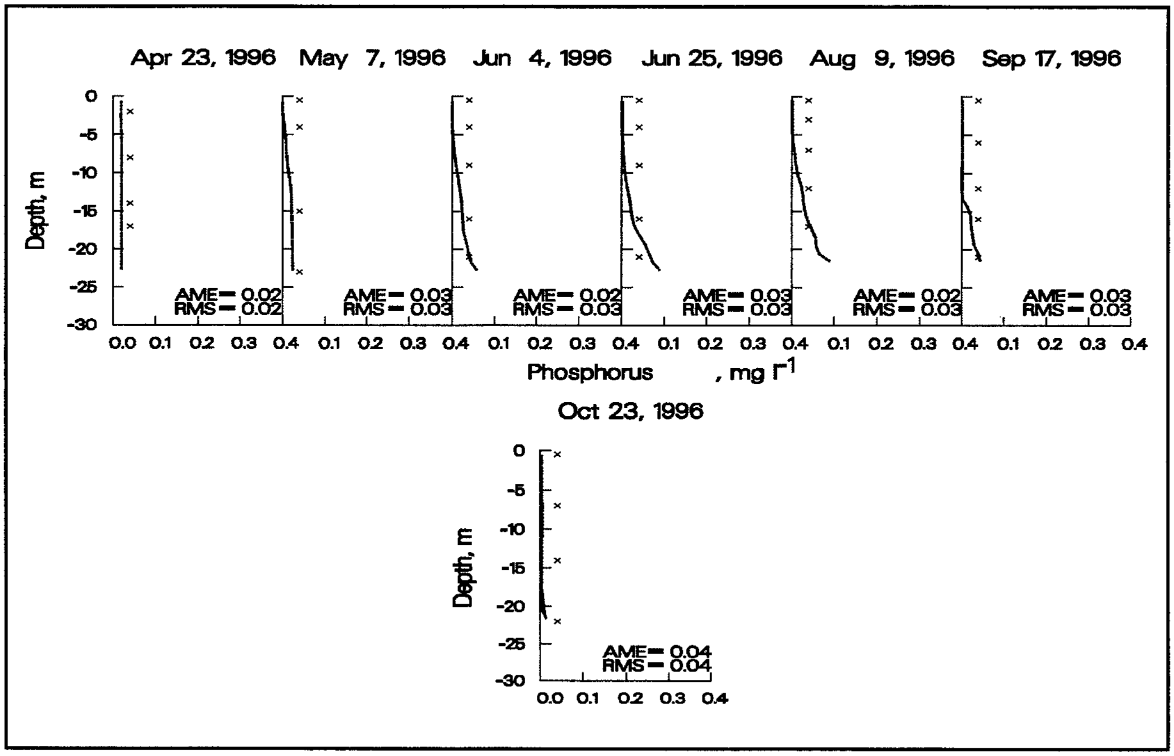

Figure 54. 1996 computed (...) vs. observed (x) phosphorus at station 03

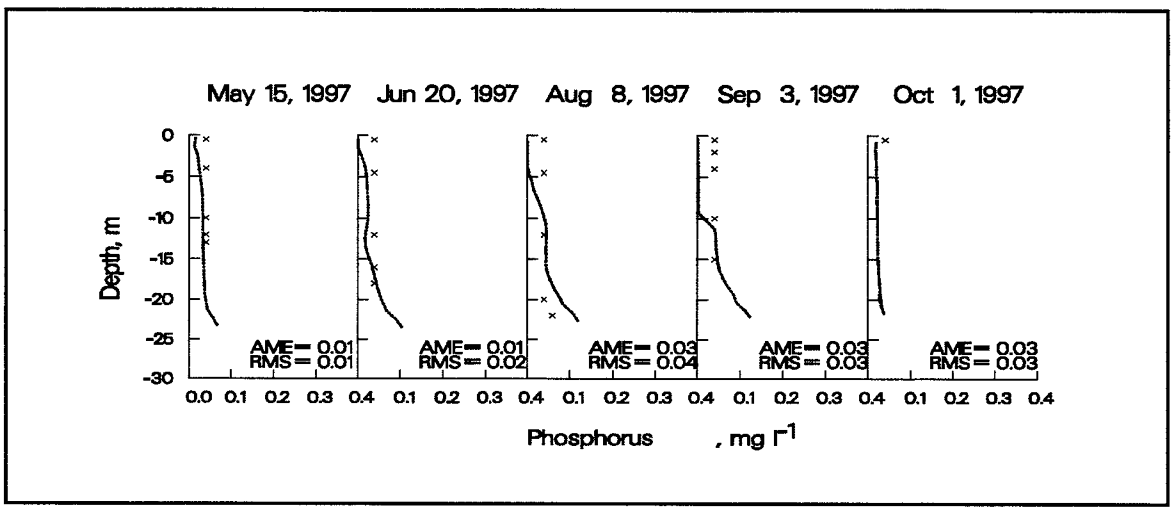

Figure 55. 1997 computed (...) vs. observed (x) phosphorus at station 03

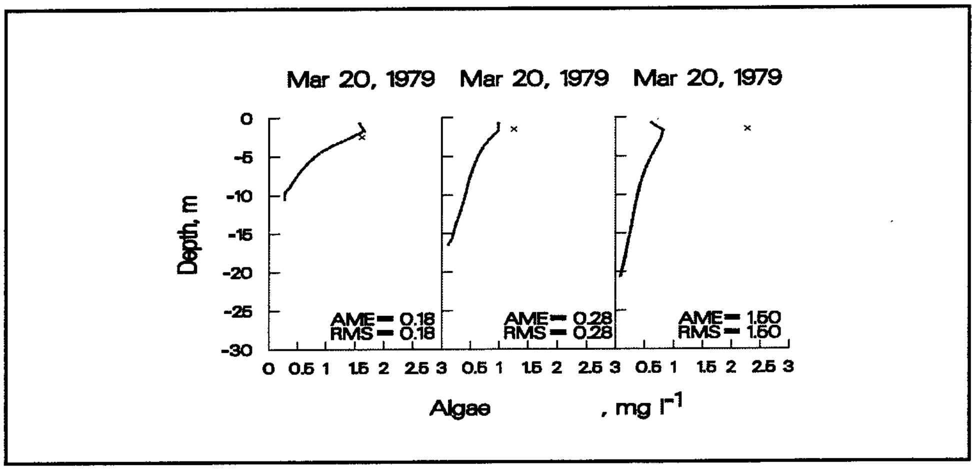

Figure 56. Computed (...) versus observed (x) algal concentrations for stations 10, 05, and 03 for March 20, 1979

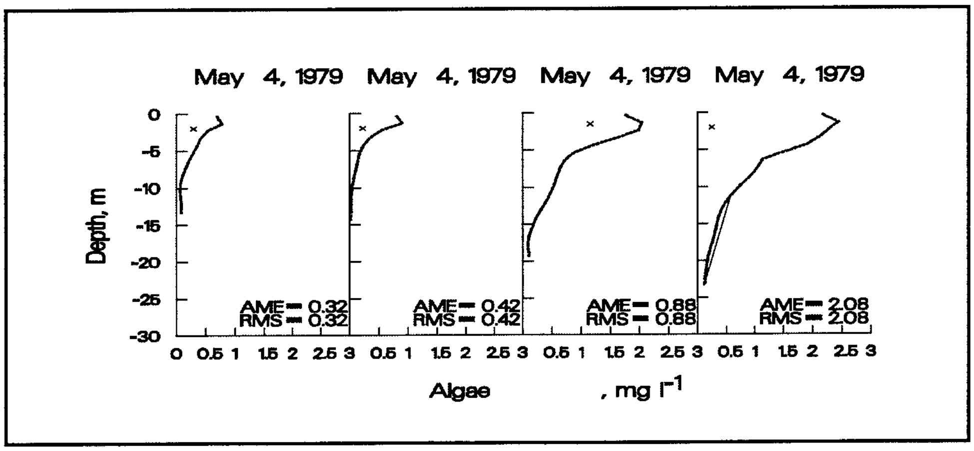

Figure 57. Computed (...) versus observed (x) algal concentrations for stations 10, 07, 05, and 03 for May 4, 1979

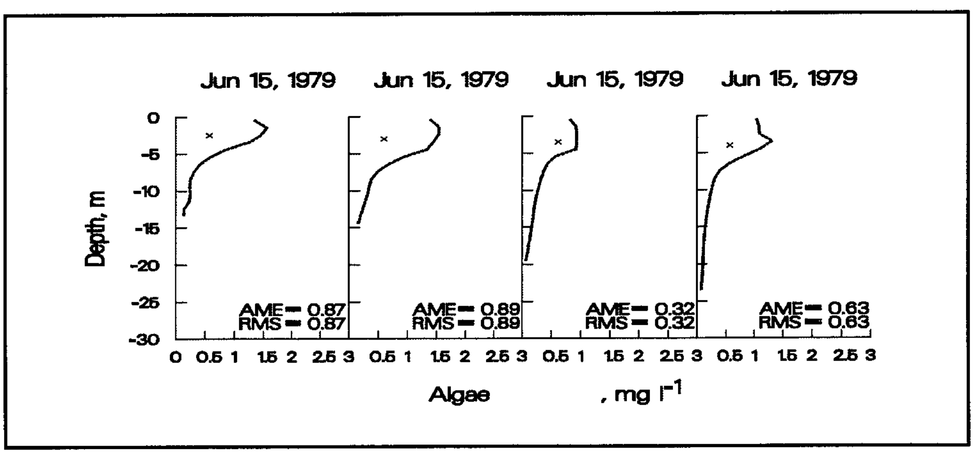

Figure 58. Computed (...) versus observed (x) algal concentrations for stations 10, 07, 05, and 03 for June 15, 1979

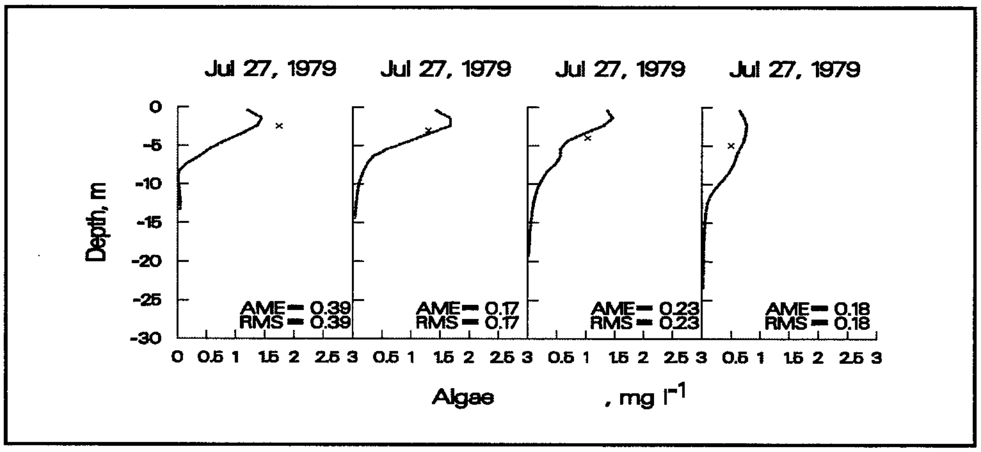

Figure 59. Computed (...) versus observed (x) algal concentrations for stations 10, 07, 05, and 03 for July 27, 1979

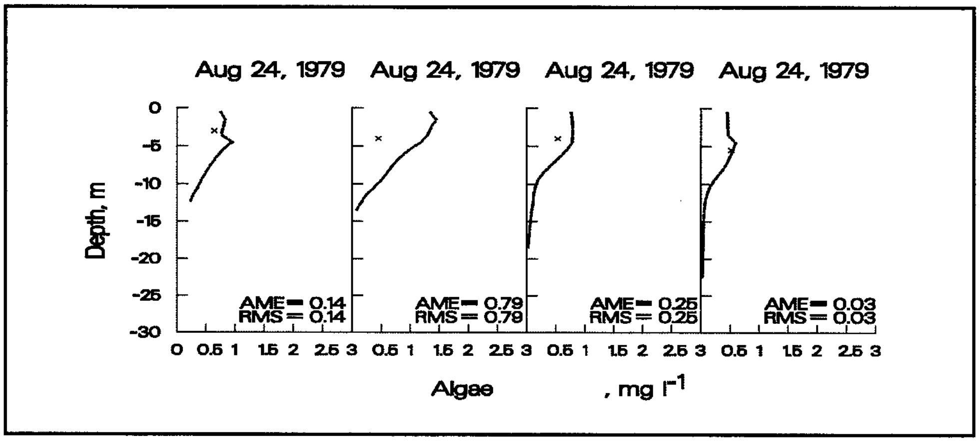

Figure 60. Computed (...) versus observed (x) algal concentrations for stations 10, 07, 05, and 03 for August 24, 1979

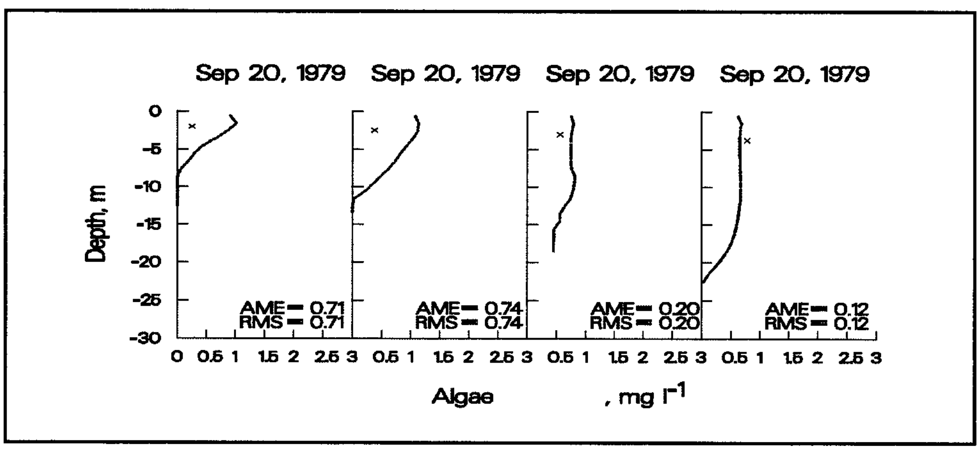

Figure 61. Computed (...) versus observed (x) algal concentrations for stations 10, 07, 05, and 03 for September 20, 1979

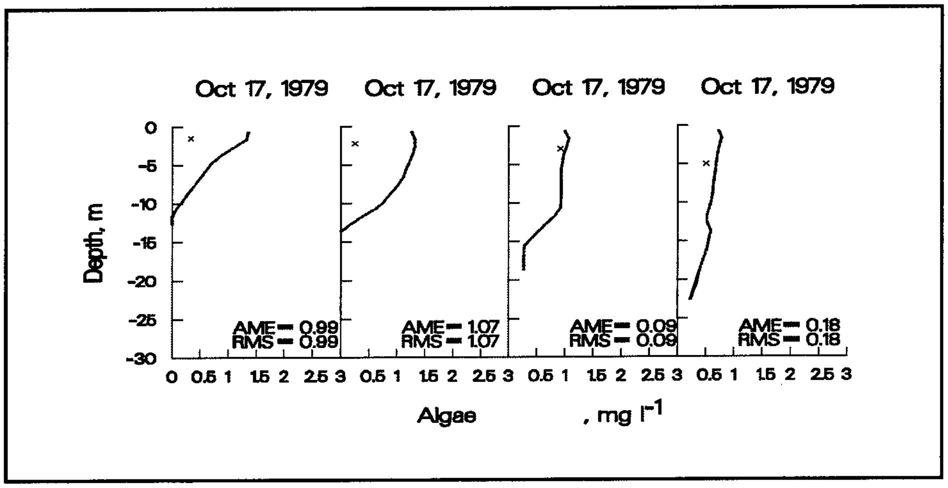

Figure 62. Computed (...) versus observed (x) algal concentrations for stations 10, 07, 05, and 03 for October 17, 1979

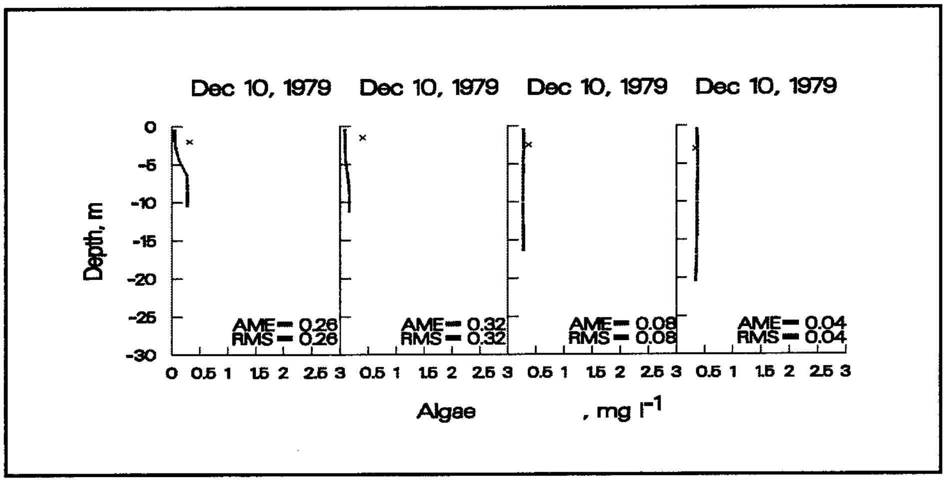

Figure 63. Computed (...) versus observed (x) algal concentrations for stations 10, 07, 05, and 03 for December 10, 1979

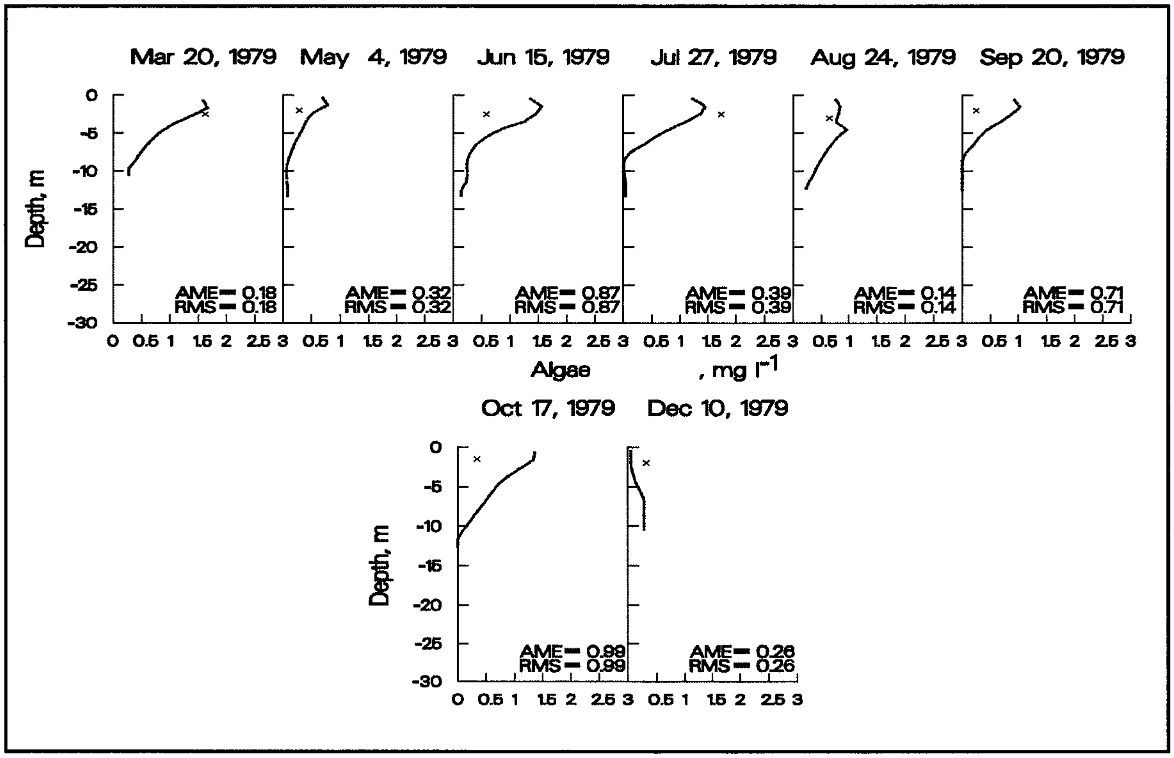

Figure 64. 1979 computed (...) versus observed (x) algal concentrations at station 10 for all observed dates

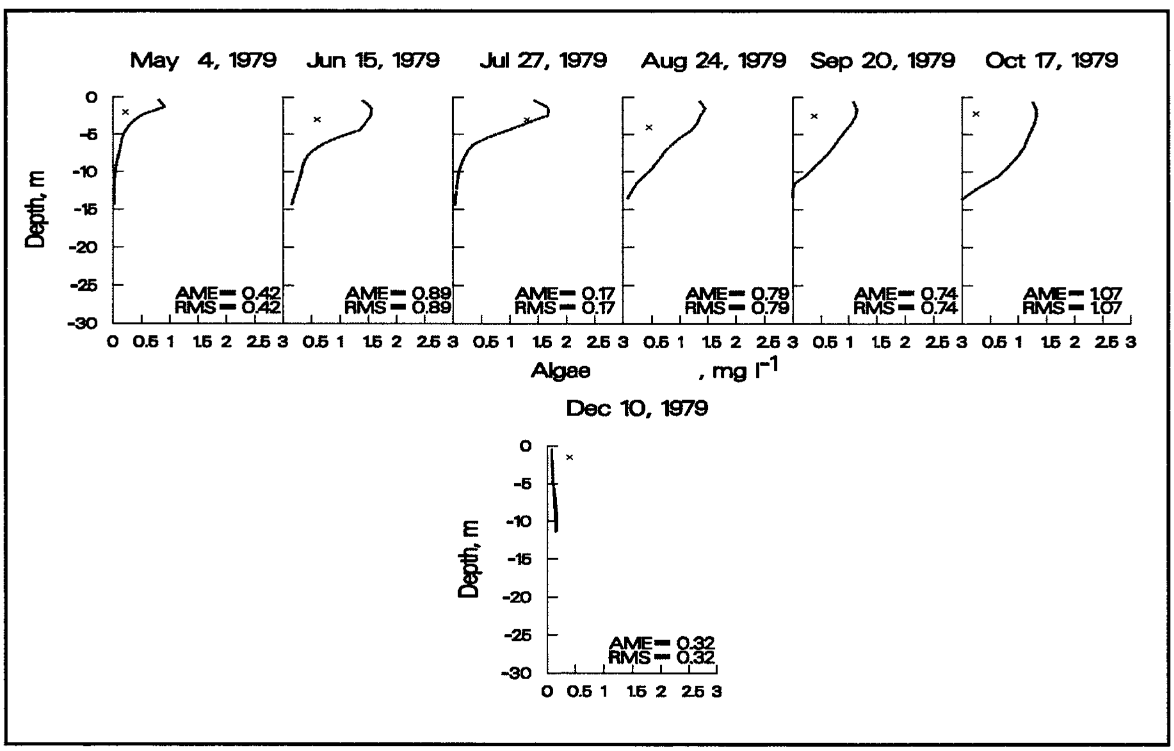

Figure 65. 1979 computed (...) versus observed (x) algal concentrations at station 07 for all observed dates

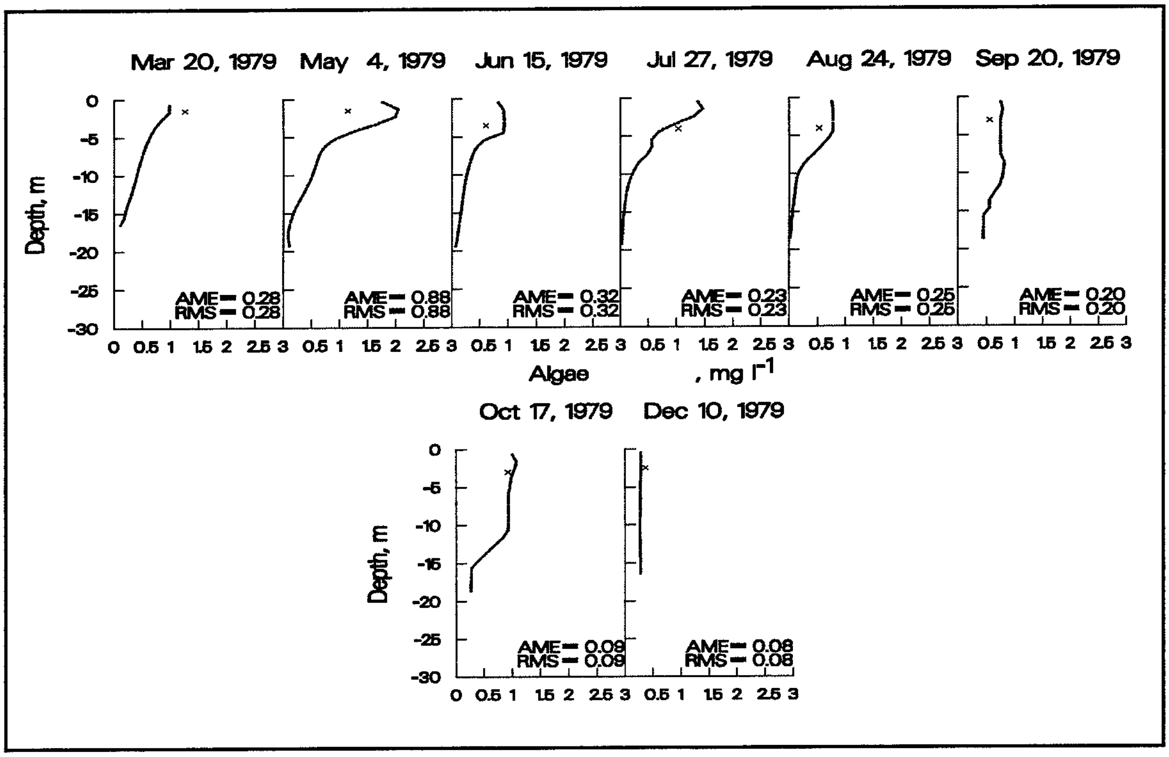

Figure 66. 1979 computed (...) versus observed (x) algal concentrations at station 05 for all observed dates

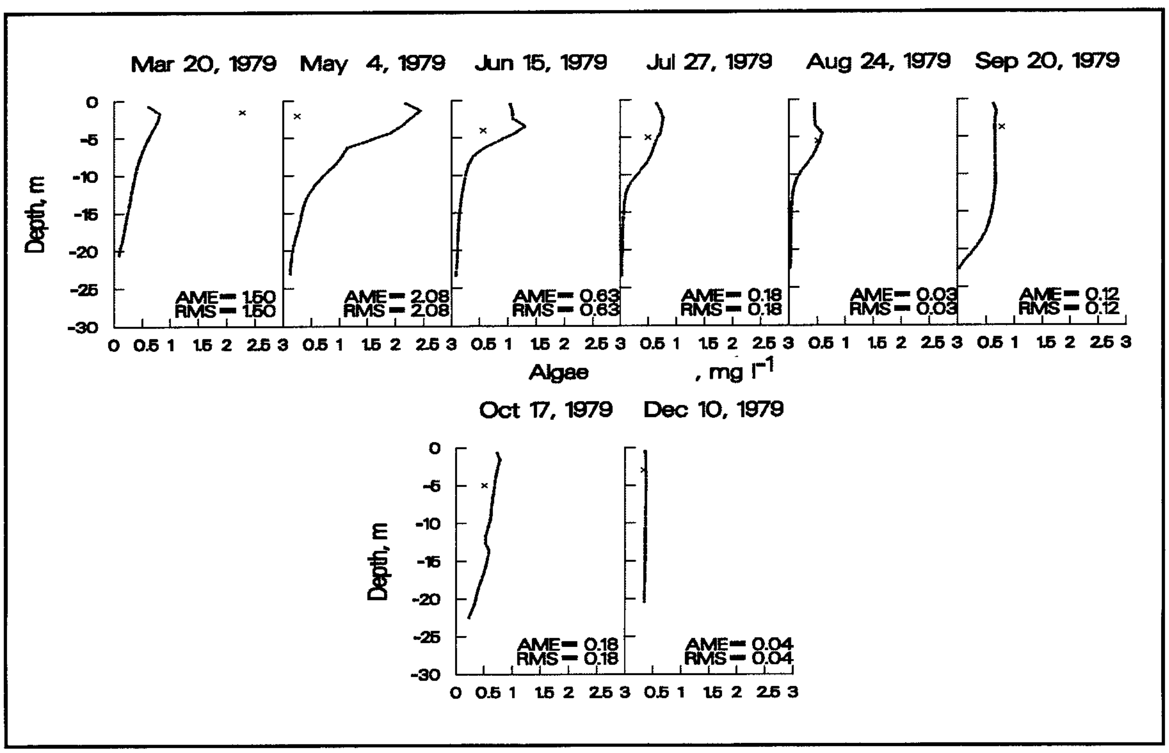

Figure 67. 1979 computed (...) versus observed (x) algal concentrations at station 03 for all observed dates

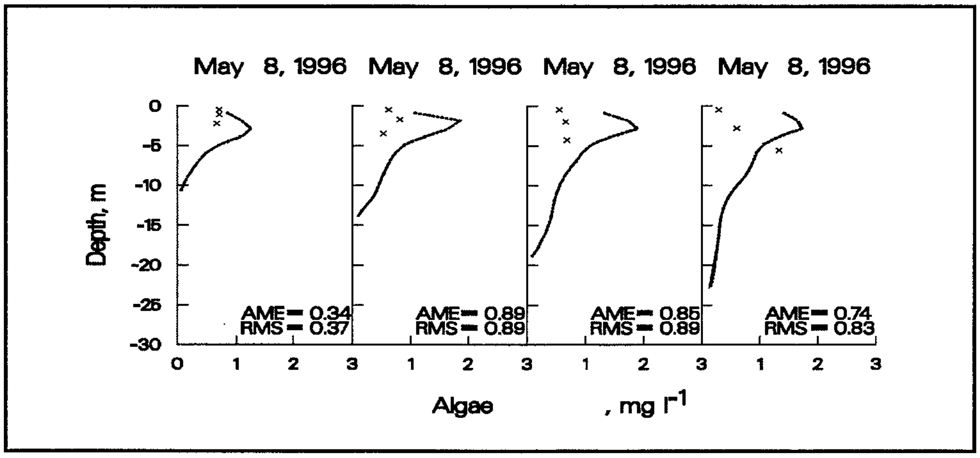

Figure 68. Computed (...) versus observed (x) algal concentrations for stations 10, 07, 05, and 03 for May 8, 1996

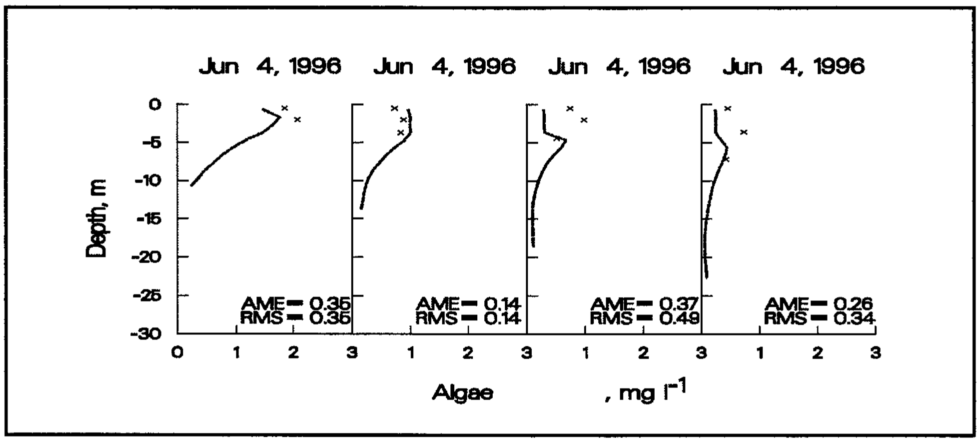

Figure 69. Computed (...) versus observed (x) algal concentrations for stations 10, 07, 05, and 03 for June 4, 1996

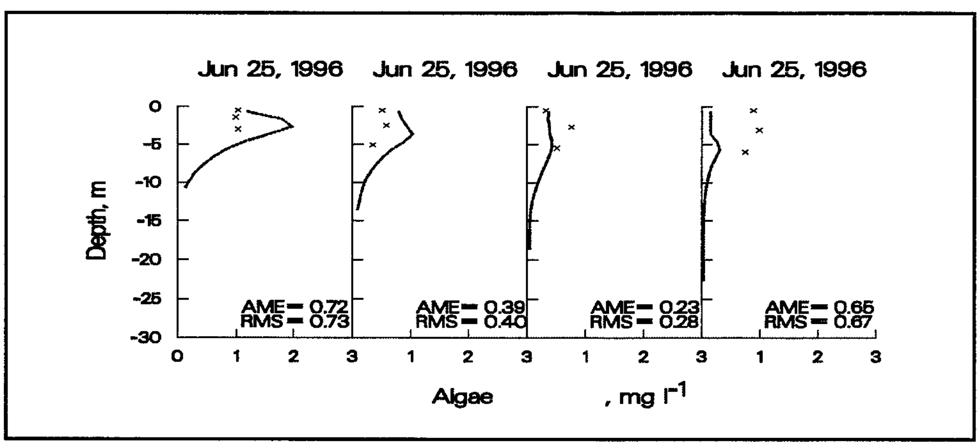

Figure 70. Computed (...) versus observed (x) algal concentrations for stations 10, 07, 05, and 03 for June 25, 1996

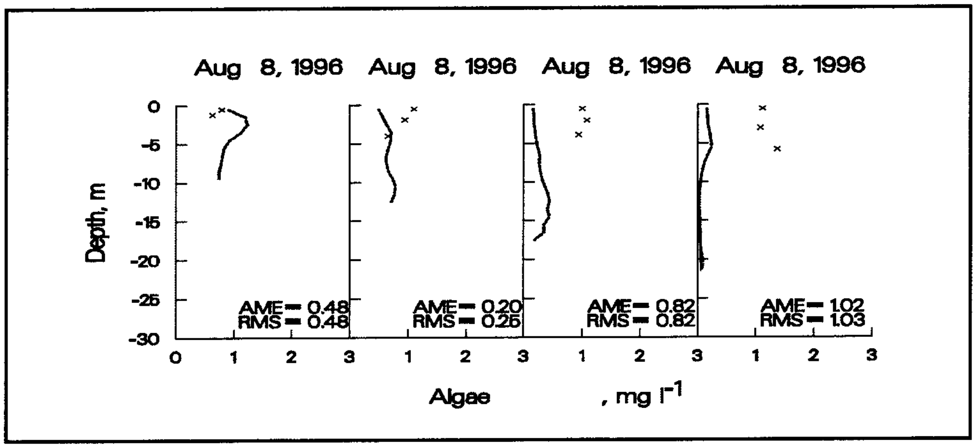

Figure 71. Computed (...) versus observed (x) algal concentrations for stations 10, 07, 05, and 03 for August 8, 1996

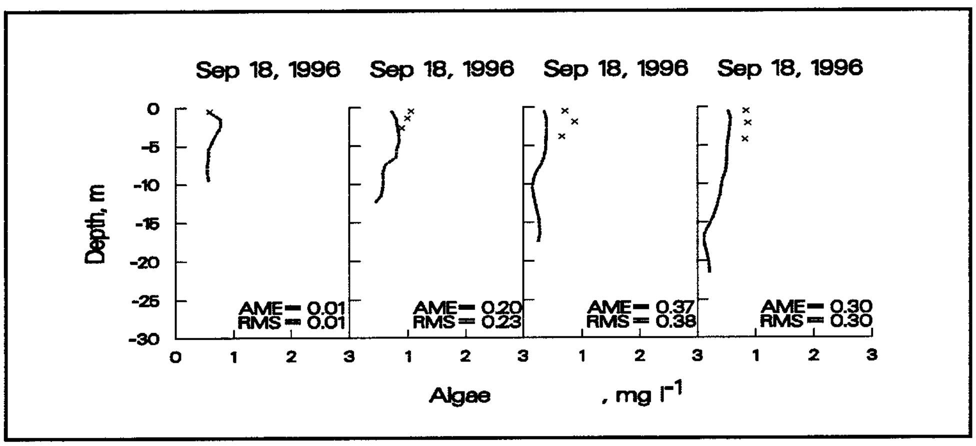

Figure 72. Computed (...) versus observed (x) algal concentrations for stations 10, 07, 05, and 03 for September 18, 1996

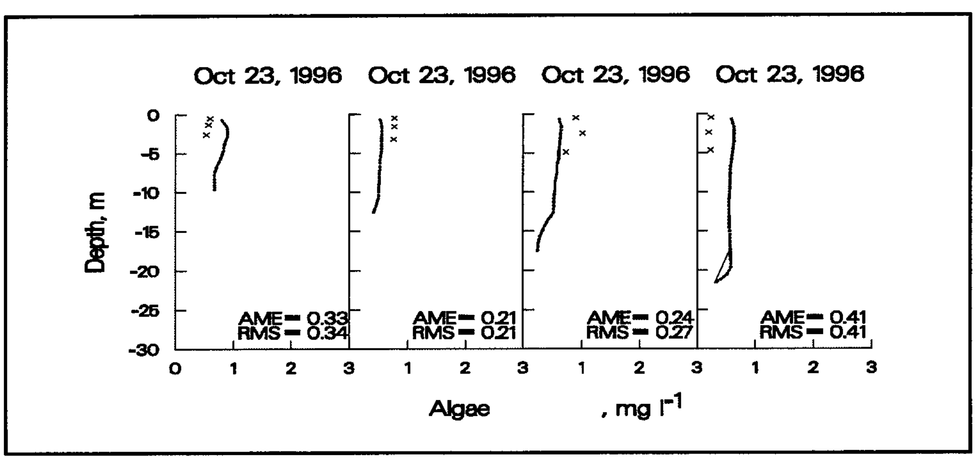

Figure 73. Computed (...) versus observed (x) algal concentrations for stations 10, 07, 05, and 03 for October 23, 1996

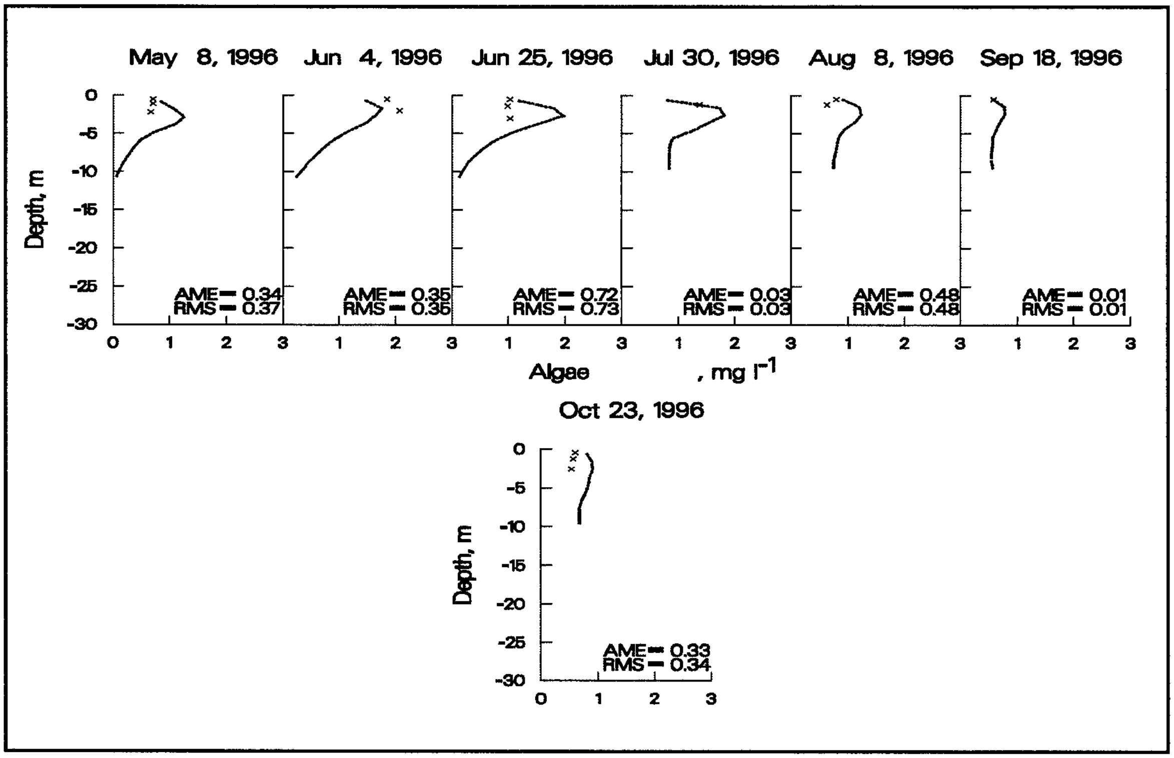

Figure 74. 1996 computed (...) versus observed (x) algal concentrations at station 10 for all observed dates

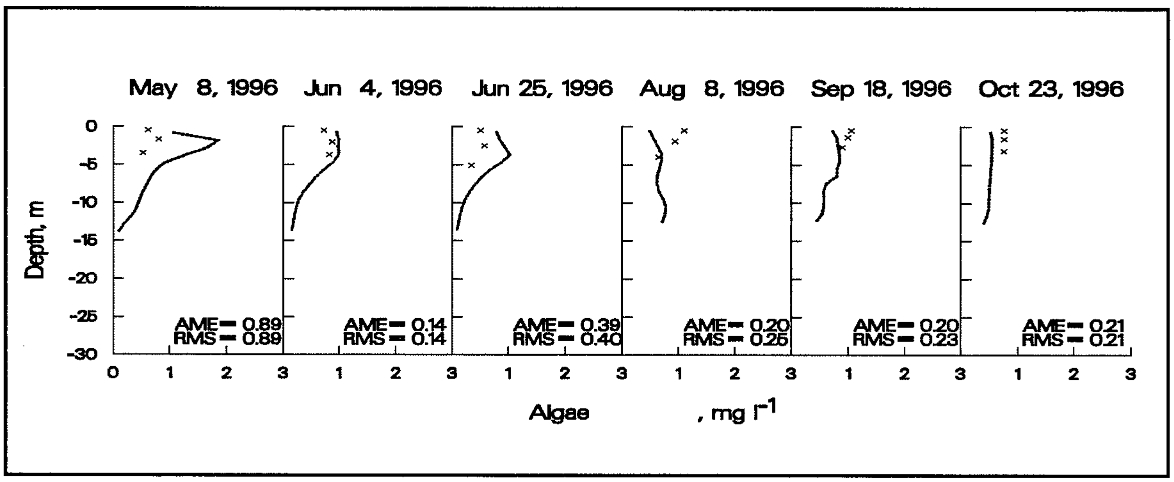

Figure 75. 1996 computed (...) versus observed (x) algal concentrations at station 07 for all observed dates

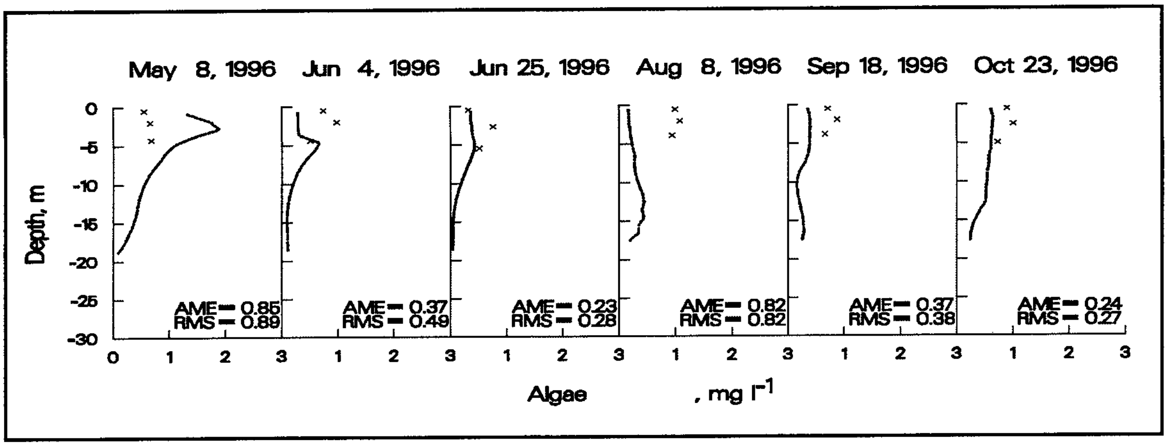

Figure 76. 1996 computed (...) versus observed (x) algal concentrations at station 05 for all observed dates

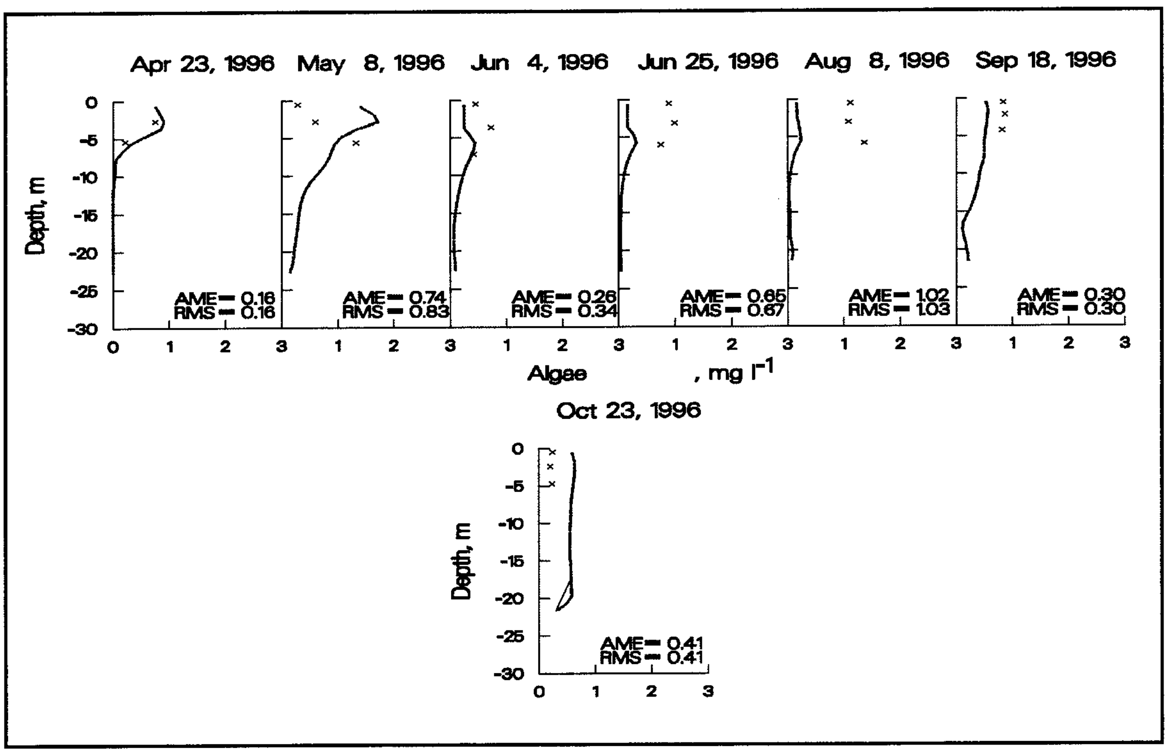

Figure 77. 1996 computed (...) versus observed (x) algal concentrations at station 03 for all observed dates

4 Discussion

A water quality model is a simplified description of what in reality is a very complex world. Numerous problems are associated with numerical water quality models. First, the solutions of the governing equations are only approximations since they cannot be solved analytically. As a result, error is immediately introduced at the start of any model development and subsequent application. Second, simplifying assumptions are normally made about the fully three-dimensional governing equations that may or may not have an effect on the results depending upon the application. In the case of CE-QUAL-W2, the most important assumptions are the lateral averaging, hydrostatic pressure, and the turbulence model. Lastly, model predictions are assumed to be constant for a given model cell, whereas the real world is a continuum of gradients in water quality.

For water quality, the most serious limitation is that the model assumes that only one algal assemblage is sufficient to describe what is occurring over time. Additionally, zooplankton are not modeled, thus eliminating any top-down control of algal standing crop. Carbon is modeled using two DOM fractions and a single fraction for POM, when in reality there are a multitude of carbon forms. Carbon deposition, decay, and subsequent nutrient recycling in the sediments are modeled in a very simplistic manner. Lastly, and probably most importantly, the boundary conditions for water quality are scant at best. This is most important for systems like West Point with a relatively short hydraulic residence time.

Despite all these problems, numerical models have been shown to be one of the most cost-effective tools for managing water quality among our Nation's water resources when used appropriately. For the application of CE-QUAL-W2 to Allatoona and West Point, the model accurately captured their thermal regimes. Dissolved oxygen and nutrients were also well represented by the model.

The largest discrepancies were in comparisons of observed and computed algal concentrations. Factors contributing to this discrepancy are the use of one algal compartment, no zooplankton compartment, and sparse data for inflow concentrations of algae and nutrients. However, for both reservoirs, the model was able to capture the spatial trend going from upstream to downstream for many of the sampling dates. Also keep in mind that much of the observed data were a mixture over the photic zone depth and model results are an approximation to a mixture over the photic zone.

The overpredictions of algal biomass in early spring could have been due to carbon to chlorophyll ratios used in converting model output (grams organic matter dry weight) to measured chl*a* data. If the dominant algal group in the spring was diatoms, then the C:chl*a* ratio in the prototype would be much lower than what was used in the model. Using a more appropriate value for diatoms would bring the predictions much closer to observed values while still retaining the model's ability to capture the spatial trends.

5 Conclusions

CE-QUAL-W2 has been calibrated for temperature and algal/nutrient/DO interactions for Allatoona and West Point Reservoirs. When using the calibrated model as a management tool, one would have the most confidence using the model to investigate how operational changes would affect temperature and water quality – particularly DO. The model accurately captures the physics of both reservoirs. Any alteration in the physics should be predicted with a high degree of accuracy.

Although the model is not as accurate regarding its representation of algal dynamics, the model is responsive to changes in loadings as is evidenced by the different behavior of the model's algal predictions for different calibration years. When used to address reductions in nutrient loadings, the model would provide a worst-case scenario since the model does not include a sediment diagenesis compartment that keeps track of nutrient delivery, transformation, and subsequent release back into the water column. Thus, the long-term removal of nutrients from internal recycling is not modeled. Conversely, when evaluating the effects of increased nutrient loadings, the model would provide a best-case scenario since an increase in internal nutrient recycling would not be represented.

As with nearly every water quality model study, the most serious shortcoming of the present calibration is lack of loading information sufficient to have a high level of confidence that the model is accurately reproducing the observed data. However, one important point to keep in mind is that these results were obtained for four calibration years for Allatoona and three calibration years for West Point. Additionally, none of the kinetic coefficients differed between the two reservoirs except for sediment nutrient release rates, nitrate decay, and sediment oxygen demand. Kinetic coefficients that did not vary between reservoirs used the default values. These are the same values used in the application of the model to Weiss, Neely Henry, and Walter F. George for the Alabama-Coosa-Tallapoosa/ Apalachicola-Chattahoochee-Flint study. The results were obtained with an absolute minimum of "curve fitting" (Tillman, Cole, and Bunch 1999).

Depending upon the amount of scrutiny that the model application will receive, it may be prudent to collect an additional year's worth of data with the sampling designed specifically to provide the necessary information to support the model – particularly for the algal compartment. This would primarily entail obtaining more frequent inflow and outflow boundary conditions and delineation of the dominant algal populations over the growing season. The next version of the model will include the ability to model any number of algal groups.

References

American Public Health Association, American Water Works Association, and Water Pollution Control Federation. (1985). *Standard methods for the examination of water and wastewater. 16th ed.,* Washington, DC.

Brown, L. C., and Barnwell, T. O., Jr. (1987). "The enhanced stream water quality models QUAL2E and QUAL2E-UNCAS: Documentation and user manual," Environmental Research Laboratory, Office of Research and Development, U.S. Environmental Protection Agency, Athens, GA.

Cole, T. M., and Buchak, E. M. (1995). "CE-QUAL-W2: A two-dimensional, laterally averaged, hydrodynamic and water quality model, Version 2.0," Instruction Report EL-95-1, U.S. Army Engineer Waterways Experiment Station, Vicksburg, MS.

Georgia Department of Natural Resources. (1993). "Water quality investigation of West Point Lake study, 1993 Report," Water Quality Management Program, Atlanta, GA.

Kennedy, R. H. (1994). "Limnological assessment of West Point Lake, Georgia," Technical Report EL-94-6, U.S. Army Engineer Waterways Experiment Station, Vicksburg, MS.

Radtke, D. B., Buell, G. R., and Perlman, H. A. (1984). "Water quality management studies: West Point Lake, Chattahoochee River, Alabama-Georgia, April 1978–December 1979," Report prepared for U.S. Army Engineer District, Mobile, Environmental Quality Section, Mobile, AL.

Tillman, D. H., Cole, T. M., and Bunch, B. W. (1999). "Detailed reservoir water quality modeling (CE-QUAL-W2), Alabama-Coosa-Tallapoosa/Apalachicola-Chattahoochee-Flint (ACT/ACF) comprehensive water resource study," Report prepared for U.S. Army Engineer District, Mobile, AL.

Appendix A
Temporal and Spatial Trends in Water Quality

The following plots are included to provide a complete assessment of how well the model is capturing temporal and spatial trends in the water quality data. Two types of plots are presented. The first type of plot includes all the dates at one station location to allow assessment of the model's ability to reproduce temporal trends in water quality at the given station. The second type of plot includes all the mainstem stations on a given date in order to allow assessment of the model's ability to reproduce spatial trends in water quality.

Temperature

Allatoona

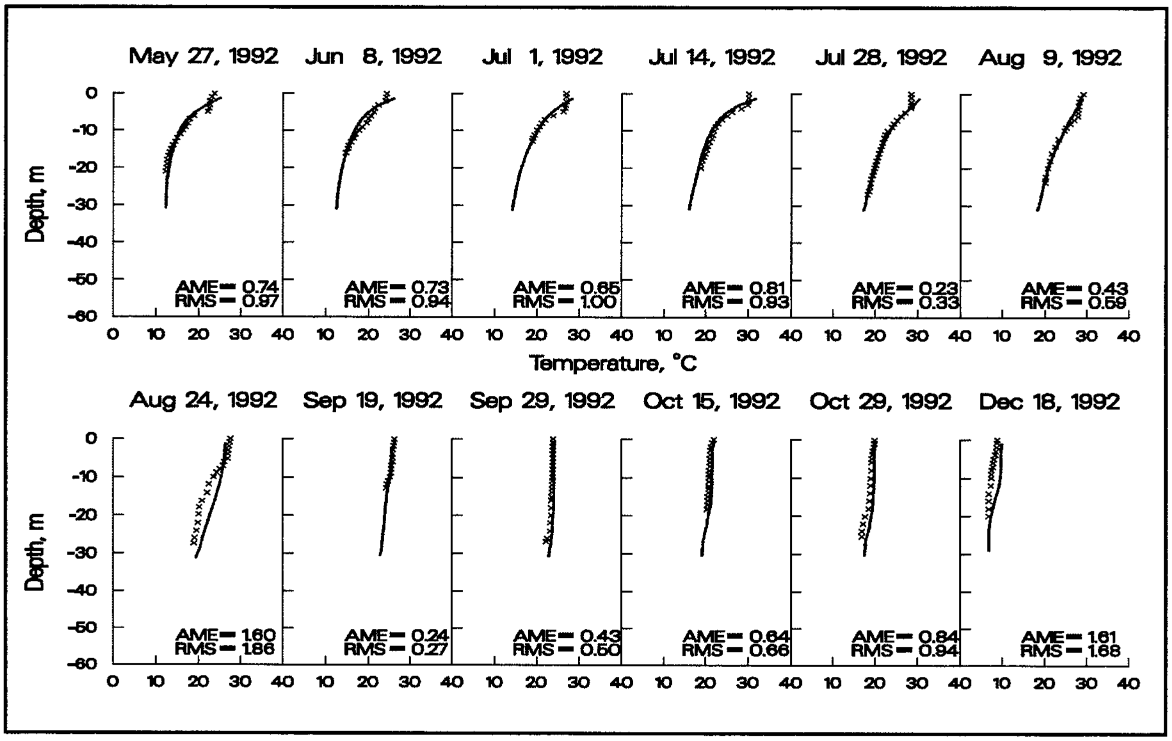

Figure A1. 1992 Allatoona Reservoir computed (...) versus observed (x) temperatures for station 03

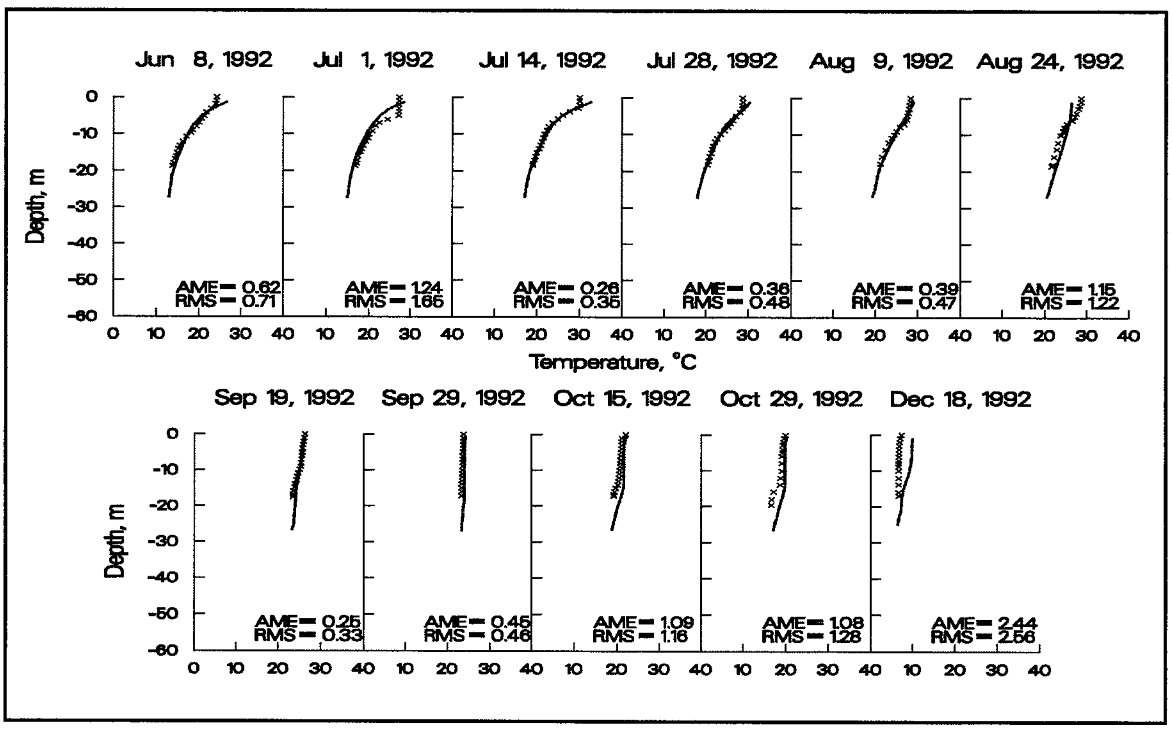

Figure A2. 1992 Allatoona Reservoir computed (...) versus observed (x) temperatures for station 09

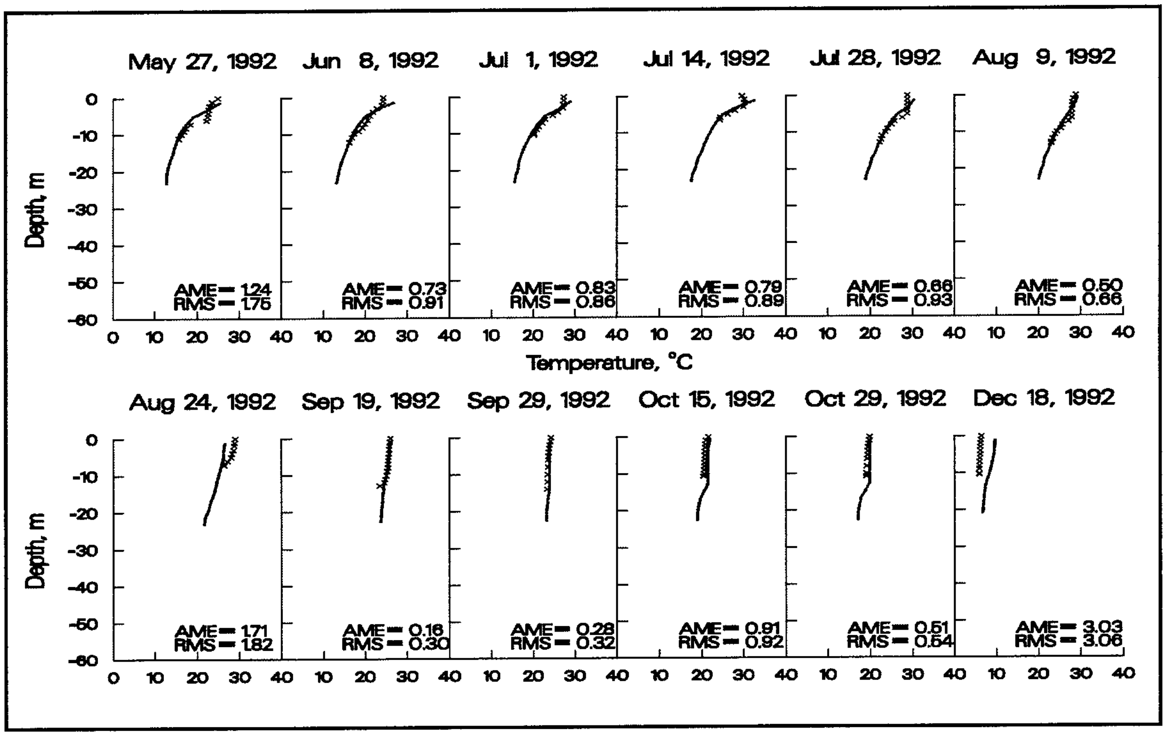

Figure A3. 1992 Allatoona Reservoir computed (...) versus observed (x) temperatures for station 18

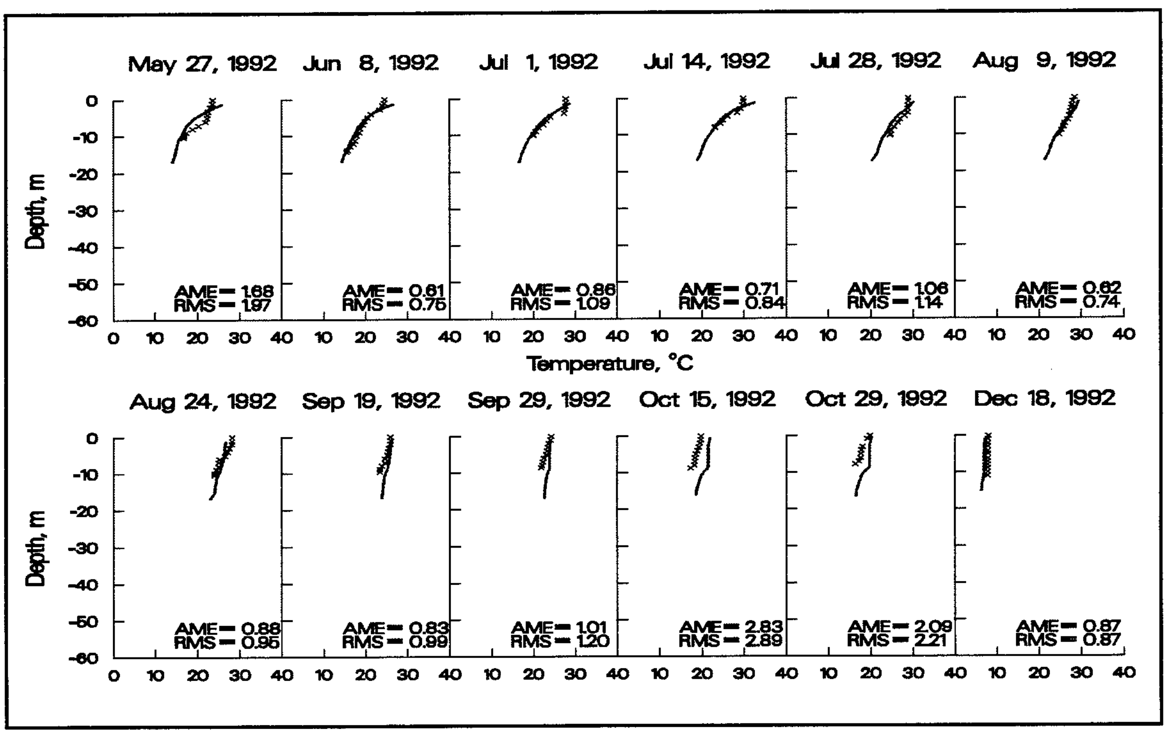

Figure A4. 1992 Allatoona Reservoir computed (...) versus observed (x) temperatures for station 39

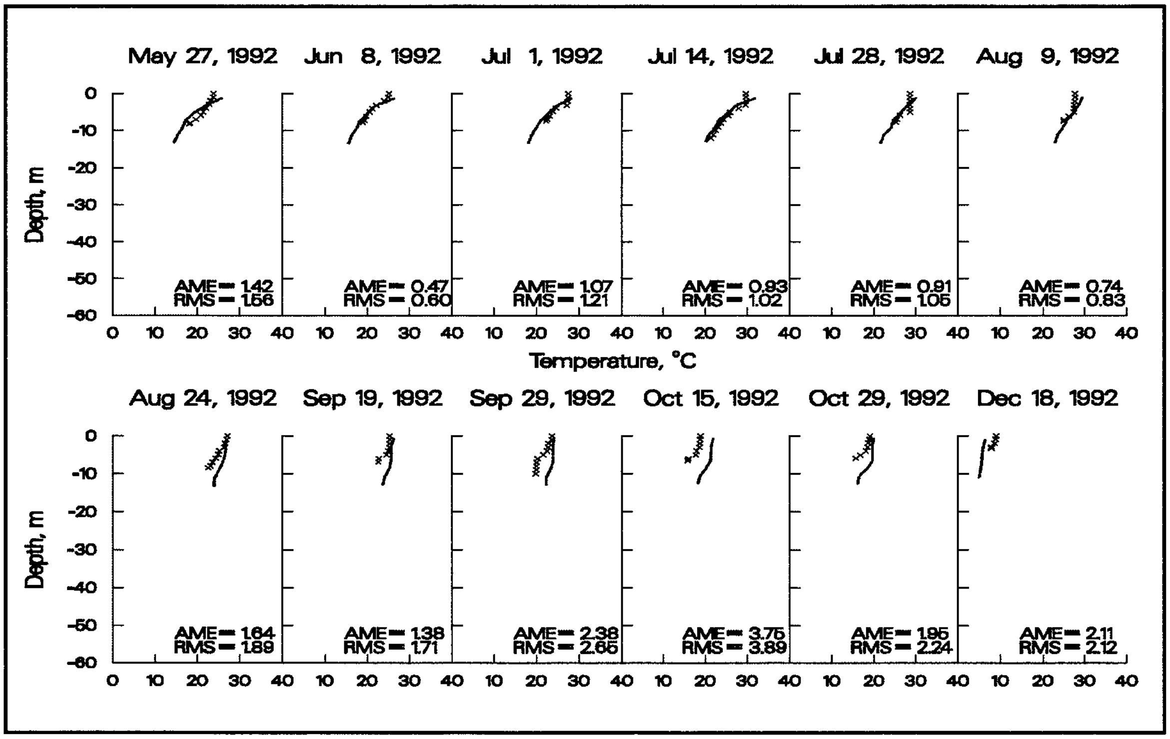

Figure A5. 1992 Allatoona Reservoir computed (...) versus observed (x) temperatures for station 45

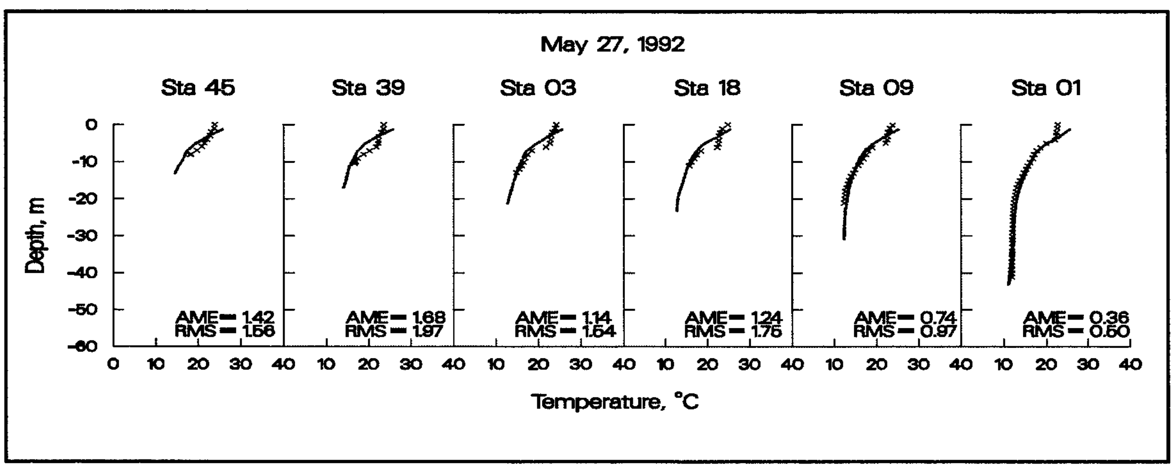

Figure A6. 1992 Allatoona Reservoir computed (...) versus observed (x) temperatures for stations along the mainstem, May 27

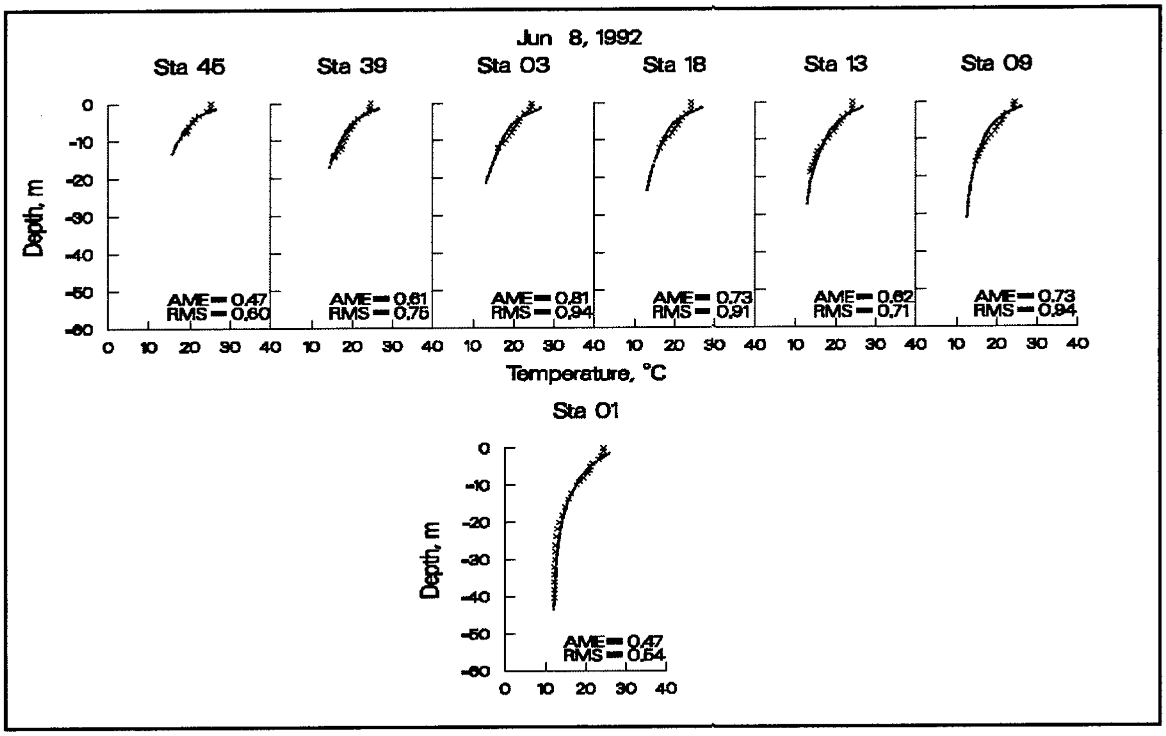

Figure A7. 1992 Allatoona Reservoir computed (...) versus observed (x) temperatures for stations along the mainstem, June 8

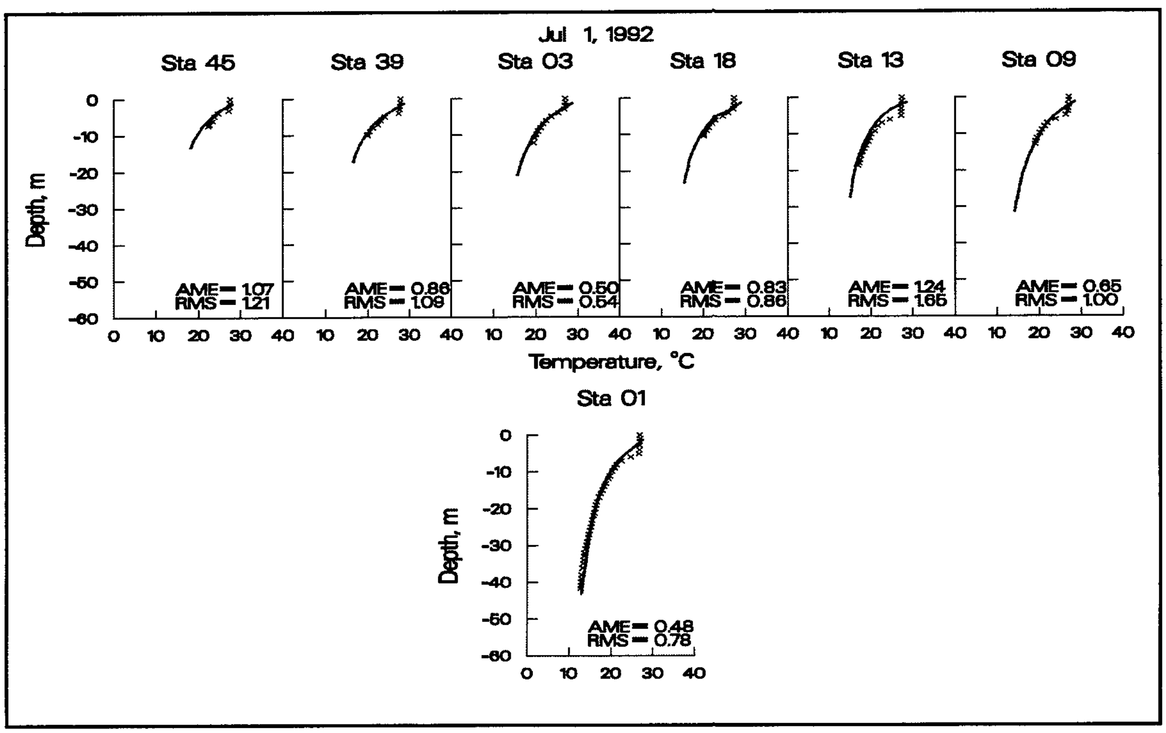

Figure A8. 1992 Allatoona Reservoir computed (...) versus observed (x) temperatures for stations along the mainstem, July 1

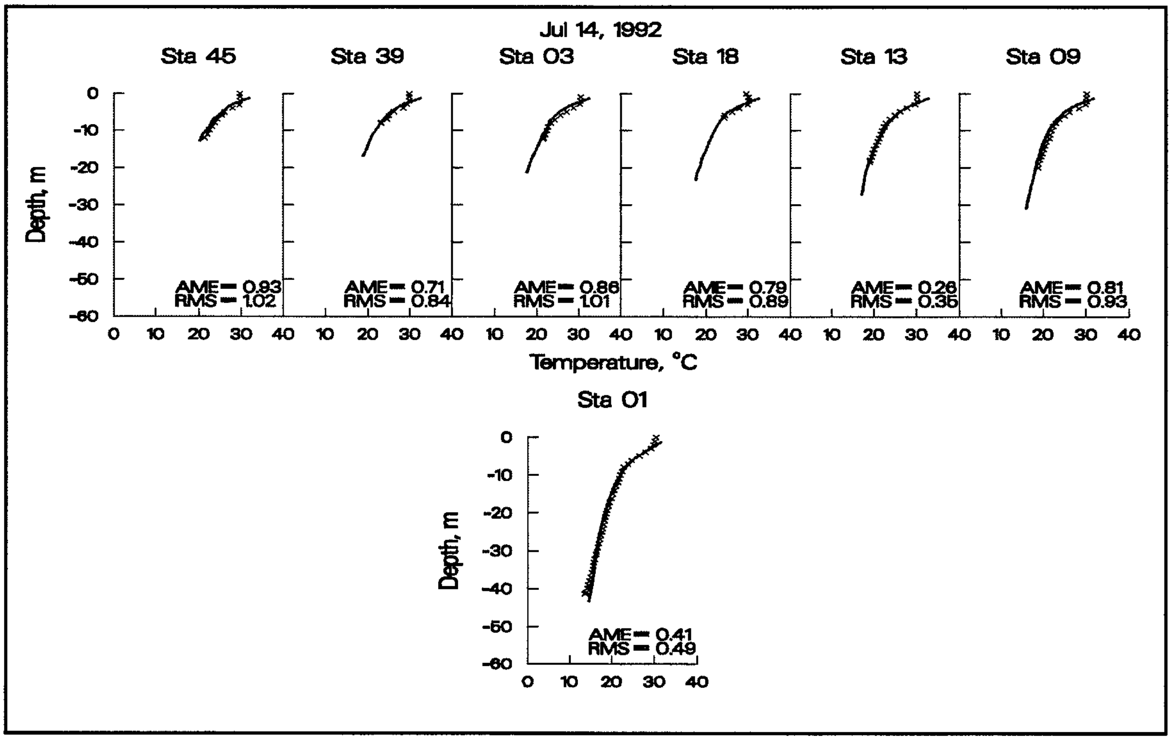

Figure A9. 1992 Allatoona Reservoir computed (...) versus observed (x) temperatures for stations along the mainstem, July 14

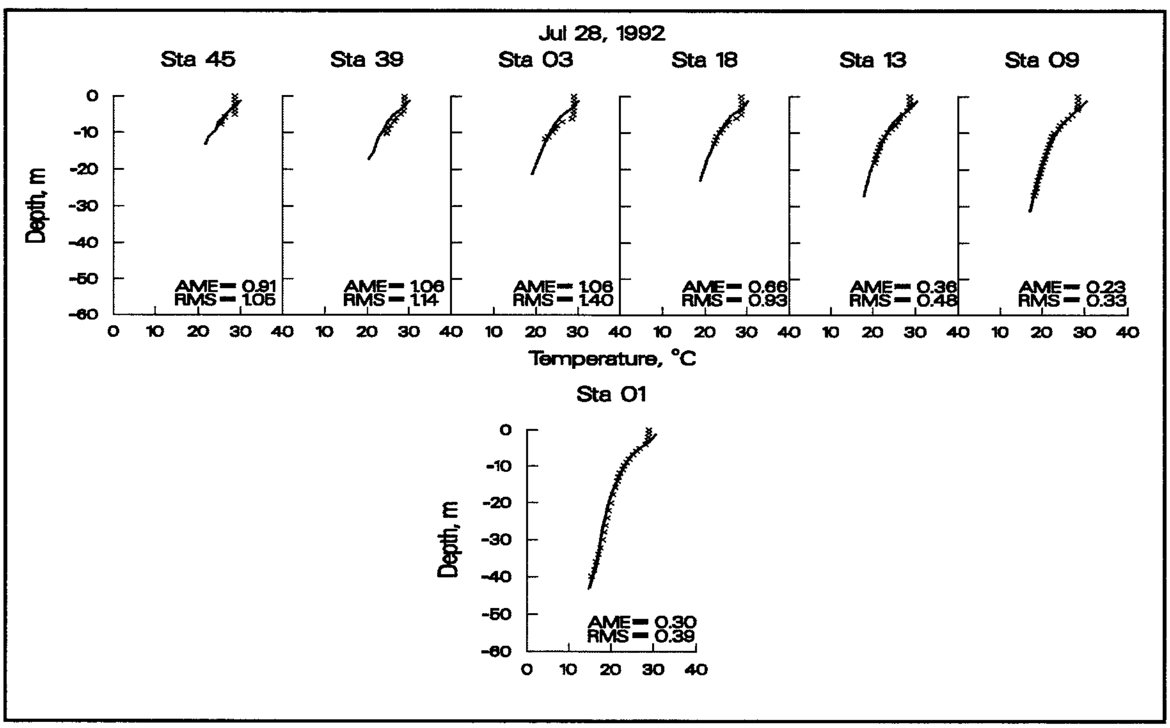

Figure A10. 1992 Allatoona Reservoir computed (...) versus observed (x) temperatures for stations along the mainstem, July 28

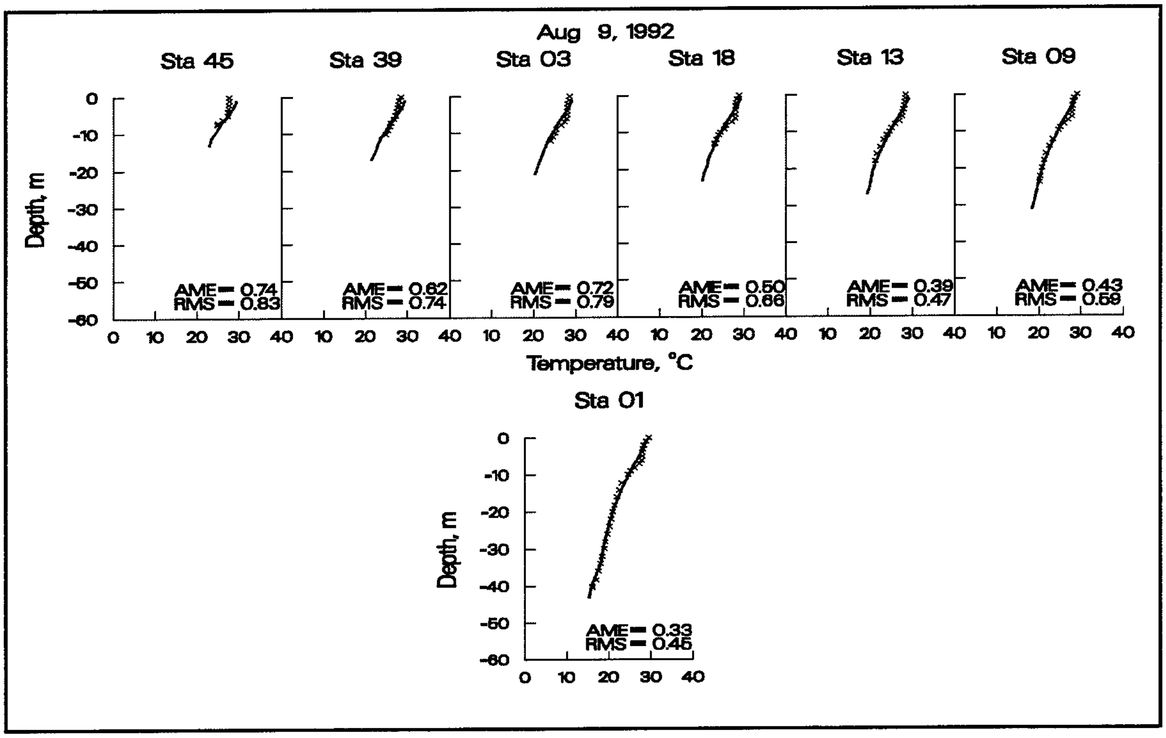

Figure A11. 1992 Allatoona Reservoir computed (...) versus observed (x) temperatures for stations along the mainstem, August 9

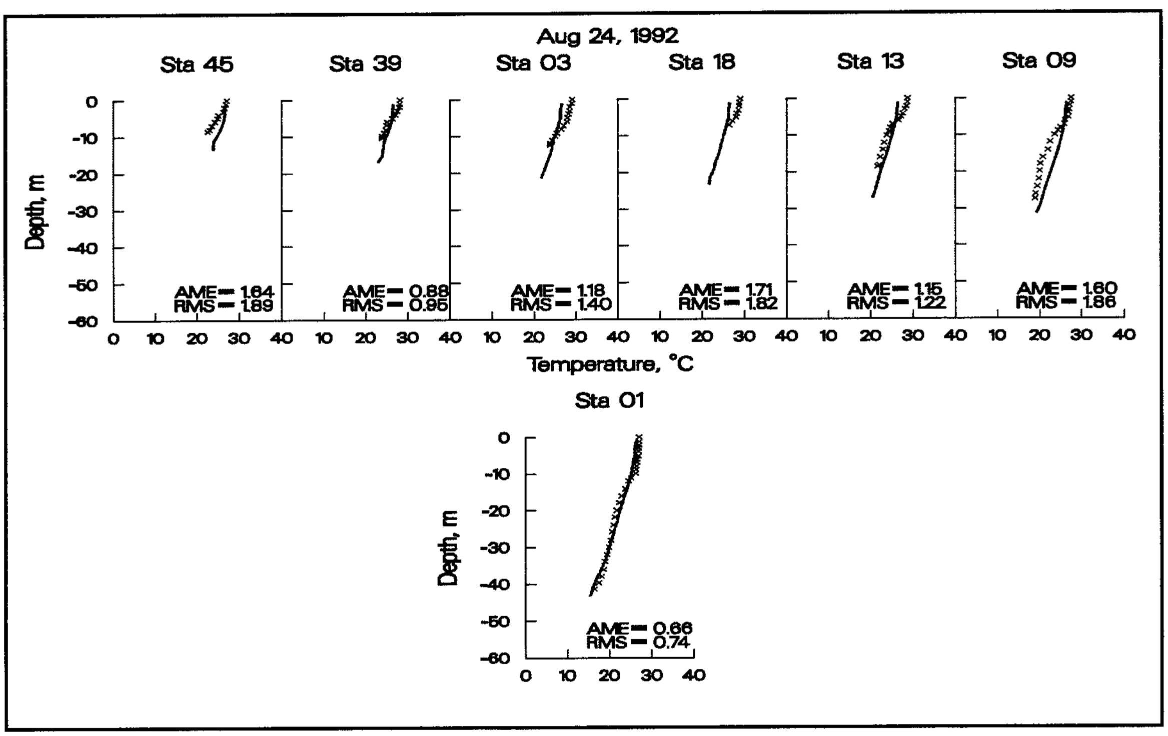

Figure A12. 1992 Allatoona Reservoir computed (...) versus observed (x) temperatures for stations along the mainstem, August 24

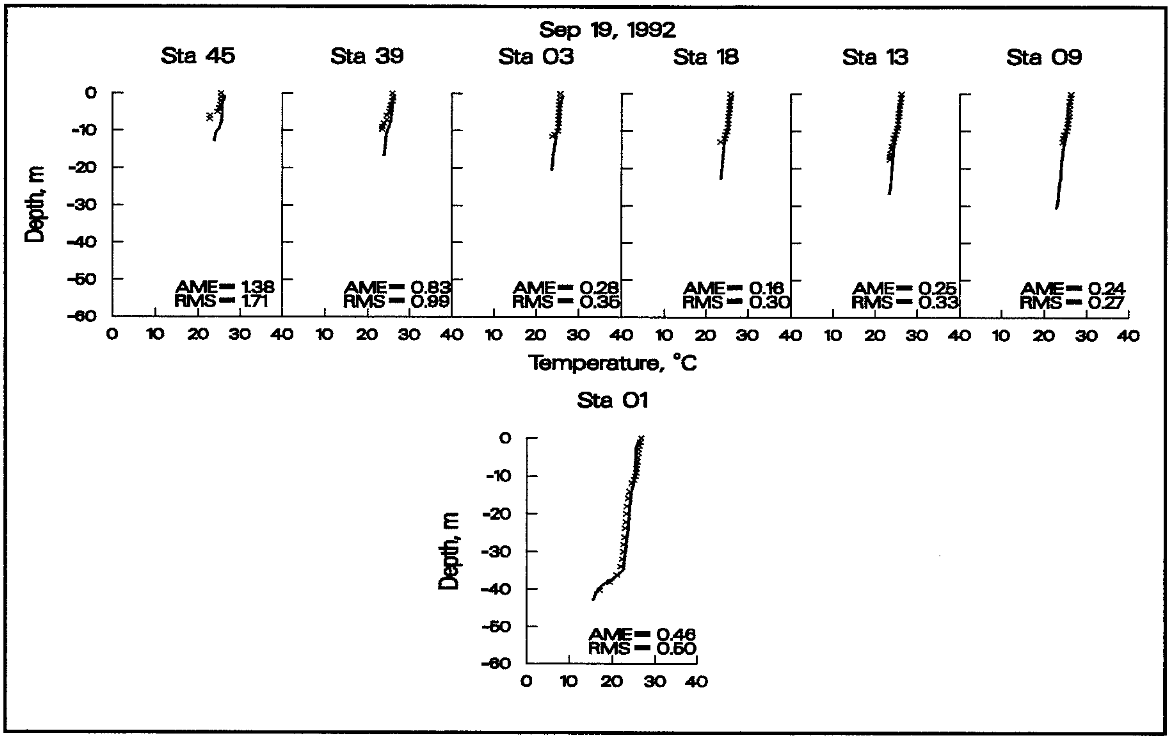

Figure A13. 1992 Allatoona Reservoir computed (...) versus observed (x) temperatures for stations along the mainstem, September 19

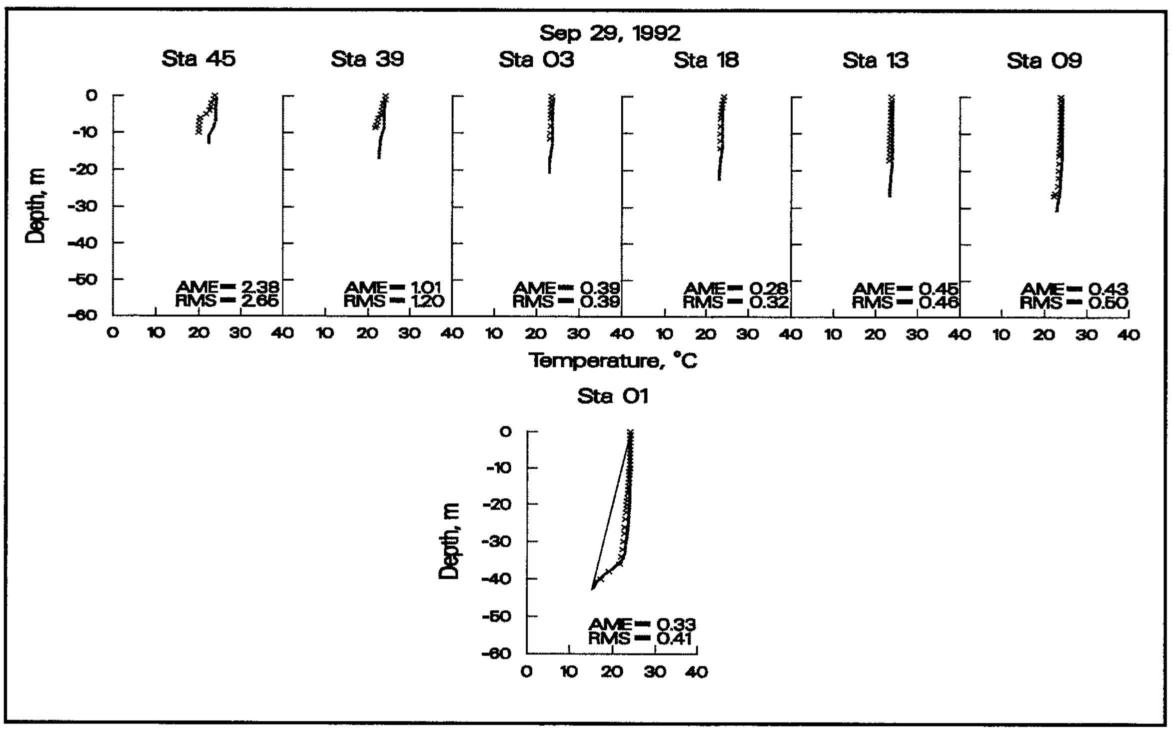

Figure A14. 1992 Allatoona Reservoir computed (...) versus observed (x) temperatures for stations along the mainstem, September 29

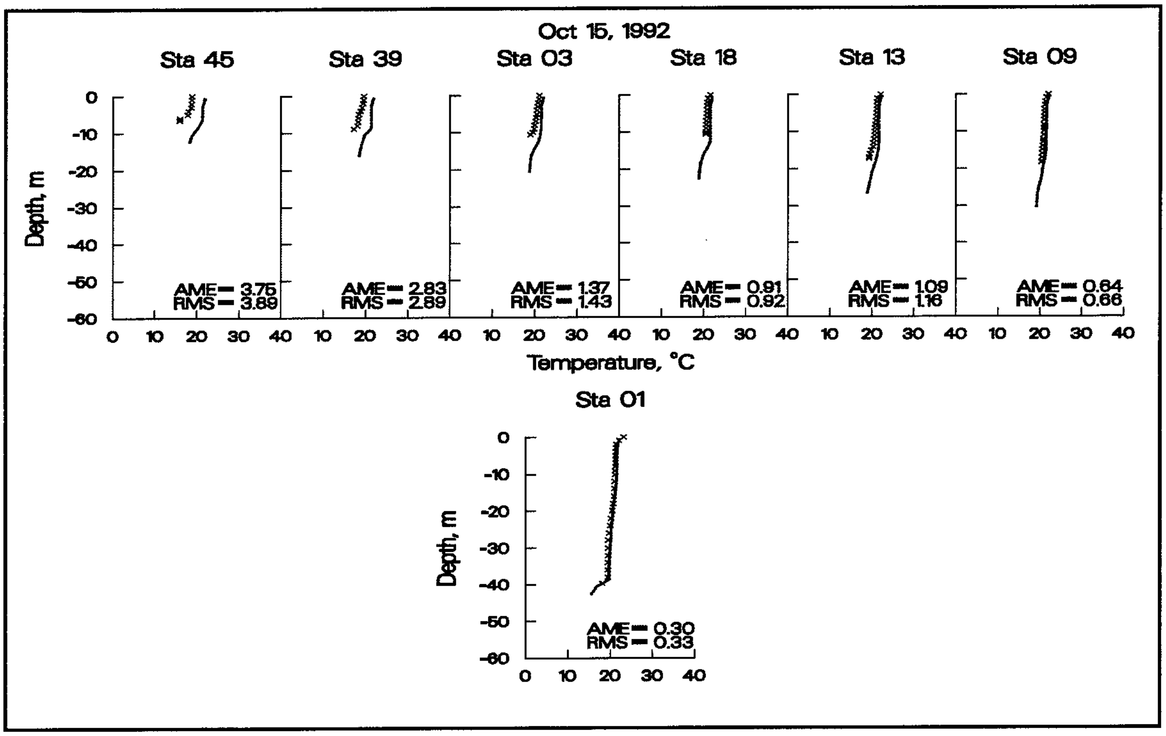

Figure A15. 1992 Allatoona Reservoir computed (...) versus observed (x) temperatures for stations along the mainstem, October 15

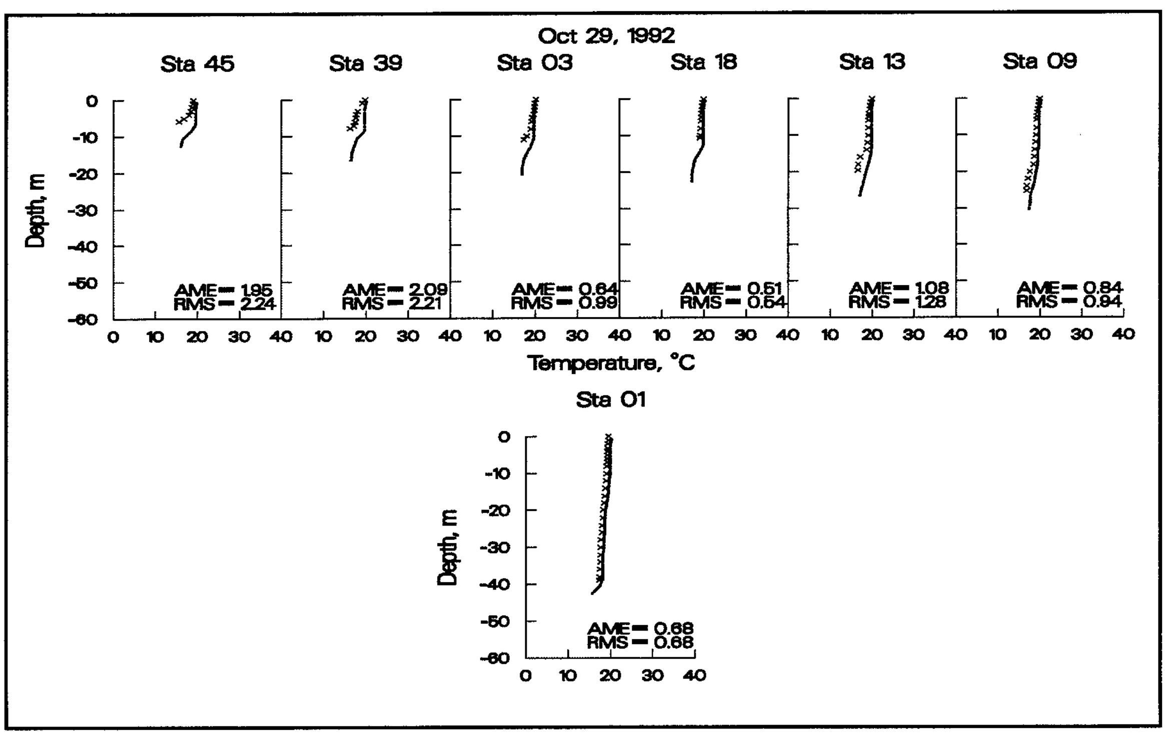

Figure A16. 1992 Allatoona Reservoir computed (...) versus observed (x) temperatures for stations along the mainstem, October 29

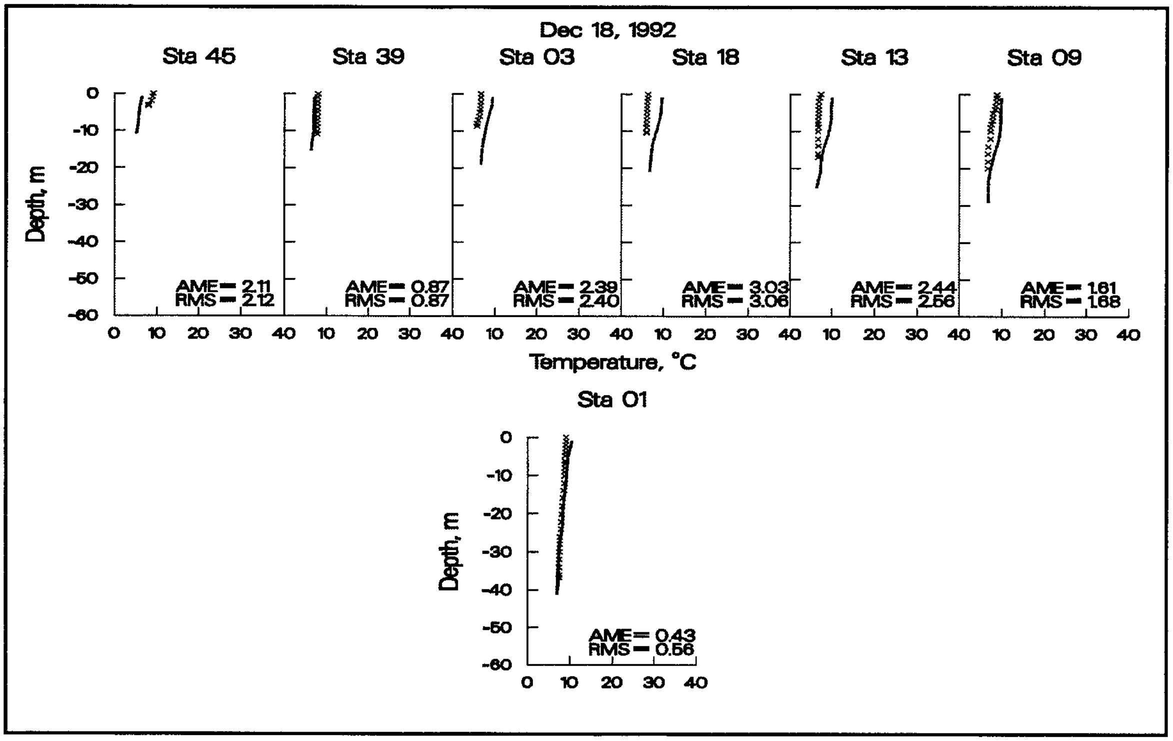

Figure A17. 1992 Allatoona Reservoir computed (...) versus observed (x) temperatures for stations along the mainstem, December 18

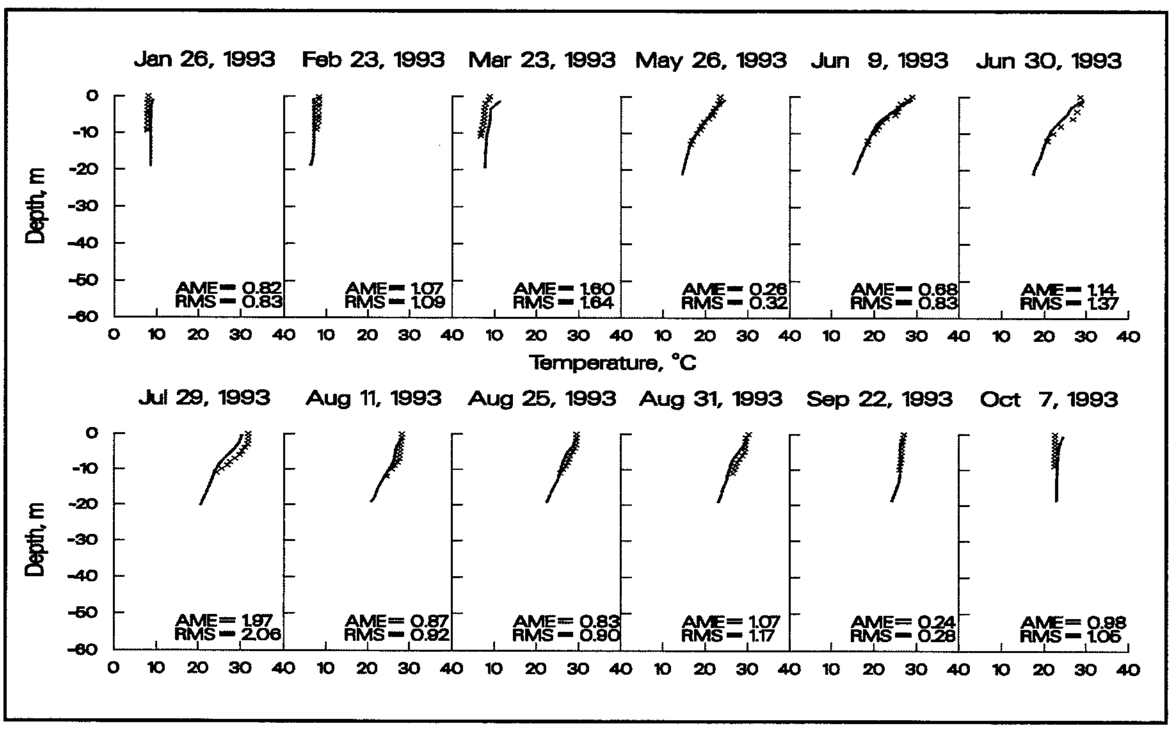

Figure A18. 1993 Allatoona Reservoir computed (...) versus observed (x) temperatures for station 09

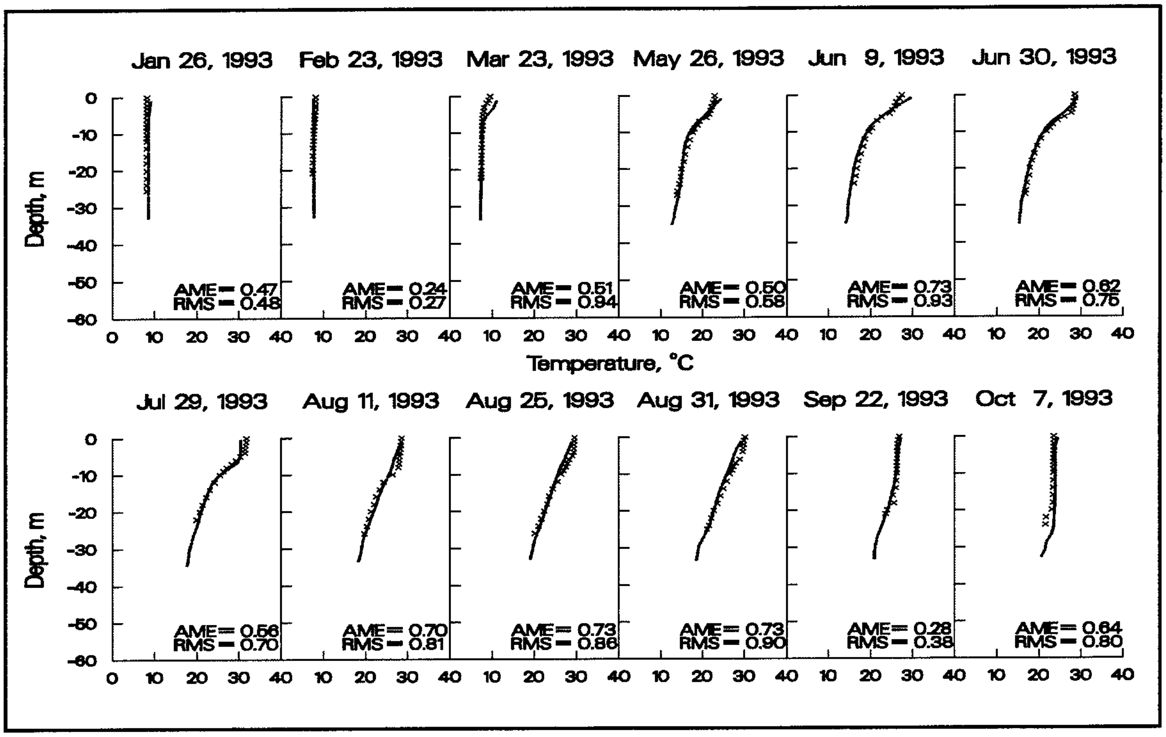

Figure A19. 1993 Allatoona Reservoir computed (...) versus observed (x) temperatures for station 18

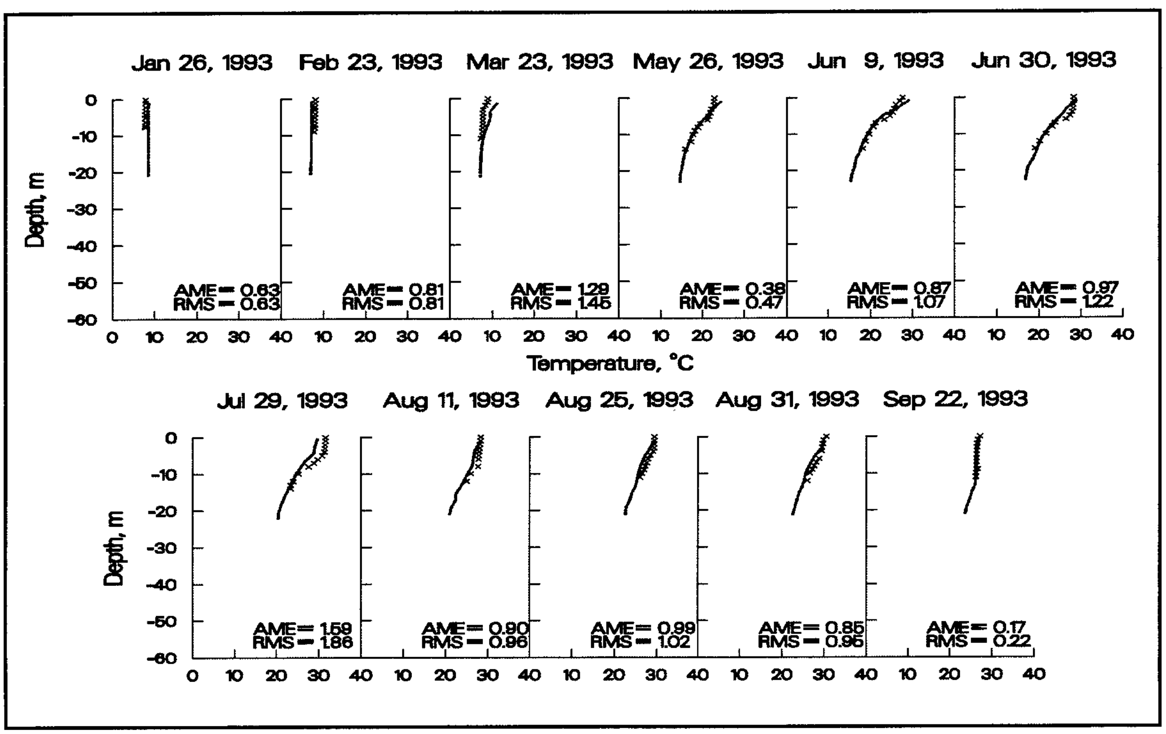

Figure A20. 1993 Allatoona Reservoir computed (...) versus observed (x) temperatures for station 39

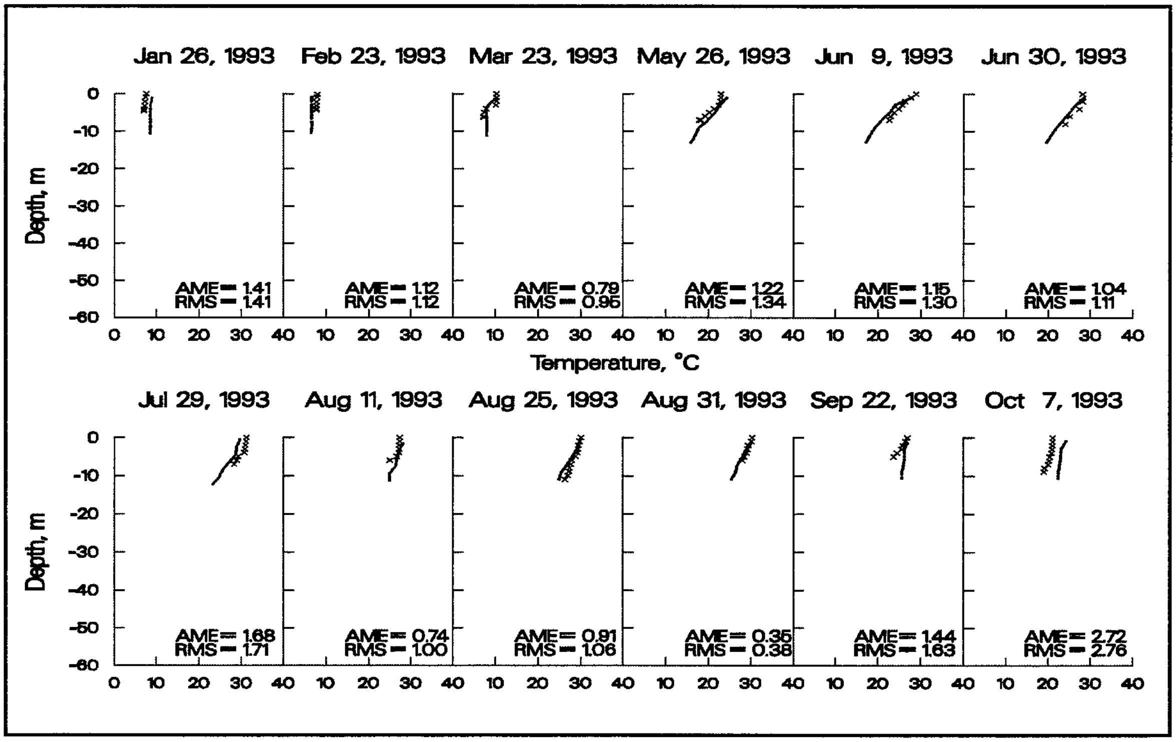

Figure A21. 1993 Allatoona Reservoir computed (...) versus observed (x) temperatures for station 45

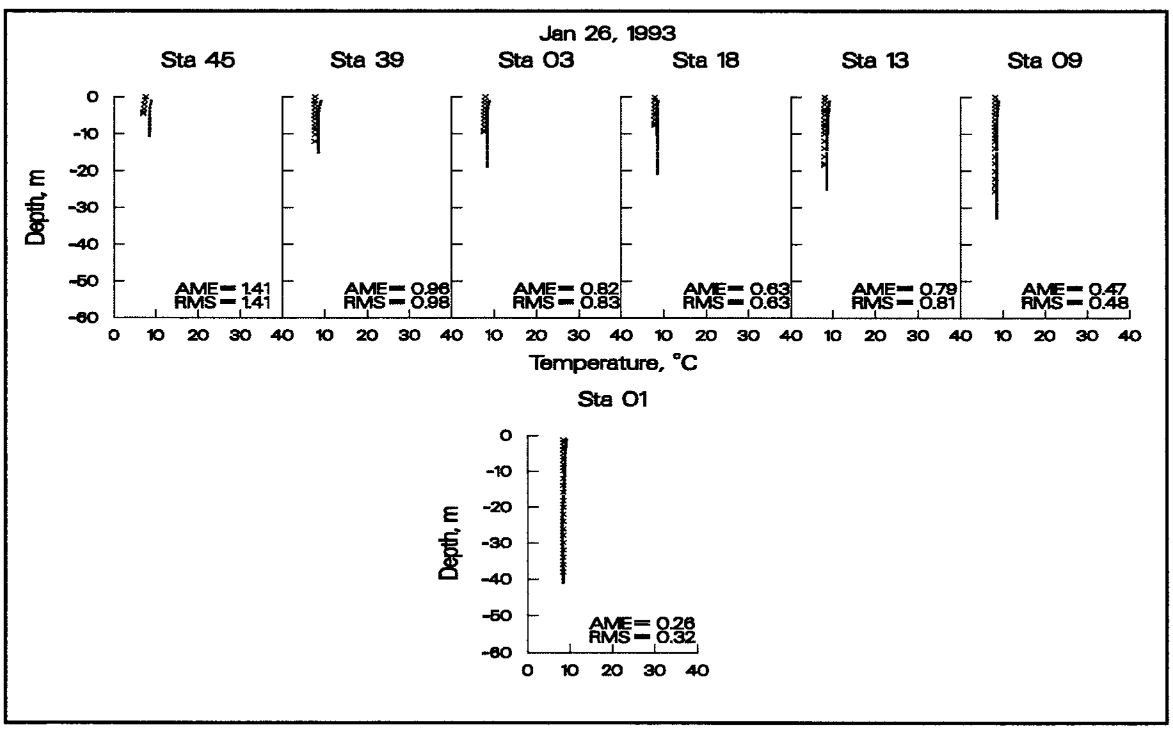

Figure A22. 1993 Allatoona Reservoir computed (...) versus observed (x) temperatures for stations located along main axis of the reservoir, January 26

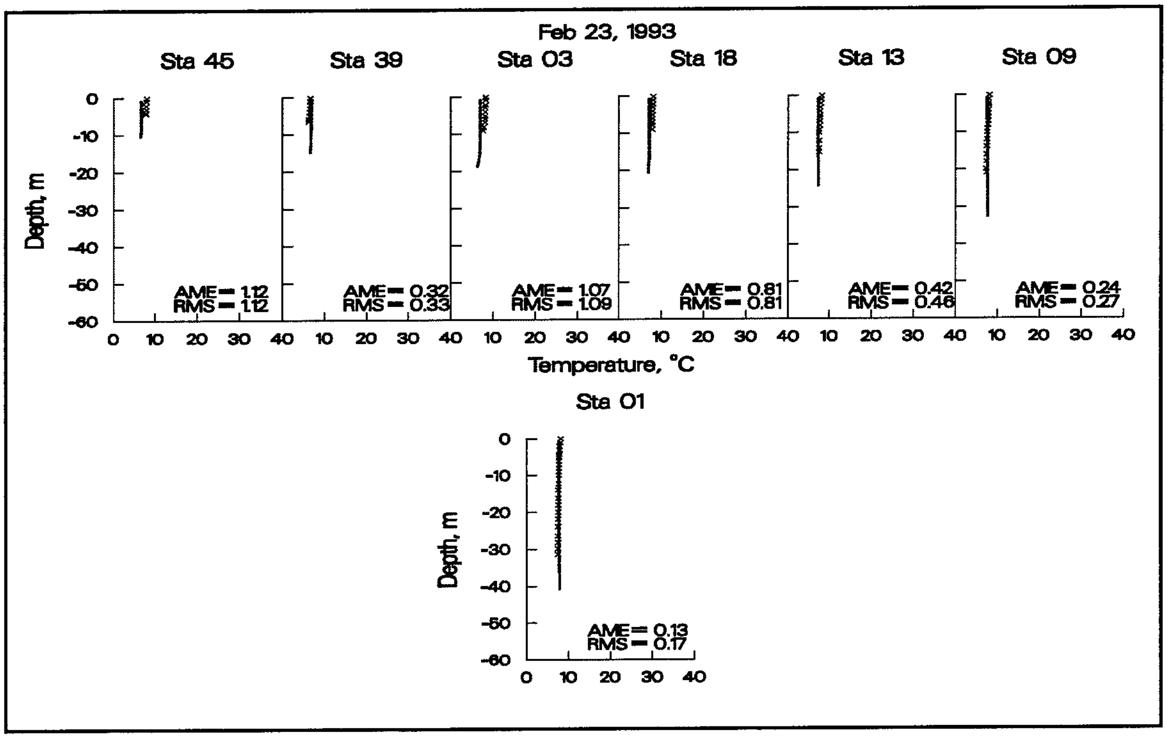

Figure A23. 1993 Allatoona Reservoir computed (...) versus observed (x) temperatures for stations located along main axis of the reservoir, February 23

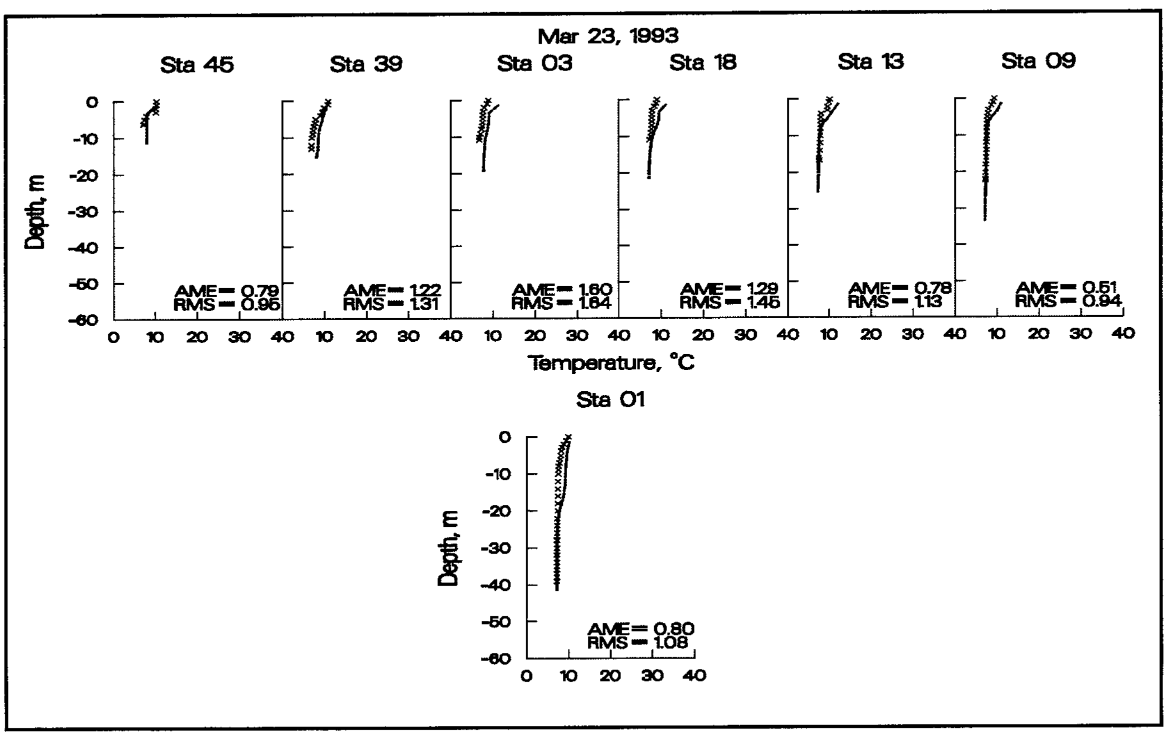

Figure A24. 1993 Allatoona Reservoir computed (...) versus observed (x) temperatures for stations located along main axis of the reservoir, March 23

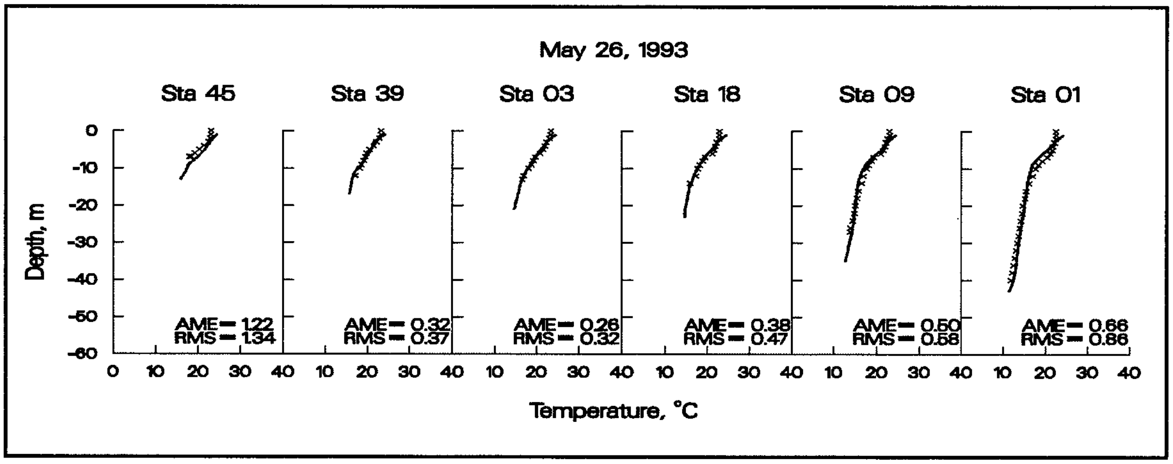

Figure A25. 1993 Allatoona Reservoir computed (...) versus observed (x) temperatures for stations located along main axis of the reservoir, May 26

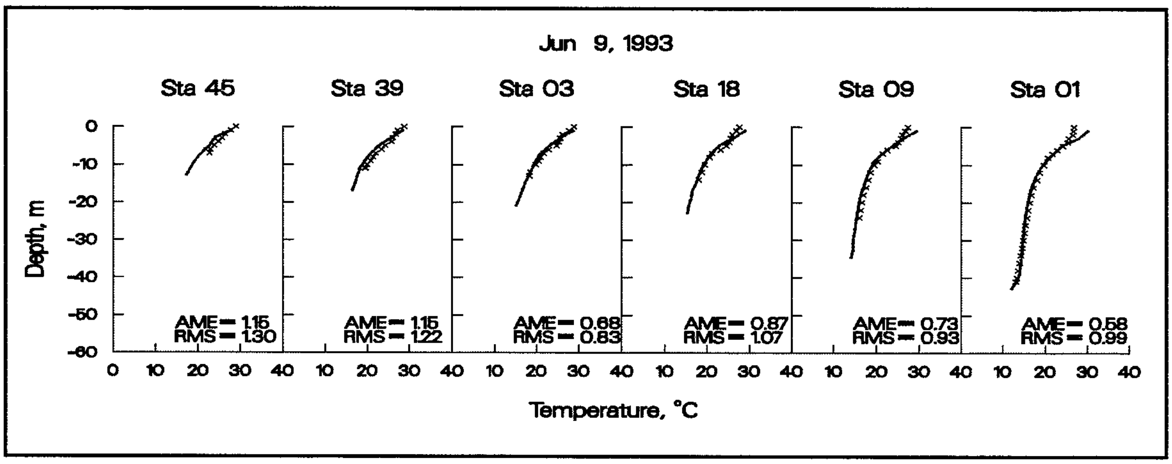

Figure A26. 1993 Allatoona Reservoir computed (...) versus observed (x) temperatures for stations located along main axis of the reservoir, June 9

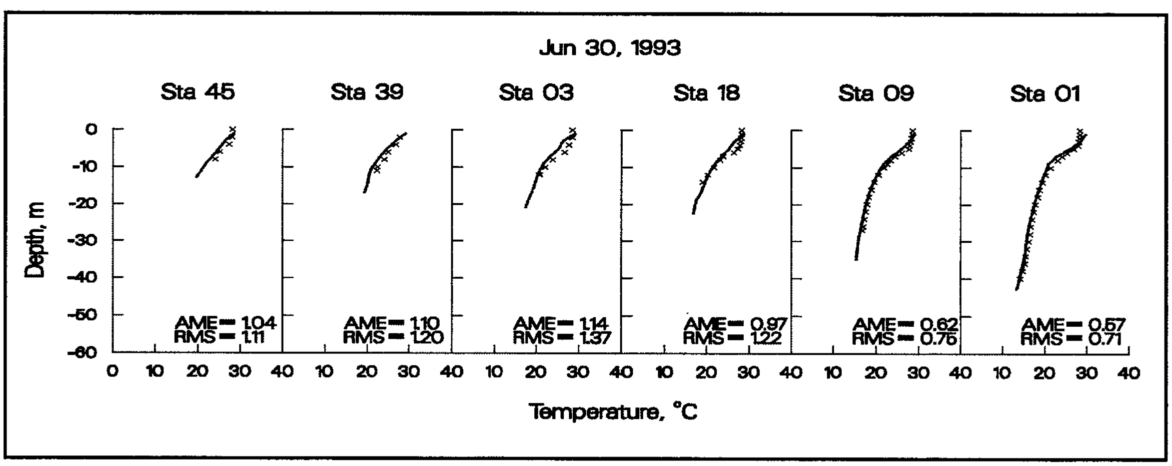

Figure A27. 1993 Allatoona Reservoir computed (...) versus observed (x) temperatures for stations located along main axis of the reservoir, June 30

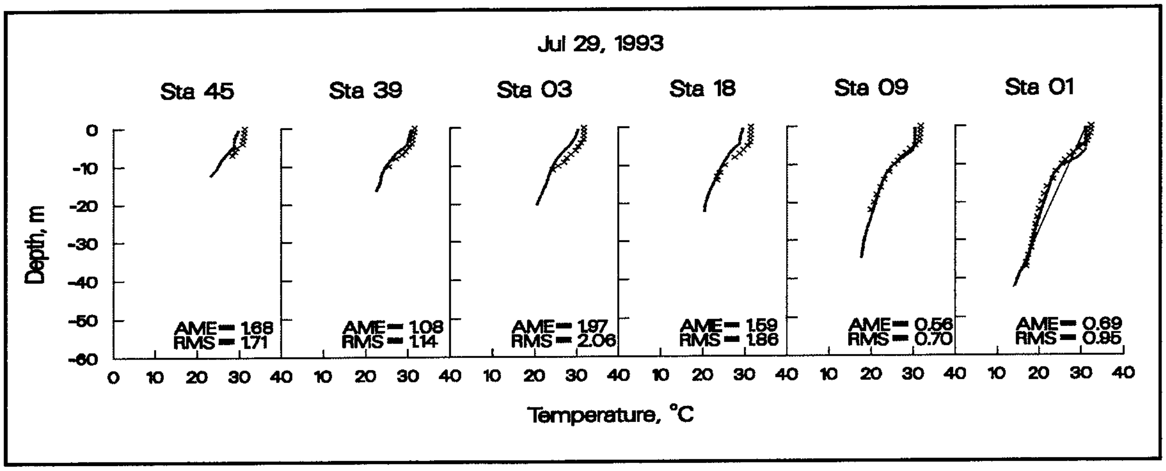

Figure A28. 1993 Allatoona Reservoir computed (...) versus observed (x) temperatures for stations located along main axis of the reservoir, July 29

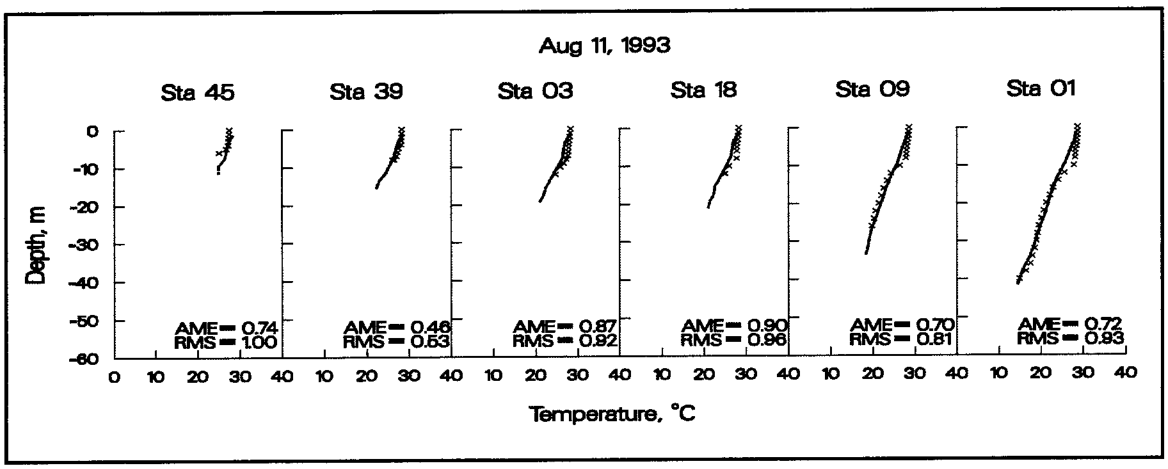

Figure A29. 1993 Allatoona Reservoir computed (...) versus observed (x) temperatures for stations located along main axis of the reservoir, August 11

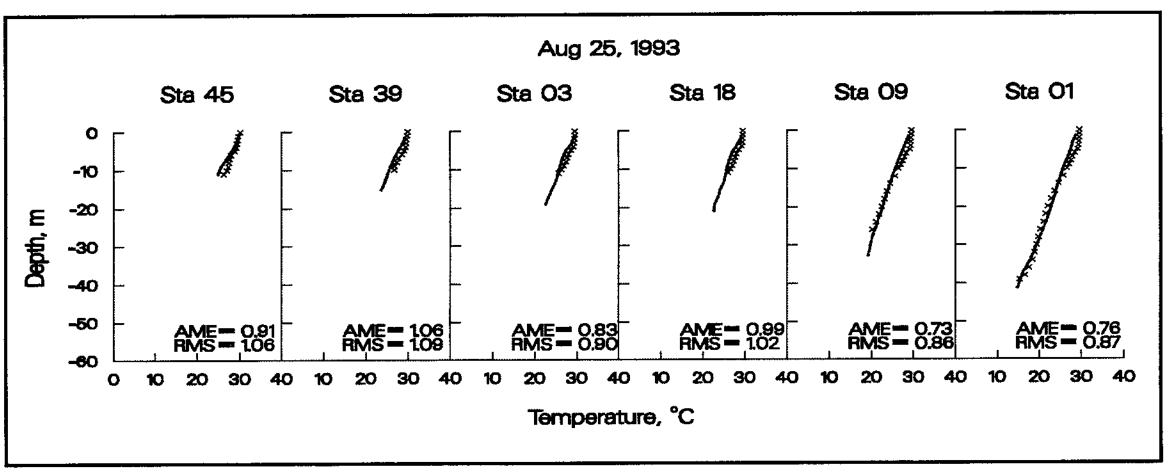

Figure A30. 1993 Allatoona Reservoir computed (...) versus observed (x) temperatures for stations located along main axis of the reservoir, August 25

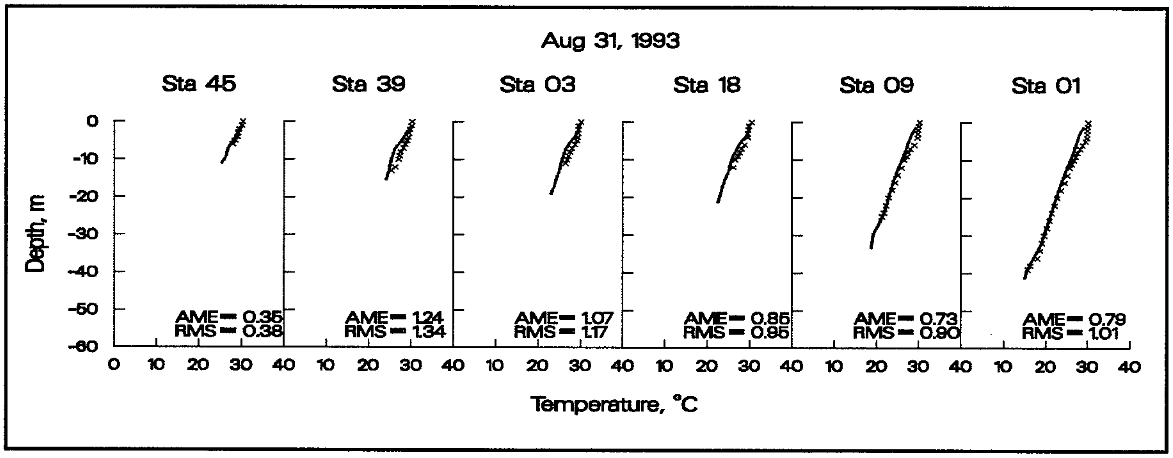

Figure A31. 1993 Allatoona Reservoir computed (...) versus observed (x) temperatures for stations located along main axis of the reservoir, August 31

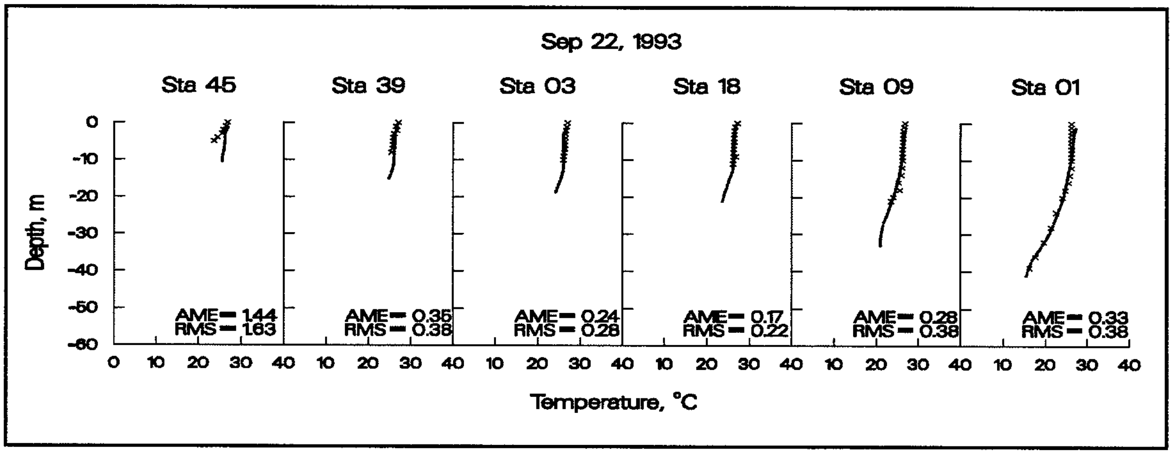

Figure A32. 1993 Allatoona Reservoir computed (...) versus observed (x) temperatures for stations located along main axis of the reservoir, September 22

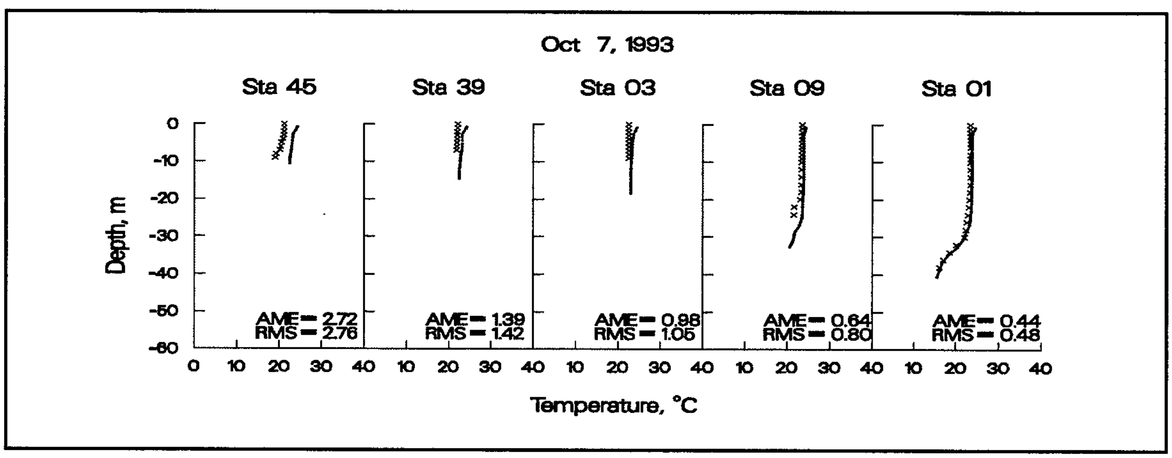

Figure A33. 1993 Allatoona Reservoir computed (...) versus observed (x) temperatures for stations located along main axis of the reservoir, October 7

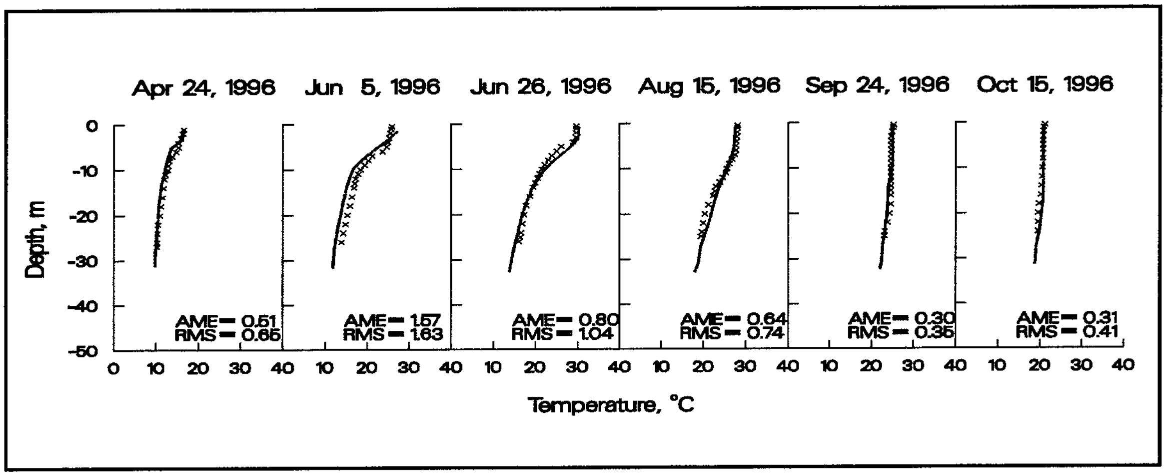

Figure A34. 1996 Allatoona Reservoir computed (...) versus observed (x) temperatures for station 09

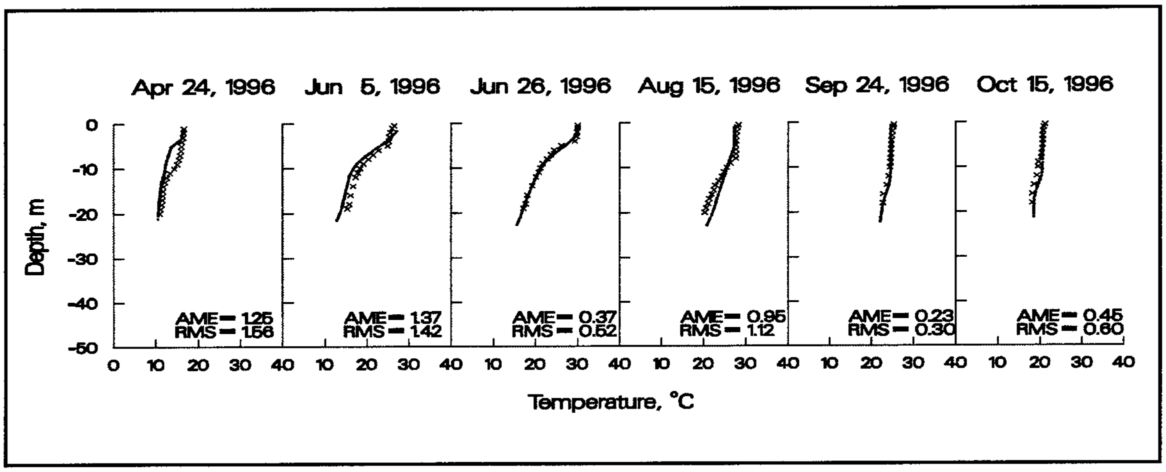

Figure A35. 1996 Allatoona Reservoir computed (...) versus observed (x) temperatures for station 18

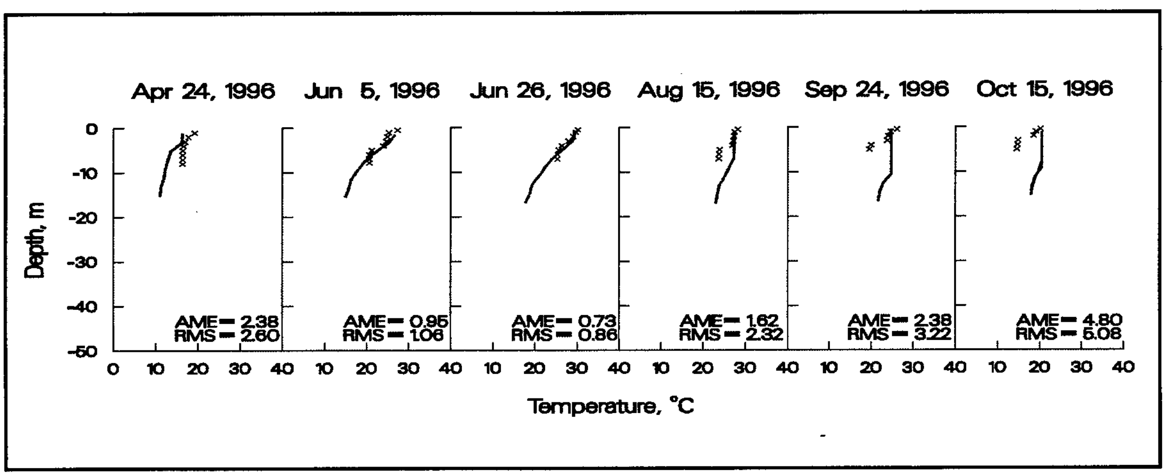

Figure A36. 1996 Allatoona Reservoir computed (...) versus observed (x) temperatures for station 45

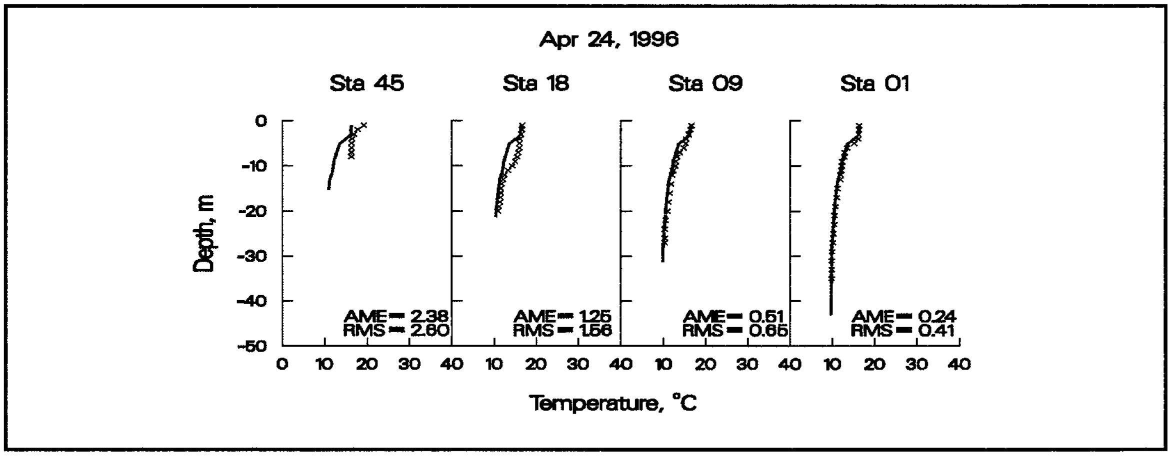

Figure A37. 1996 Allatoona Reservoir computed (...) versus observed (x) temperatures for stations along the mainstem, April 24

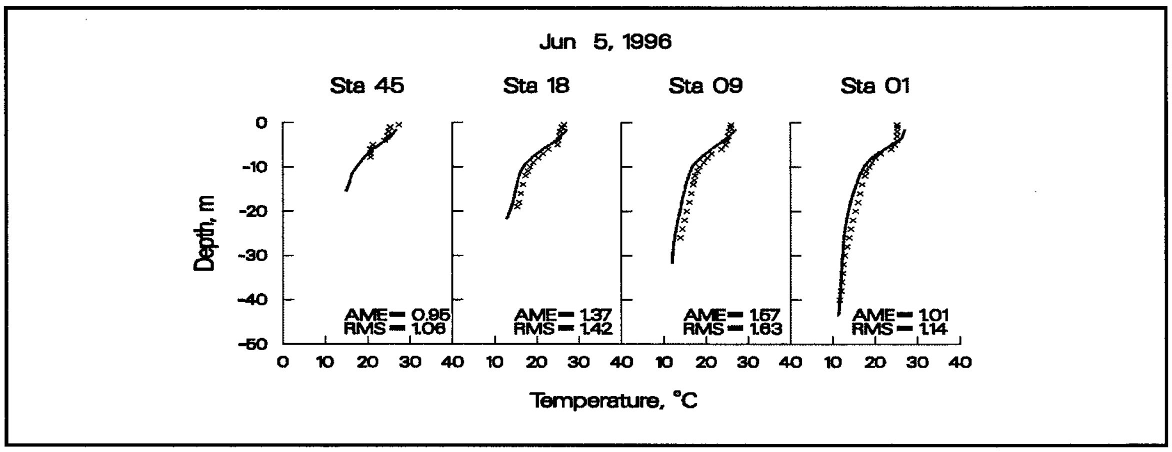

Figure A38. 1996 Allatoona Reservoir computed (...) versus observed (x) temperatures for stations along the mainstem, June 5

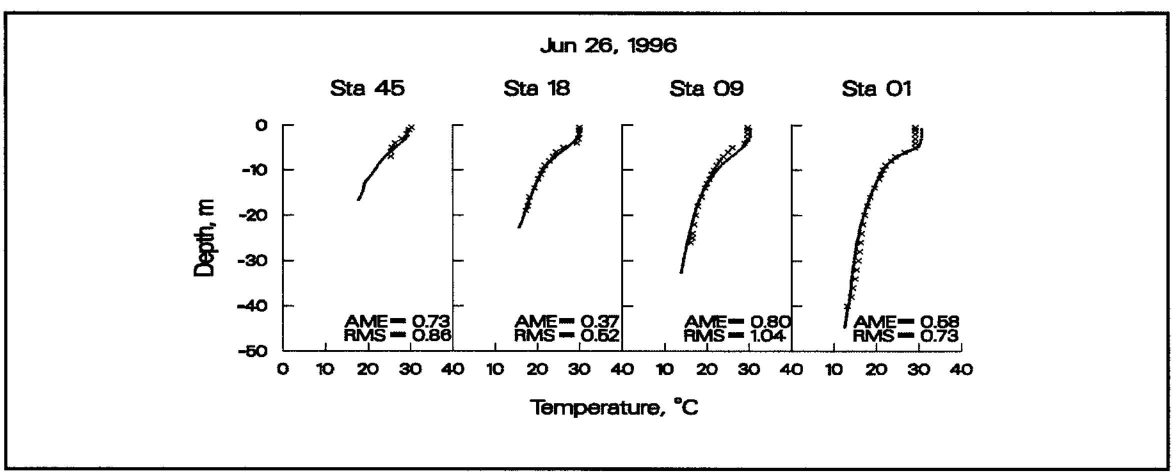

Figure A39. 1996 Allatoona Reservoir computed (...) versus observed (x) temperatures for stations along the mainstem, June 26

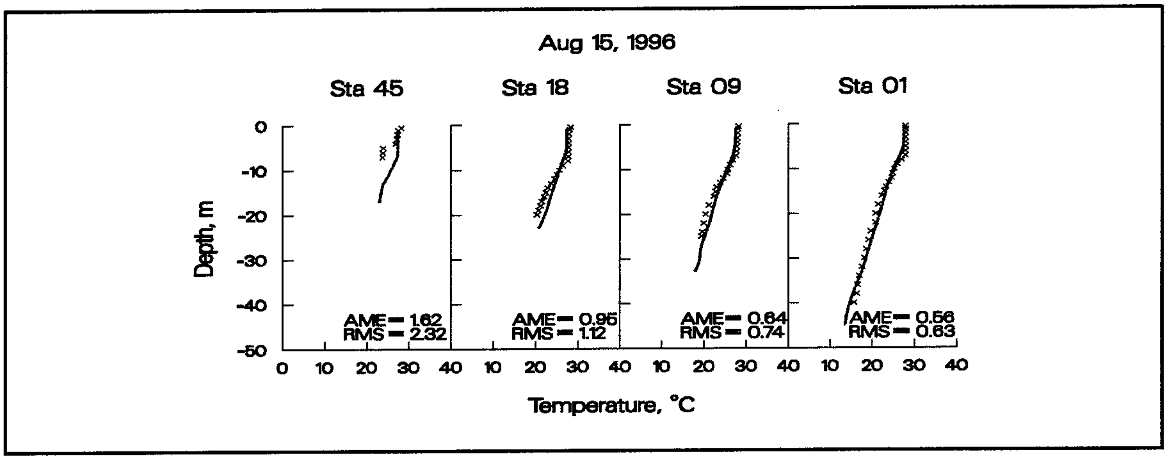

Figure A40. 1996 Allatoona Reservoir computed (...) versus observed (x) temperatures for stations along the mainstem, August 15

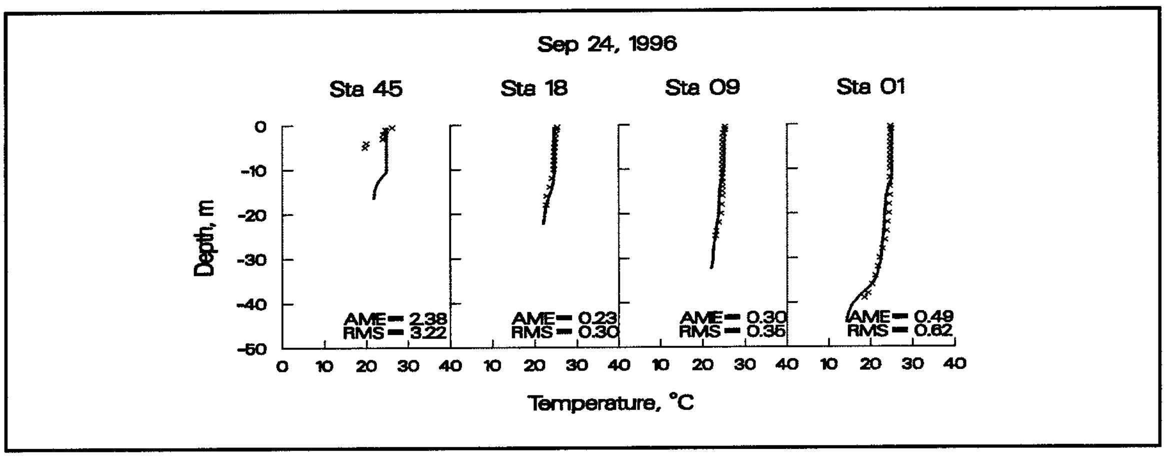

Figure A41. 1996 Allatoona Reservoir computed (...) versus observed (x) temperatures for stations along the mainstem, September 24

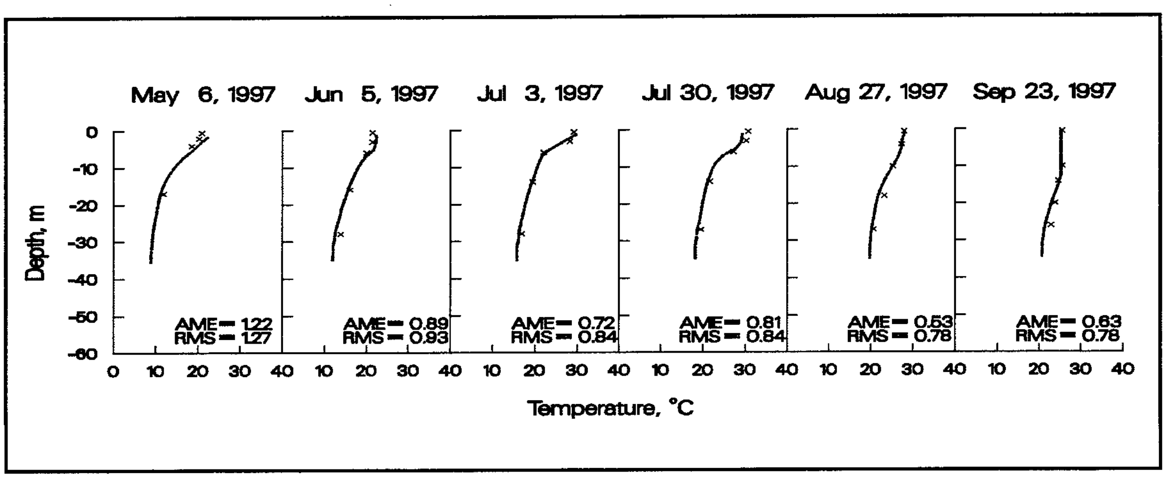

Figure A42. 1997 Allatoona Reservoir computed (...) versus observed (x) temperatures for station 09

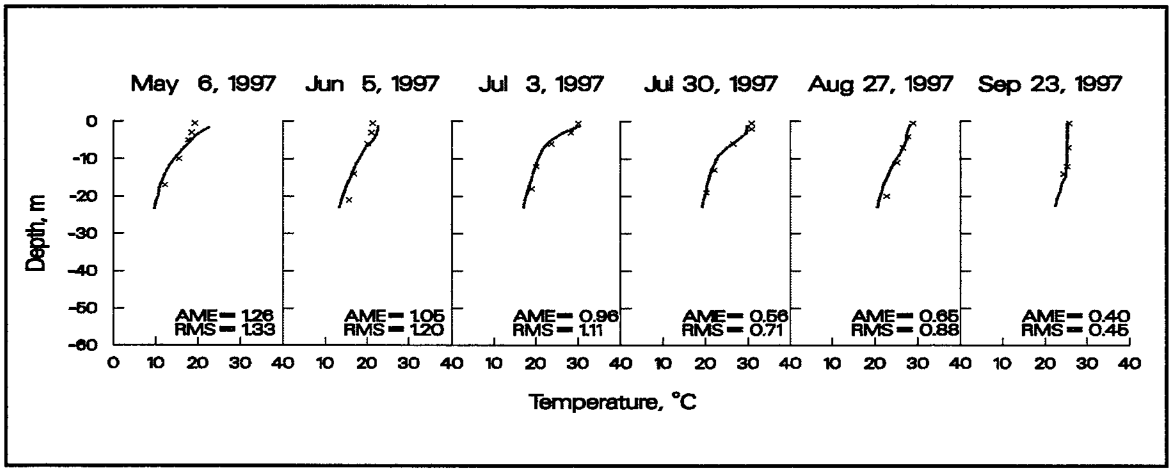

Figure A43. 1997 Allatoona Reservoir computed (...) versus observed (x) temperatures for station 18

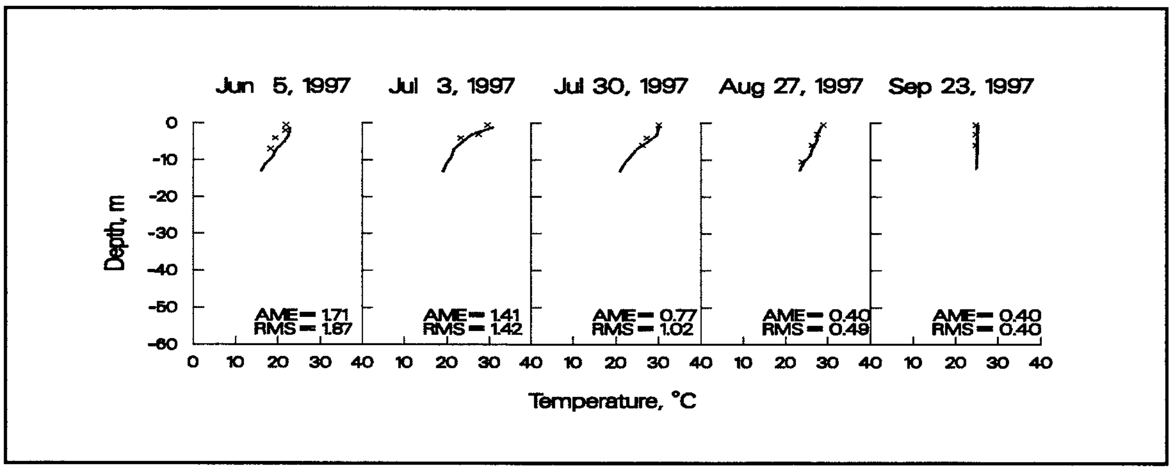

Figure A44. 1997 Allatoona Reservoir computed (...) versus observed (x) temperatures for station 45

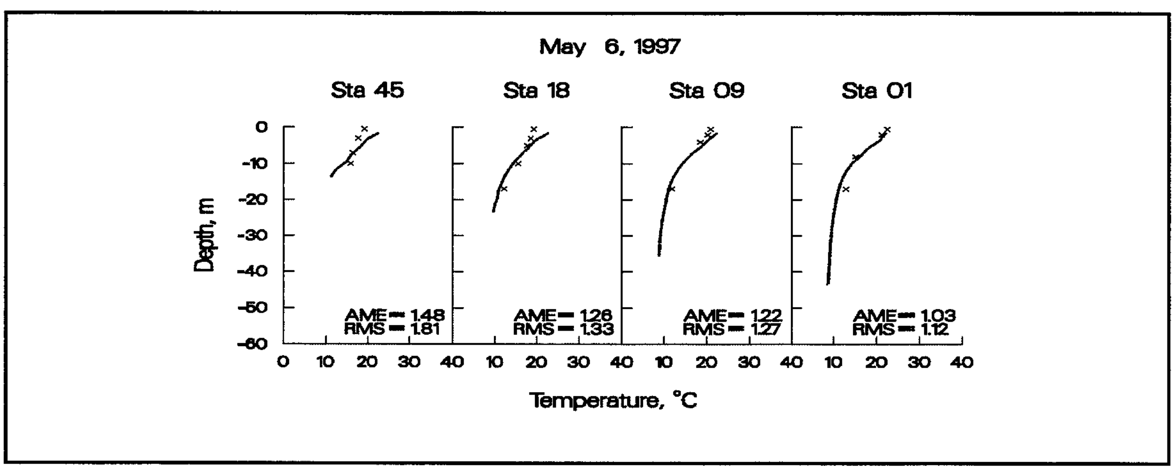

Figure A45. 1997 Allatoona Reservoir computed (...) versus observed (x) temperatures for stations along the mainstem, May 6

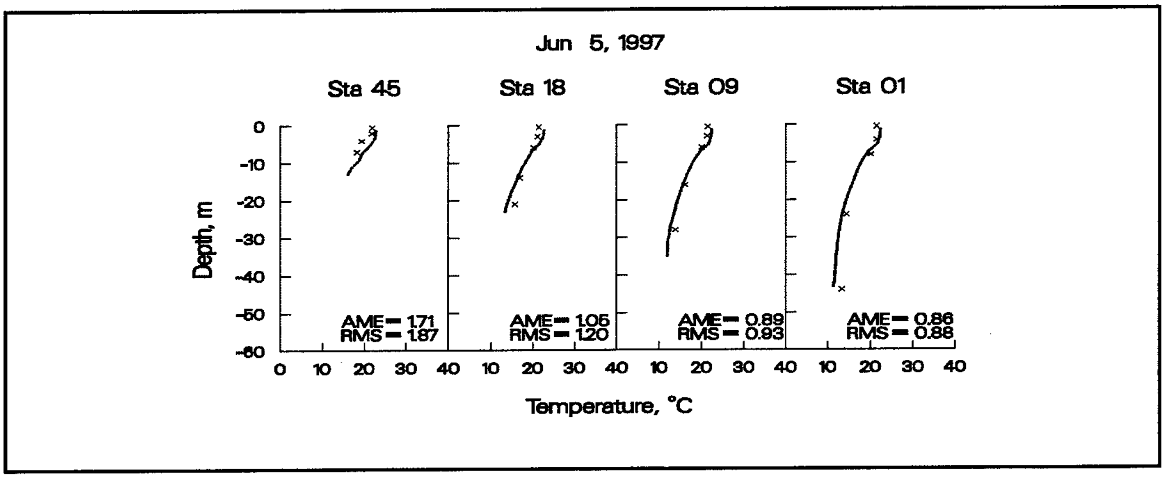

Figure A46. 1997 Allatoona Reservoir computed (...) versus observed (x) temperatures for stations along the mainstem, June 5

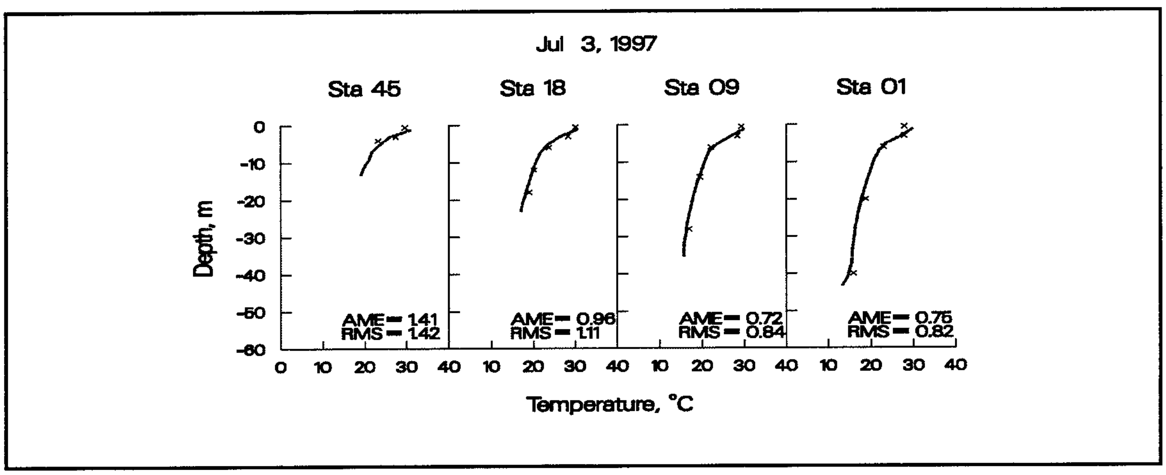

Figure A47. 1997 Allatoona Reservoir computed (...) versus observed (x) temperatures for stations along the mainstem, July 3

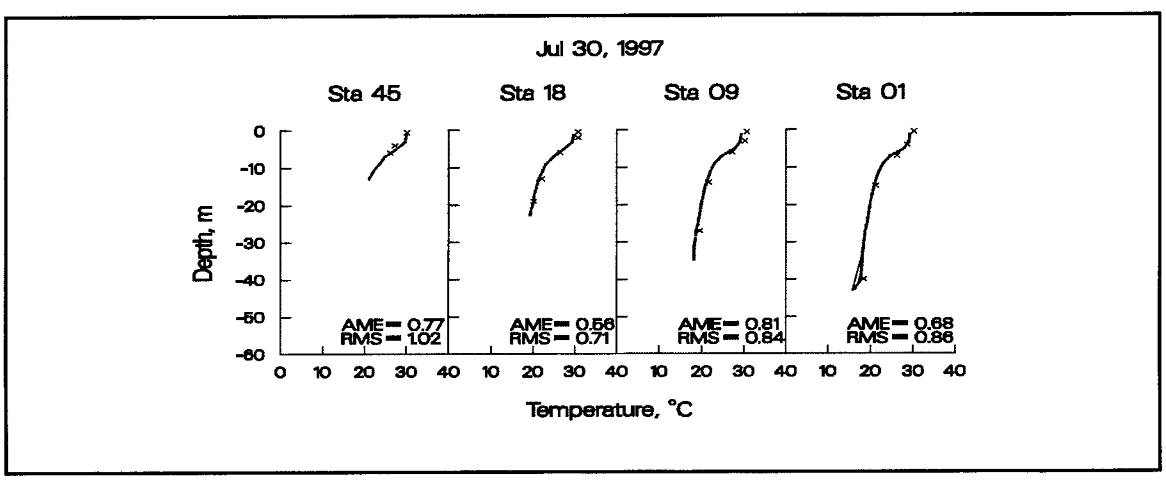

Figure A48. 1997 Allatoona Reservoir computed (...) versus observed (x) temperatures for stations along the mainstem, July 30

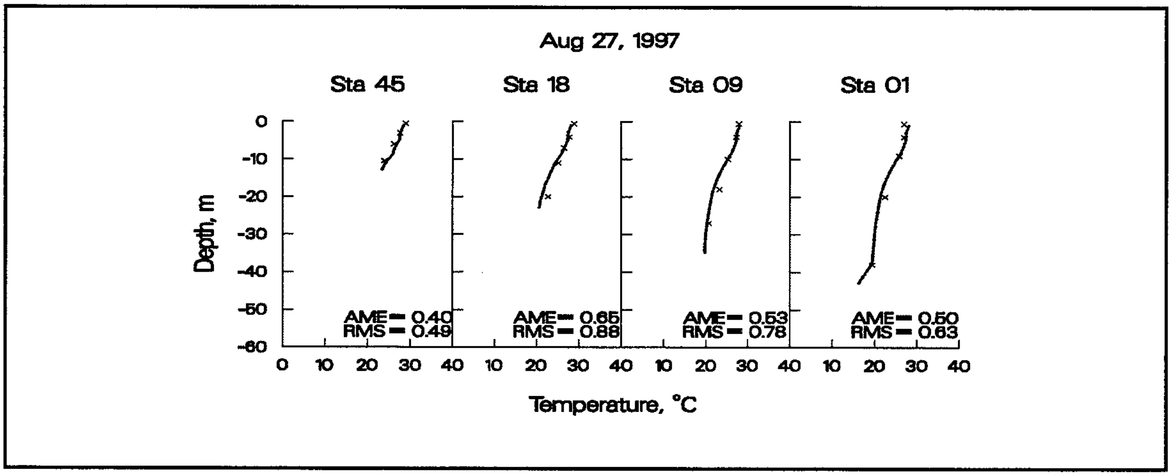

Figure A49. 1997 Allatoona Reservoir computed (...) versus observed (x) temperatures for stations along the mainstem, August 27

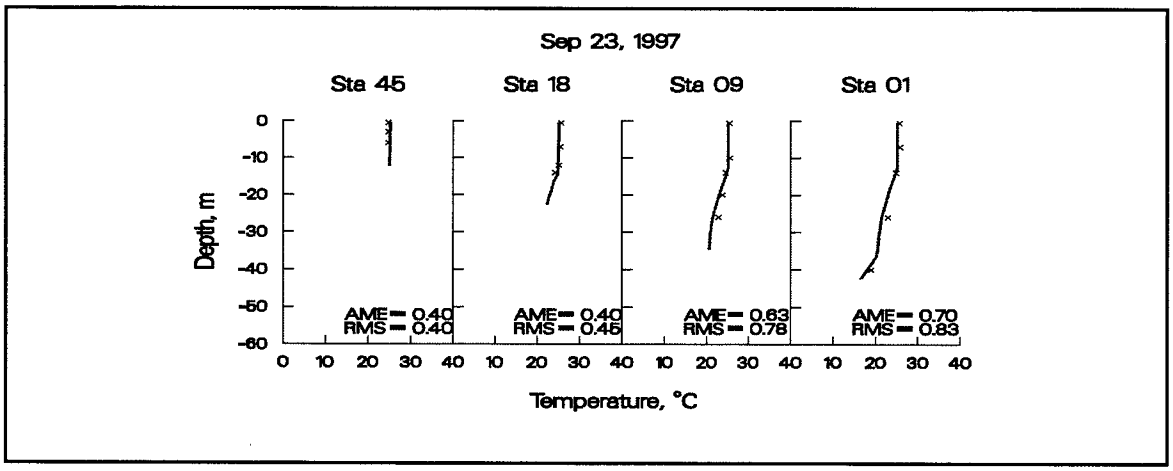

Figure A50. 1997 Allatoona Reservoir computed (...) versus observed (x) temperatures for stations along the mainstem, September 23

West Point

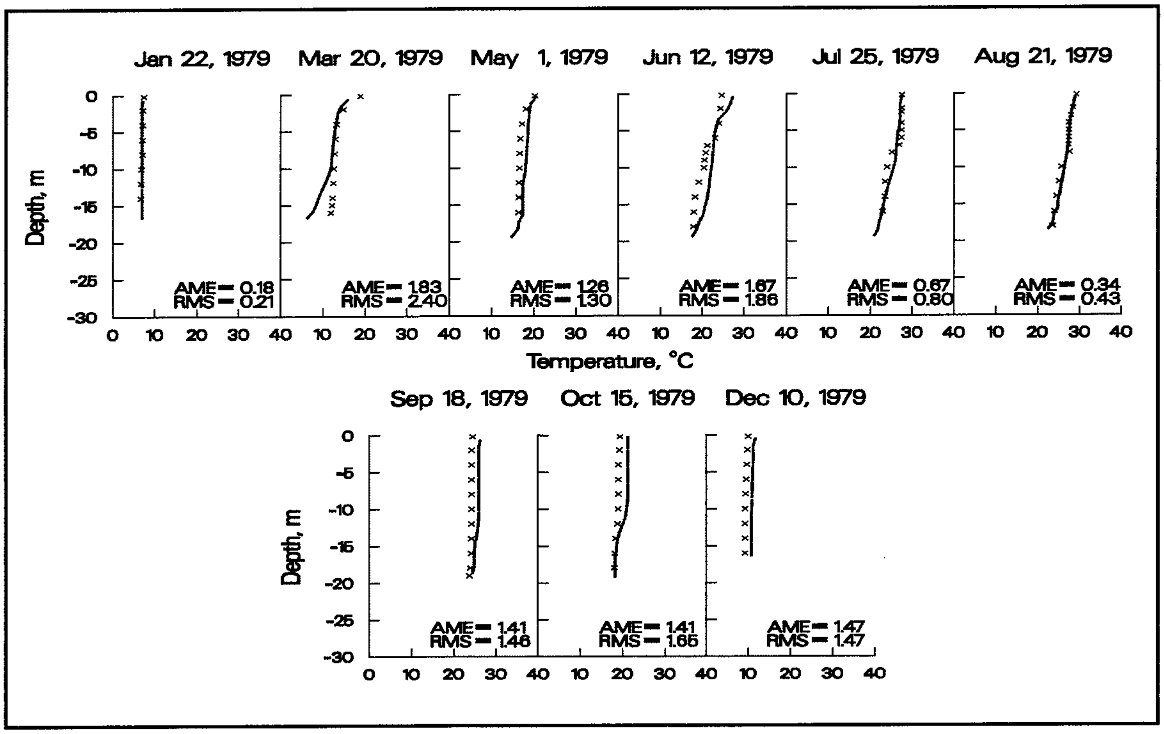

Figure A51. 1979 West Point Reservoir computed (...) versus observed (x) temperatures for station 05

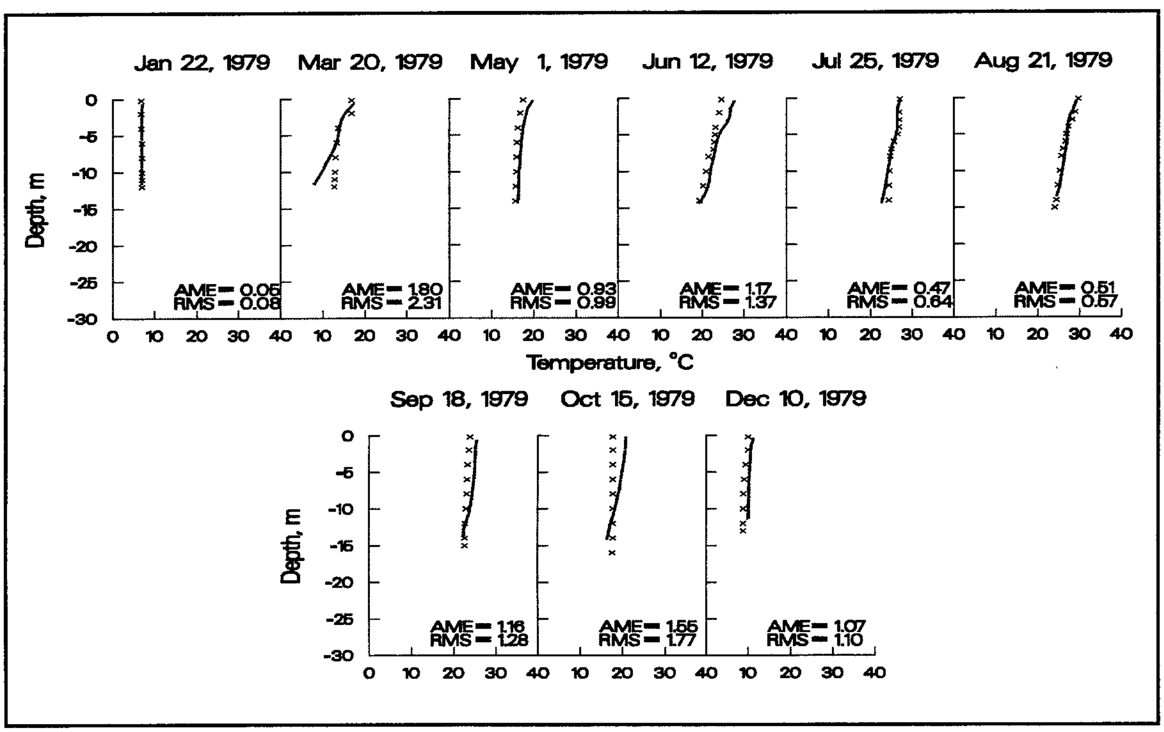

Figure A52. 1979 West Point Reservoir computed (...) versus observed (x) temperatures for station 07

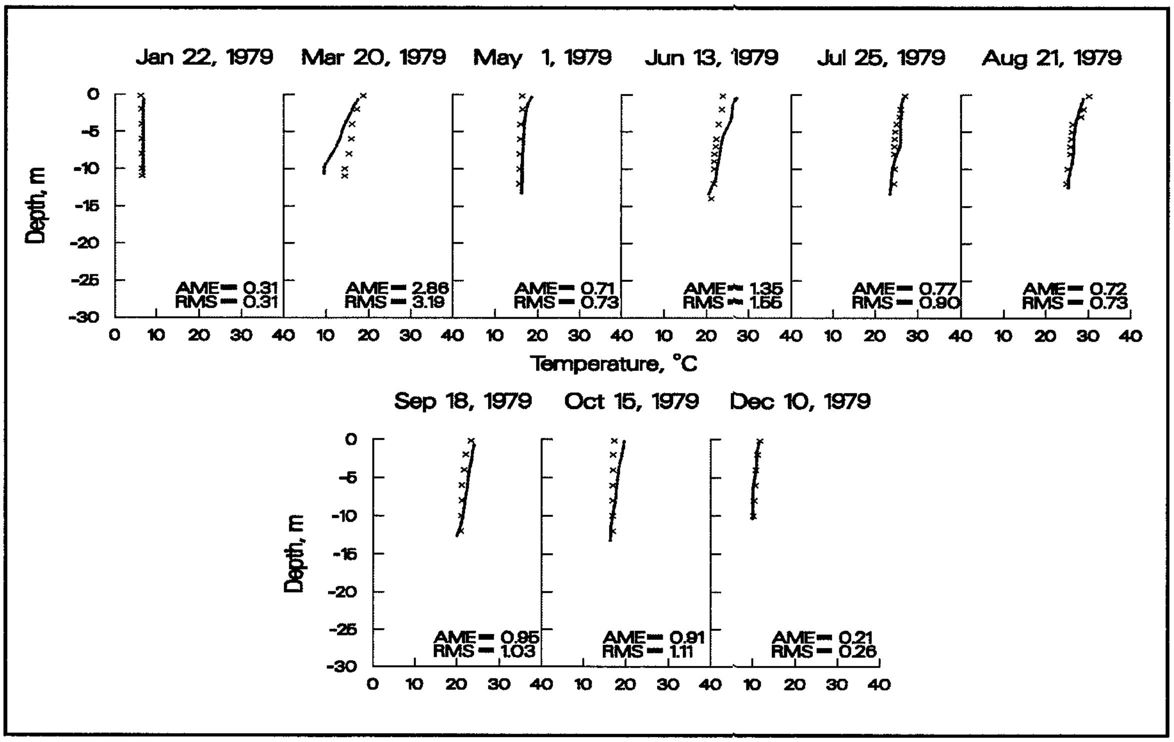

Figure A53. 1979 West Point Reservoir computed (...) versus observed (x) temperatures for station 10

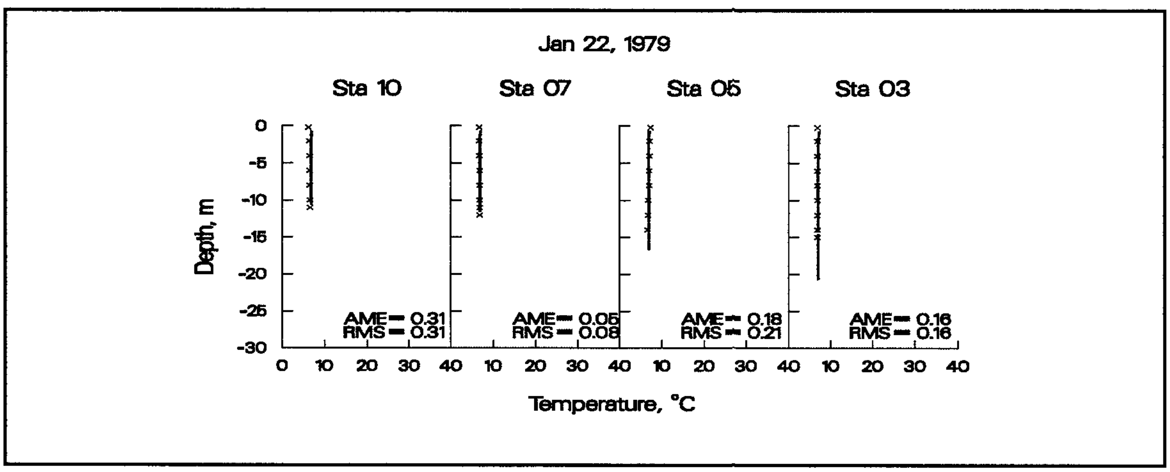

Figure A54. 1979 West Point Reservoir computed (...) versus observed (x) temperatures for stations along the mainstem, January 22

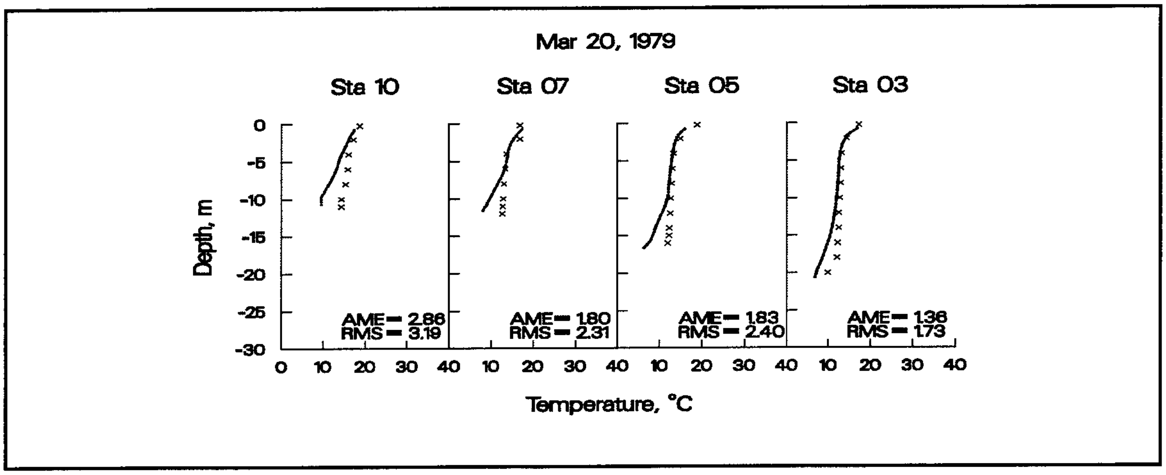

Figure A55. 1979 West Point Reservoir computed (...) versus observed (x) temperatures for stations along the mainstem, March 20

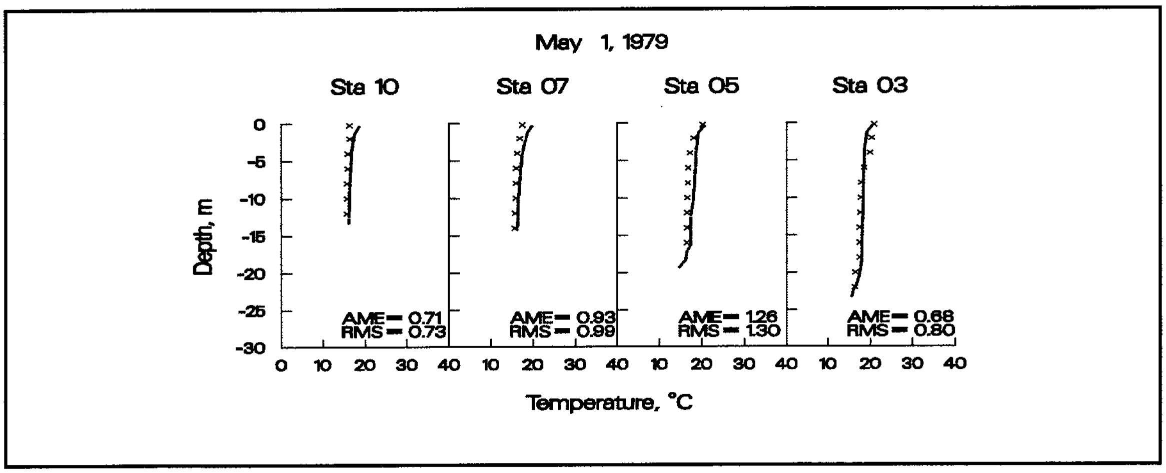

Figure A56. 1979 West Point Reservoir computed (...) versus observed (x) temperatures for stations along the mainstem, May 1

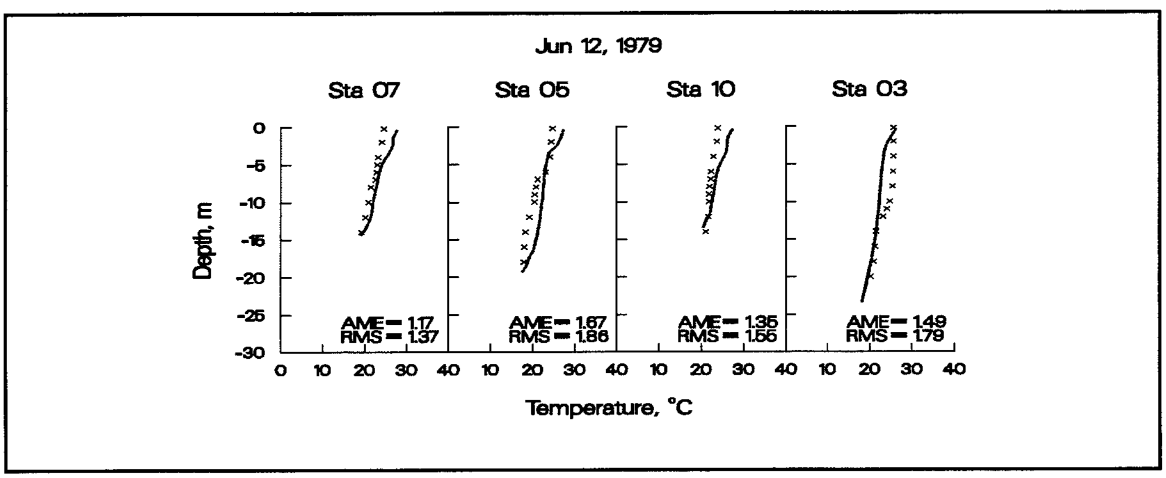

Figure A57. 1979 West Point Reservoir computed (...) versus observed (x) temperatures for stations along the mainstem, June 12

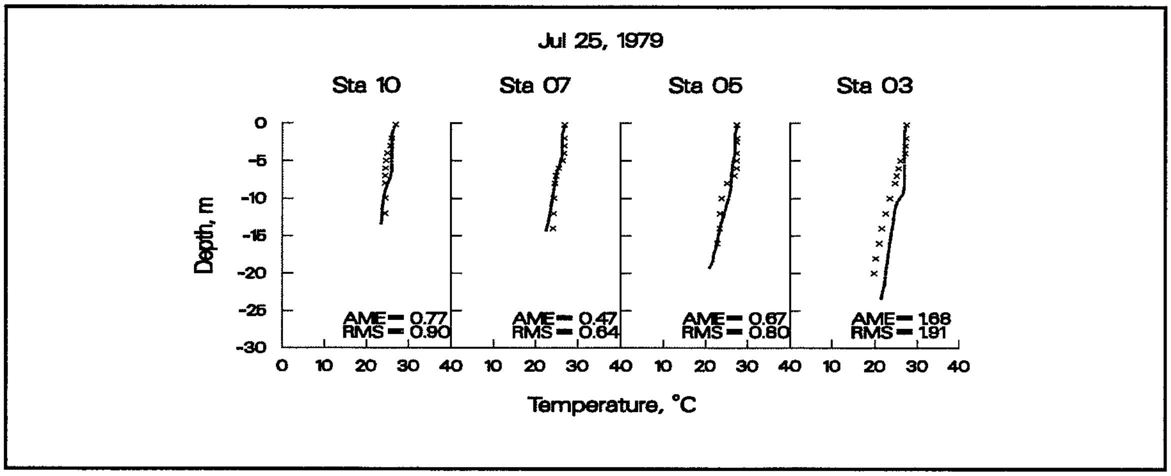

Figure A58. 1979 West Point Reservoir computed (...) versus observed (x) temperatures for stations along the mainstem, July 25

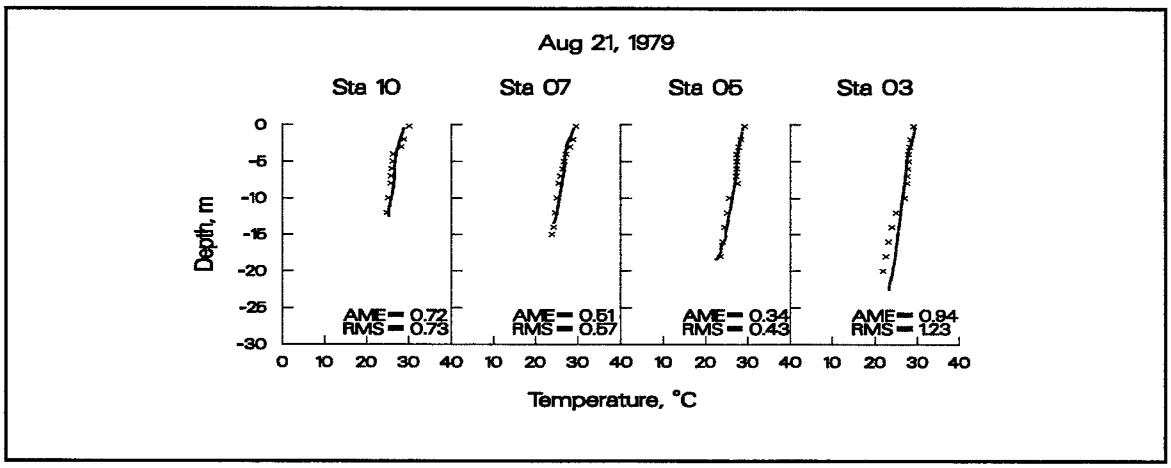

Figure A59. 1979 West Point Reservoir computed (...) versus observed (x) temperatures for stations along the mainstem, August 21

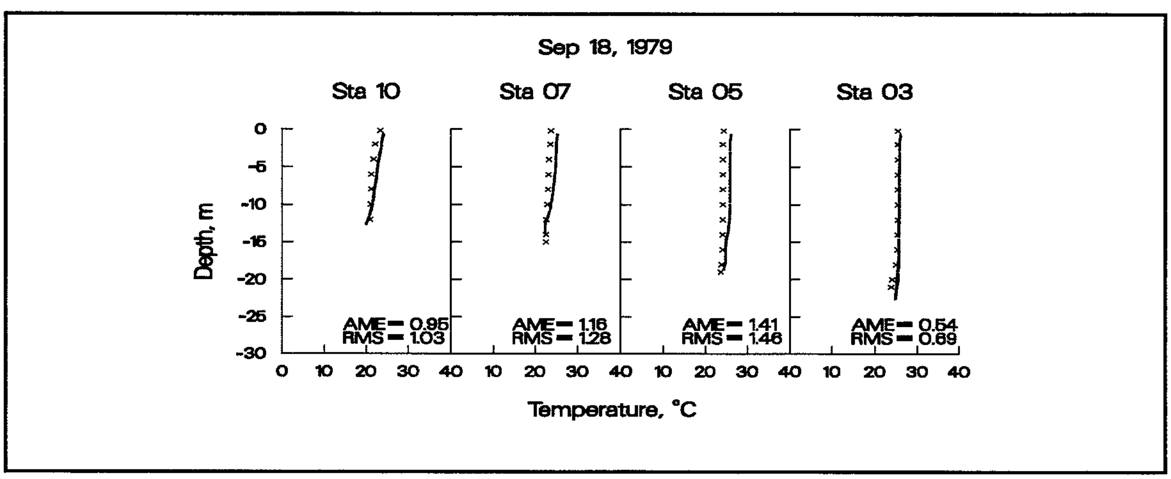

Figure A60. 1979 West Point Reservoir computed (...) versus observed (x) temperatures for stations along the mainstem, September 18

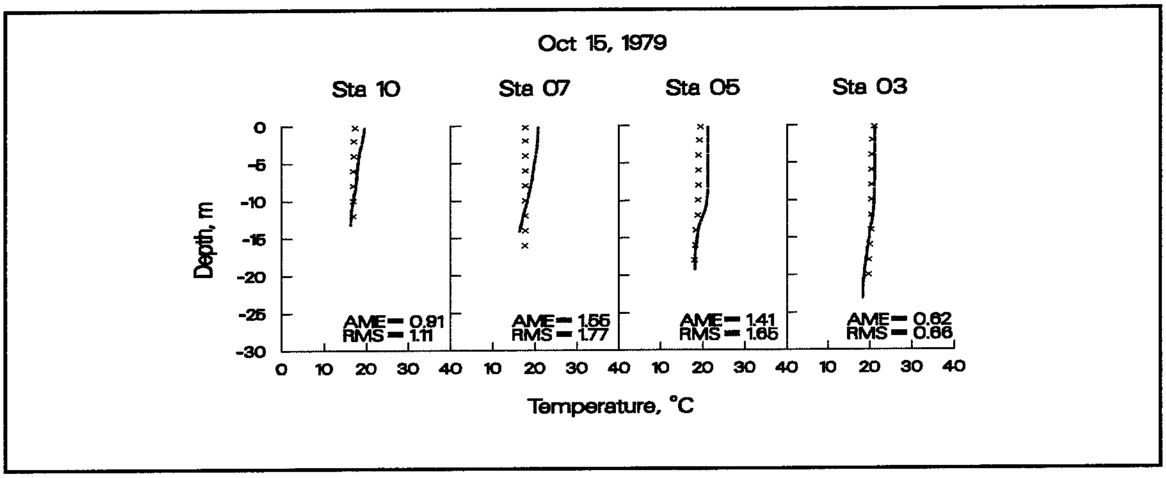

Figure A61. 1979 West Point Reservoir computed (...) versus observed (x) temperatures for stations along the mainstem, October 15

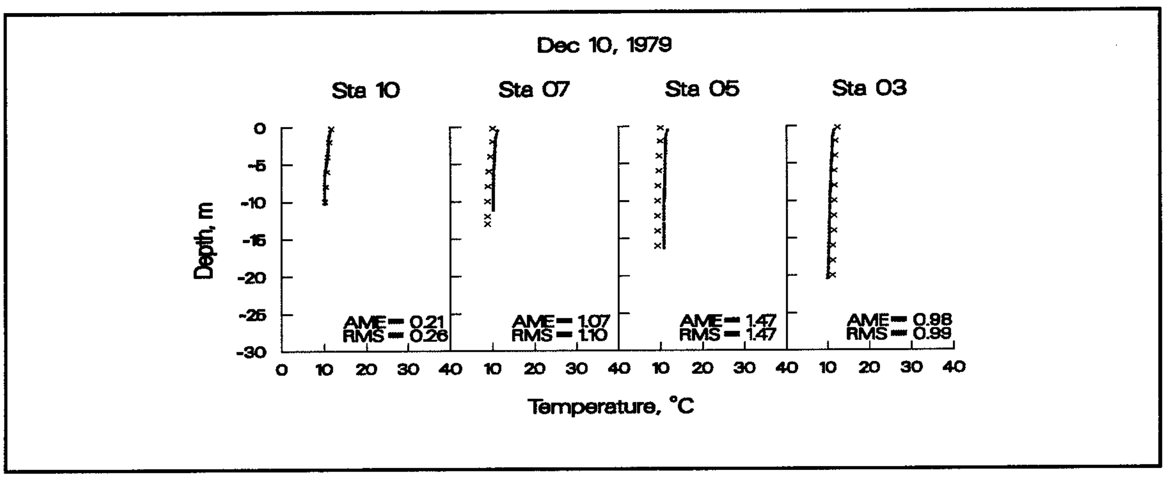

Figure A62. 1979 West Point Reservoir computed (...) versus observed (x) temperatures for stations along the mainstem, December 10

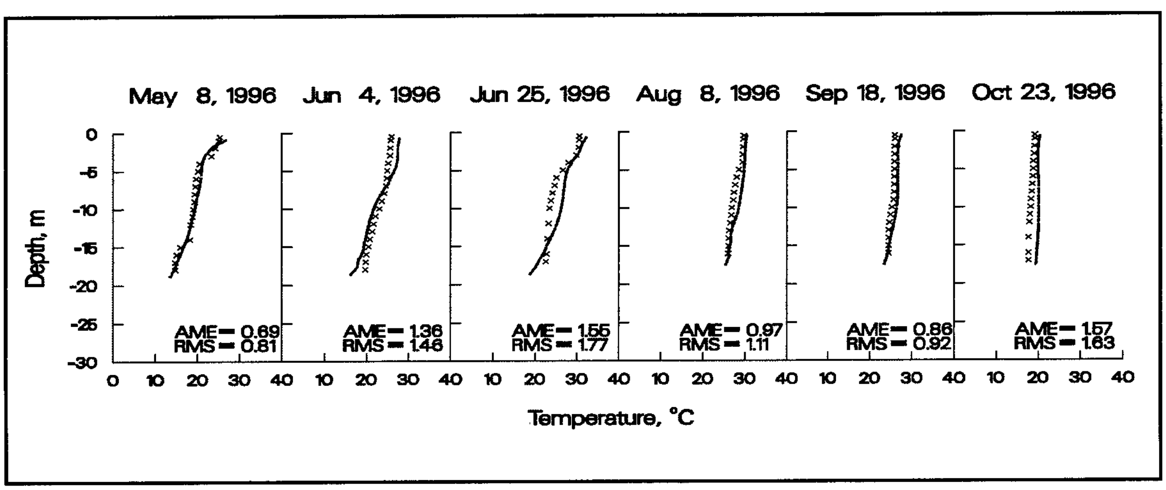

Figure A63. 1996 West Point Reservoir computed (...) versus observed (x) temperatures for station 05

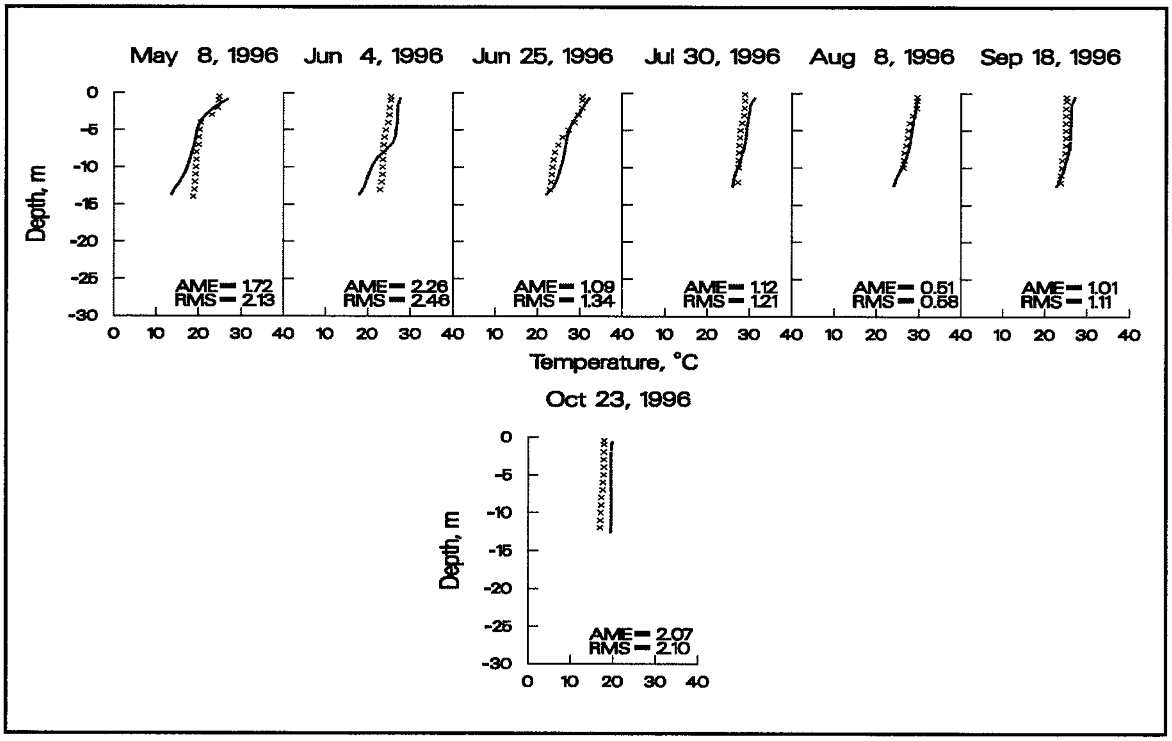

Figure A64. 1996 West Point Reservoir computed (...) versus observed (x) temperatures for station 07

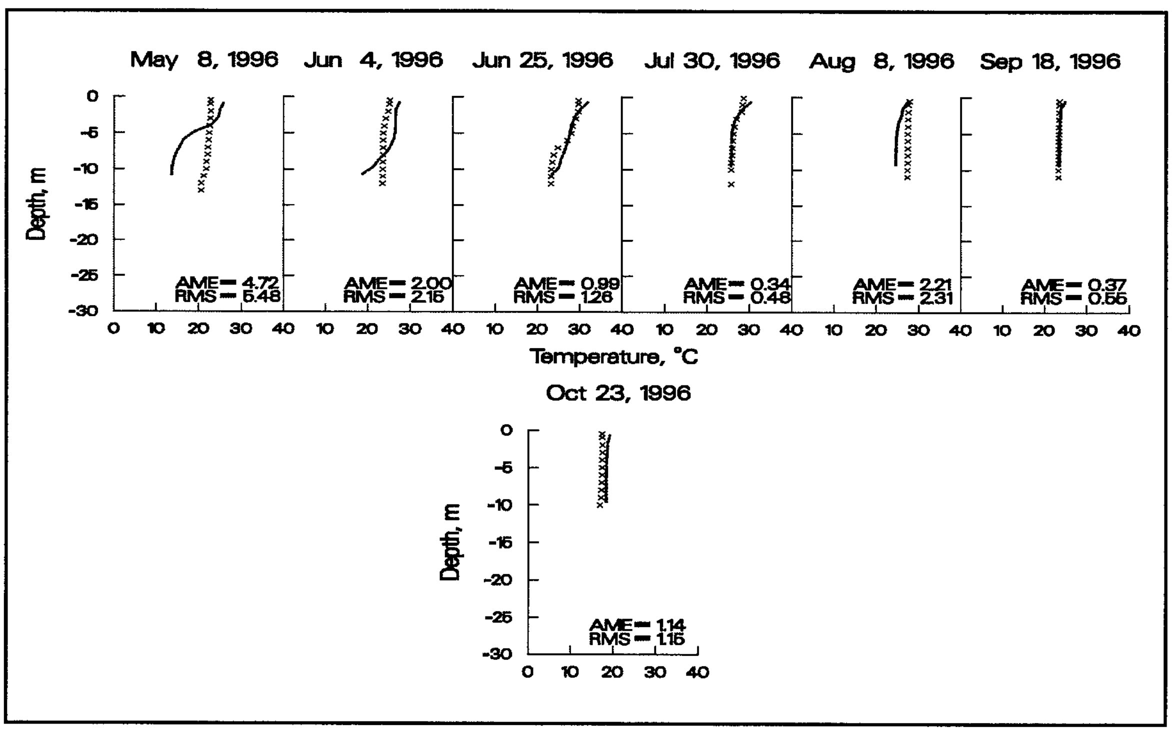

Figure A65. 1996 West Point Reservoir computed (...) versus observed (x) temperatures for station 10

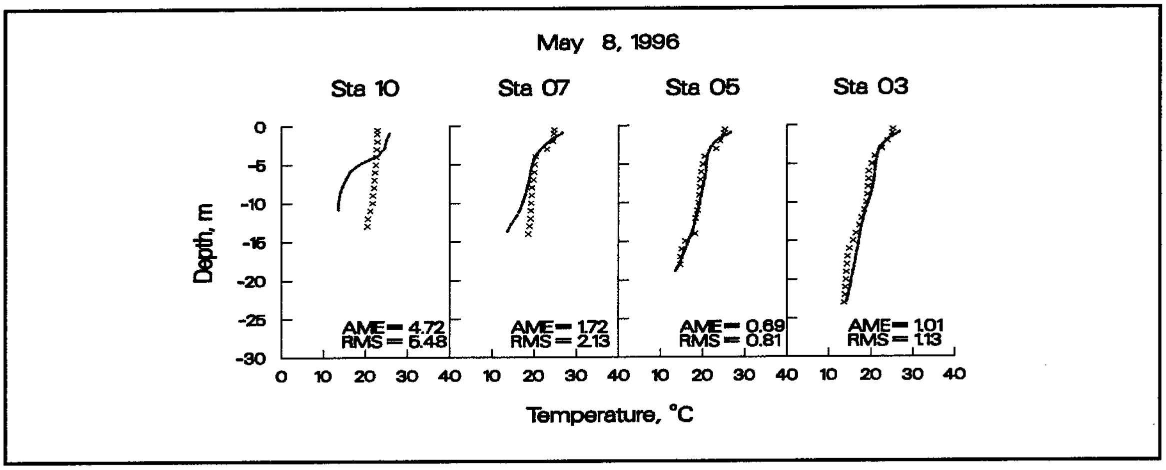

Figure A66. 1996 West Point Reservoir computed (...) versus observed (x) temperatures for stations along the mainstem, May 8

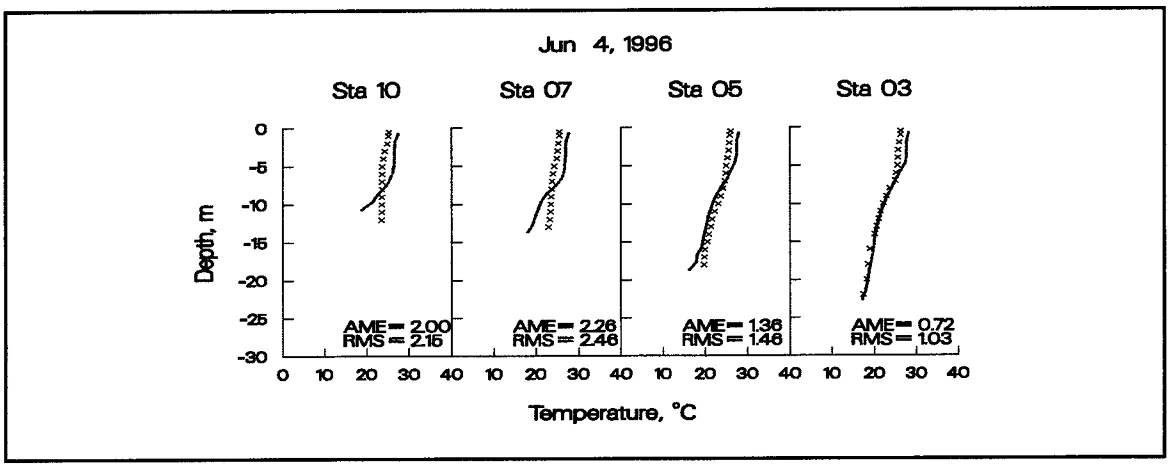

Figure A67. 1996 West Point Reservoir computed (...) versus observed (x) temperatures for stations along the mainstem, June 4

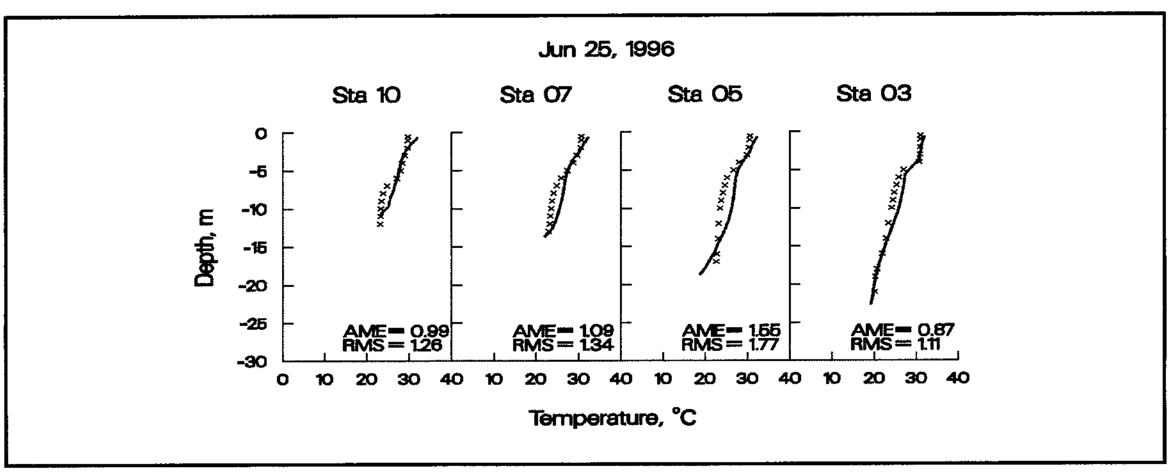

Figure A68. 1996 West Point Reservoir computed (...) versus observed (x) temperatures for stations along the mainstem, June 25

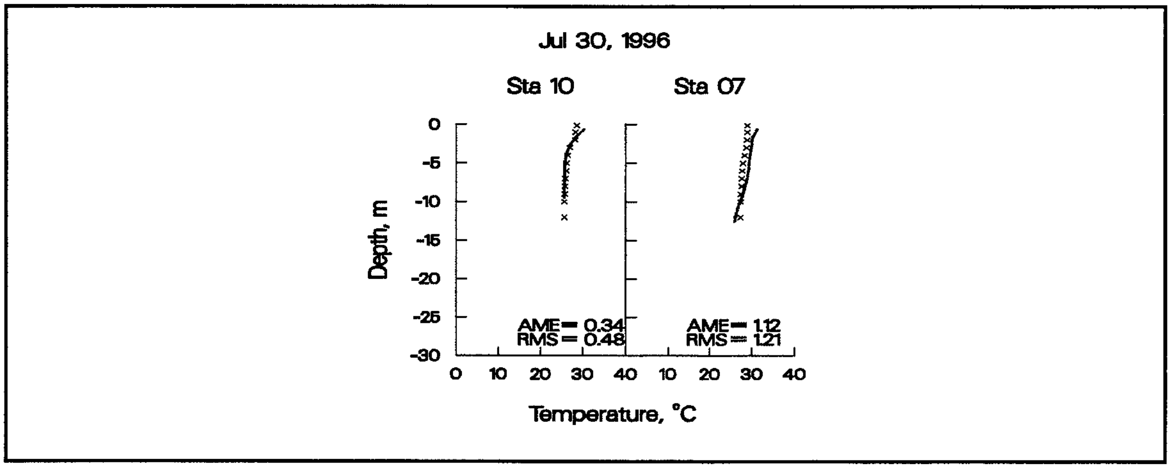

Figure A69. 1996 West Point Reservoir computed (...) versus observed (x) temperatures for stations along the mainstem, July 30

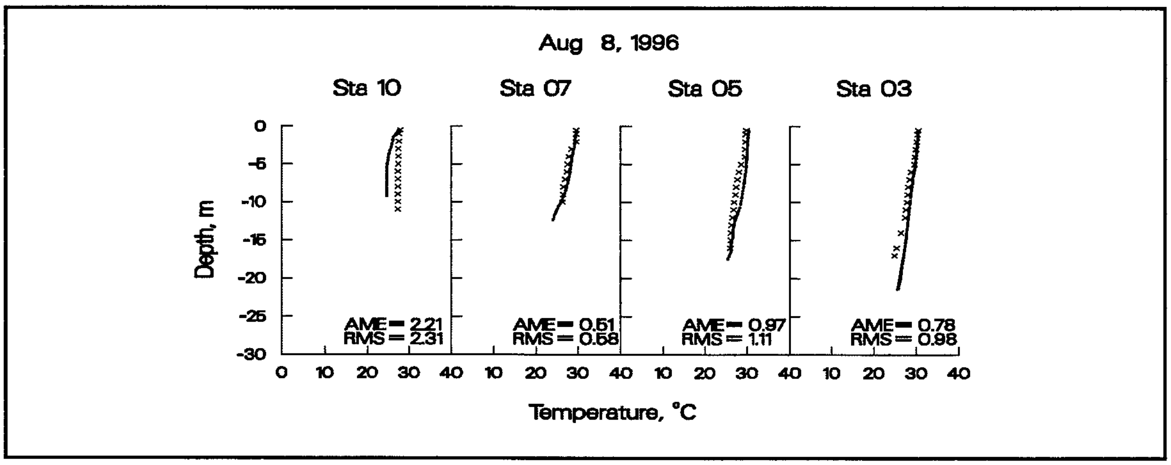

Figure A70. 1996 West Point Reservoir computed (...) versus observed (x) temperatures for stations along the mainstem, August 8

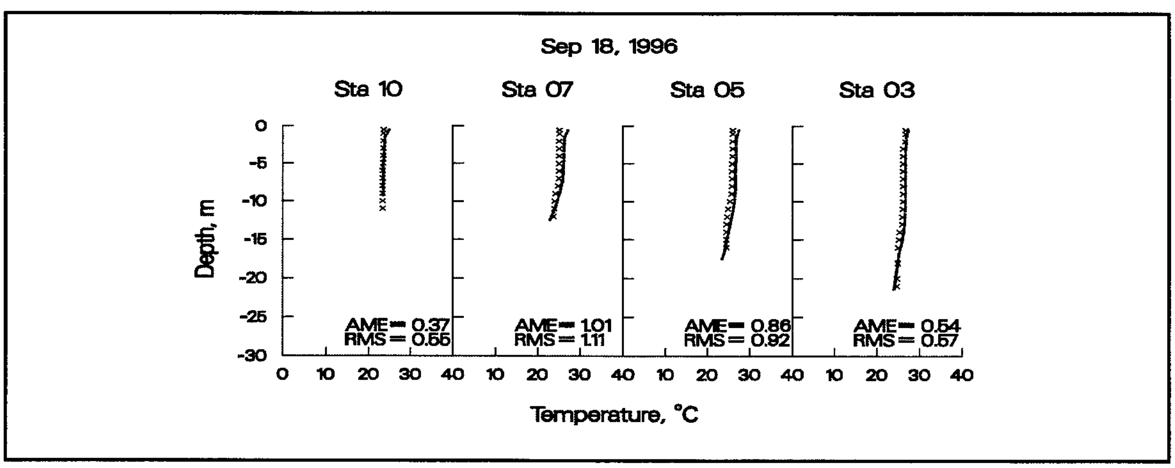

Figure A71. 1996 West Point Reservoir computed (...) versus observed (x) temperatures for stations along the mainstem, September 18

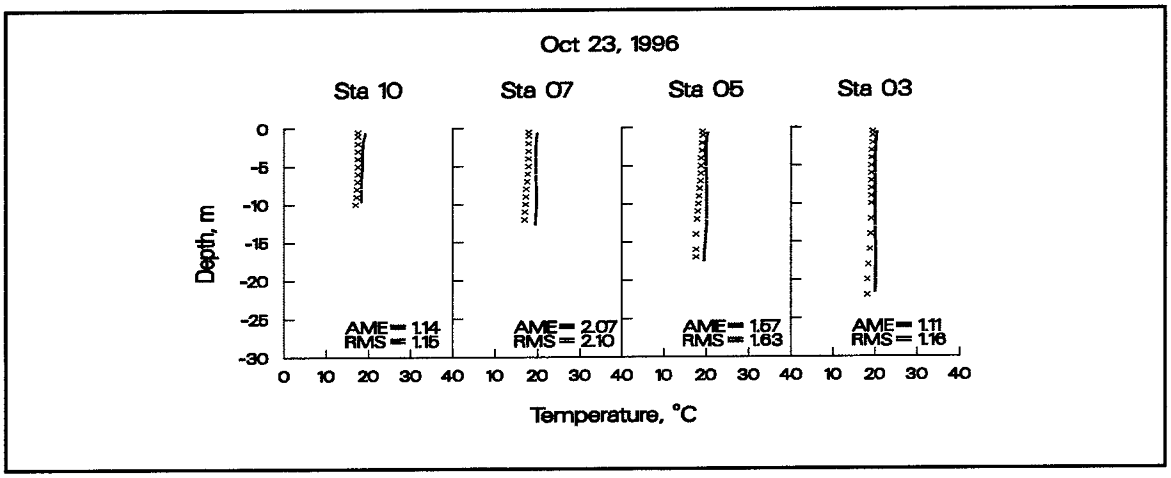

Figure A72. 1996 West Point Reservoir computed (...) versus observed (x) temperatures for stations along the mainstem, October 23

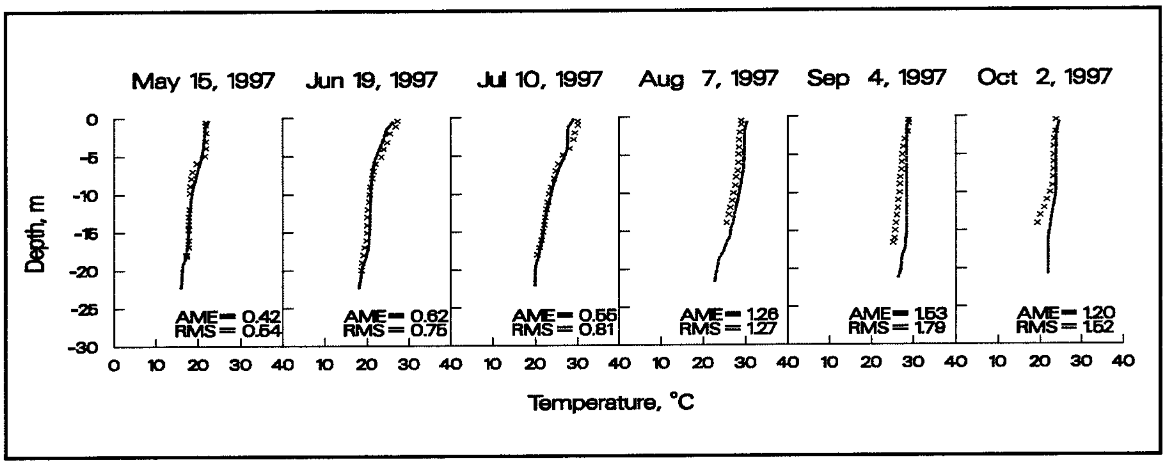

Figure A73. 1997 West Point Reservoir computed (...) versus observed (x) temperatures for station 04

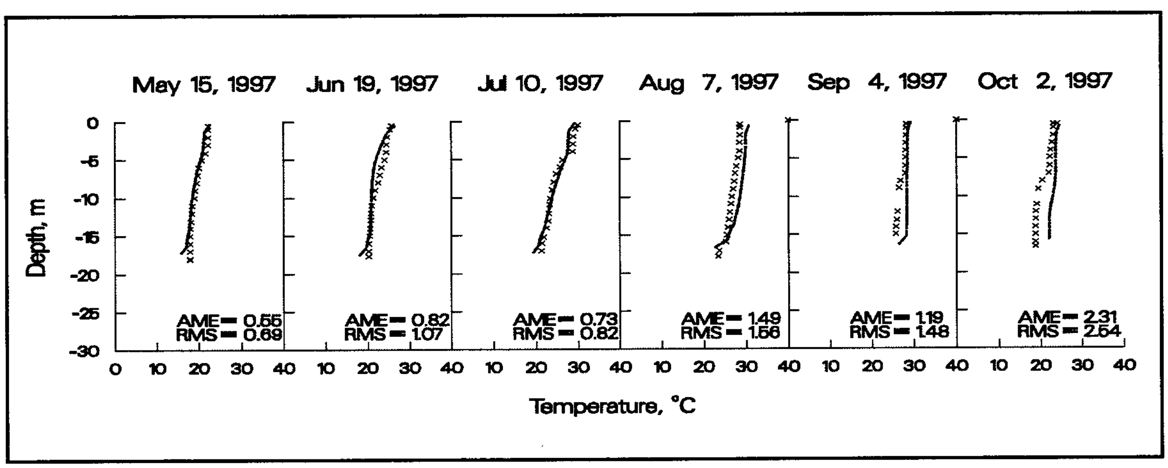

Figure A74. 1997 West Point Reservoir computed (...) versus observed (x) temperatures for station 05

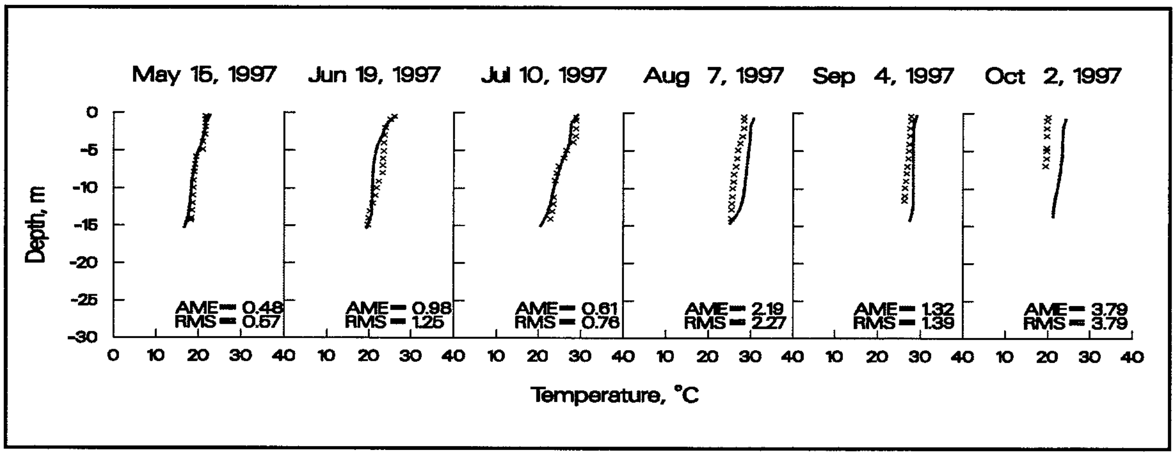

Figure A75. 1997 West Point Reservoir computed (...) versus observed (x) temperatures for station 07

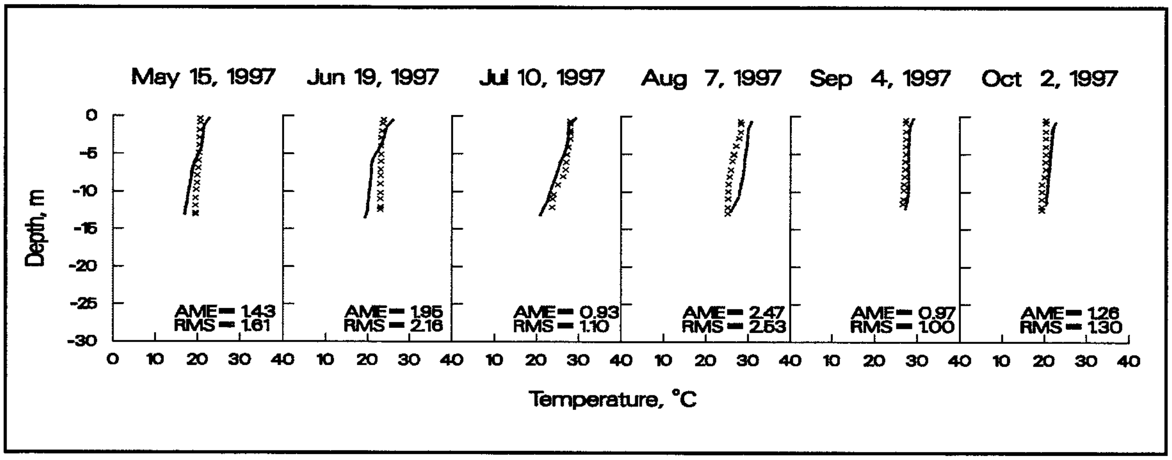

Figure A76. 1997 West Point Reservoir computed (...) versus observed (x) temperatures for station 10

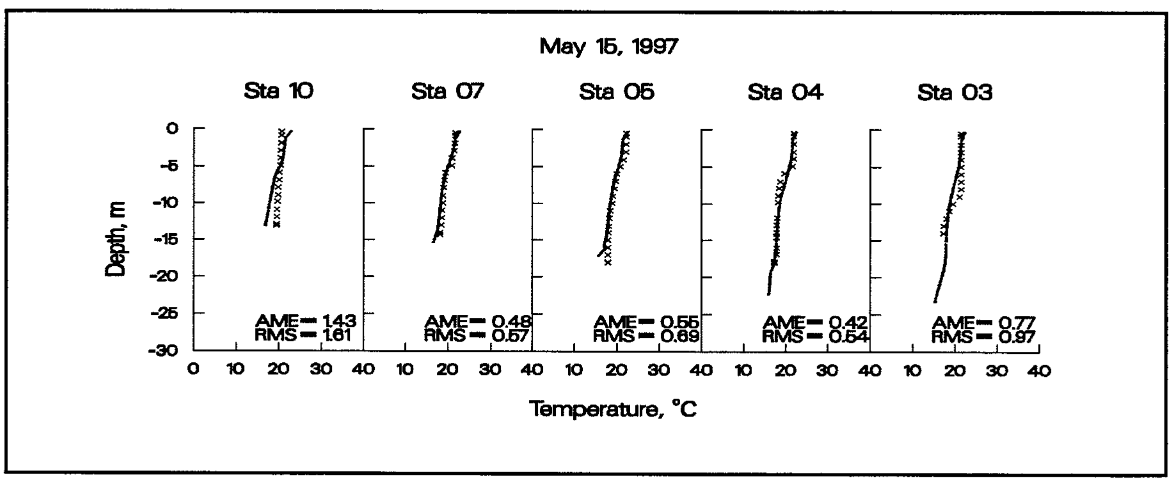

Figure A77. 1997 West Point Reservoir computed (...) versus observed (x) temperatures for stations along the mainstem, May 15

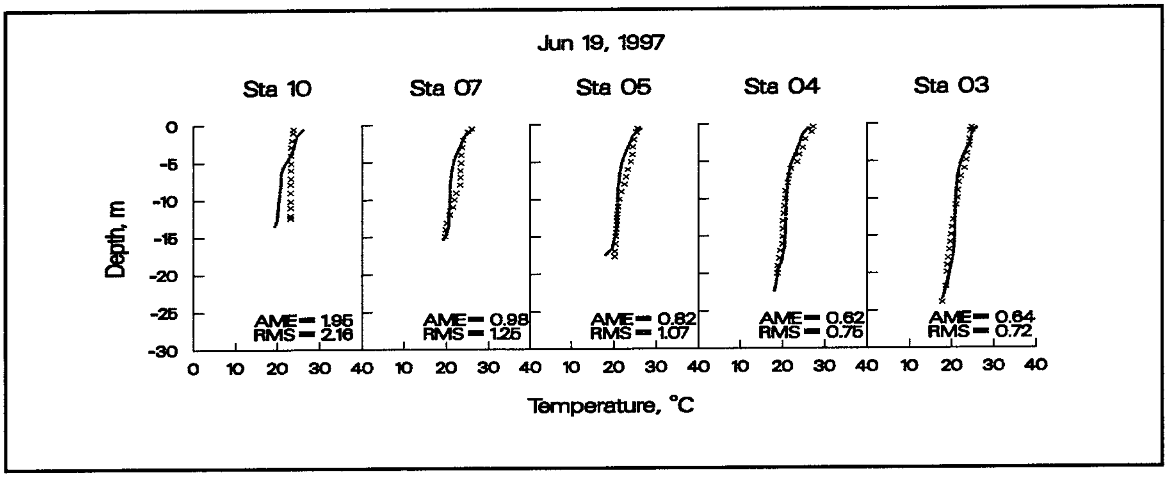

Figure A78. 1997 West Point Reservoir computed (...) versus observed (x) temperatures for stations along the mainstem, June 19

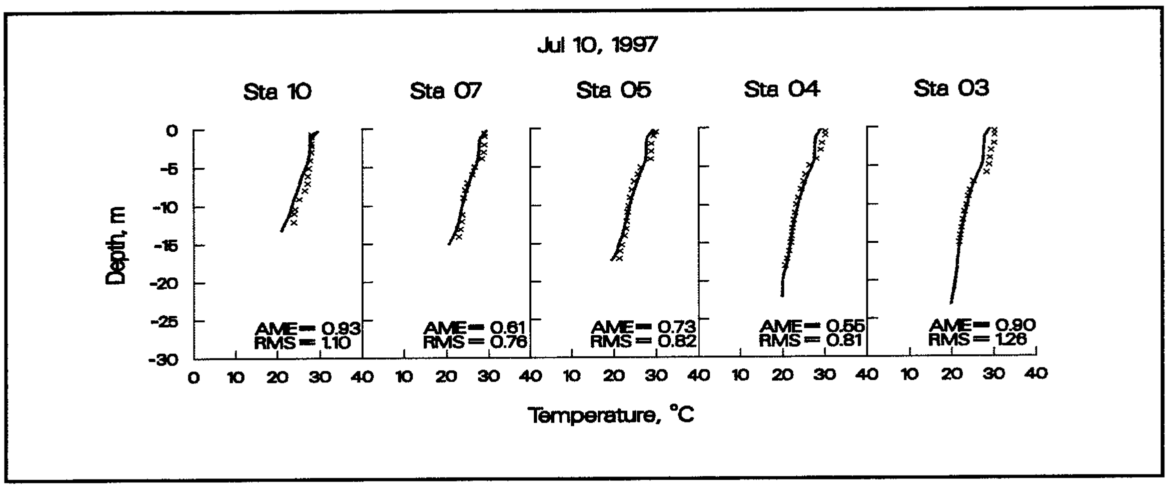

Figure A79. 1997 West Point Reservoir computed (...) versus observed (x) temperatures for stations along the mainstem, July 10

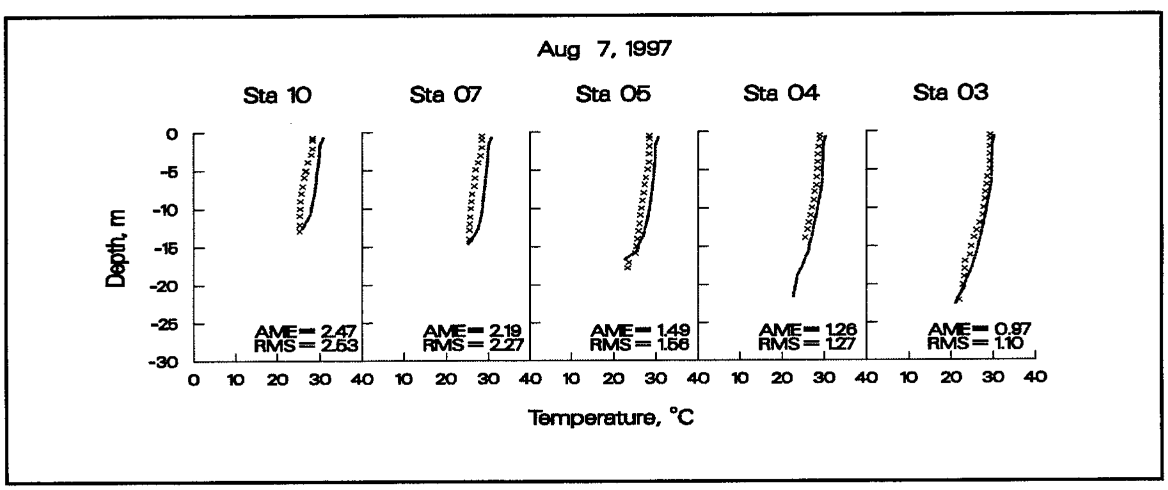

Figure A80. 1997 West Point Reservoir computed (...) versus observed (x) temperatures for stations along the mainstem, August 7

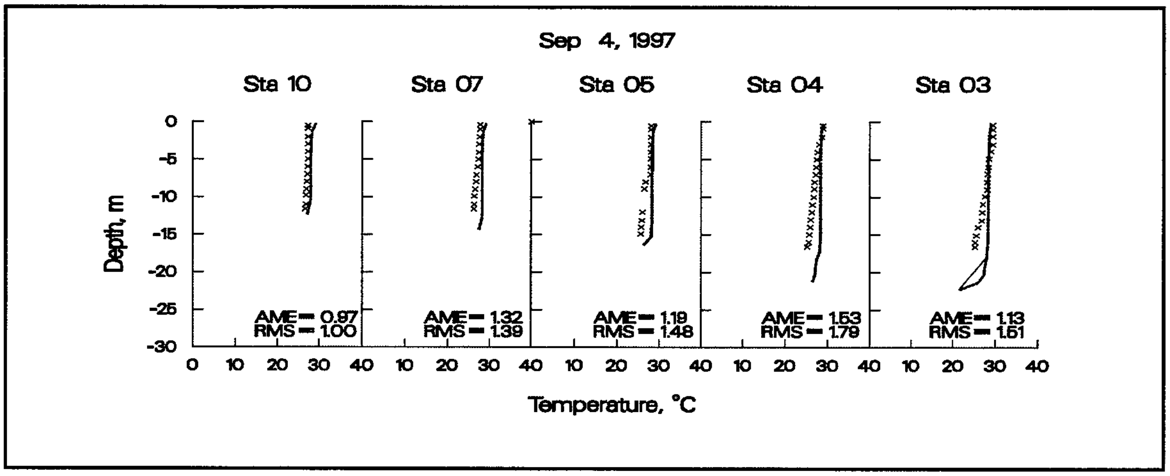

Figure A81. 1997 West Point Reservoir computed (...) versus observed (x) temperatures for stations along the mainstem, September 4

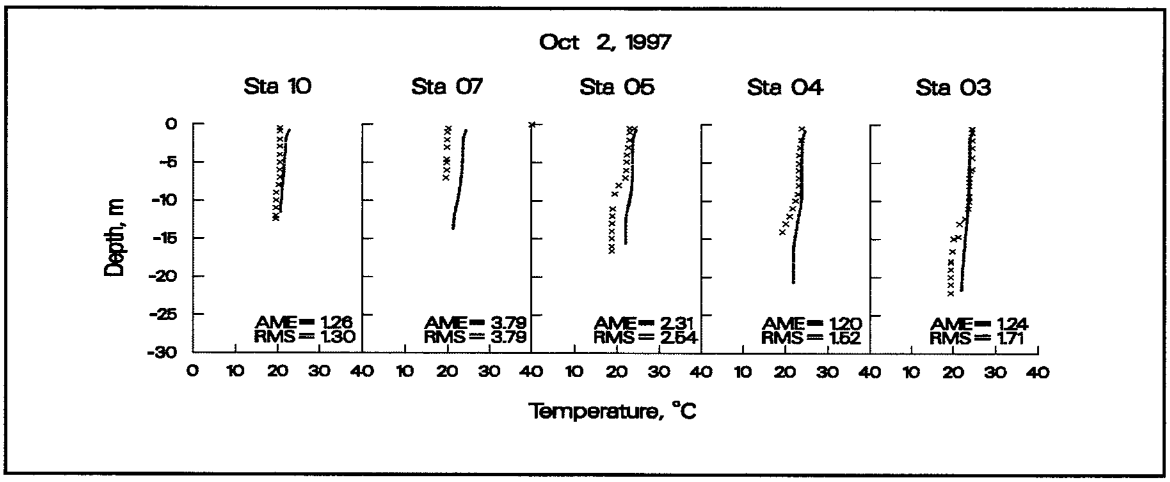

Figure A82. 1997 West Point Reservoir computed (...) versus observed (x) temperatures for stations along the mainstem, October 2

Dissolved Oxygen

Allatoona

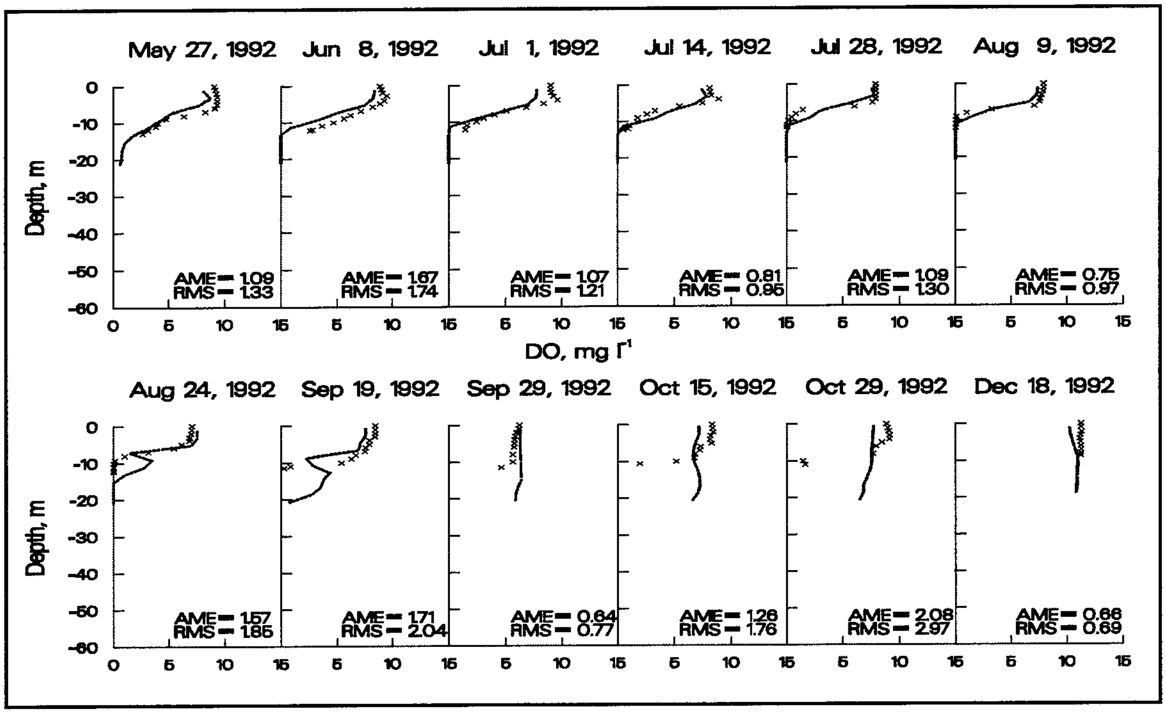

Figure A83. 1992 Allatoona Reservoir computed (...) versus observed (x) DO for station 03

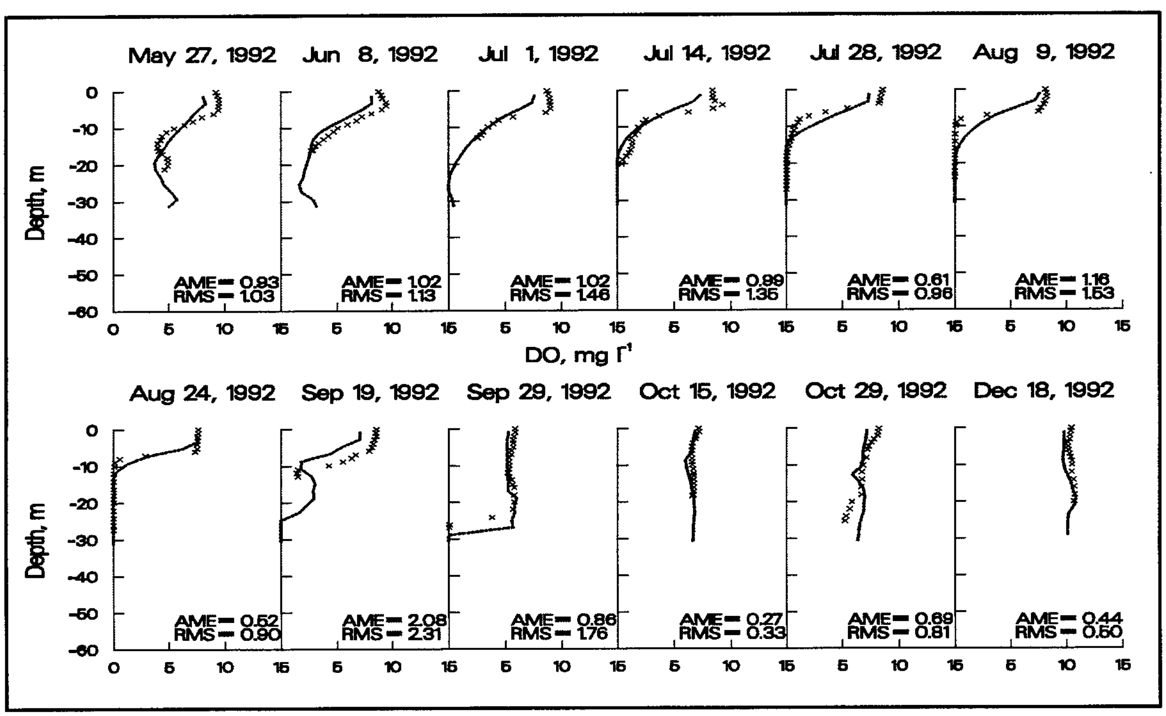

Figure A84. 1992 Allatoona Reservoir computed (...) versus observed (x) DO for station 09

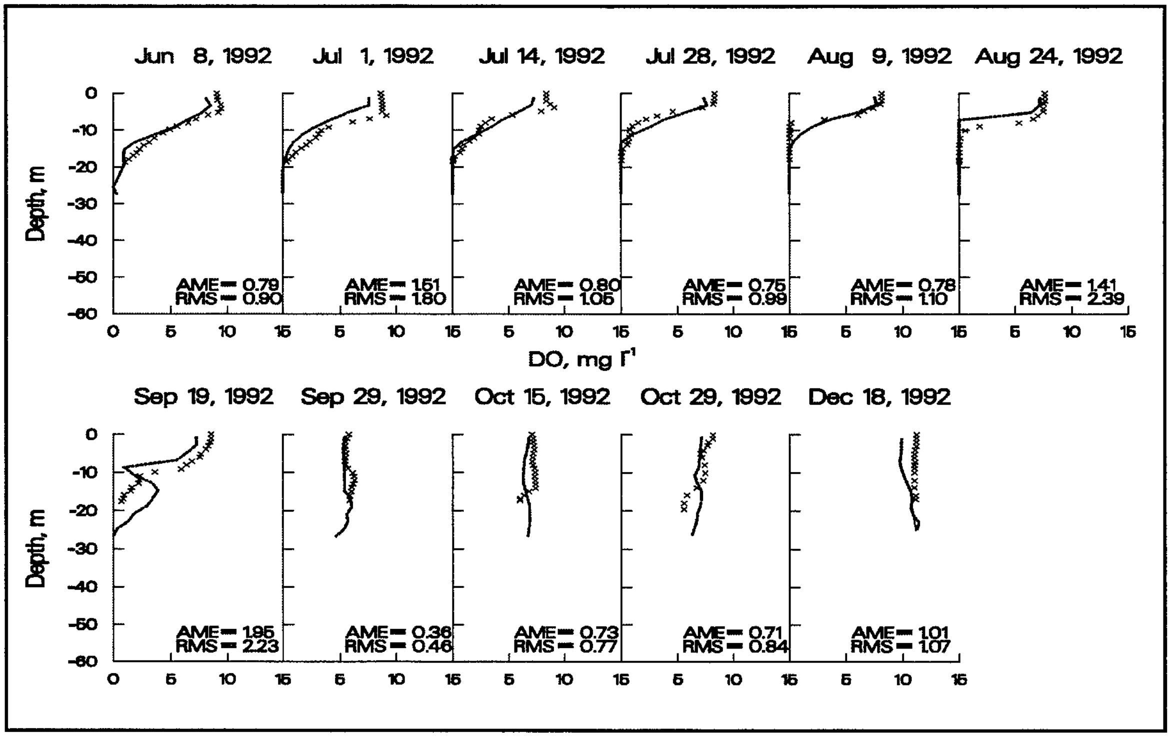

Figure A85. 1992 Allatoona Reservoir computed (...) versus observed (x) DO for station 13

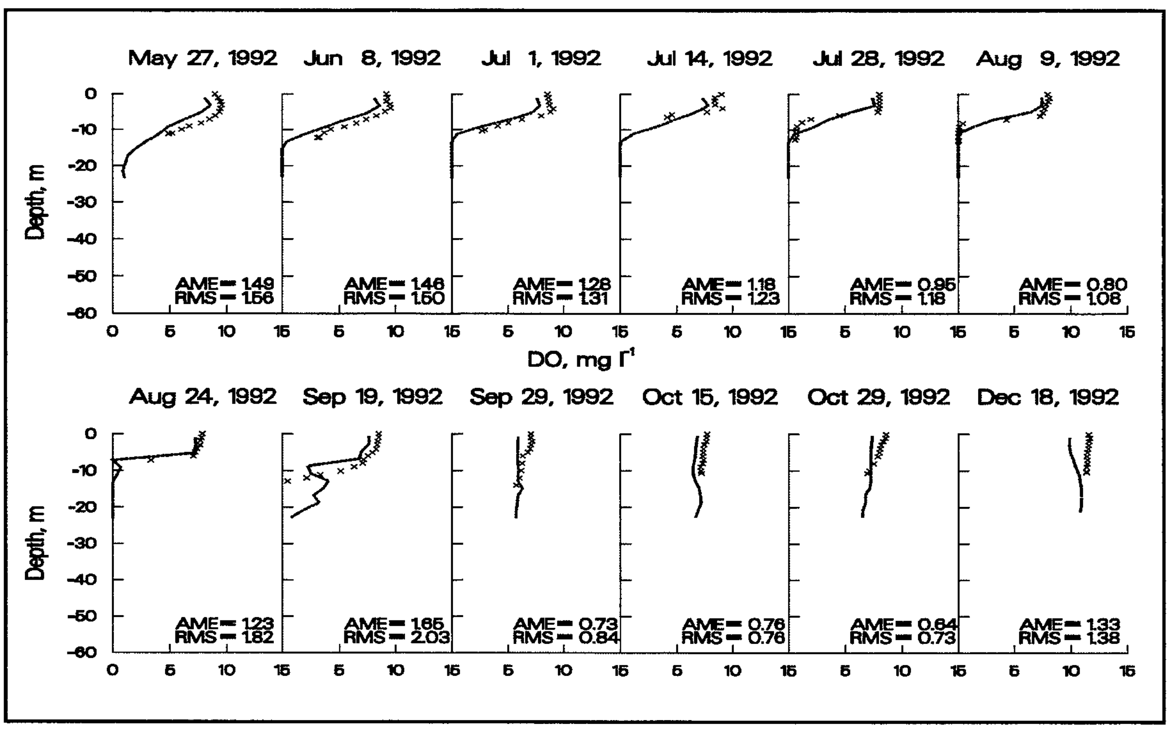

Figure A86. 1992 Allatoona Reservoir computed (...) versus observed (x) DO for station 18

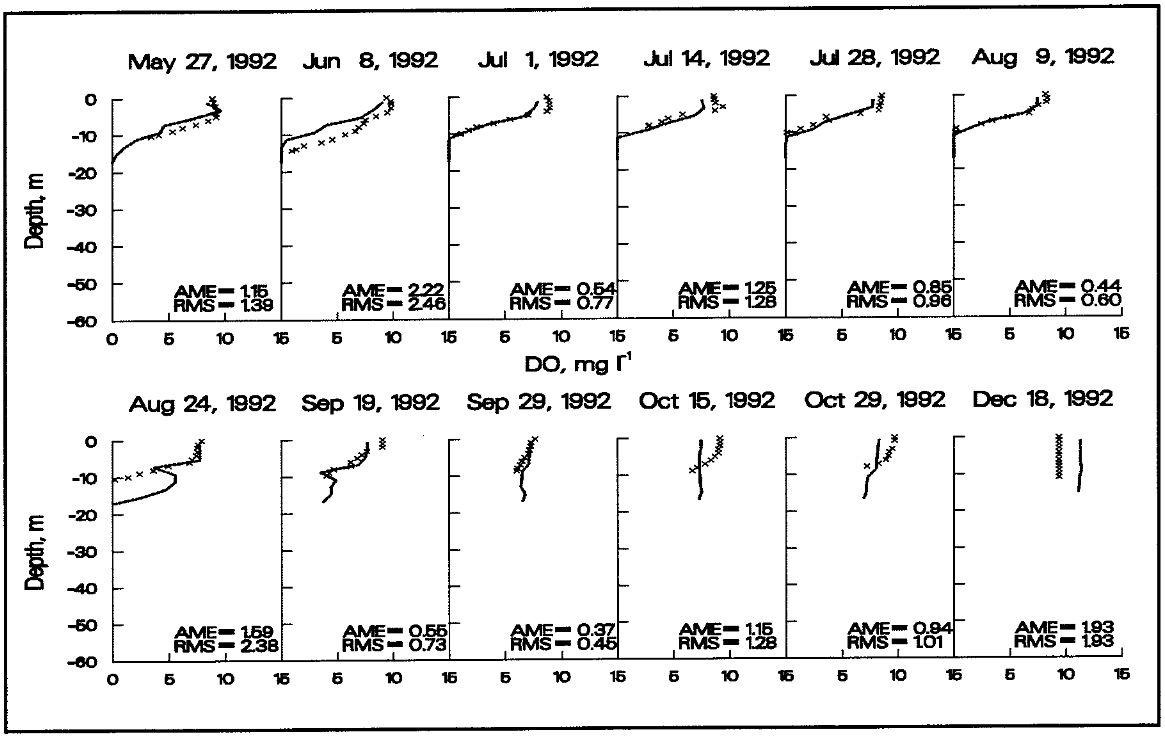

Figure A87. 1992 Allatoona Reservoir computed (...) versus observed (x) DO for station 39

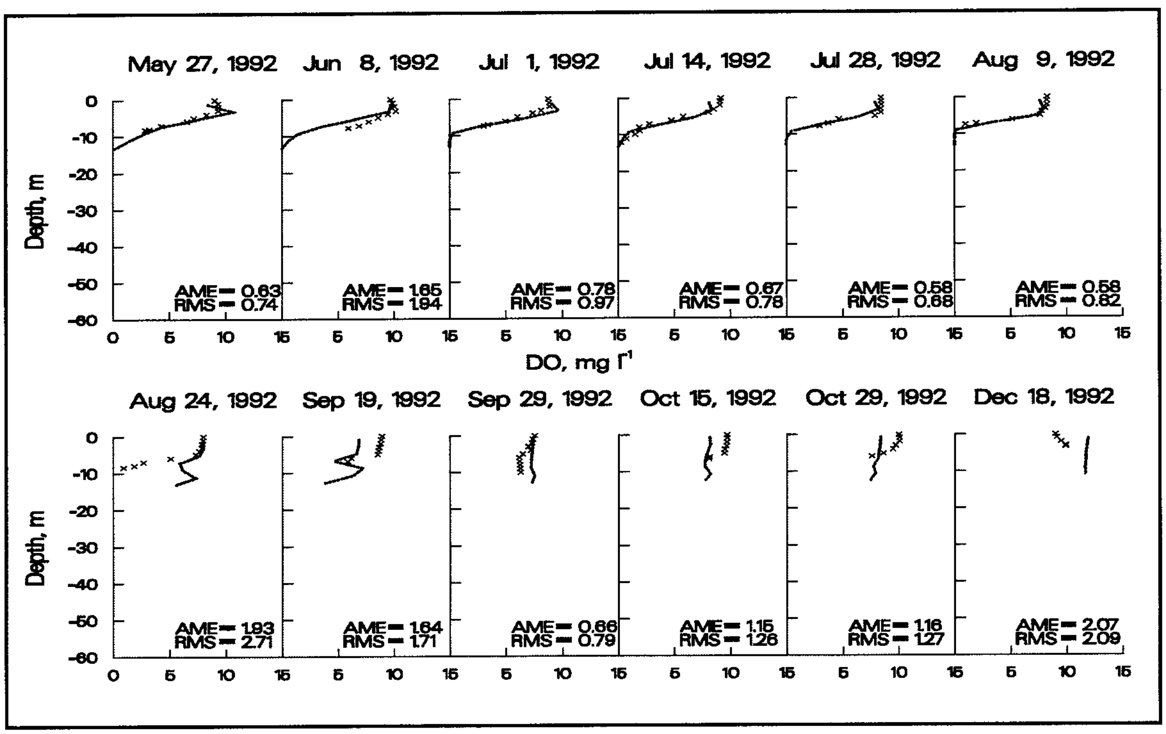

Figure A88. 1992 Allatoona Reservoir computed (...) versus observed (x) DO for station 45

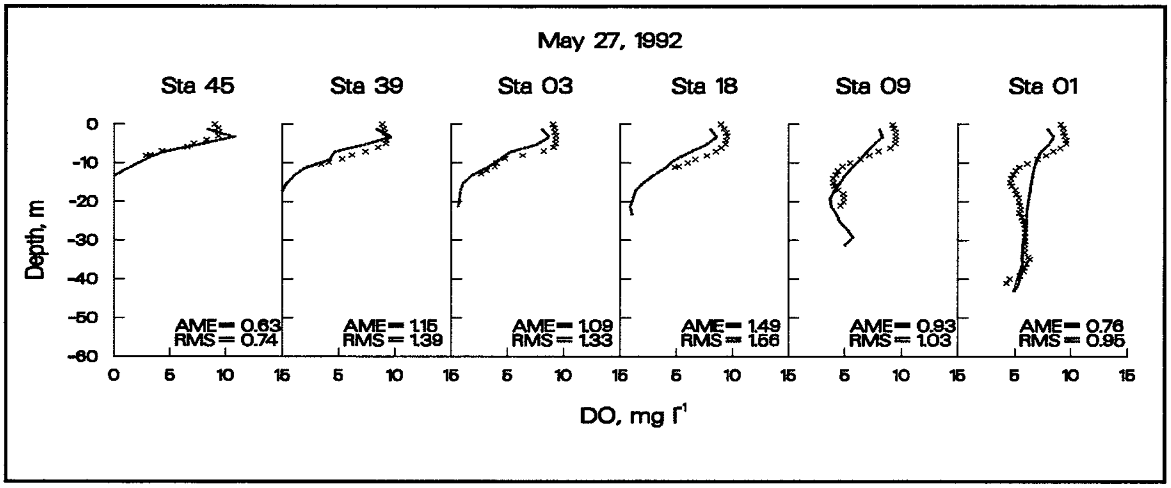

Figure A89. 1992 Allatoona Reservoir computed (...) versus observed (x) DO for stations along the mainstem, May 27

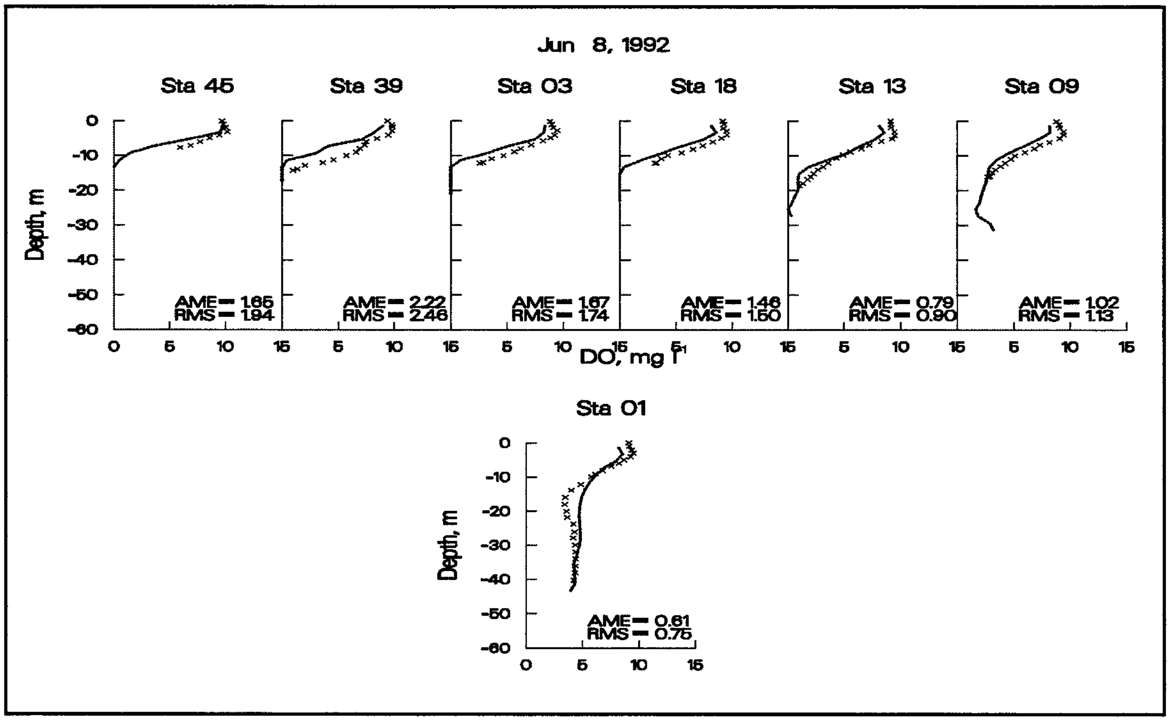

Figure A90. 1992 Allatoona Reservoir computed (...) versus observed (x) DO for stations along the mainstem, June 8

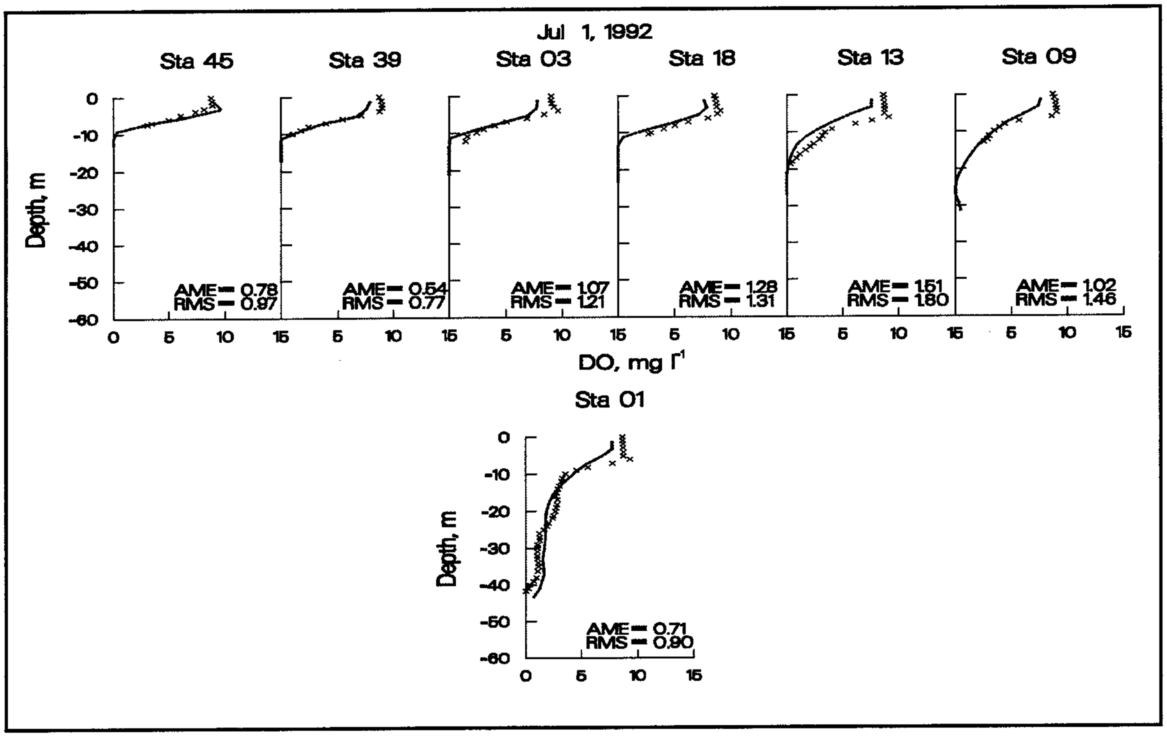

Figure A91. 1992 Allatoona Reservoir computed (...) versus observed (x) DO for stations along the mainstem, July 1

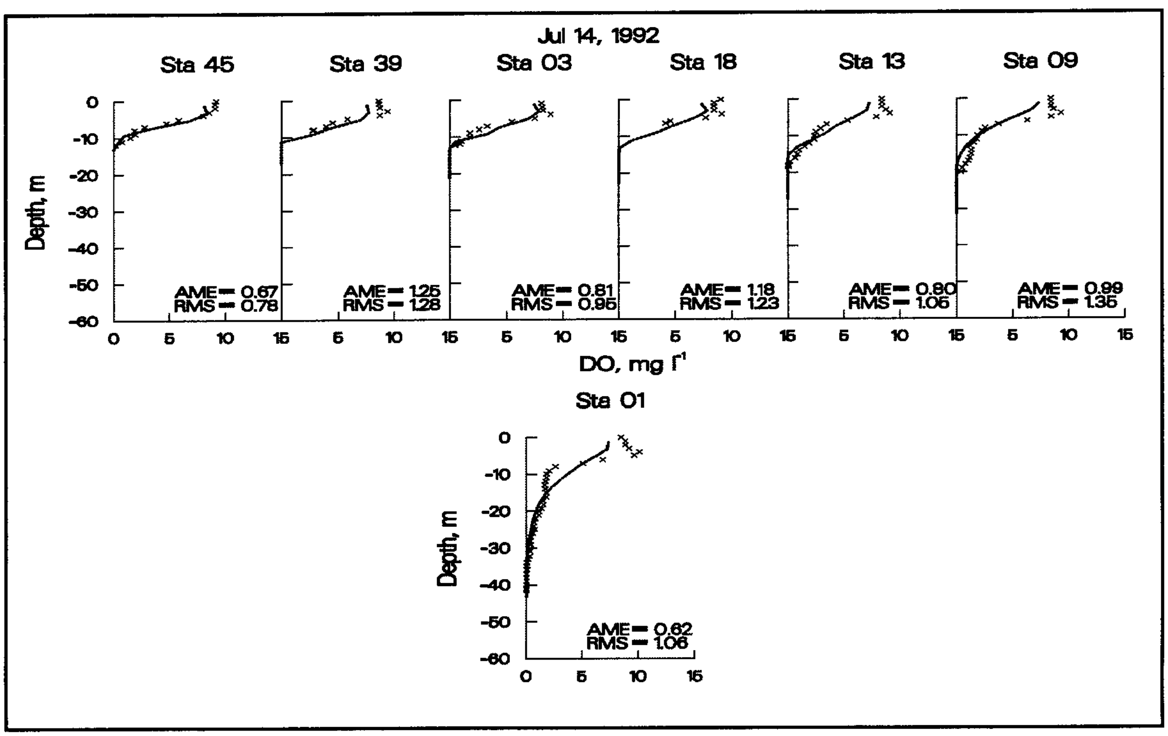

Figure A92. 1992 Allatoona Reservoir computed (...) versus observed (x) DO for stations along the mainstem, July 14

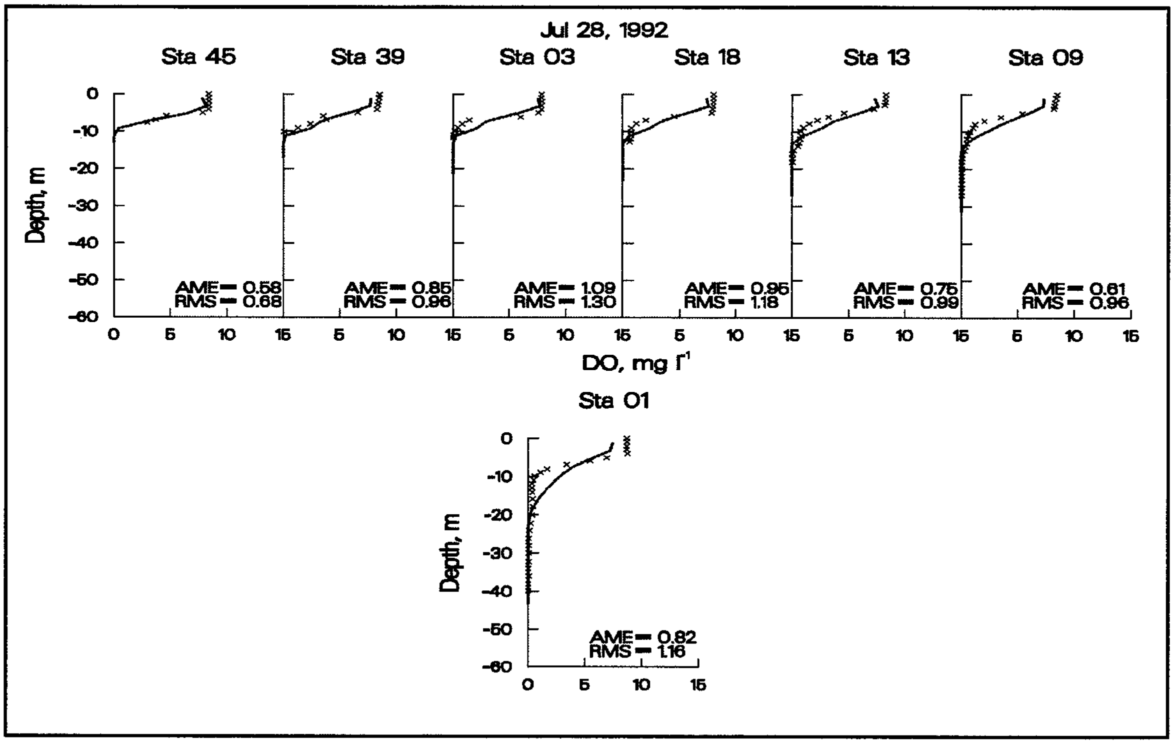

Figure A93. 1992 Allatoona Reservoir computed (...) versus observed (x) DO for stations along the mainstem, July 28

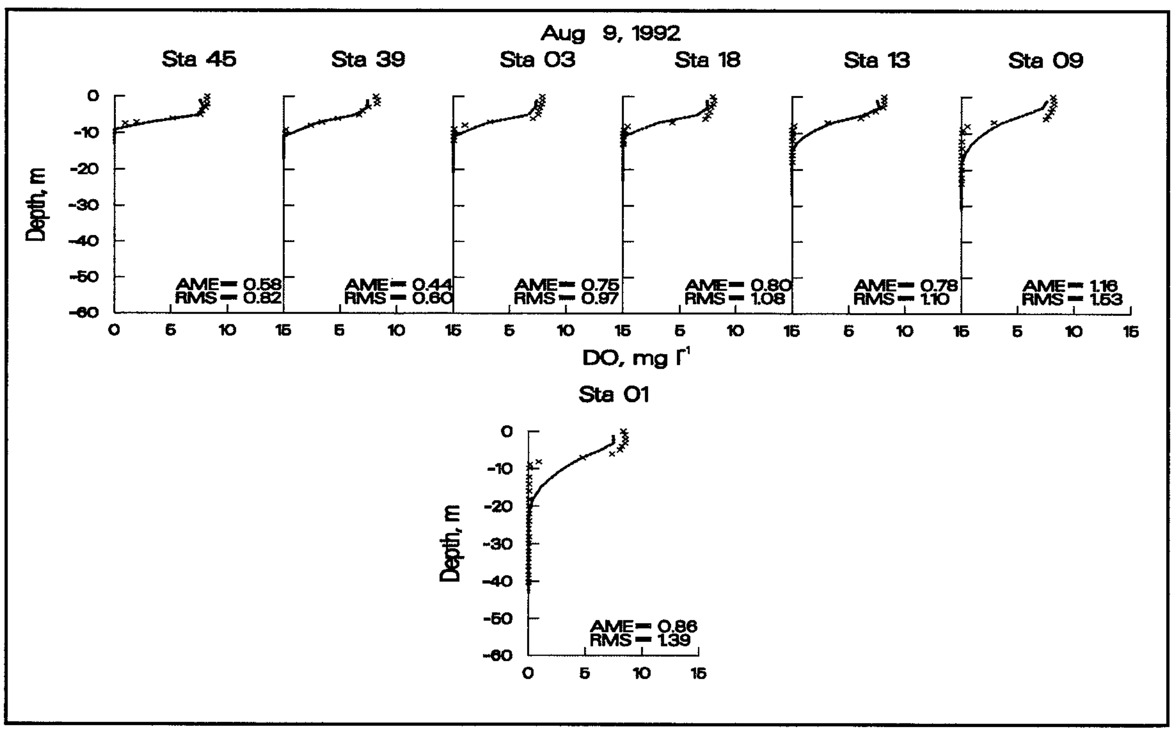

Figure A94. 1992 Allatoona Reservoir computed (...) versus observed (x) DO for stations along the mainstem, August 9

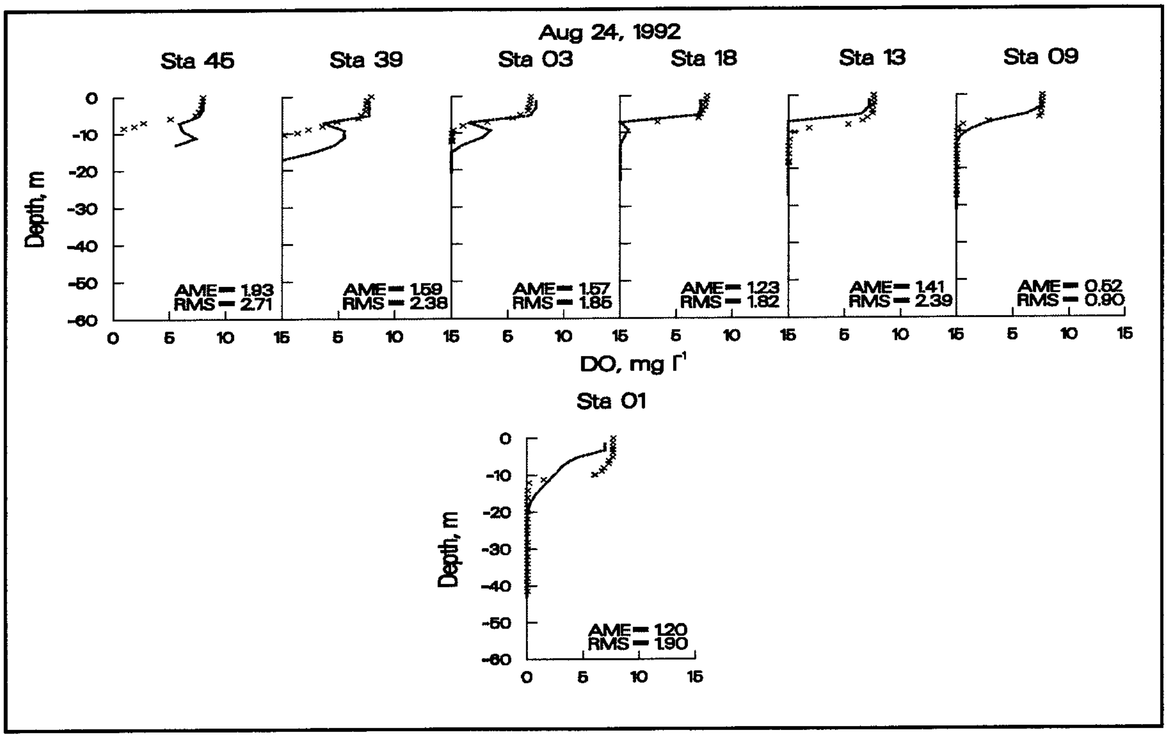

Figure A95. 1992 Allatoona Reservoir computed (...) versus observed (x) DO for stations along the mainstem, August 24

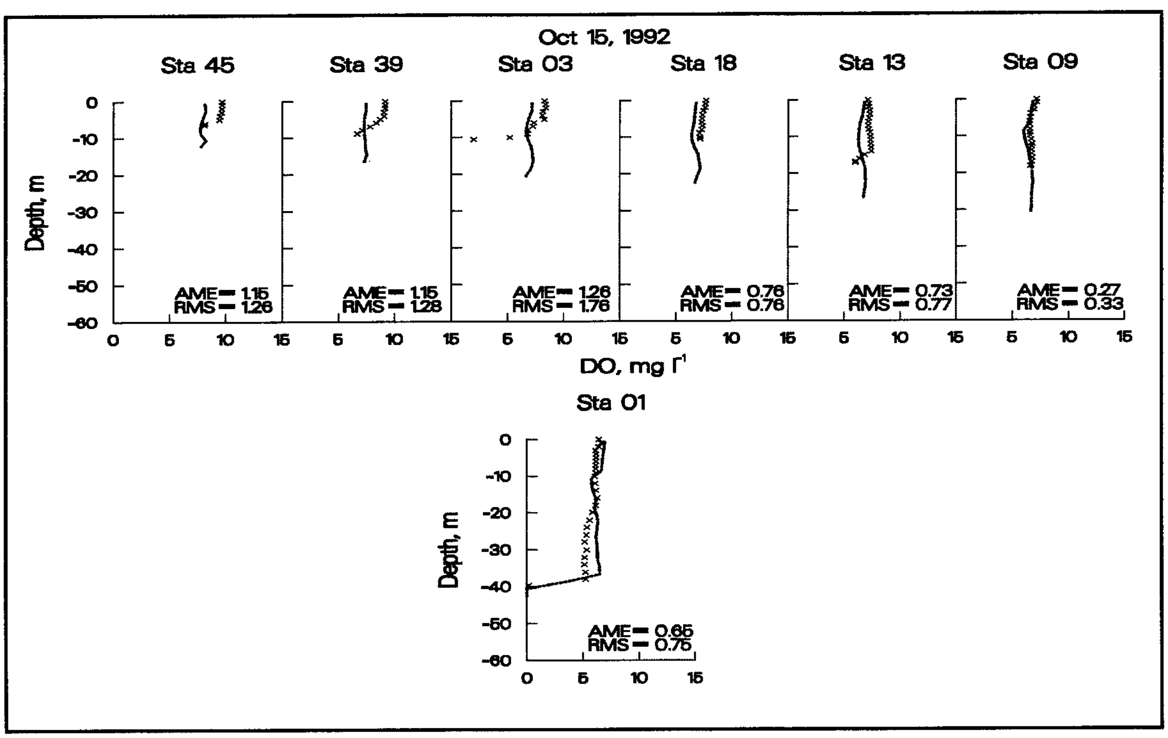

Figure A96. 1992 Allatoona Reservoir computed (...) versus observed (x) DO for stations along the mainstem, October 15

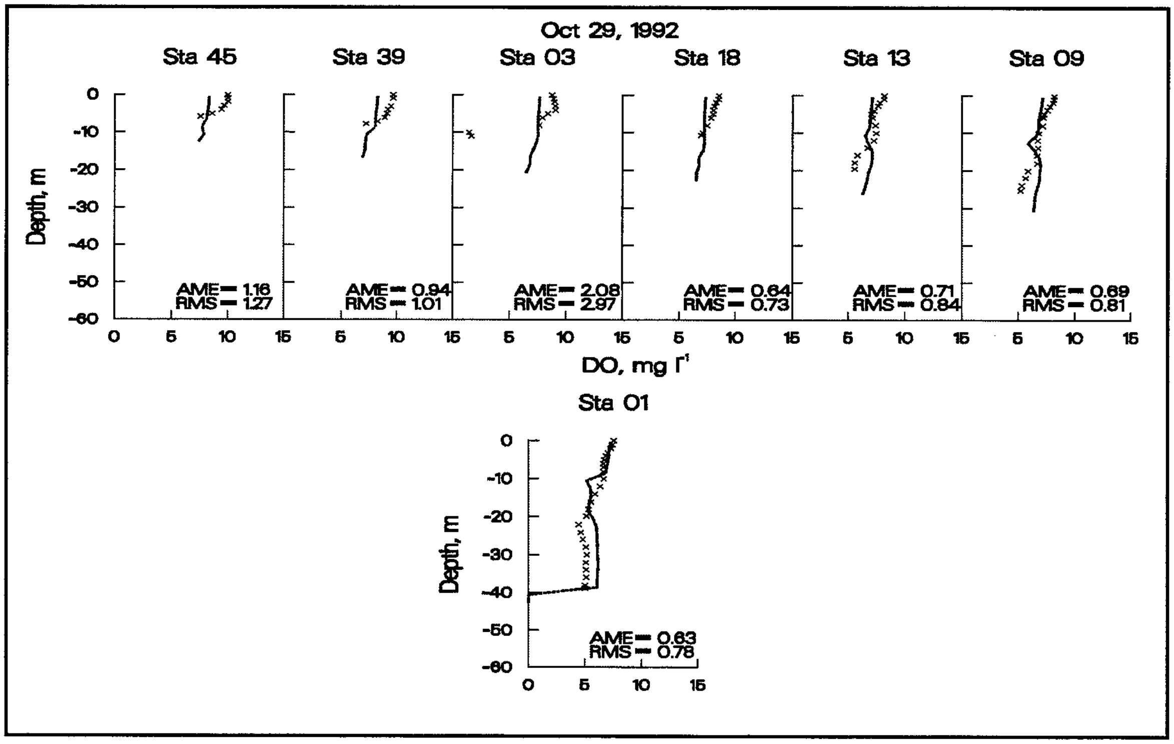

Figure A97. 1992 Allatoona Reservoir computed (...) versus observed (x) DO for stations along the mainstem, October 29

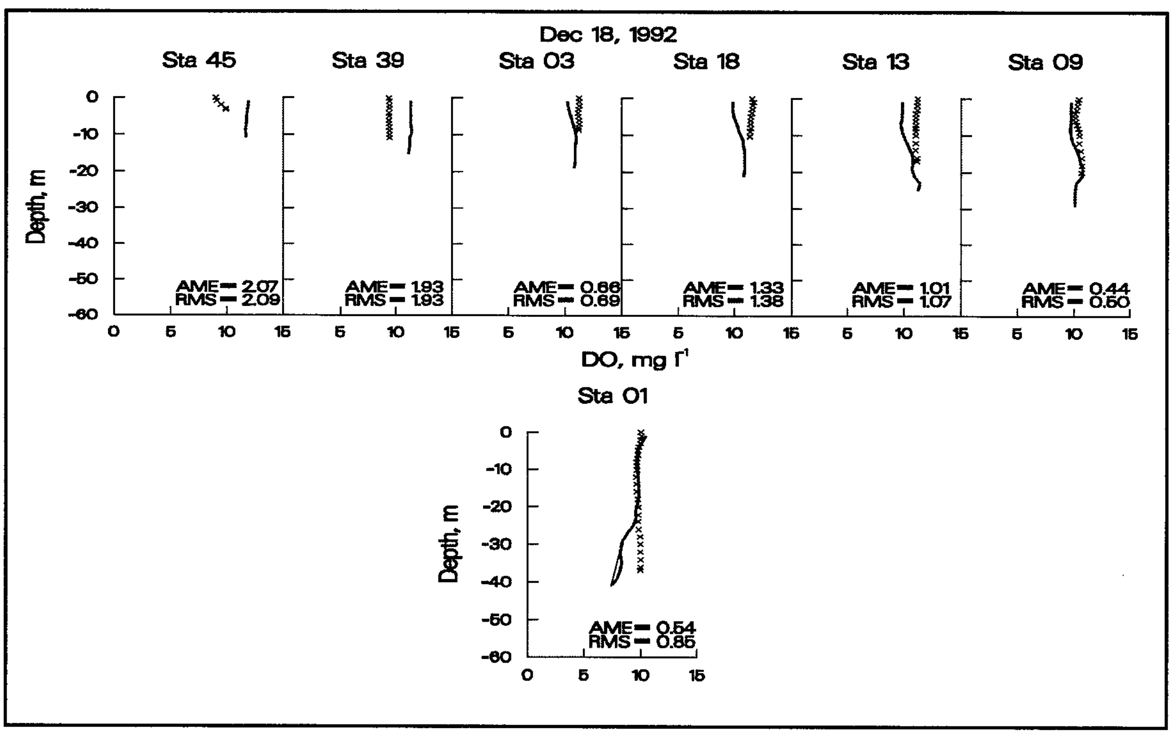

Figure A98. 1992 Allatoona Reservoir computed (...) versus observed (x) DO for stations along the mainstem, December 18

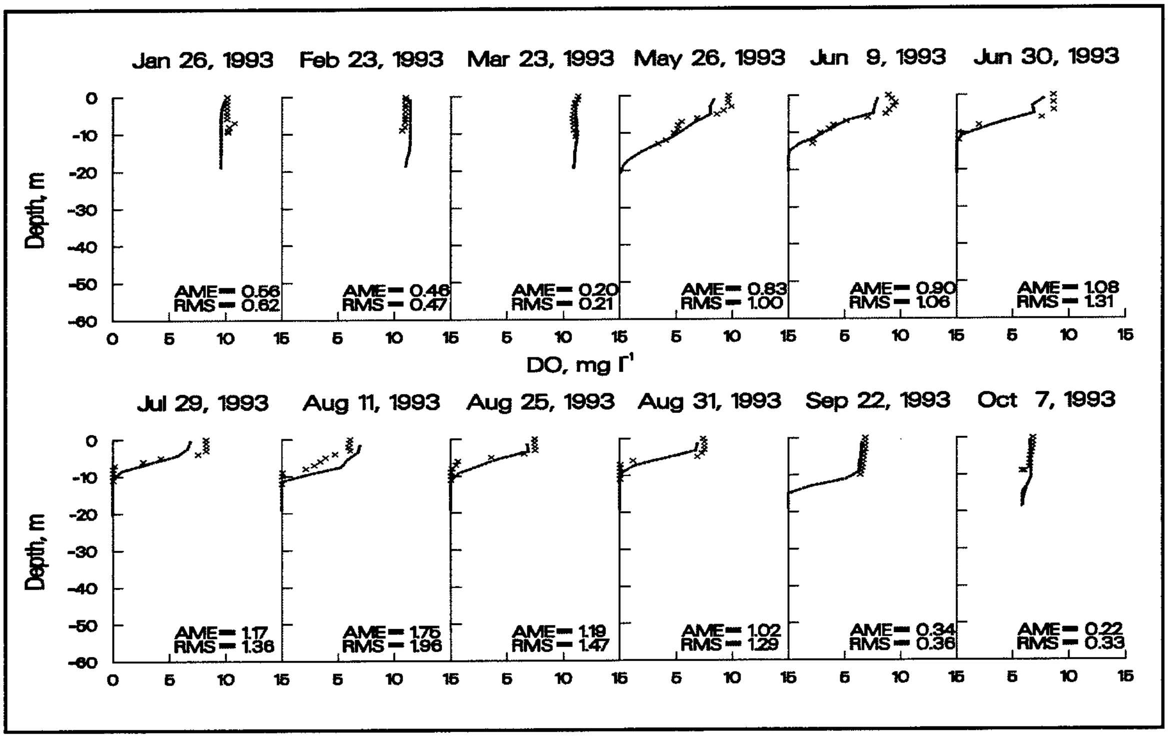

Figure A99. 1993 Allatoona Reservoir computed (...) versus observed (x) DO for station 03

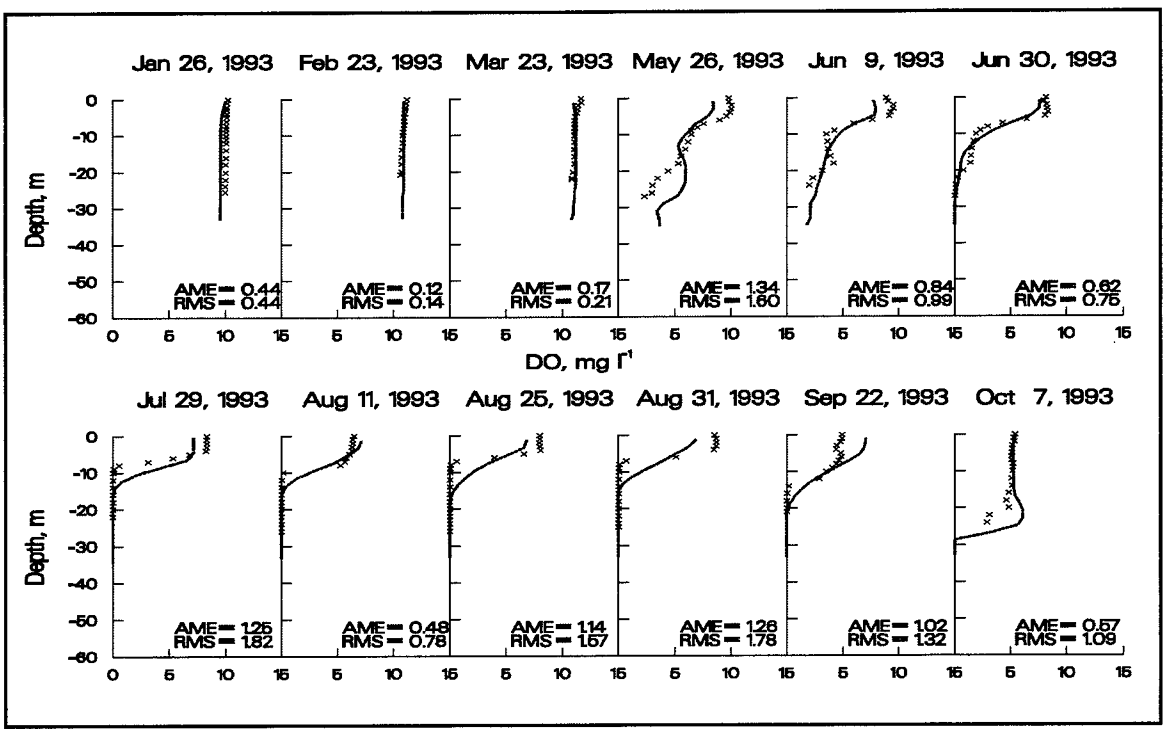

Figure A100. 1993 Allatoona Reservoir computed (...) versus observed (x) DO for station 09

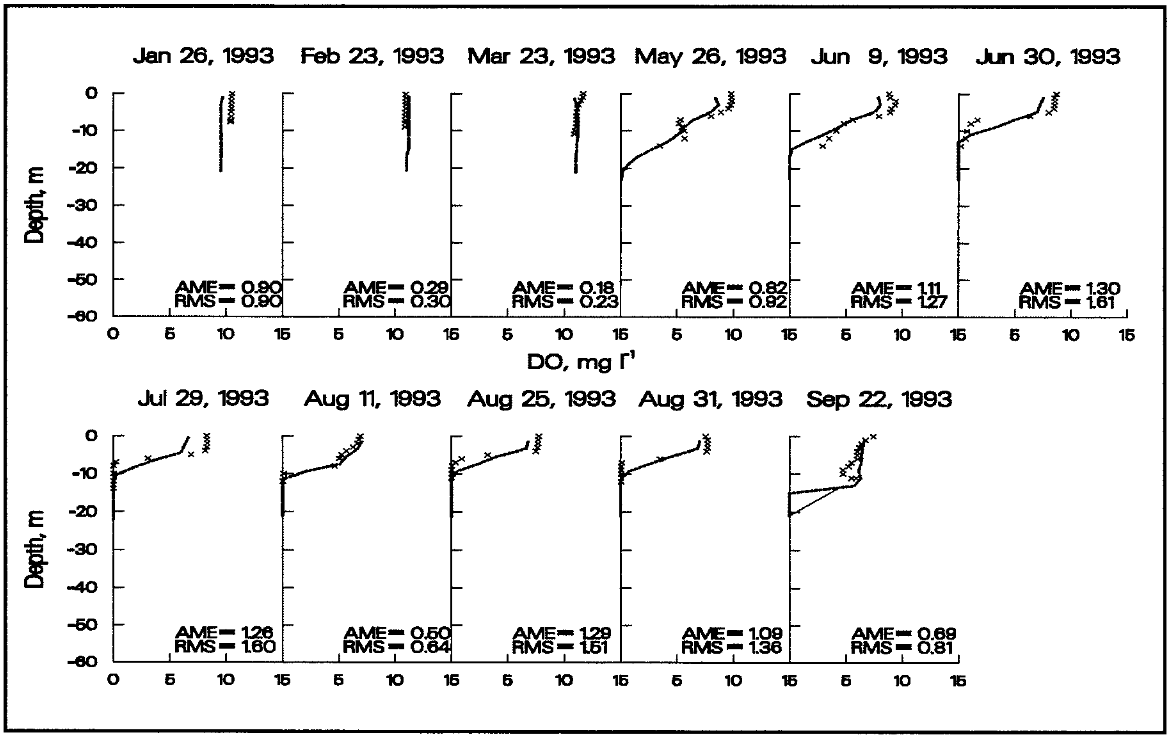

Figure A101. 1993 Allatoona Reservoir computed (...) versus observed (x) DO for station 18

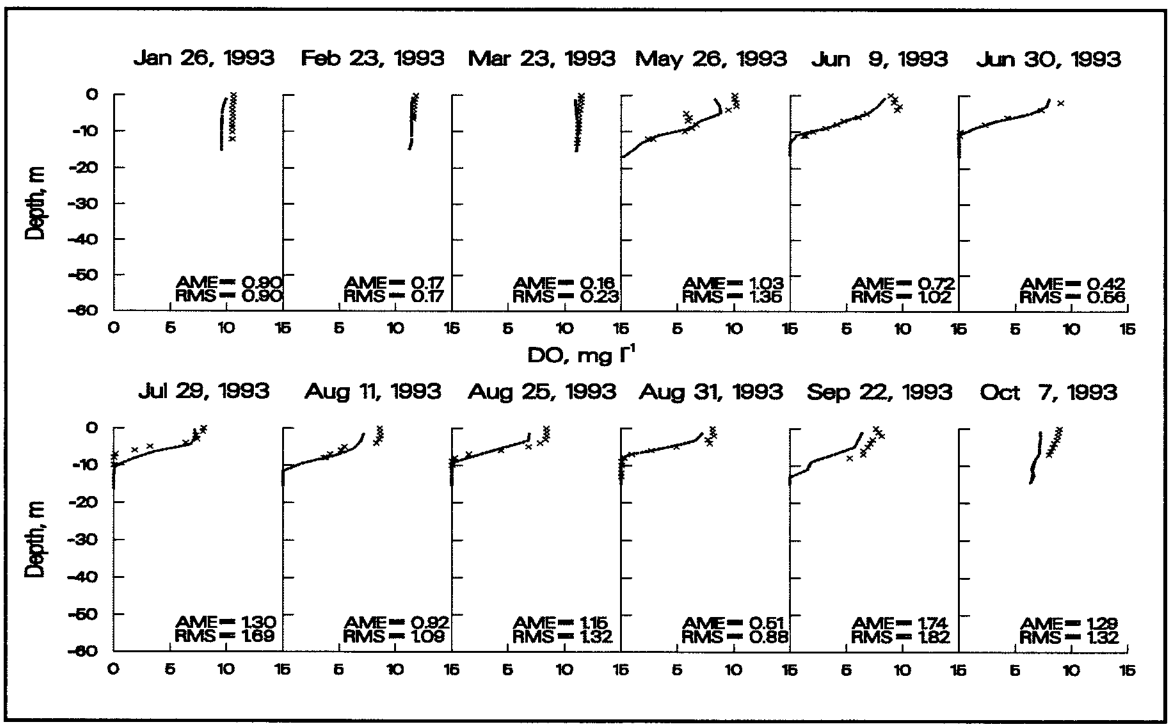

Figure A102. 1993 Allatoona Reservoir computed (...) versus observed (x) DO for station 39

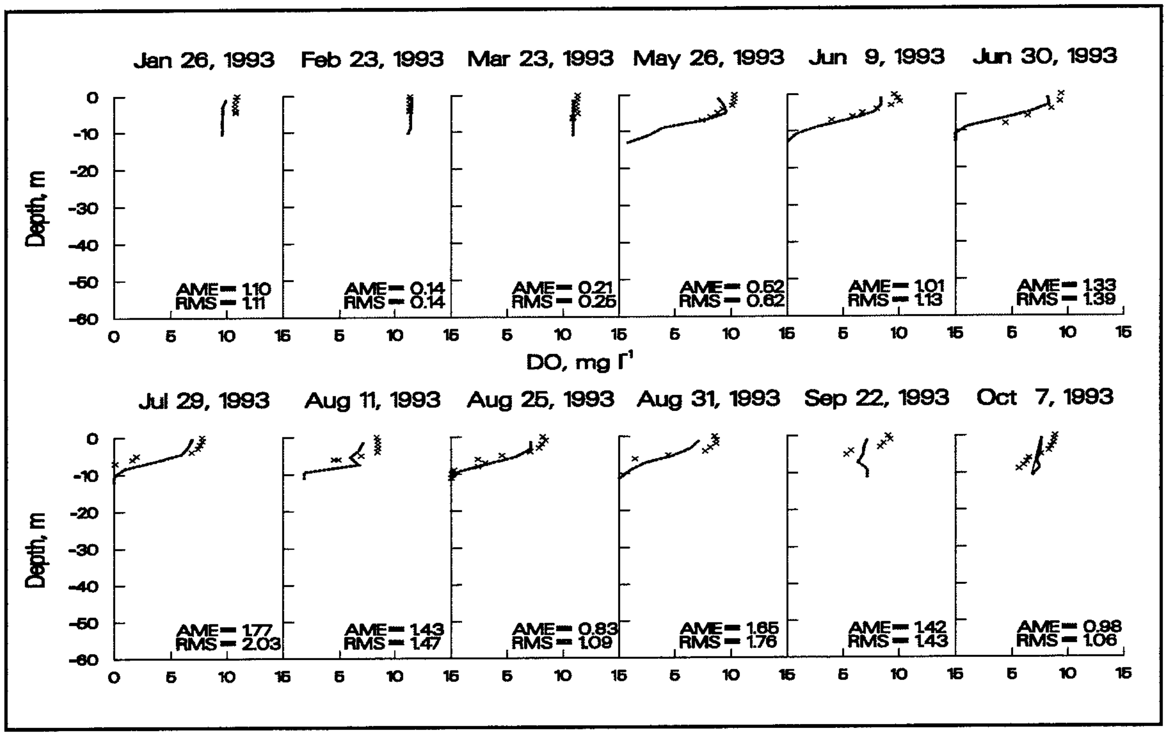

Figure A103. 1993 Allatoona Reservoir computed (...) versus observed (x) DO for station 45

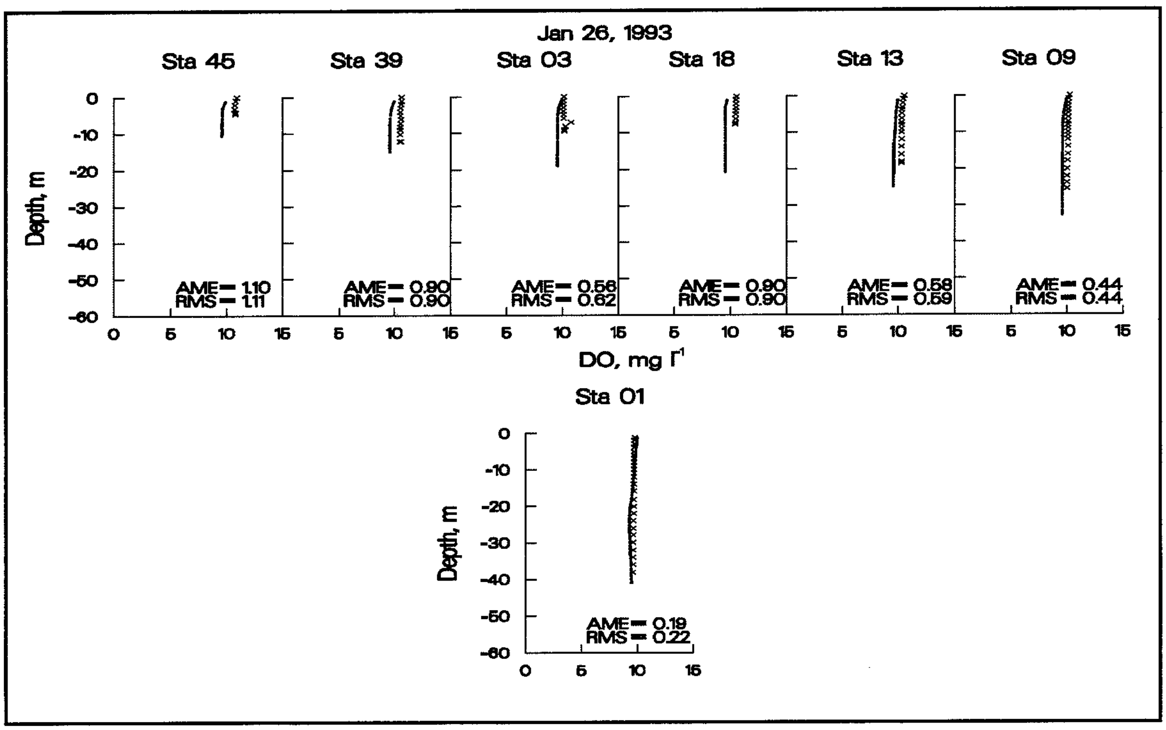

Figure A104. 1993 Allatoona Reservoir computed (...) versus observed (x) DO for stations along the mainstem, January 26

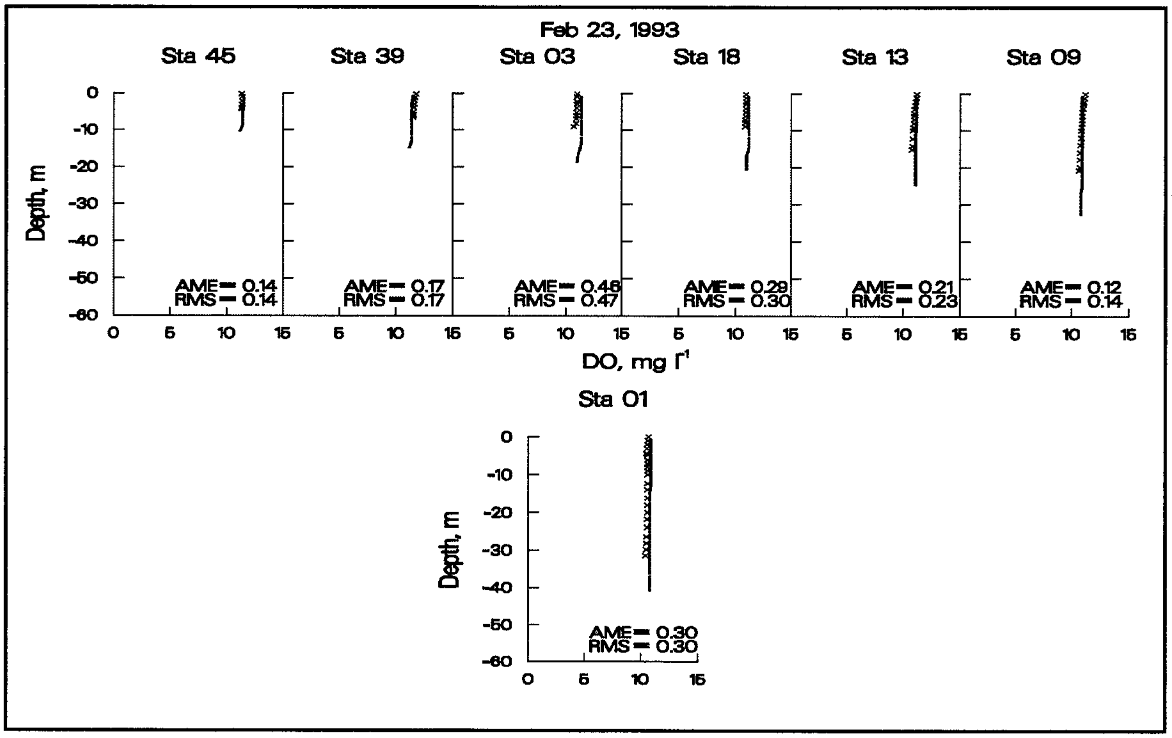

Figure A105. 1993 Allatoona Reservoir computed (...) versus observed (x) DO for stations along the mainstem, February 23

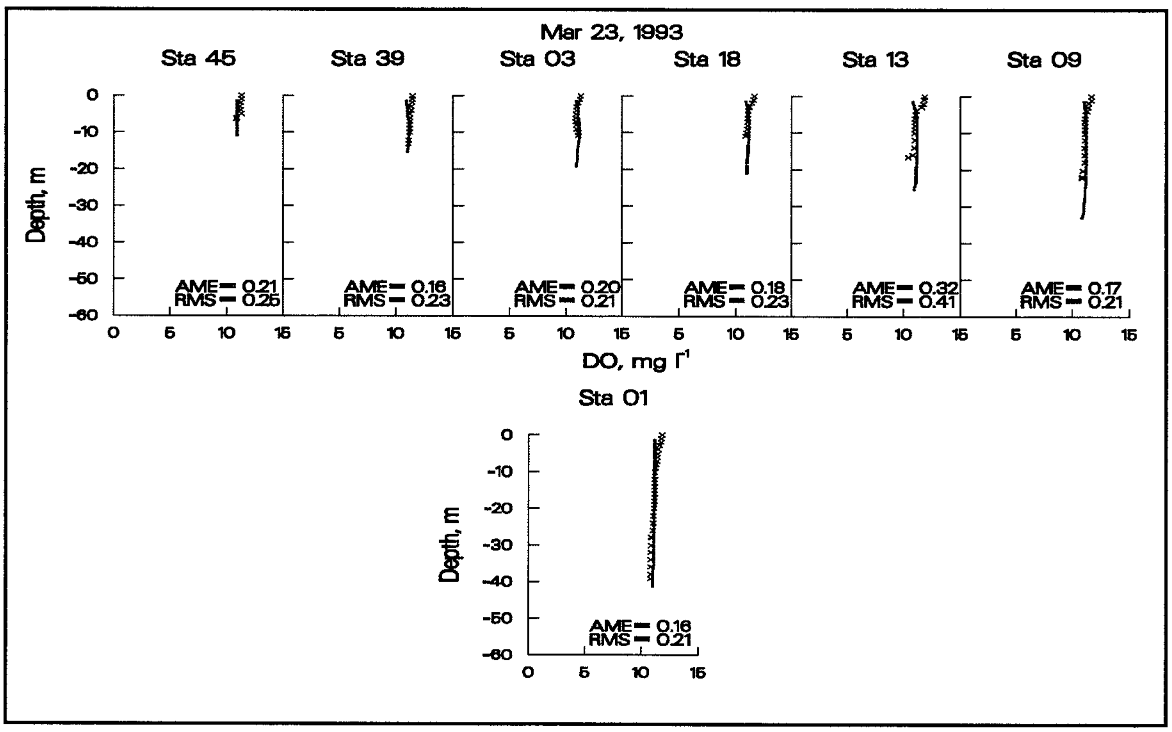

Figure A106. 1993 Allatoona Reservoir computed (...) versus observed (x) DO for stations along the mainstem, March 23

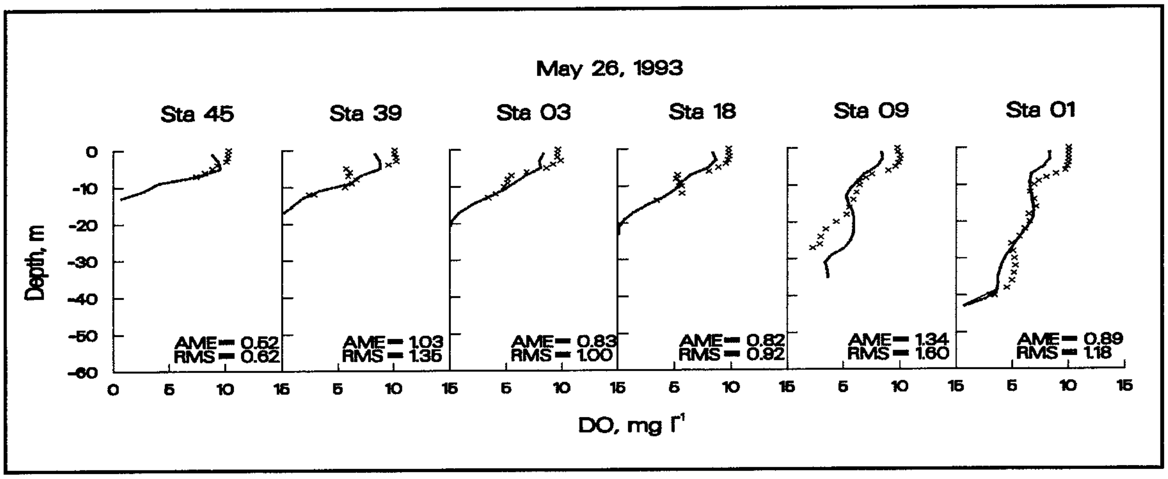

Figure A107. 1993 Allatoona Reservoir computed (...) versus observed (x) DO for stations along the mainstem, May 26

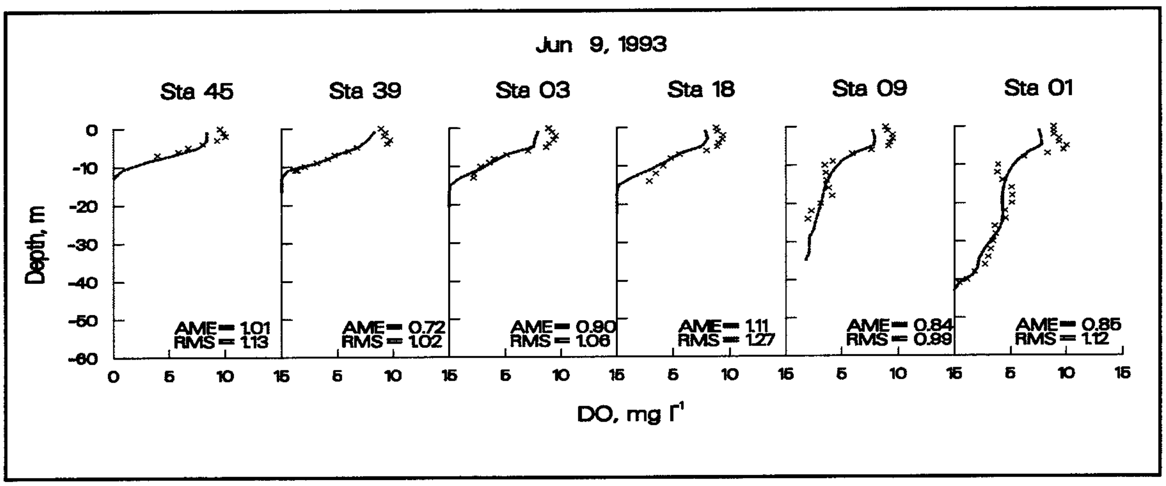

Figure A108. 1993 Allatoona Reservoir computed (...) versus observed (x) DO for stations along the mainstem, June 9

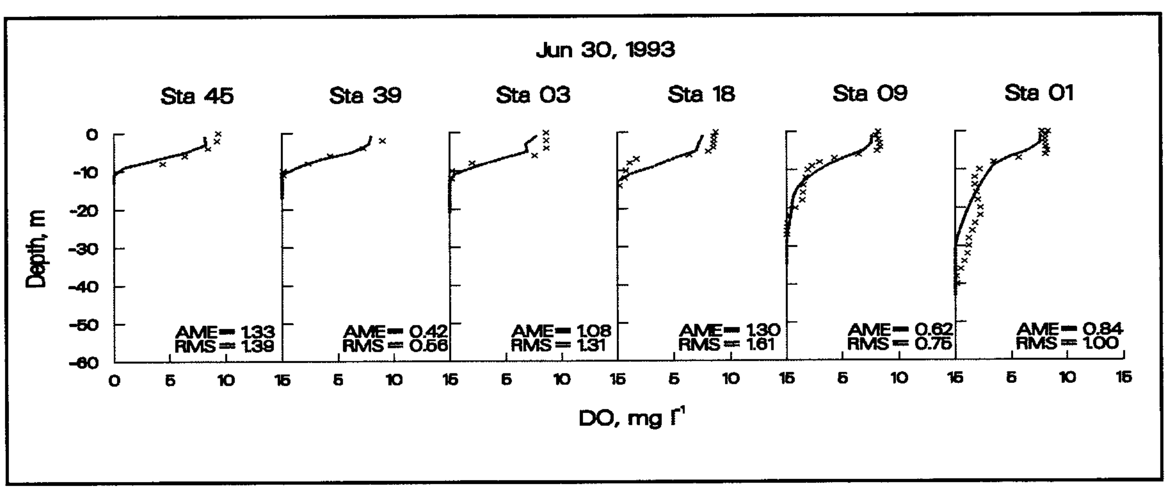

Figure A109. 1993 Allatoona Reservoir computed (...) versus observed (x) DO for stations along the mainstem, June 30

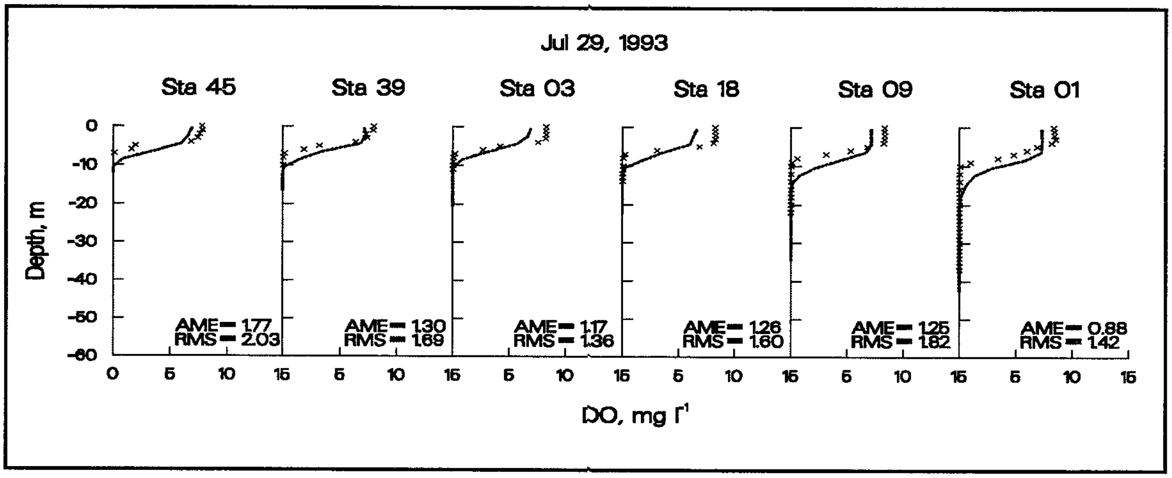

Figure A110. 1993 Allatoona Reservoir computed (...) versus observed (x) DO for stations along the mainstem, July 29

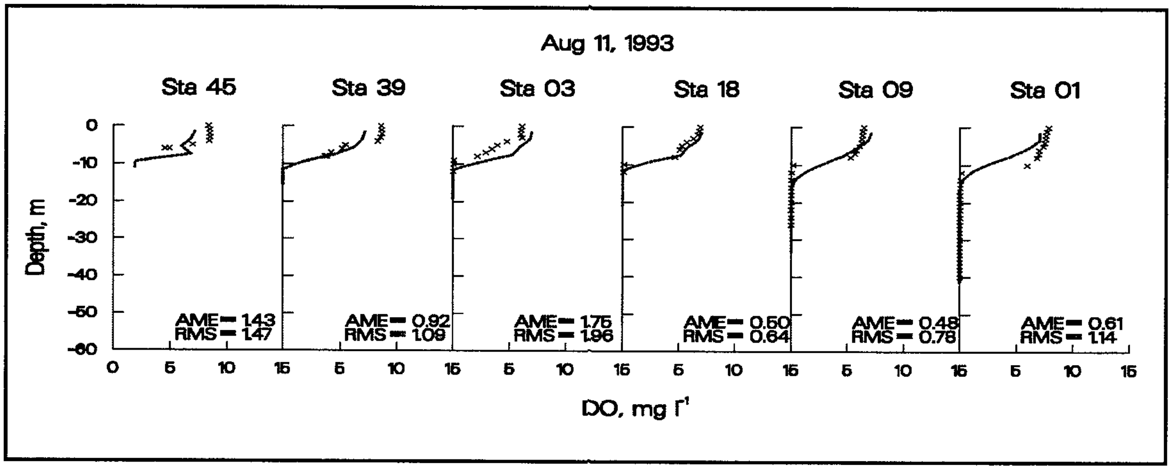

Figure A111. 1993 Allatoona Reservoir computed (...) versus observed (x) DO for stations along the mainstem, August 11

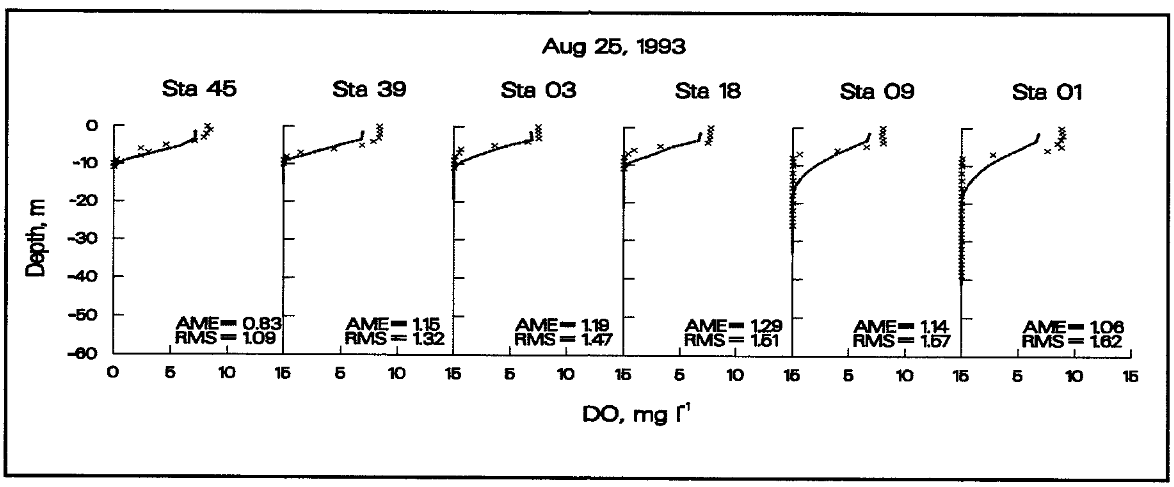

Figure A112. 1993 Allatoona Reservoir computed (...) versus observed (x) DO for stations along the mainstem, August 25

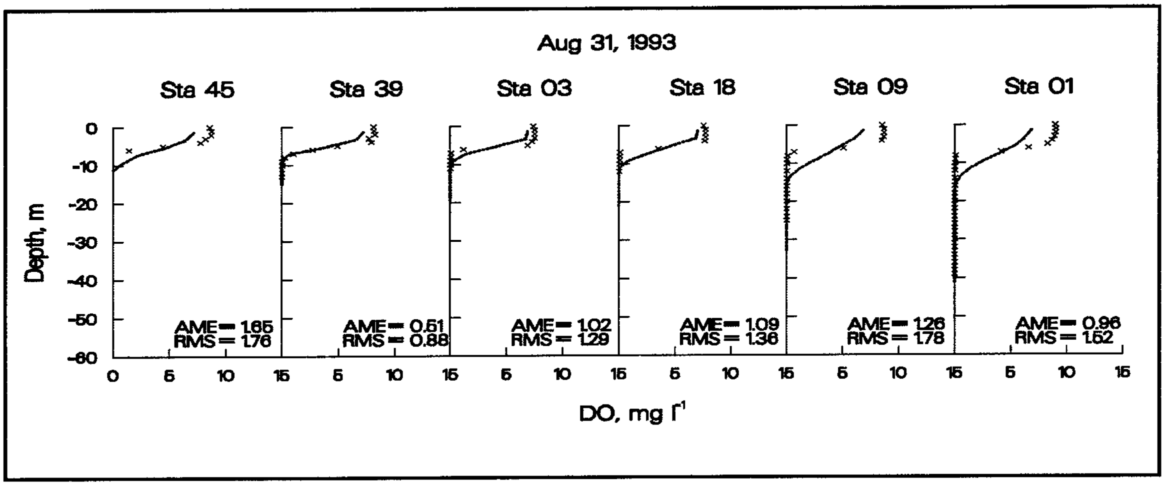

Figure A113. 1993 Allatoona Reservoir computed (...) versus observed (x) DO for stations along the mainstem, August 31

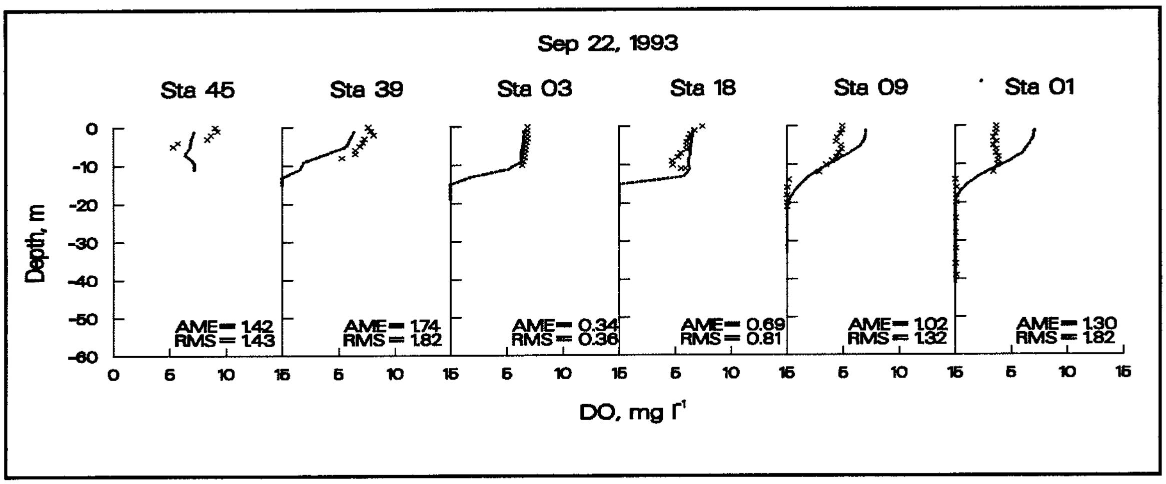

Figure A114. 1993 Allatoona Reservoir computed (...) versus observed (x) DO for stations along the mainstem, September 22

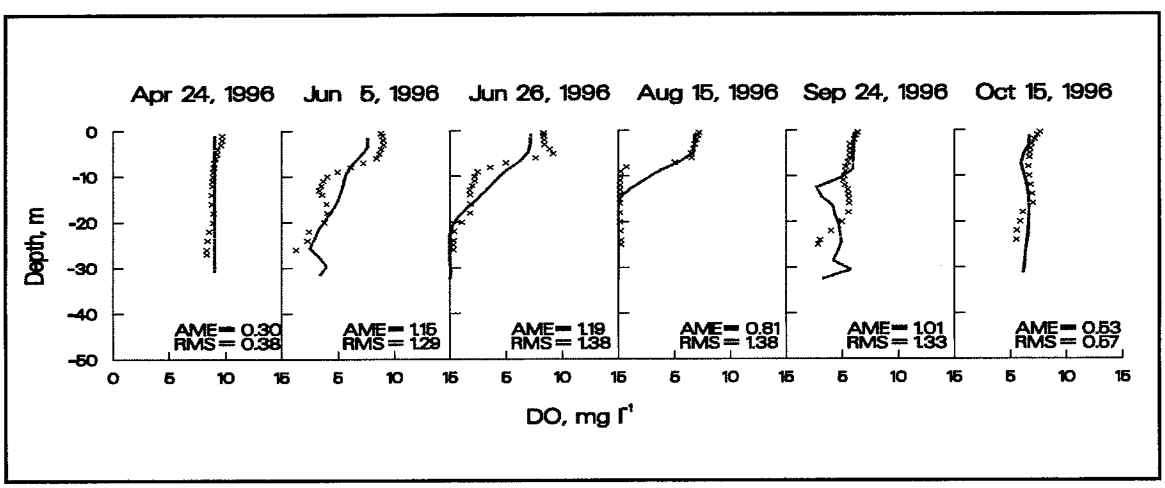

Figure A115. 1996 Allatoona Reservoir computed (...) versus observed (x) DO for station 09

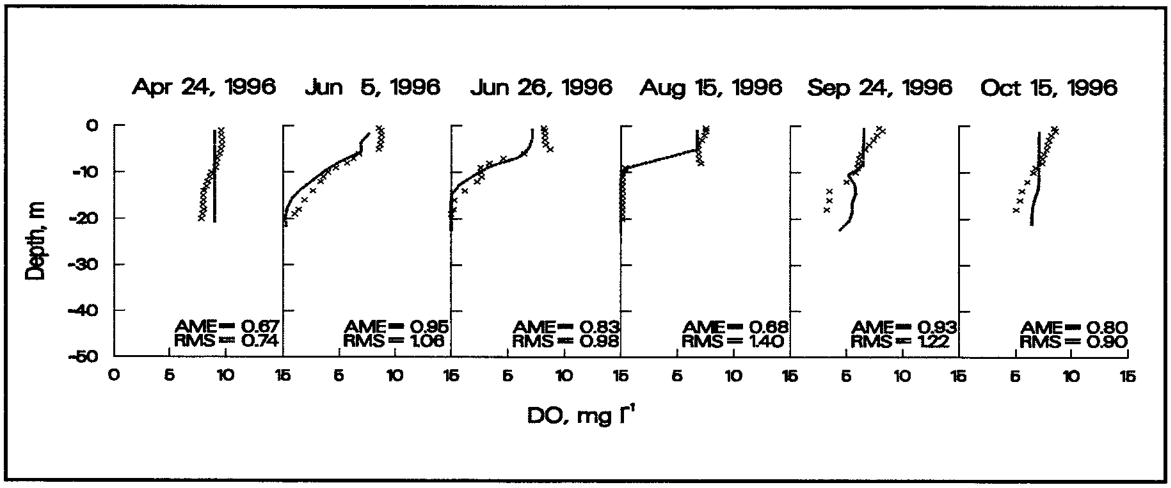

Figure A116. 1996 Allatoona Reservoir computed (...) versus observed (x) DO for station 18

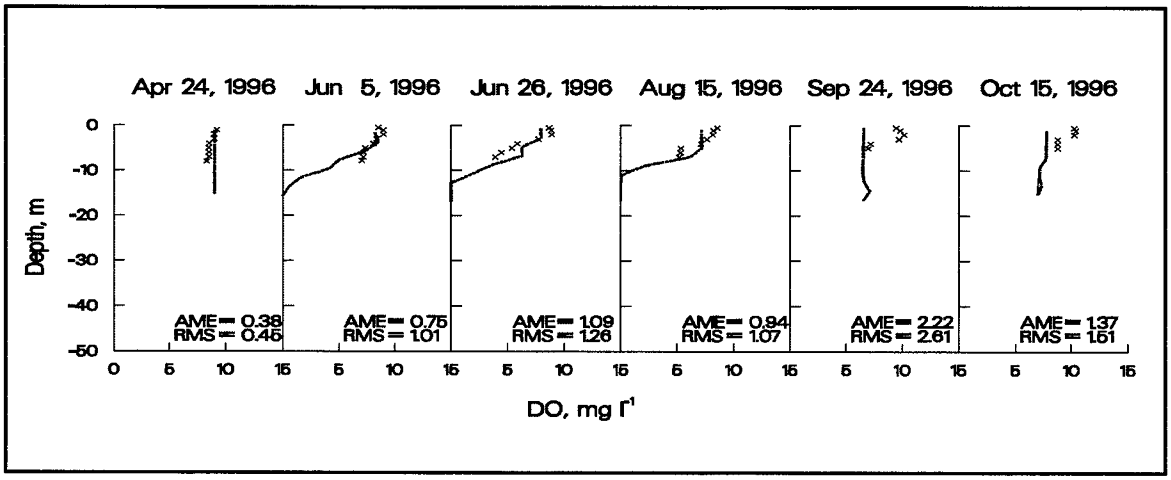

Figure A117. 1996 Allatoona Reservoir computed (...) versus observed (x) DO for station 45

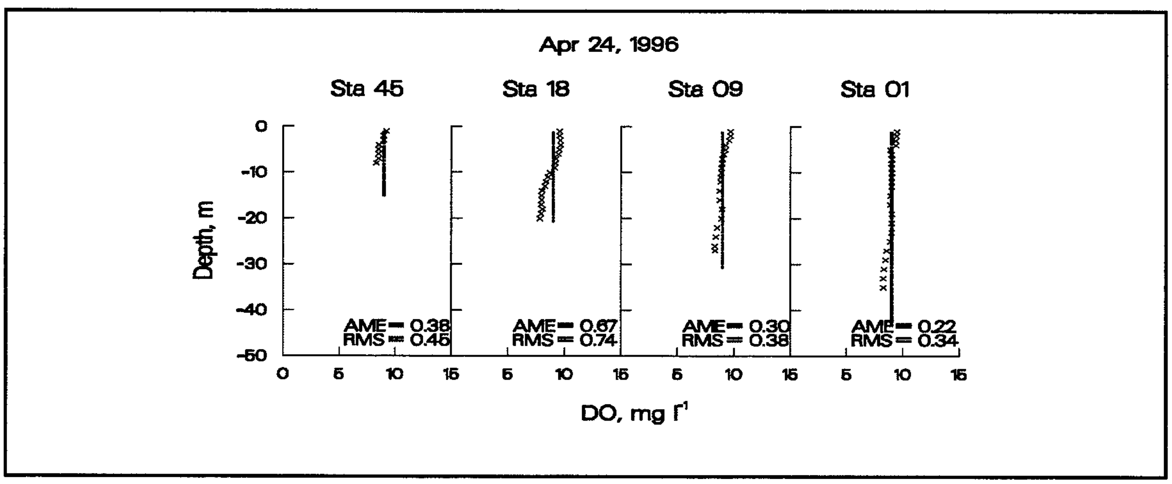

Figure A118. 1996 Allatoona Reservoir computed (...) versus observed (x) DO for stations along the mainstem, April 24

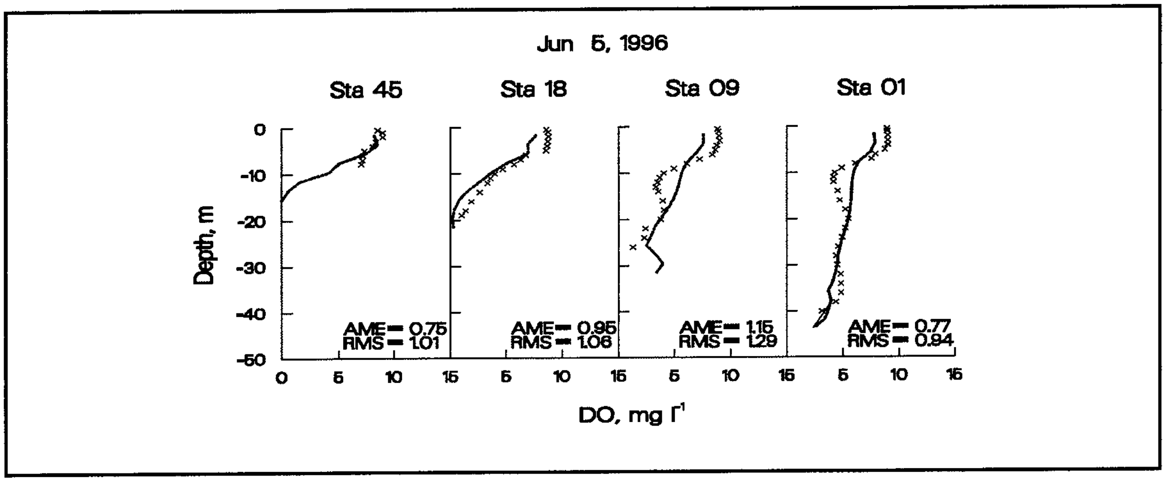

Figure A119. 1996 Allatoona Reservoir computed (...) versus observed (x) DO for stations along the mainstem, June 5

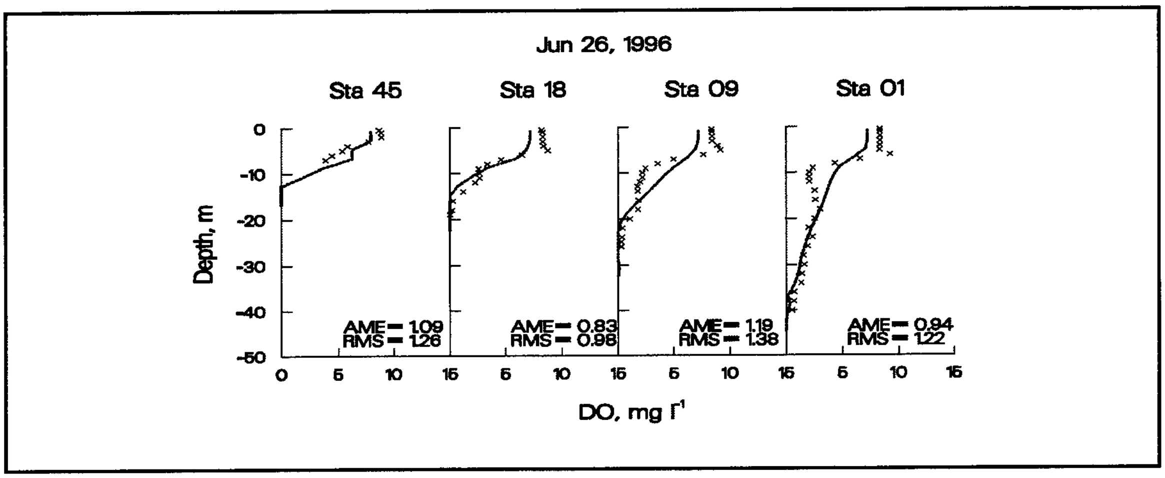

Figure A120. 1996 Allatoona Reservoir computed (...) versus observed (x) DO for stations along the mainstem, June 26

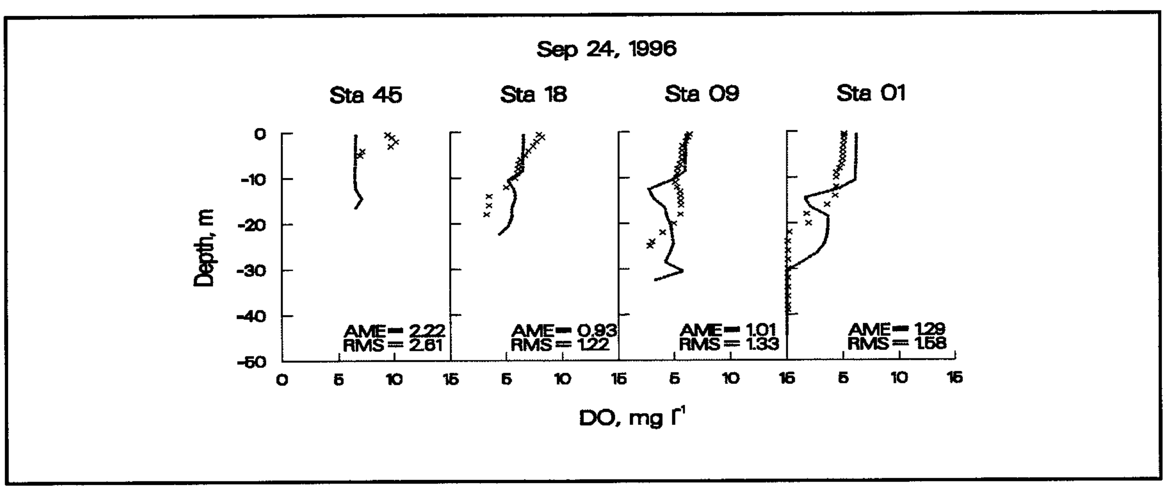

Figure A121. 1996 Allatoona Reservoir computed (...) versus observed (x) DO for stations along the mainstem, September 24

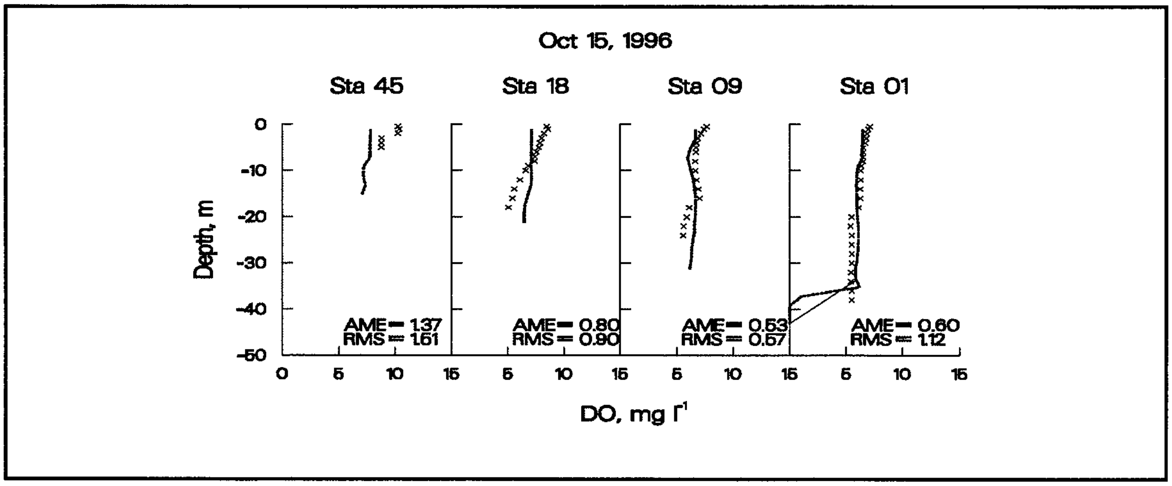

Figure A122. 1996 Allatoona Reservoir computed (...) versus observed (x) DO for stations along the mainstem, October 15

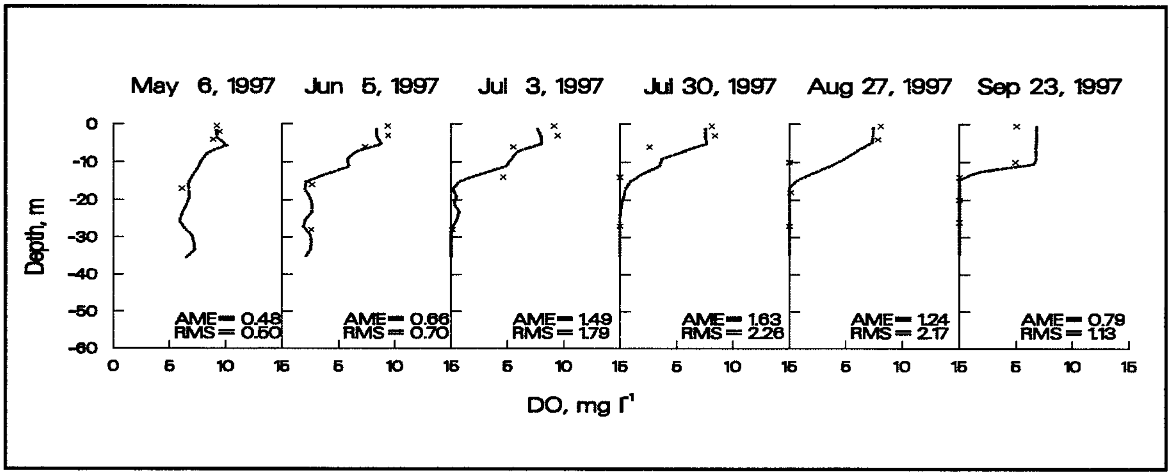

Figure A123. 1997 Allatoona Reservoir computed (...) versus observed (x) DO for station 09

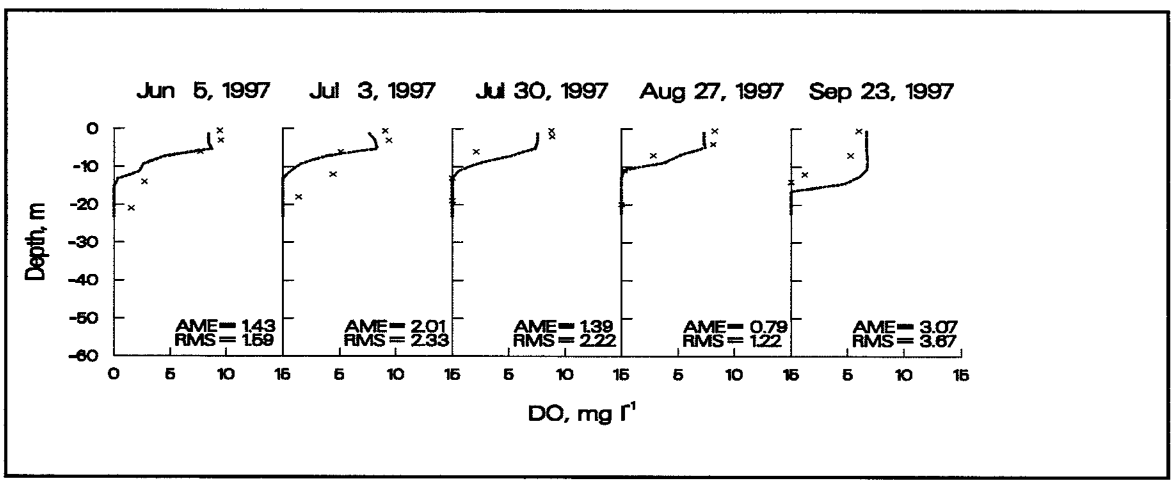

Figure A124. 1997 Allatoona Reservoir computed (...) versus observed (x) DO for station 18

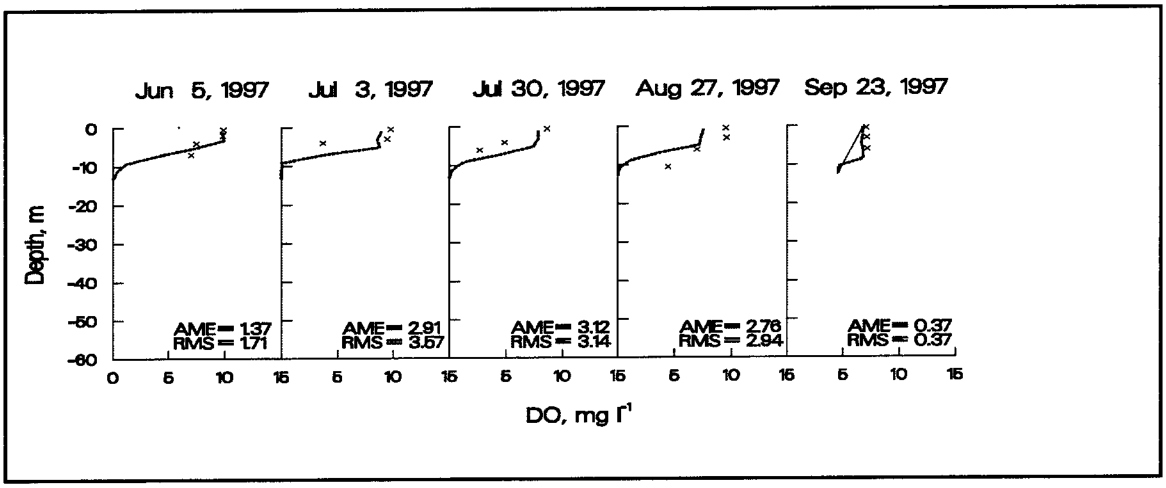

Figure A125. 1997 Allatoona Reservoir computed (...) versus observed (x) DO for station 45

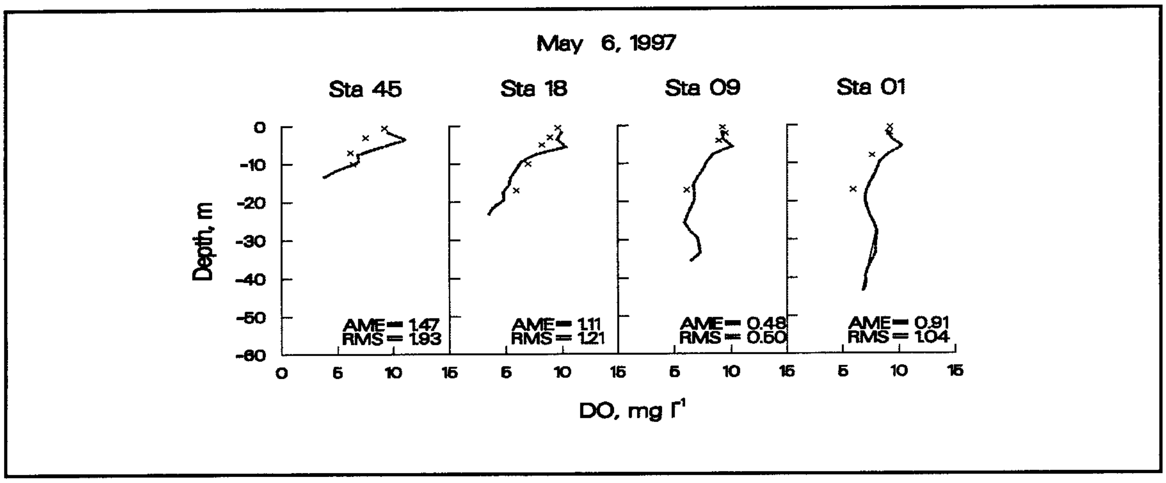

Figure A126. 1997 Allatoona Reservoir computed (...) versus observed (x) DO for stations along the mainstem, May 6

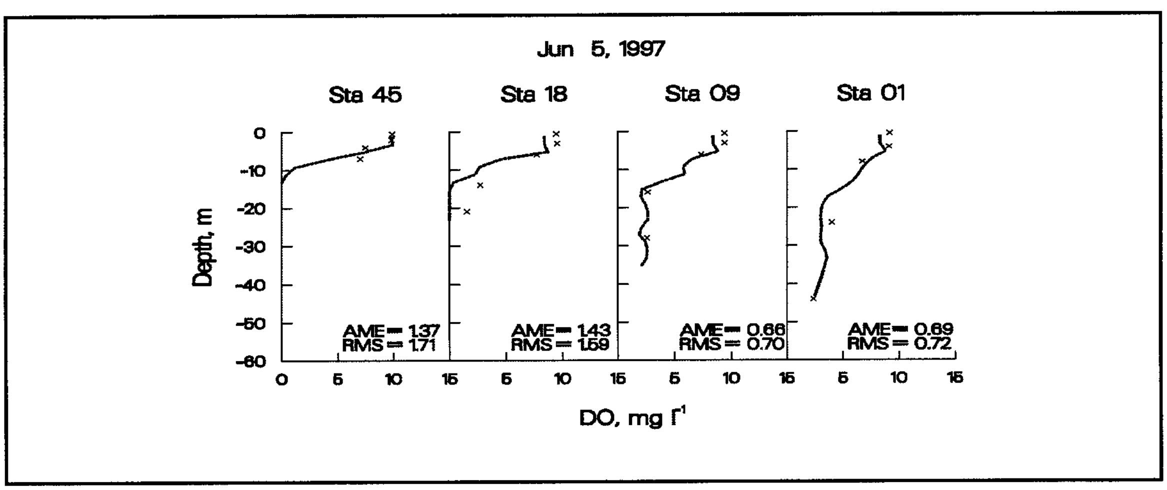

Figure A127. 1997 Allatoona Reservoir computed (...) versus observed (x) DO for stations along the mainstem, June 5

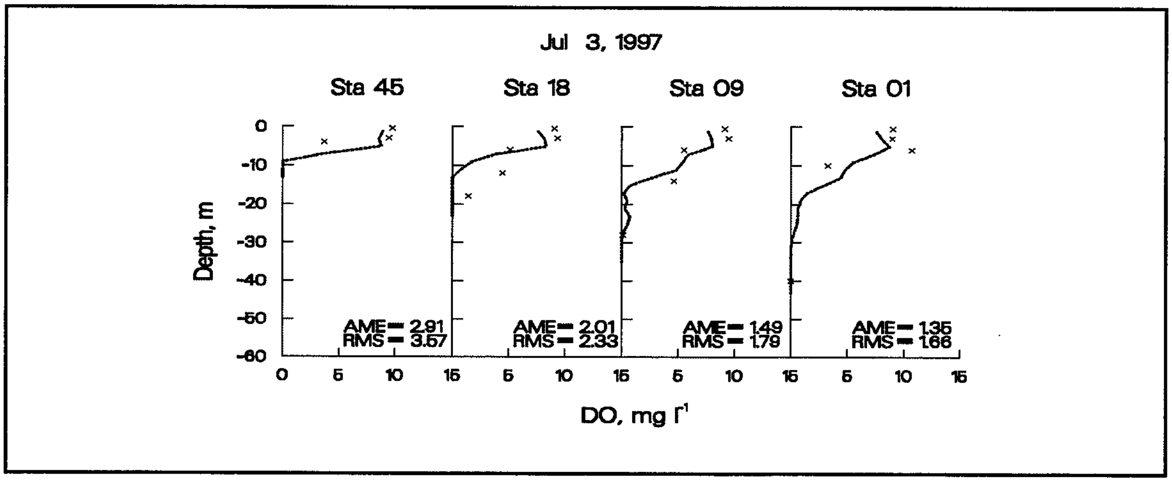

Figure A128. 1997 Allatoona Reservoir computed (...) versus observed (x) DO for stations along the mainstem, July 3

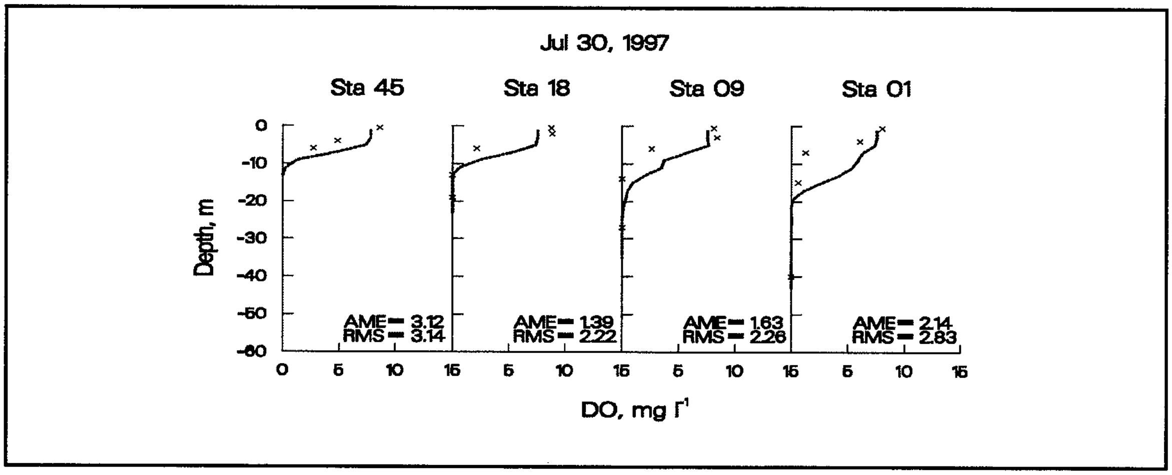

Figure A129. 1997 Allatoona Reservoir computed (...) versus observed (x) DO for stations along the mainstem, July 30

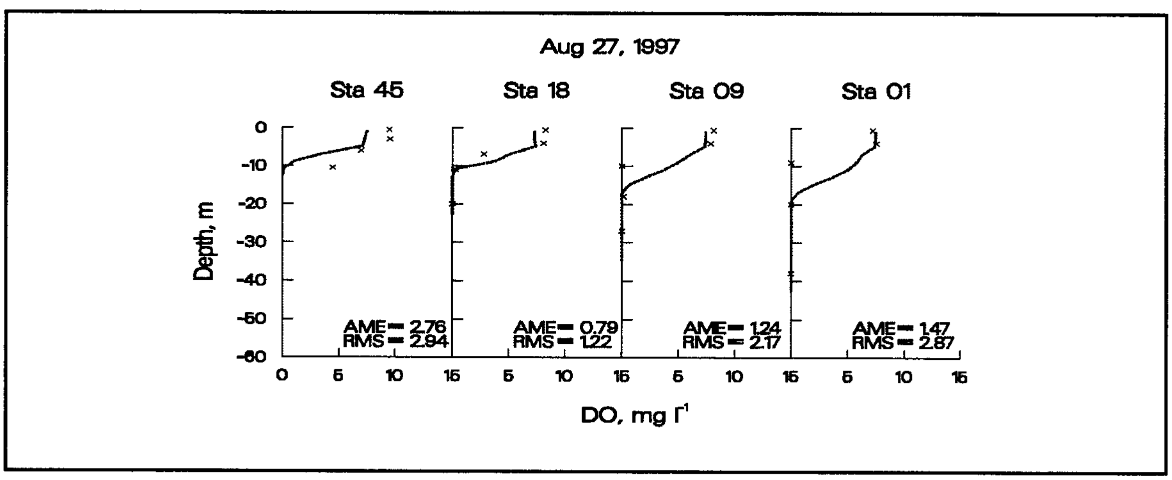

Figure A130. 1997 Allatoona Reservoir computed (...) versus observed (x) DO for stations along the mainstem, August 27

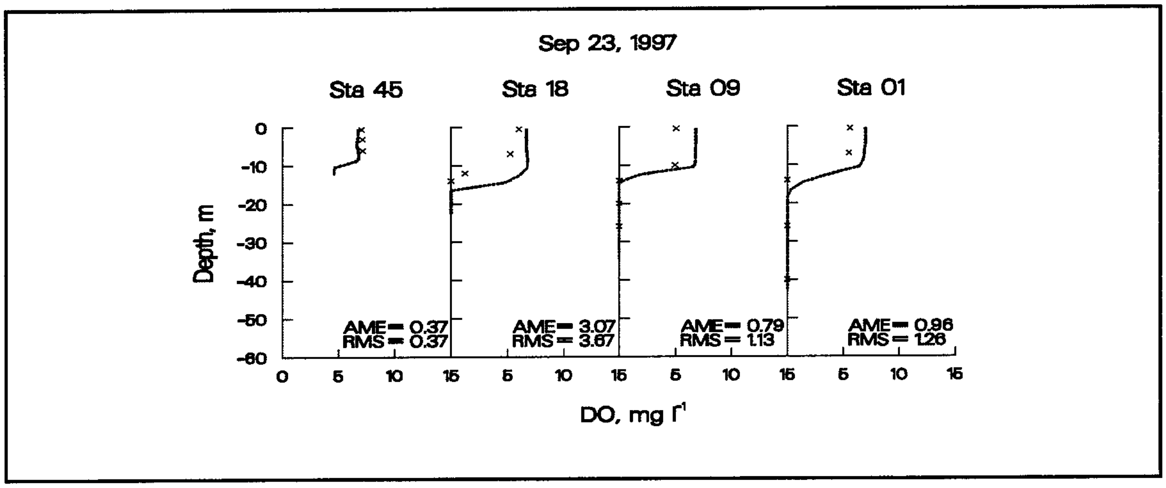

Figure A131. 1997 Allatoona Reservoir computed (...) versus observed (x) DO for stations along the mainstem, September 23

West Point

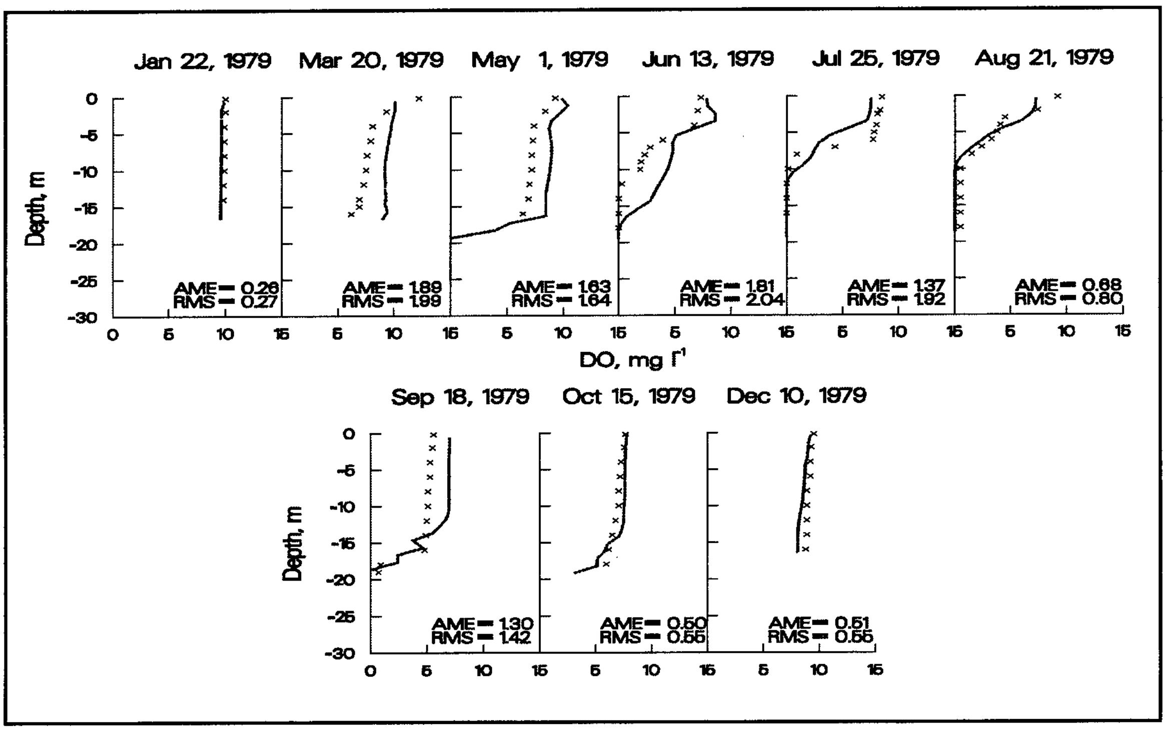

Figure A132. 1979 West Point Reservoir computed (...) versus observed (x) DO for station 05

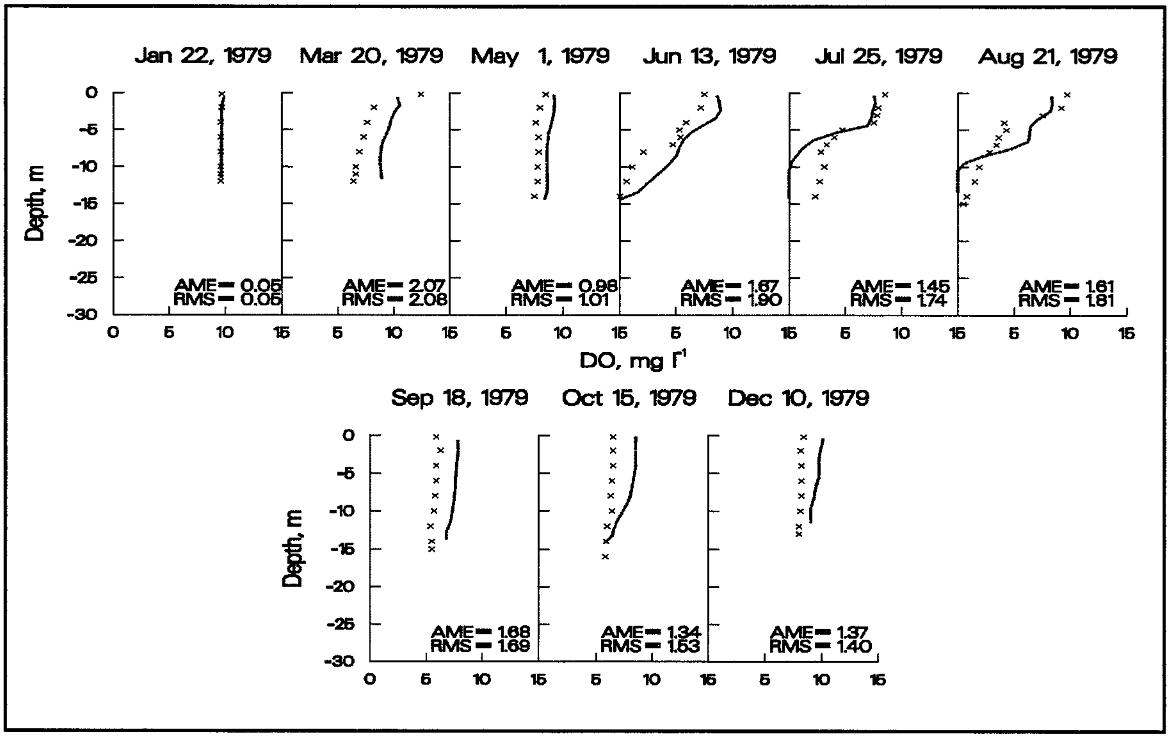

Figure A133. 1979 West Point Reservoir computed (...) versus observed (x) DO for station 07

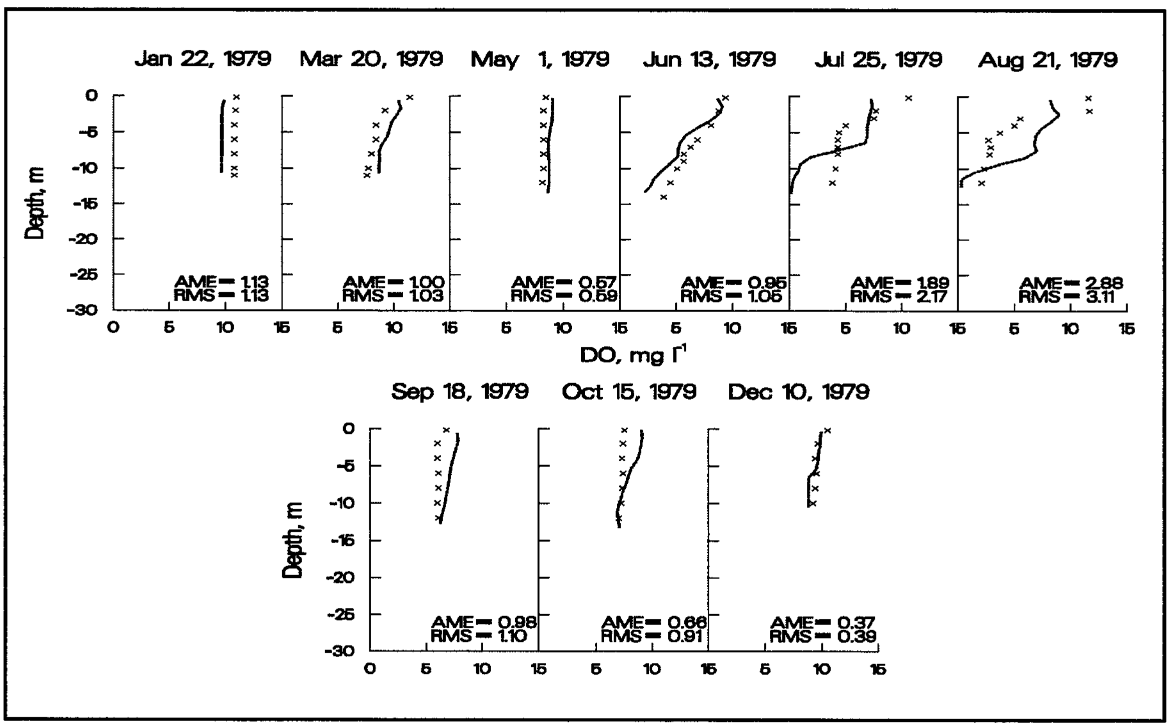

Figure A134. 1979 West Point Reservoir computed (...) versus observed (x) DO for station 10

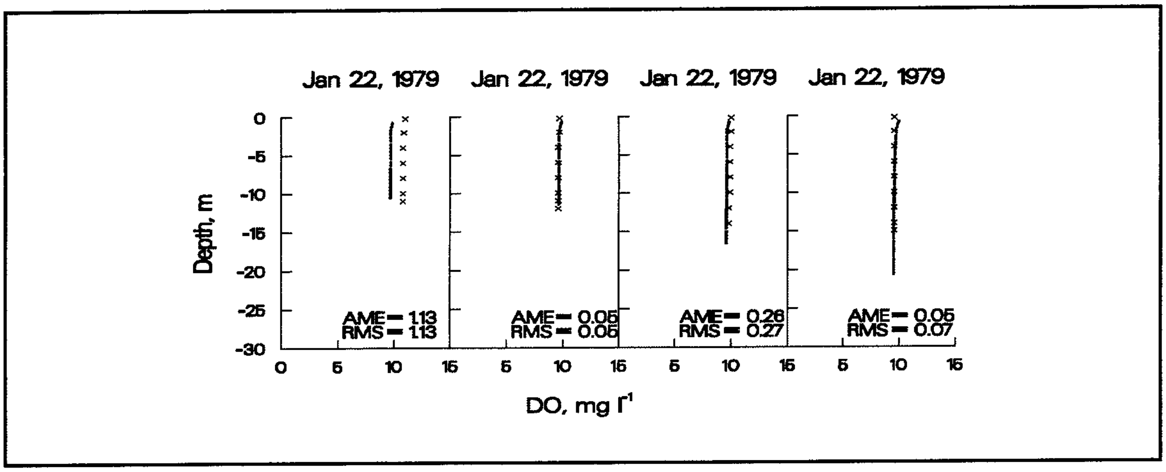

Figure A135. 1979 West Point Reservoir computed (...) versus observed (x) DO for stations along mainstem, January 22

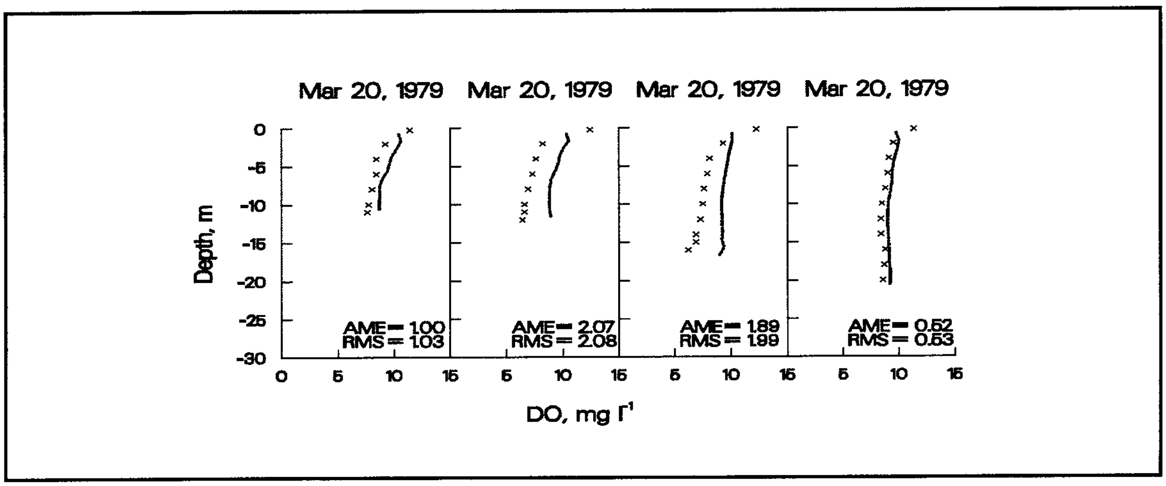

Figure A136. 1979 West Point Reservoir computed (...) versus observed (x) DO for stations along mainstem, March 20

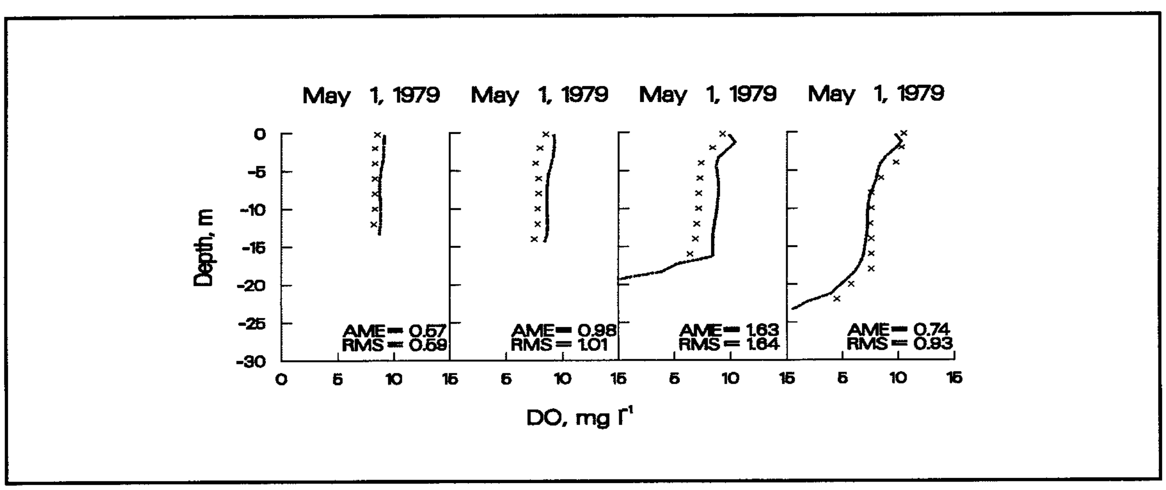

Figure A137. 1979 West Point Reservoir computed (...) versus observed (x) DO for stations along mainstem, May 1

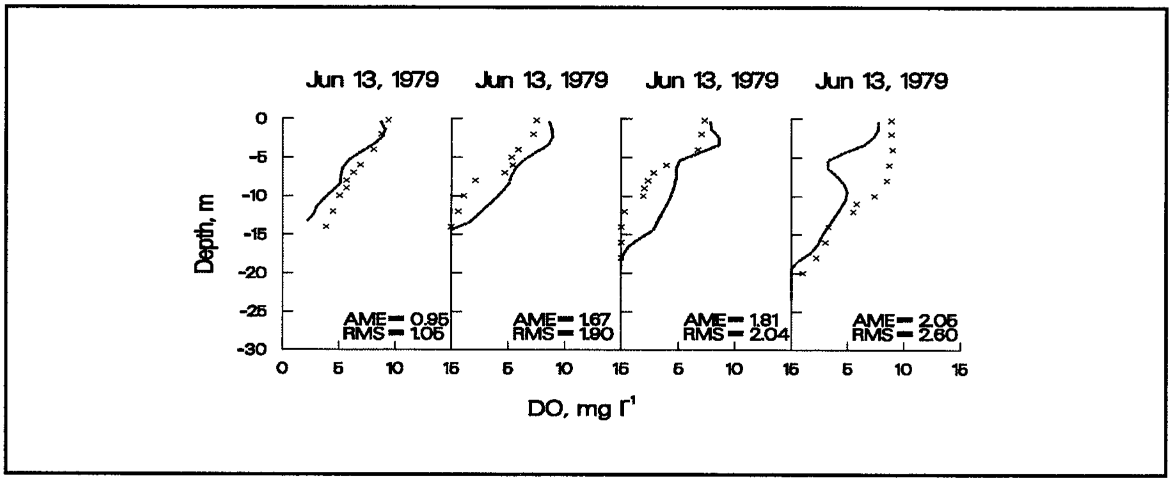

Figure A138. 1979 West Point Reservoir computed (...) versus observed (x) DO for stations along mainstem, June 13

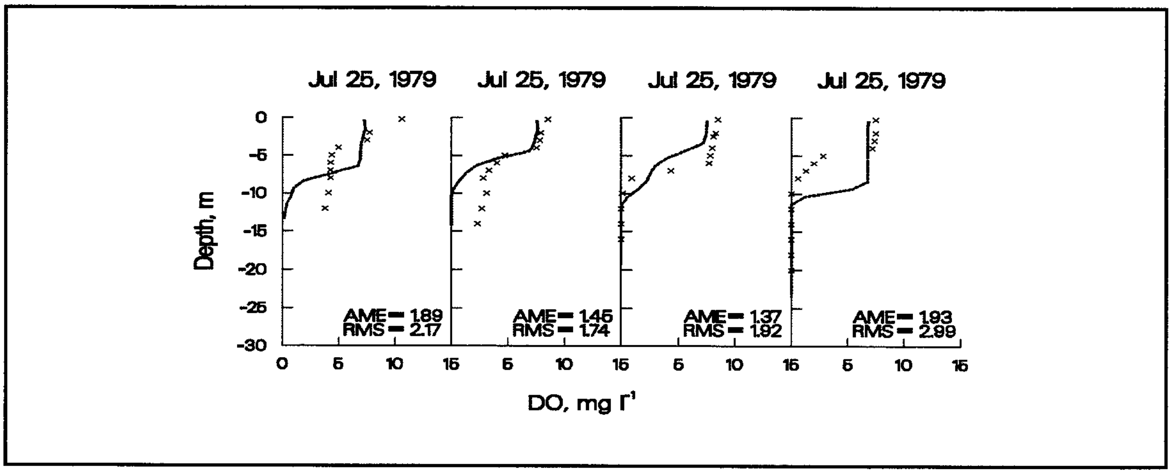

Figure A139. 1979 West Point Reservoir computed (...) versus observed (x) DO for stations along mainstem, July 25

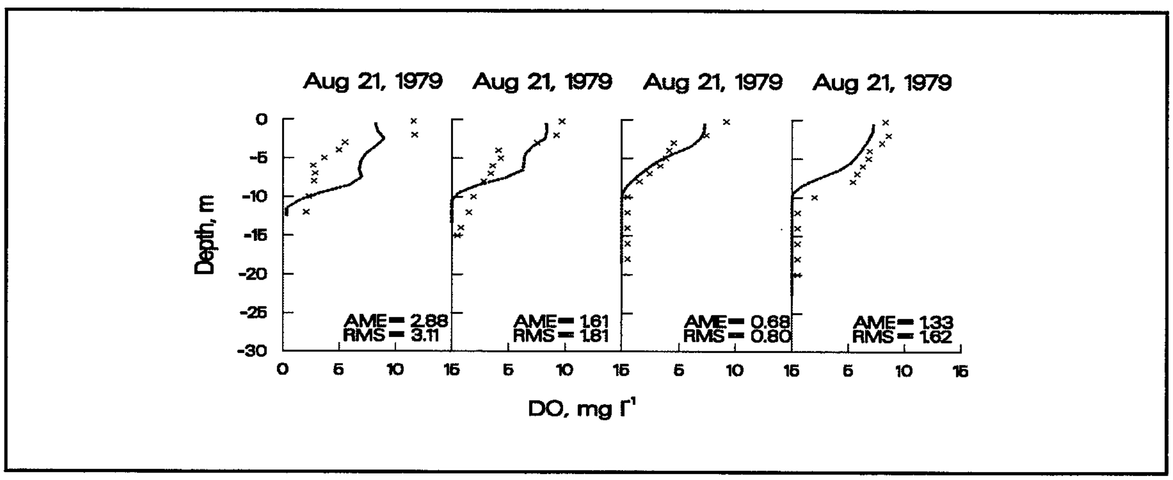

Figure A140. 1979 West Point Reservoir computed (...) versus observed (x) DO for stations along mainstem, August 21

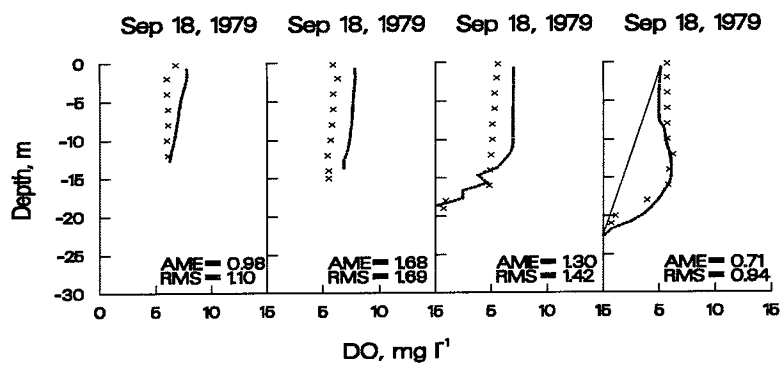

Figure A141. 1979 West Point Reservoir computed (...) versus observed (x) DO for stations along mainstem, September 18

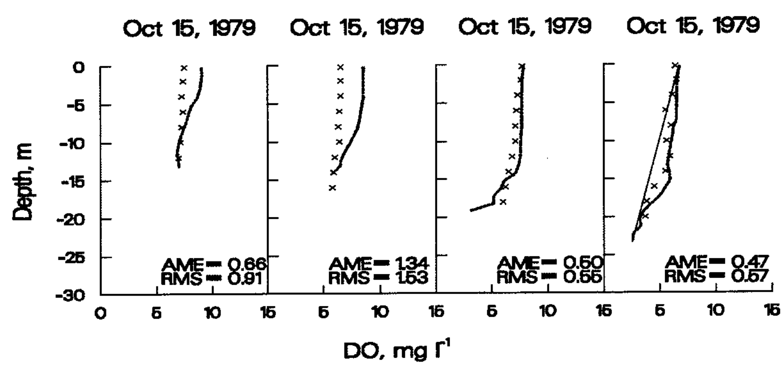

Figure A142. 1979 West Point Reservoir computed (...) versus observed (x) DO for stations along mainstem, October 15

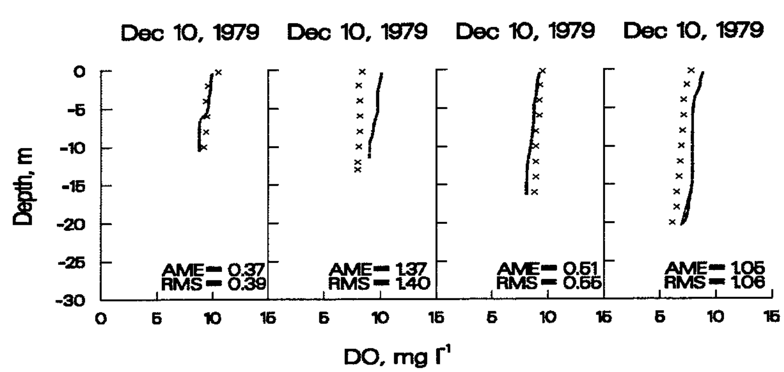

Figure A143. 1979 West Point Reservoir computed (...) versus observed (x) DO for stations along mainstem, December 10

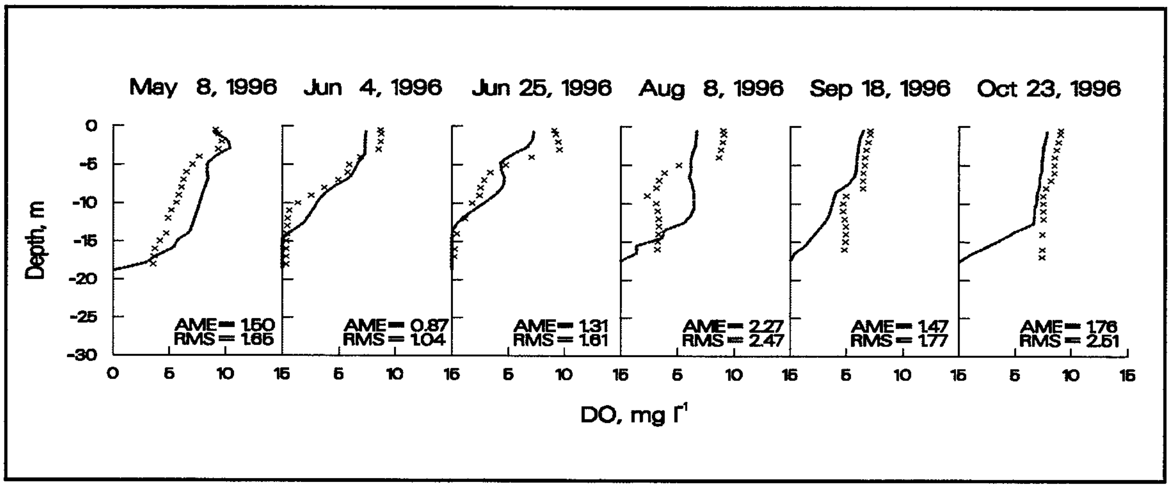

Figure A144. 1996 West Point Reservoir computed (...) versus observed (x) DO for station 05

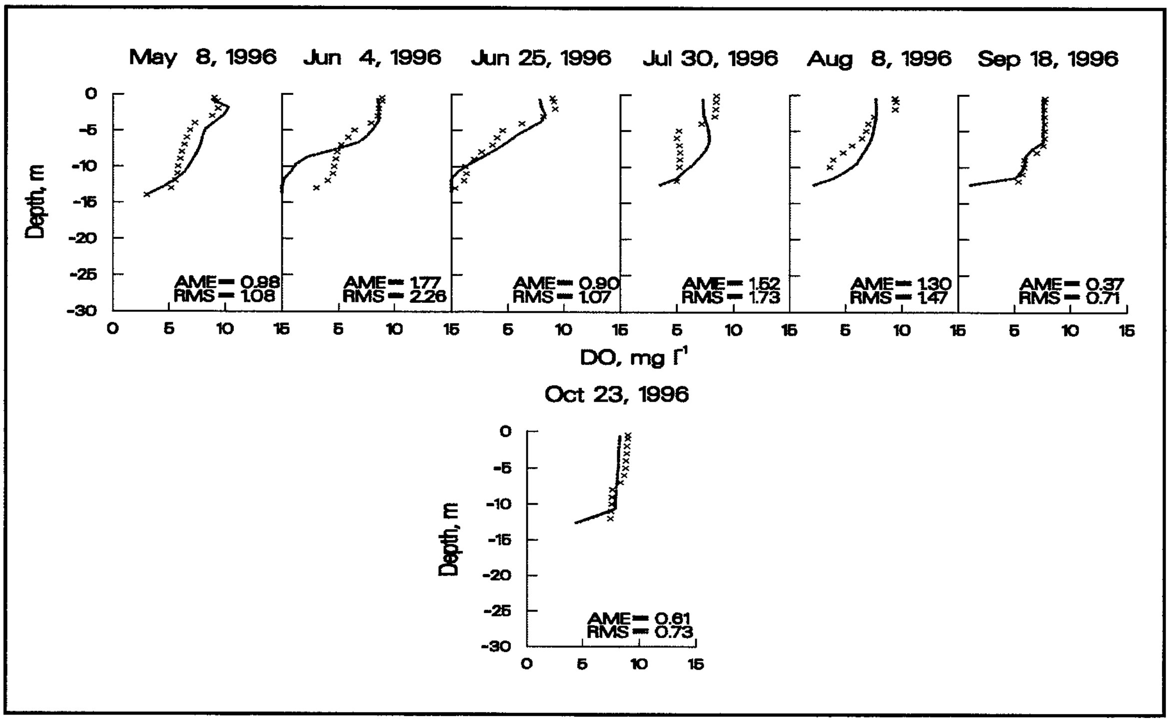

Figure A145. 1996 West Point Reservoir computed (...) versus observed (x) DO for station 07

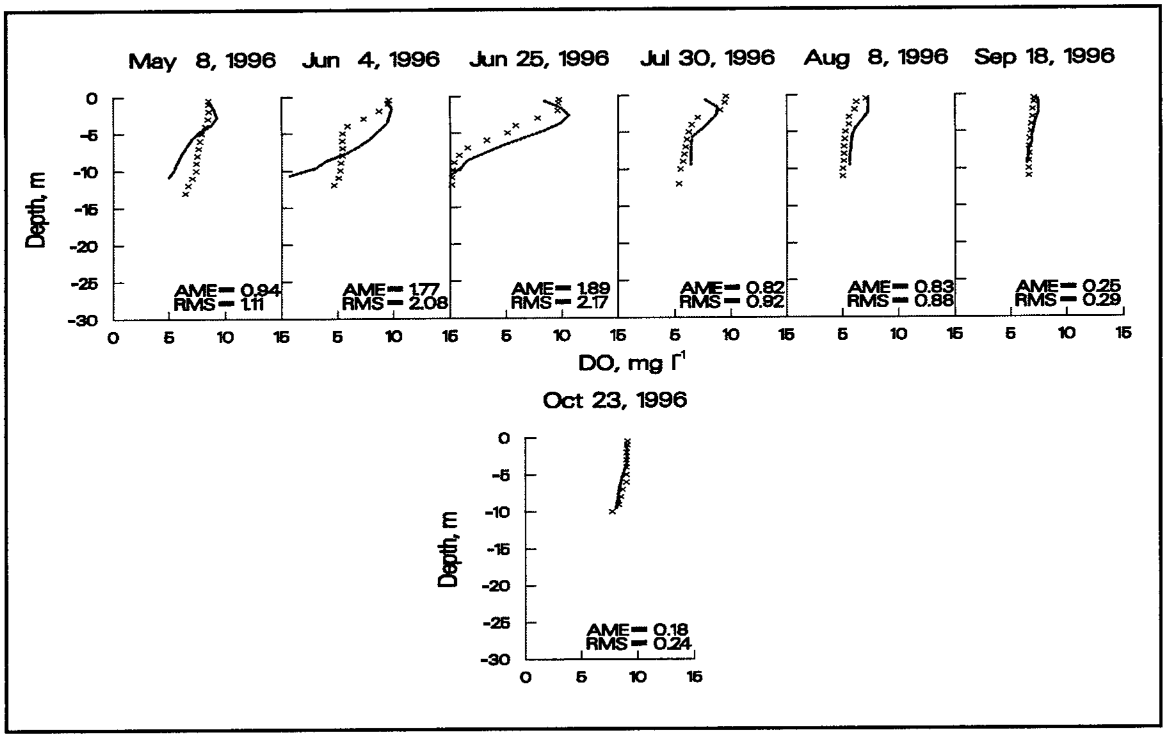

Figure A146. 1996 West Point Reservoir computed (...) versus observed (x) DO for station 10

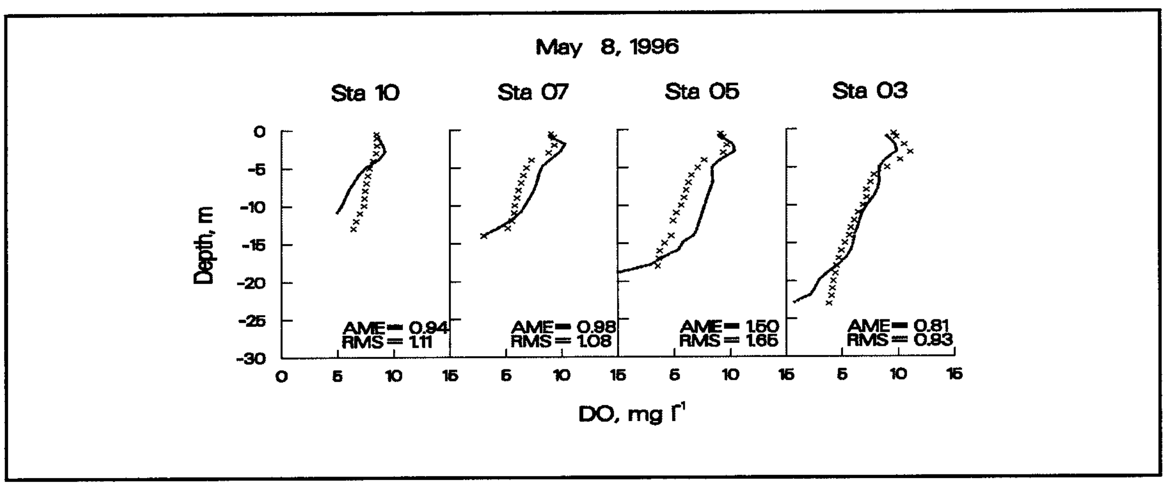

Figure A147. 1996 West Point Reservoir computed (...) versus observed (x) DO for stations along mainstem, May 8

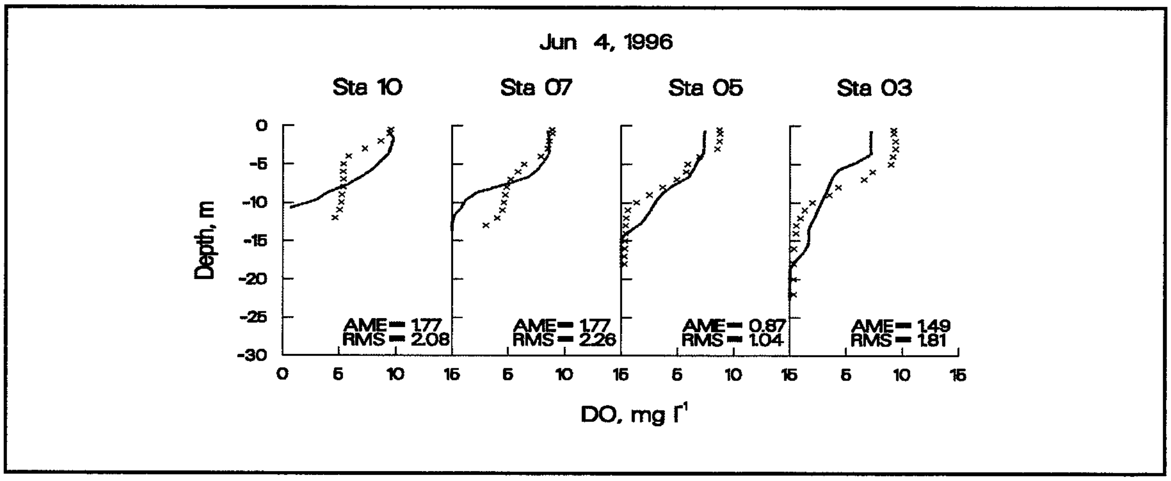

Figure A148. 1996 West Point Reservoir computed (...) versus observed (x) DO for stations along mainstem, June 4

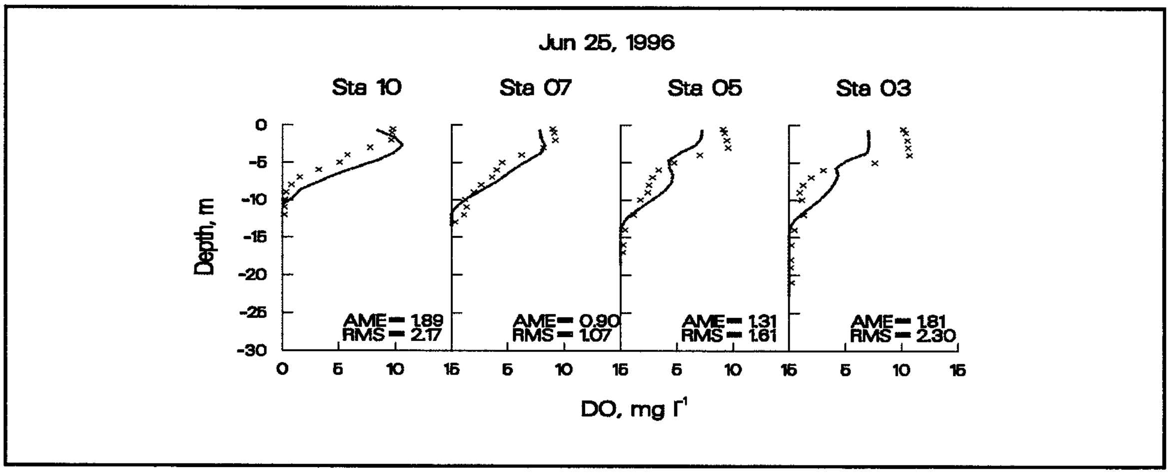

Figure A149. 1996 West Point Reservoir computed (...) versus observed (x) DO for stations along mainstem, June 25

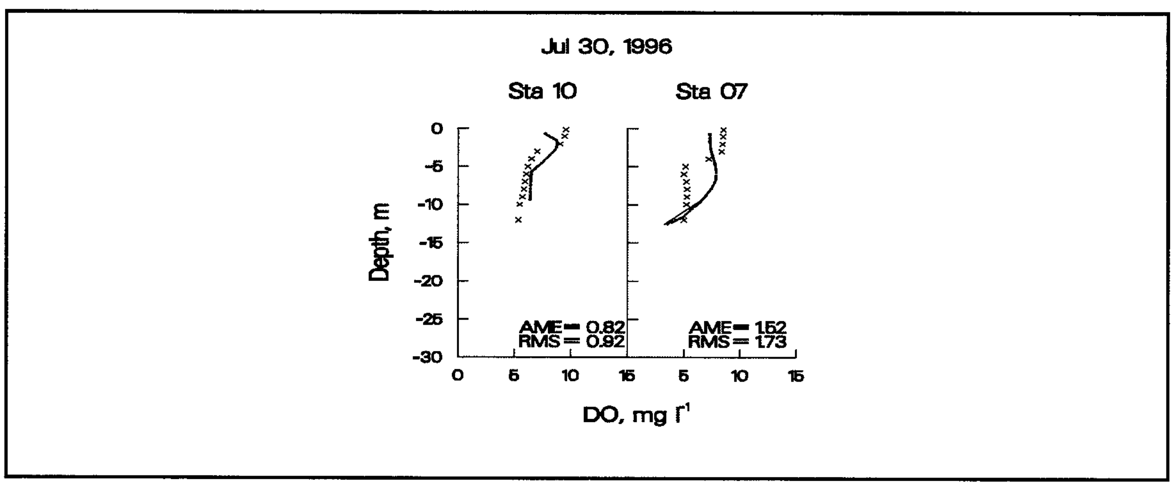

Figure A150. 1996 West Point Reservoir computed (...) versus observed (x) DO for stations along mainstem, July 30

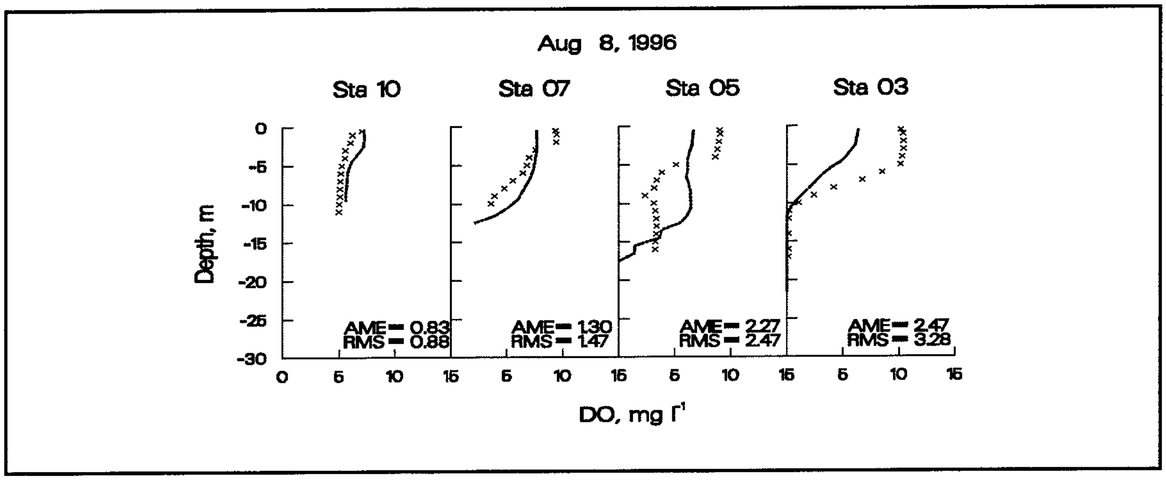

Figure A151. 1996 West Point Reservoir computed (...) versus observed (x) DO for stations along mainstem, August 8

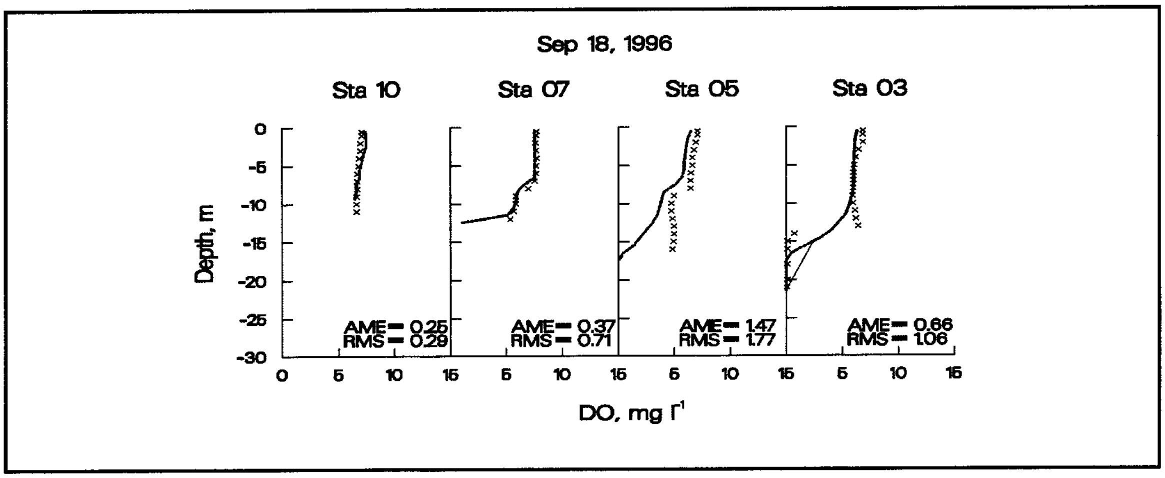

Figure A152. 1996 West Point Reservoir computed (...) versus observed (x) DO for stations along mainstem, September 18

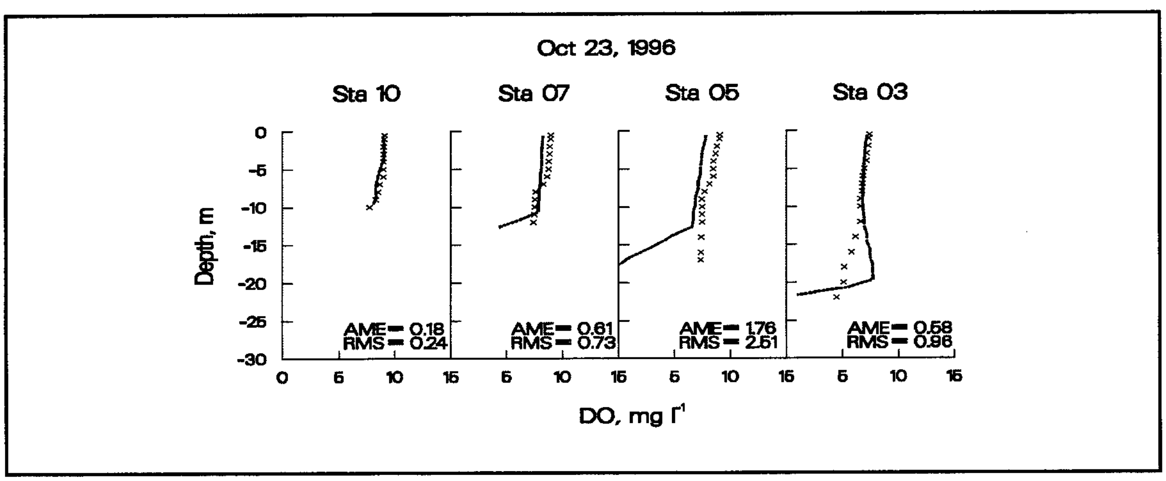

Figure A153. 1996 West Point Reservoir computed (...) versus observed (x) DO for stations along mainstem, October 23

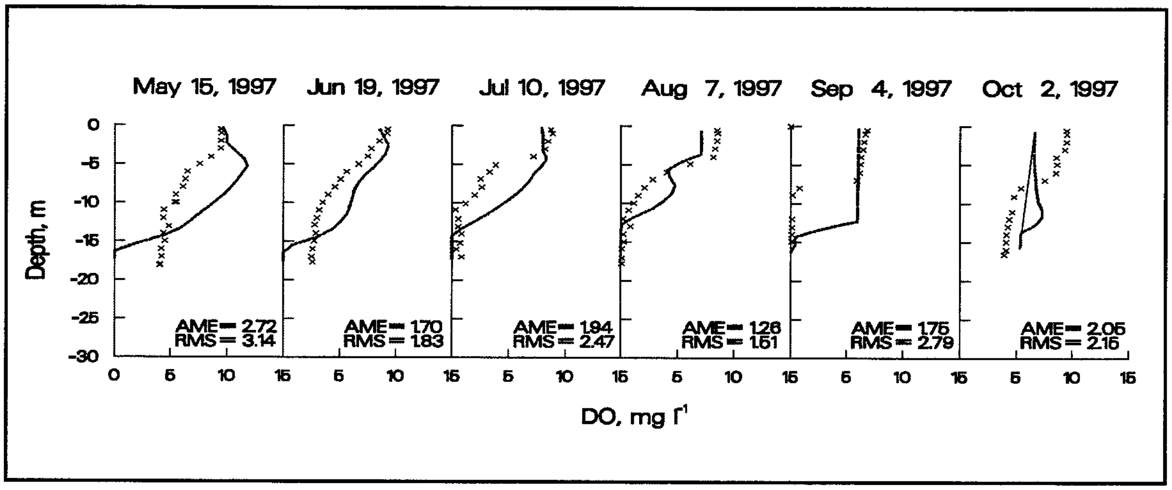

Figure A154. 1997 West Point Reservoir computed (...) versus observed (x) DO for station 05

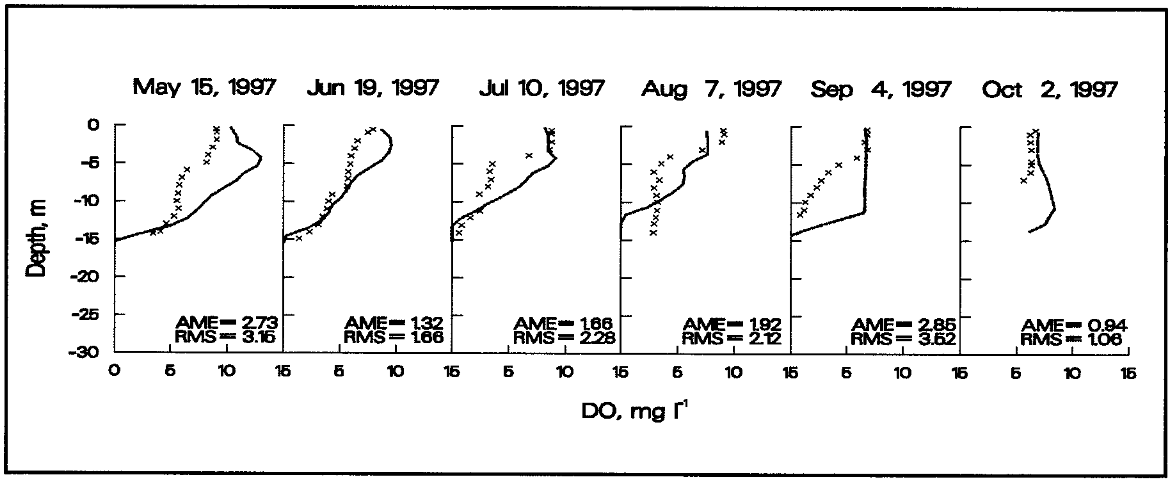

Figure A155. 1997 West Point Reservoir computed (...) versus observed (x) DO for station 07

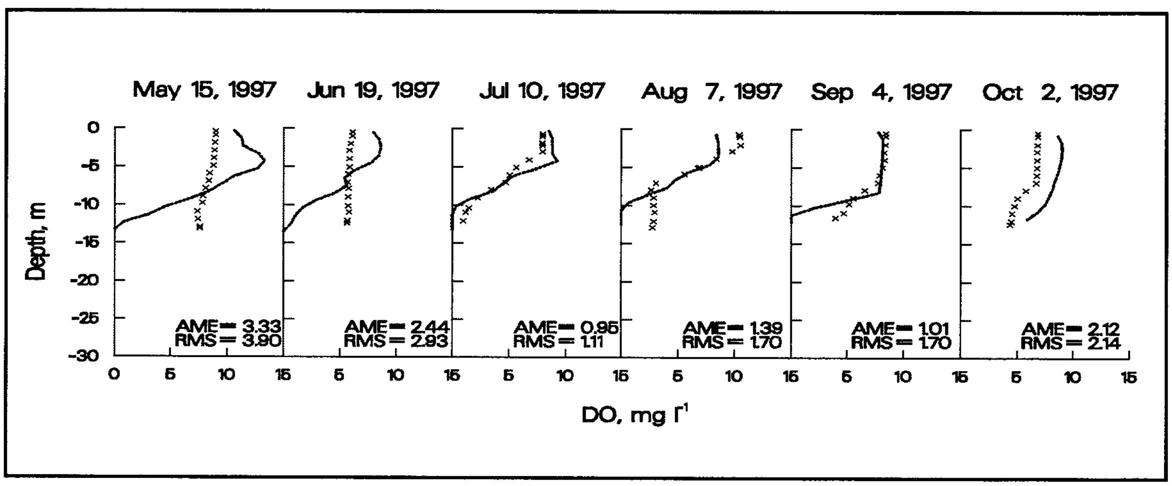

Figure A156. 1997 West Point Reservoir computed (...) versus observed (x) DO for station 10

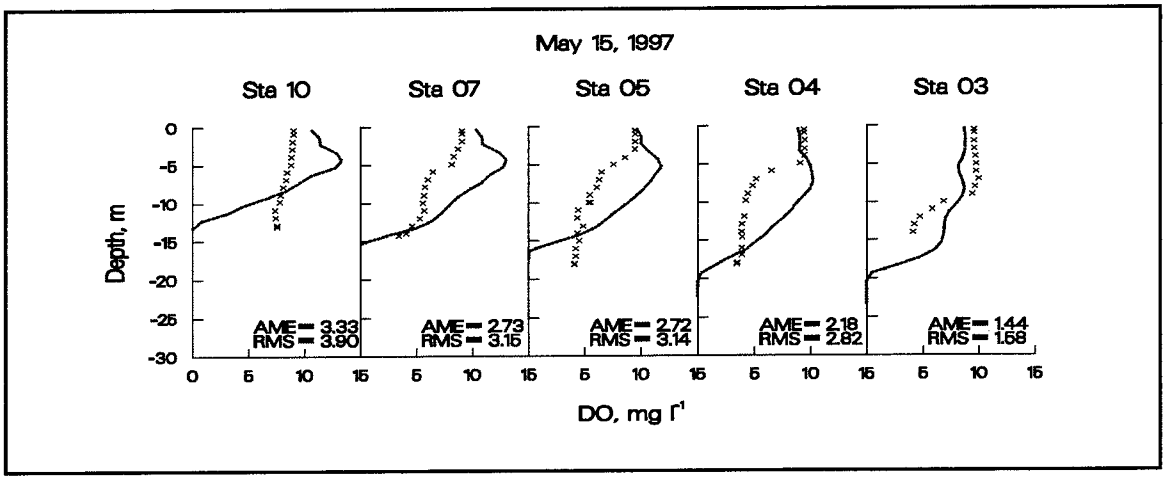

Figure A157. 1997 West Point Reservoir computed (...) versus observed (x) DO for stations along mainstem, May 15

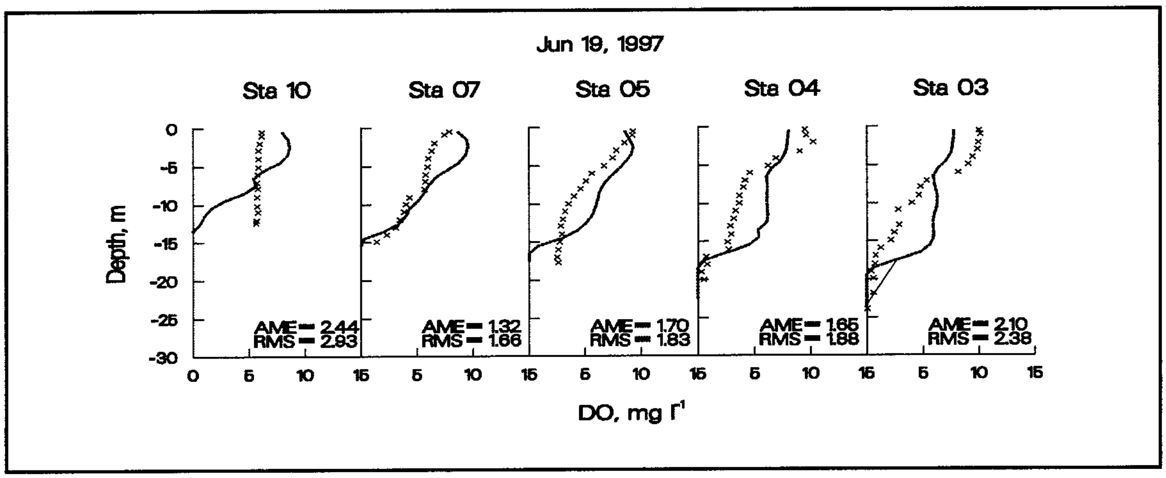

Figure A158. 1997 West Point Reservoir computed (...) versus observed (x) DO for stations along mainstem, June 19

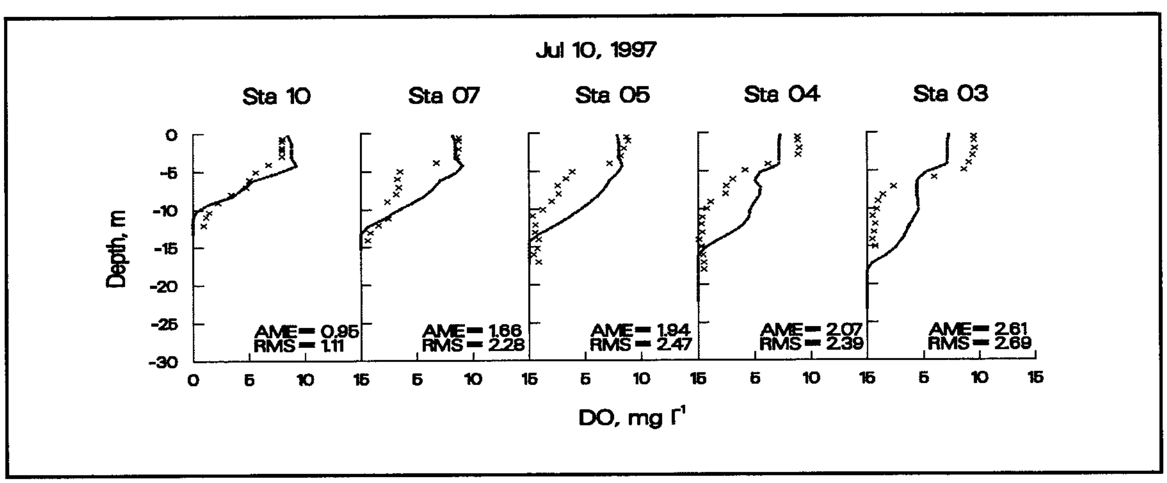

Figure A159. 1997 West Point Reservoir computed (...) versus observed (x) DO for stations along mainstem, July 10

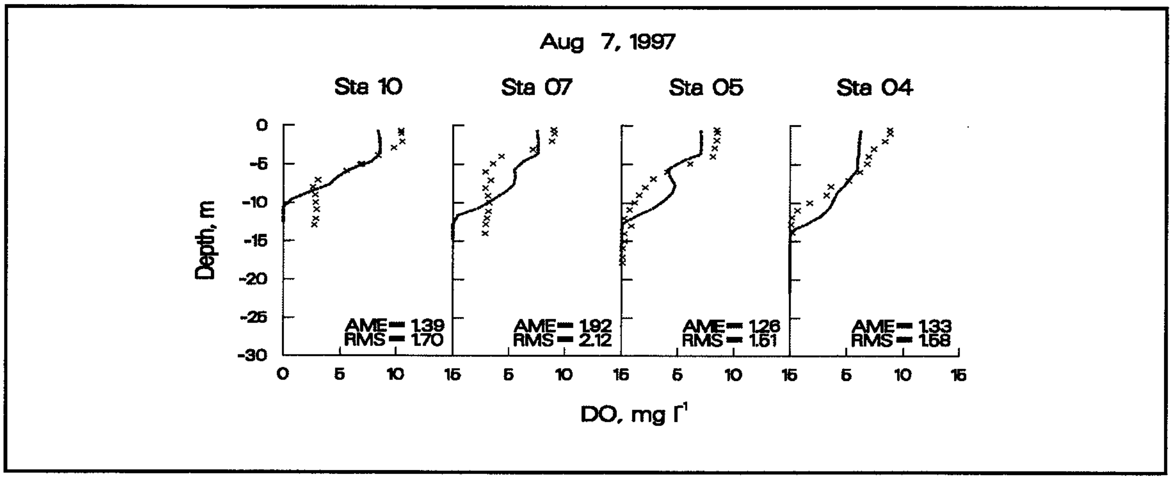

Figure A160. 1997 West Point Reservoir computed (...) versus observed (x) DO for stations along mainstem, August 7

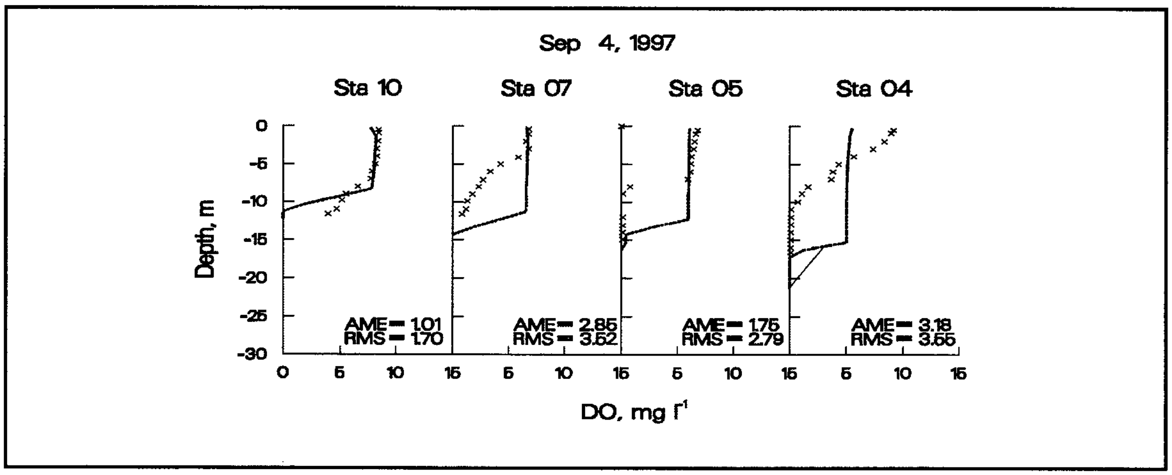

Figure A161. 1997 West Point Reservoir computed (...) versus observed (x) DO for stations along mainstem, September 4

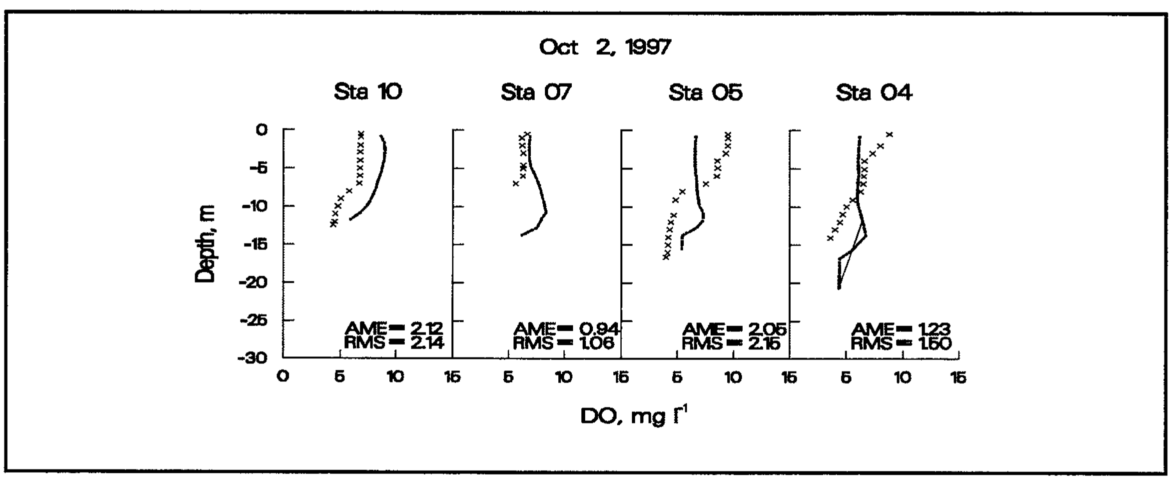

Figure A162. 1997 West Point Reservoir computed (...) versus observed (x) DO for stations along mainstem, October 2

Nutrients

Allatoona

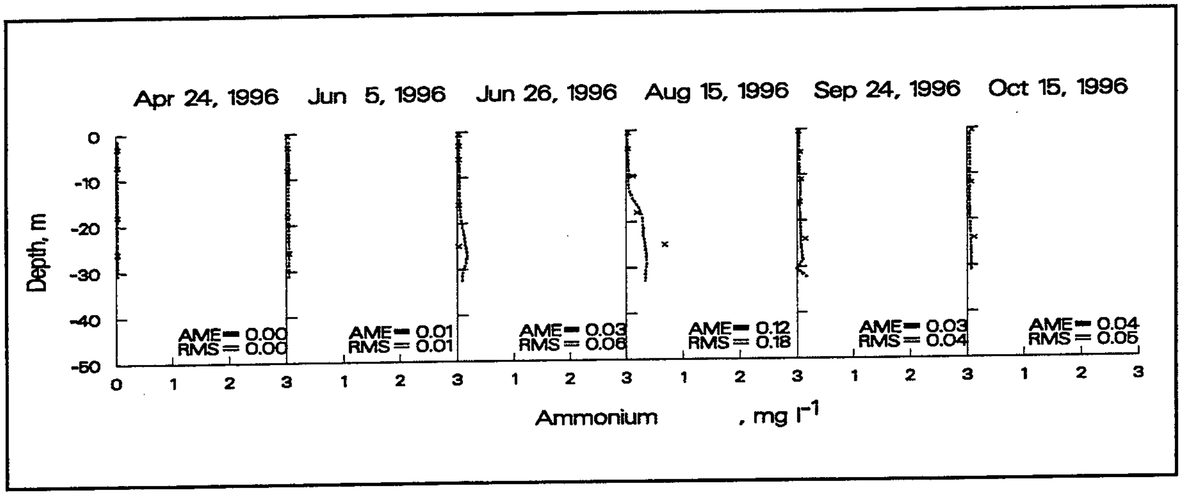

Figure A163. 1996 Allatoona Reservoir computed (...) versus observed (x) ammonium for station 09

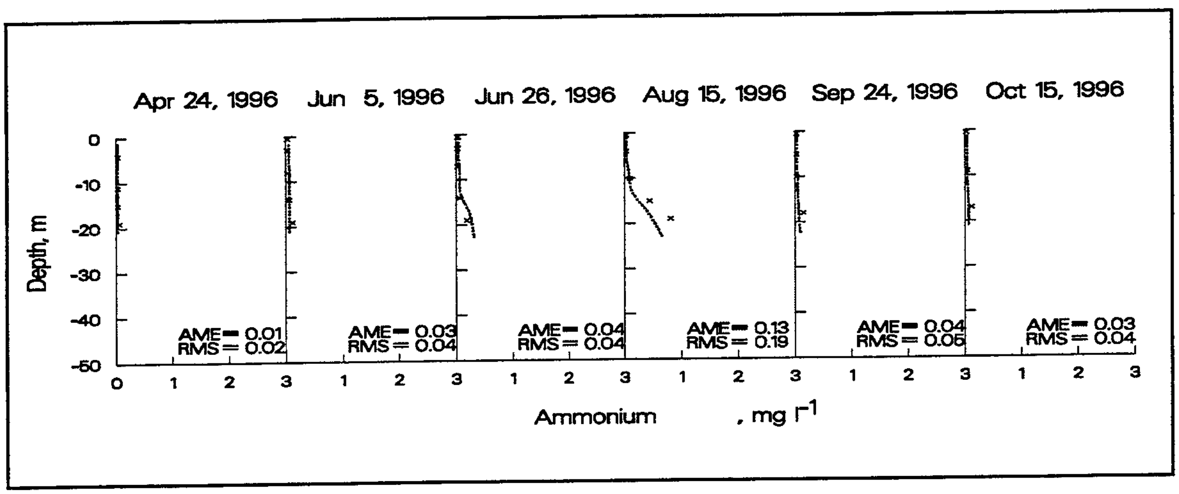

Figure A164. 1996 Allatoona Reservoir computed (...) versus observed (x) ammonium for station 18

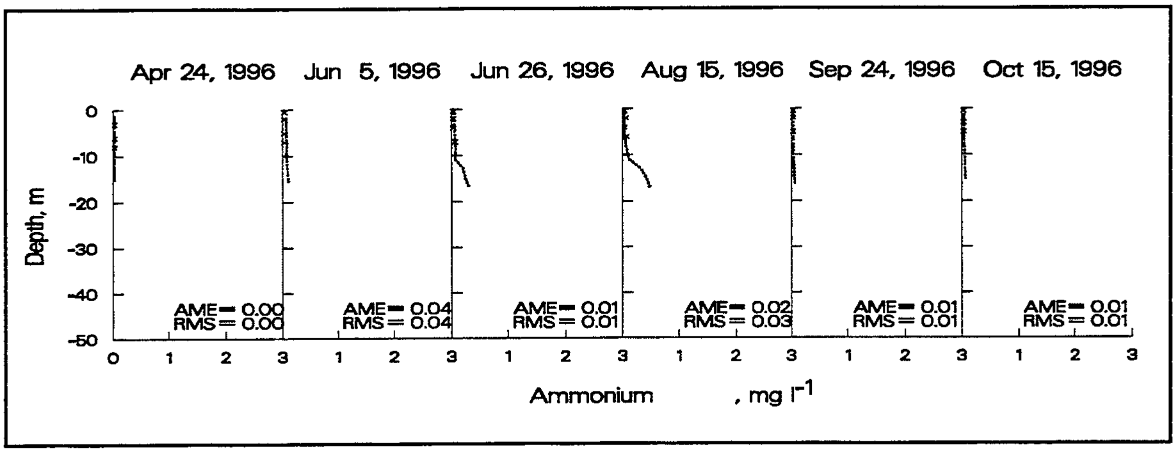

Figure A165. 1996 Allatoona Reservoir computed (...) versus observed (x) ammonium for station 45

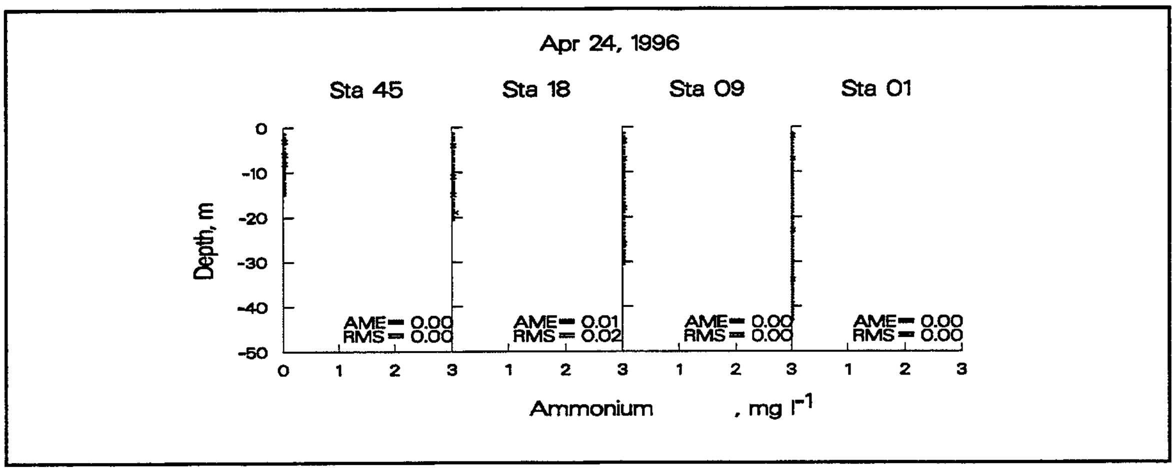

Figure A166. 1996 Allatoona Reservoir computed (...) versus observed (x) ammonium for stations along the mainstem, April 24

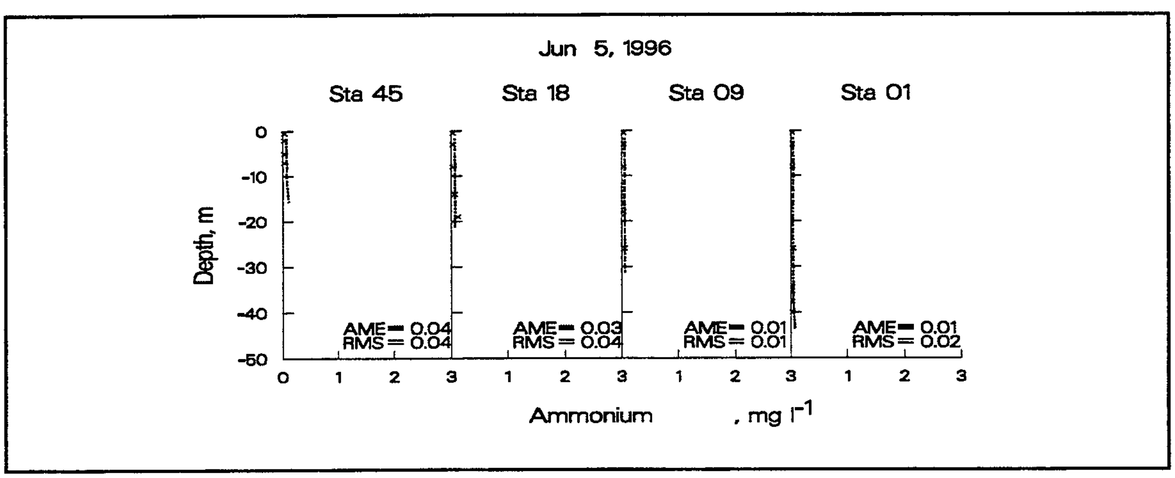

Figure A167. 1996 Allatoona Reservoir computed (...) versus observed (x) ammonium for stations along the mainstem, June 5

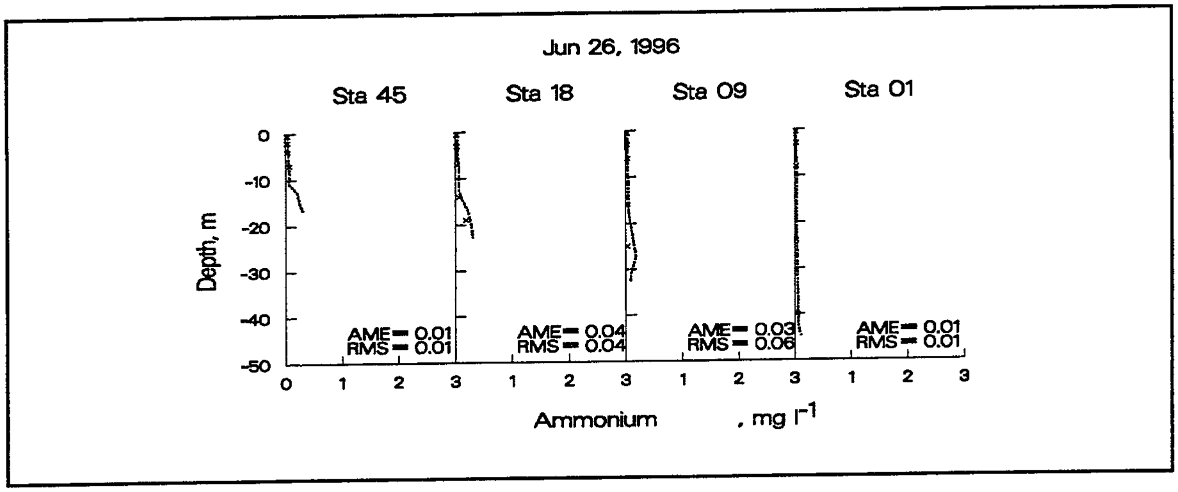

Figure A168. 1996 Allatoona Reservoir computed (...) versus observed (x) ammonium for stations along the mainstem, June 26

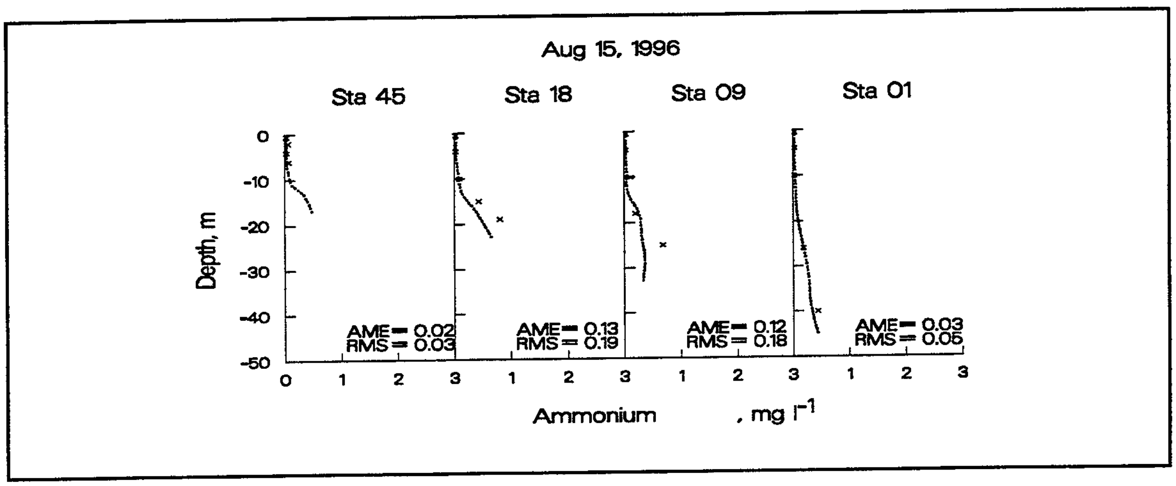

Figure A169. 1996 Allatoona Reservoir computed (...) versus observed (x) ammonium for stations along the mainstem, August 15

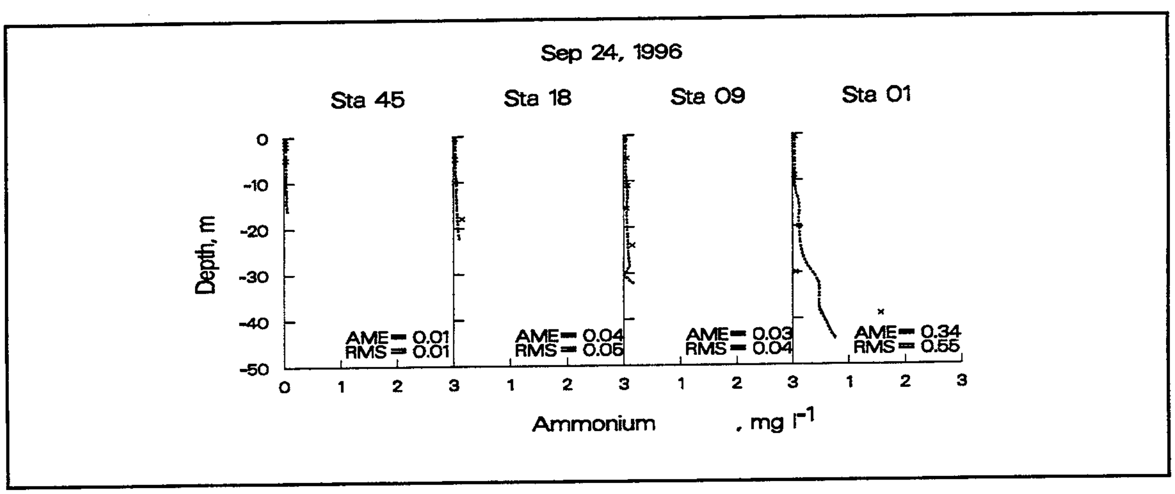

Figure A170. 1996 Allatoona Reservoir computed (...) versus observed (x) ammonium for stations along the mainstem, September 24

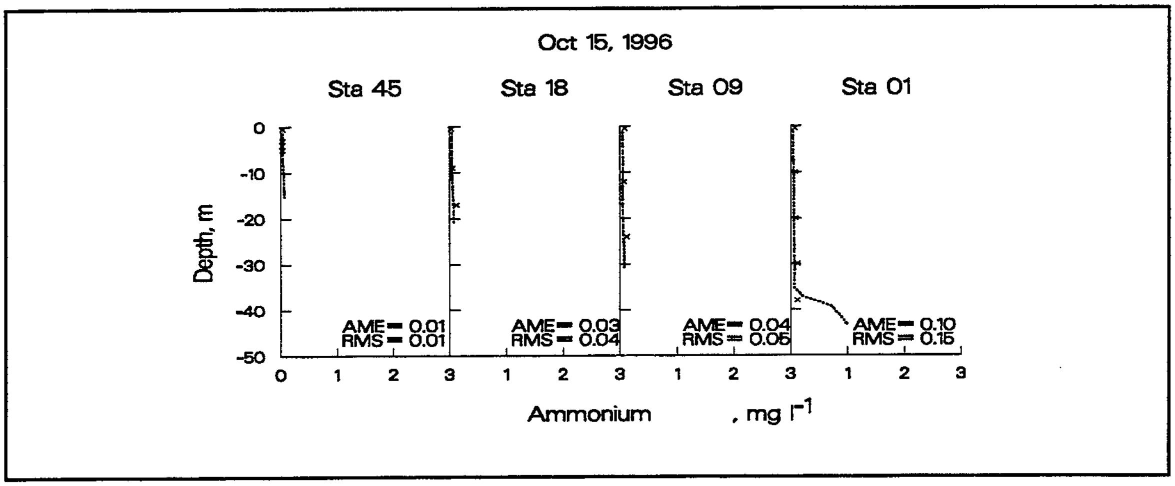

Figure A171. 1996 Allatoona Reservoir computed (...) versus observed (x) ammonium for stations along the mainstem, October 15

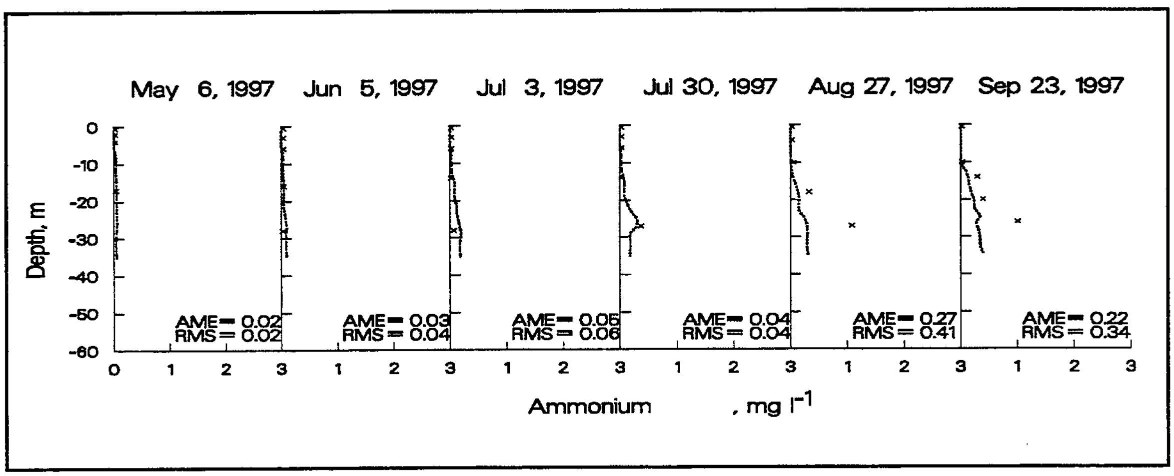

Figure A172. 1997 Allatoona Reservoir computed (...) versus observed (x) ammonium for station 09

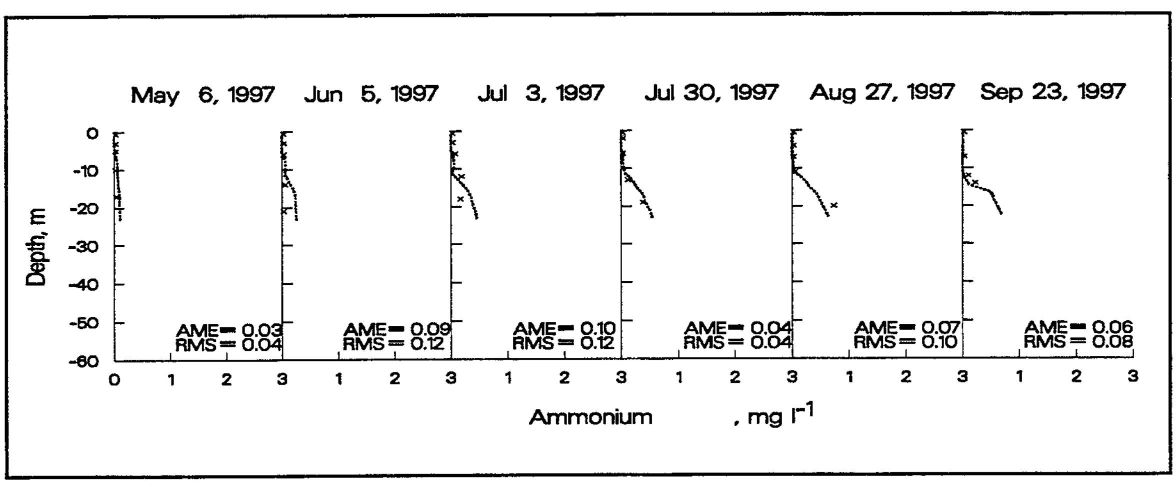

Figure A173. 1997 Allatoona Reservoir computed (...) versus observed (x) ammonium for station 18

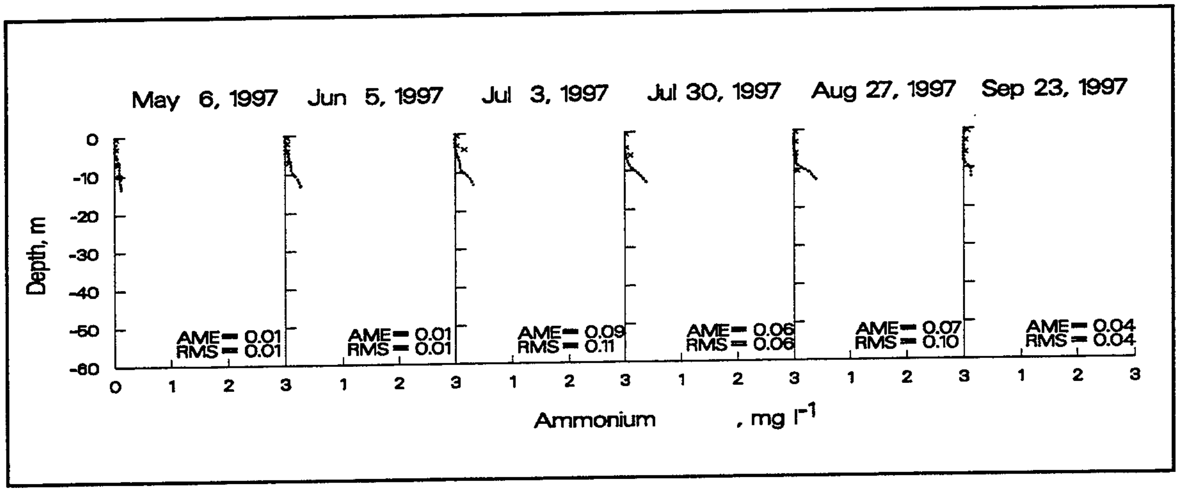

Figure A174. 1997 Allatoona Reservoir computed (...) versus observed (x) ammonium for station 45

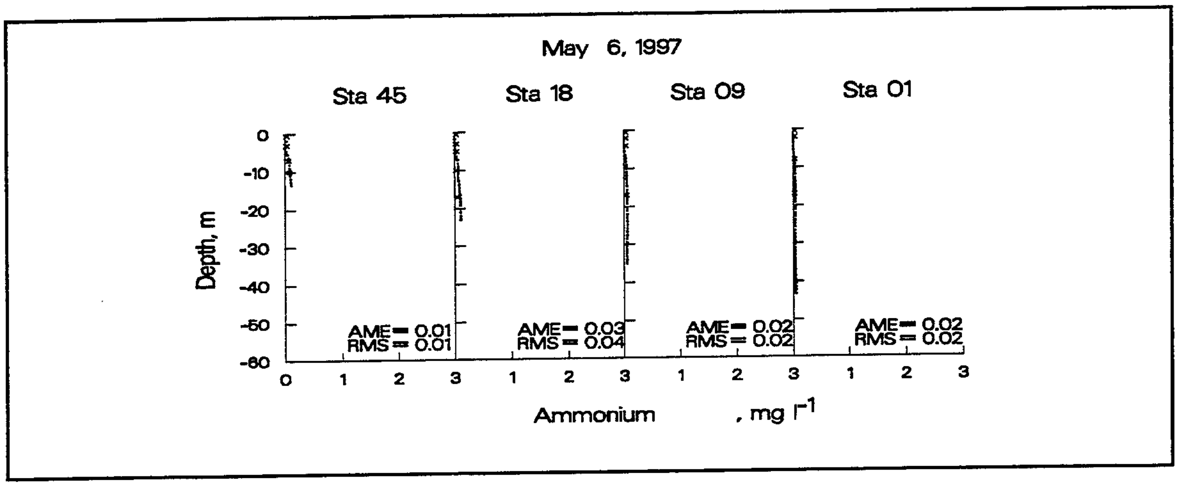

Figure A175. 1997 Allatoona Reservoir computed (...) versus observed (x) ammonium for stations along the mainstem, May 6

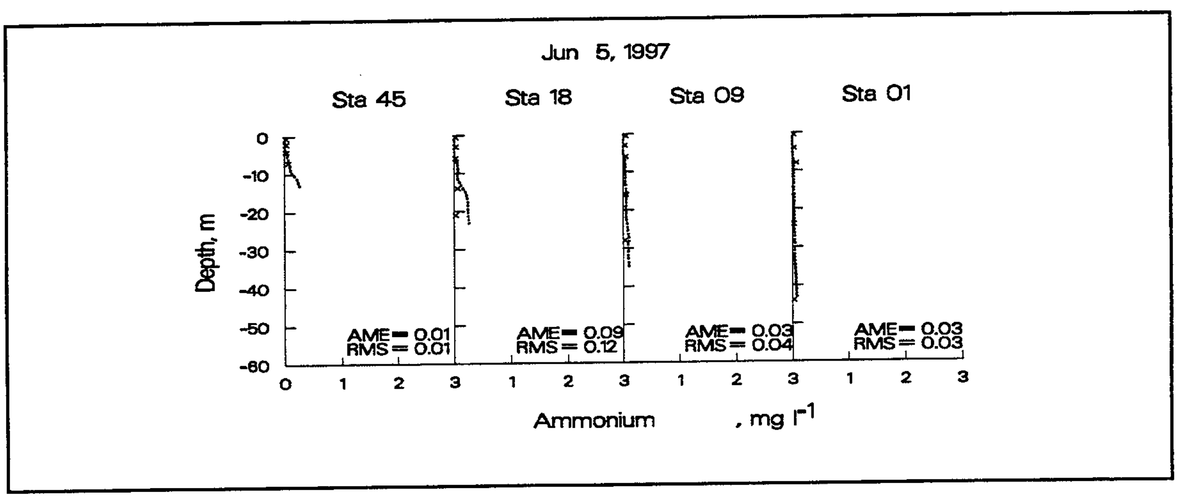

Figure A176. 1997 Allatoona Reservoir computed (...) versus observed (x) ammonium for stations along the mainstem, June 5

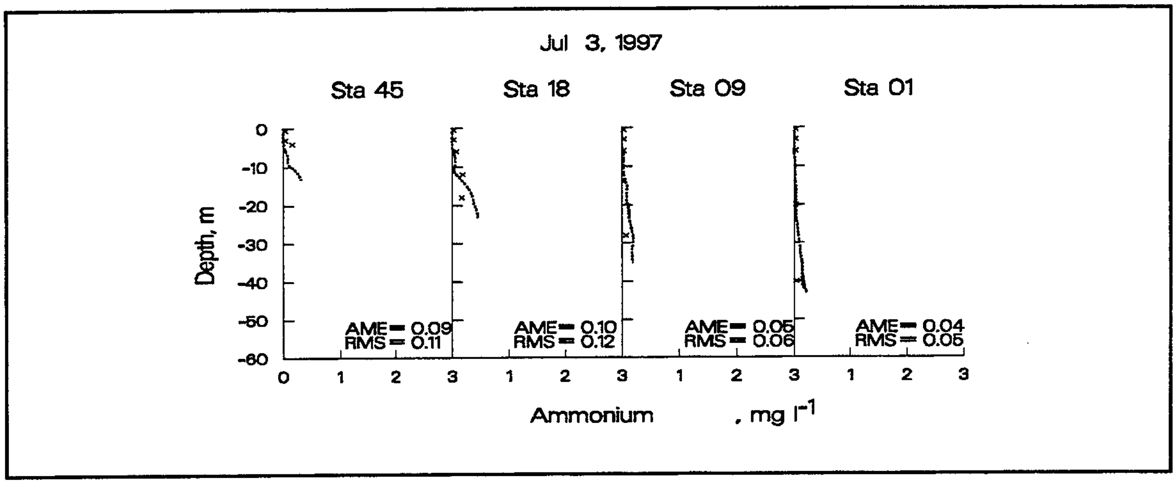

Figure A177. 1997 Allatoona Reservoir computed (...) versus observed (x) ammonium for stations along the mainstem, July 3

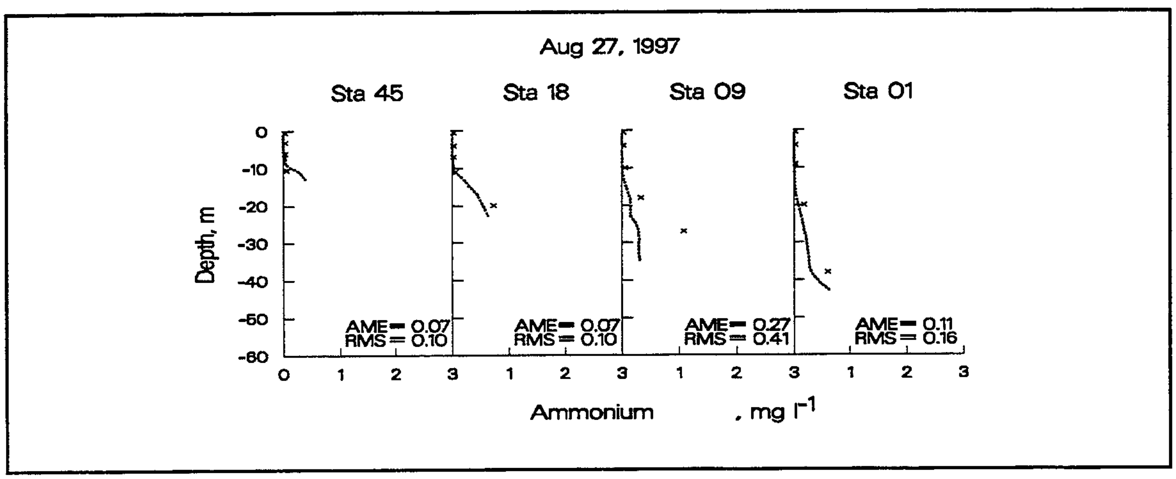

Figure A178. 1997 Allatoona Reservoir computed (...) versus observed (x) ammonium for stations along the mainstem, August 27

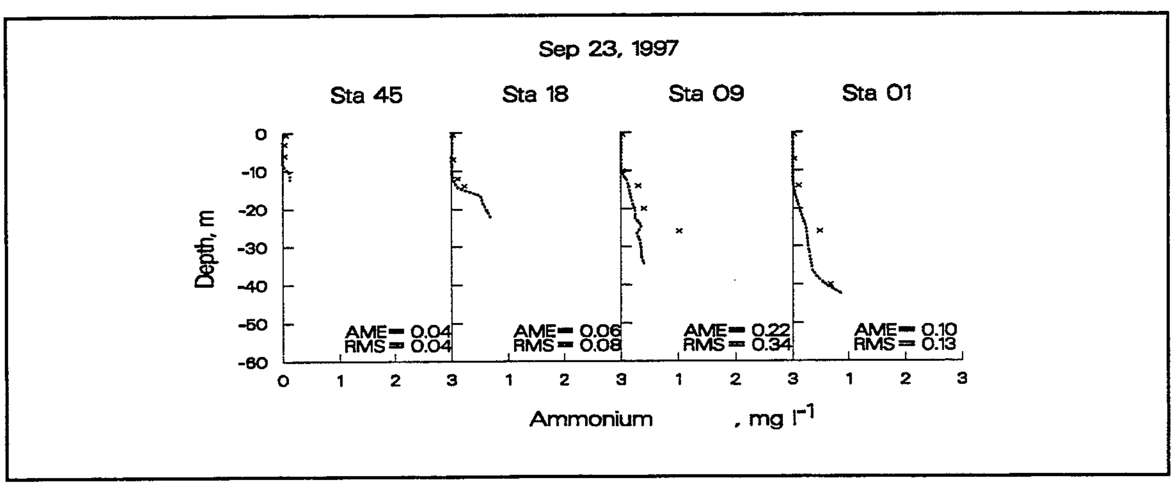

Figure A179. 1997 Allatoona Reservoir computed (...) versus observed (x) ammonium for stations along the mainstem

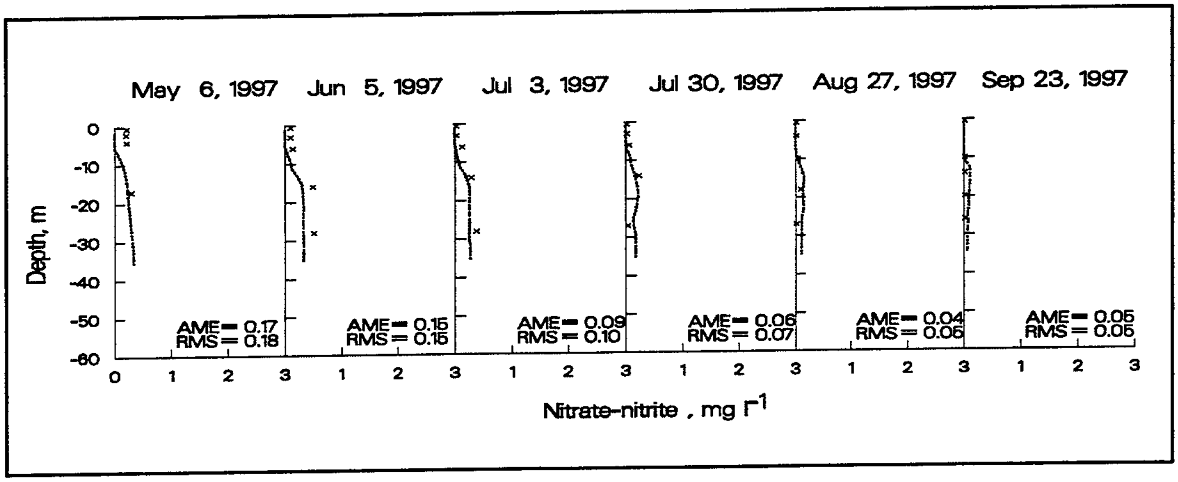

Figure A180. 1996 Allatoona Reservoir computed (...) versus observed (x) nitrate-nitrite for station 09

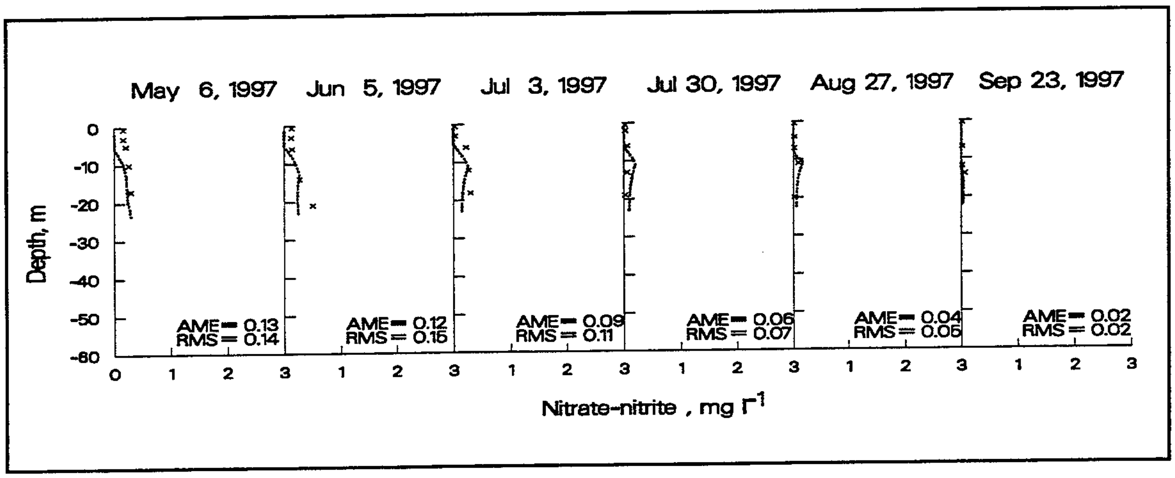

Figure A181. 1996 Allatoona Reservoir computed (...) versus observed (x) nitrate-nitrite for station 18

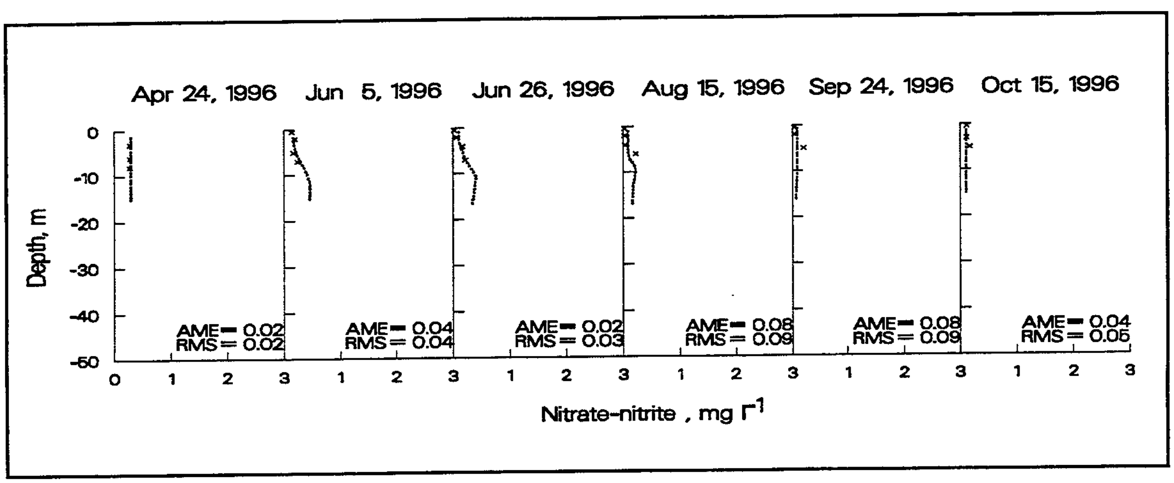

Figure A182. 1996 Allatoona Reservoir computed (...) versus observed (x) nitrate-nitrite for station 45

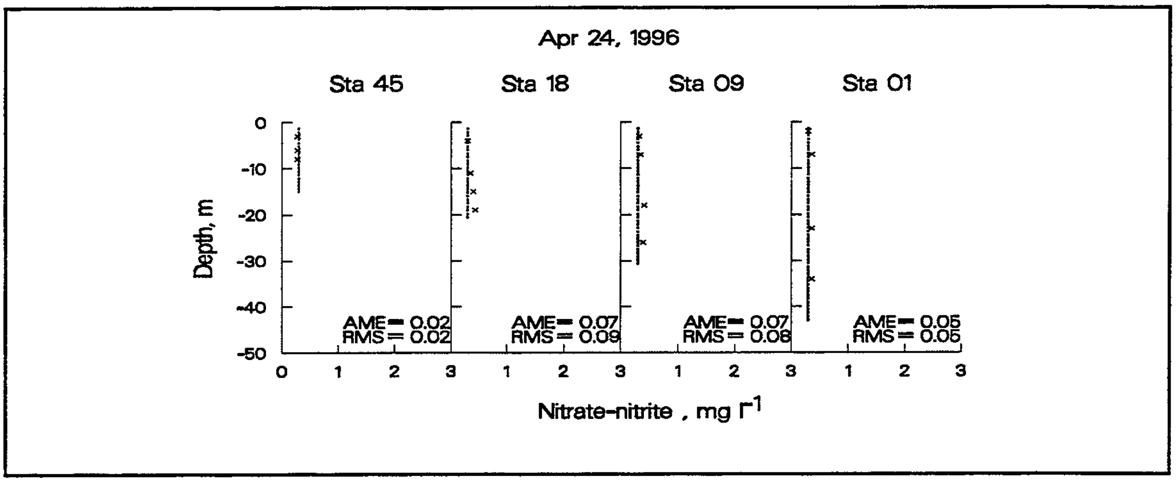

Figure A183. 1996 Allatoona Reservoir computed (...) versus observed (x) nitrate-nitrite for stations along mainstem, April 24

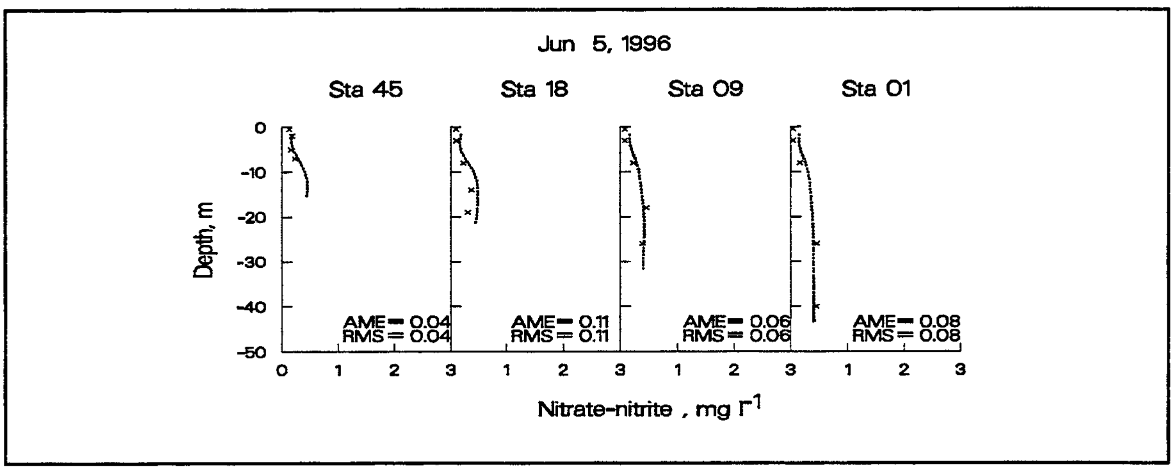

Figure A184. 1996 Allatoona Reservoir computed (...) versus observed (x) nitrate-nitrite for stations along mainstem, June 5

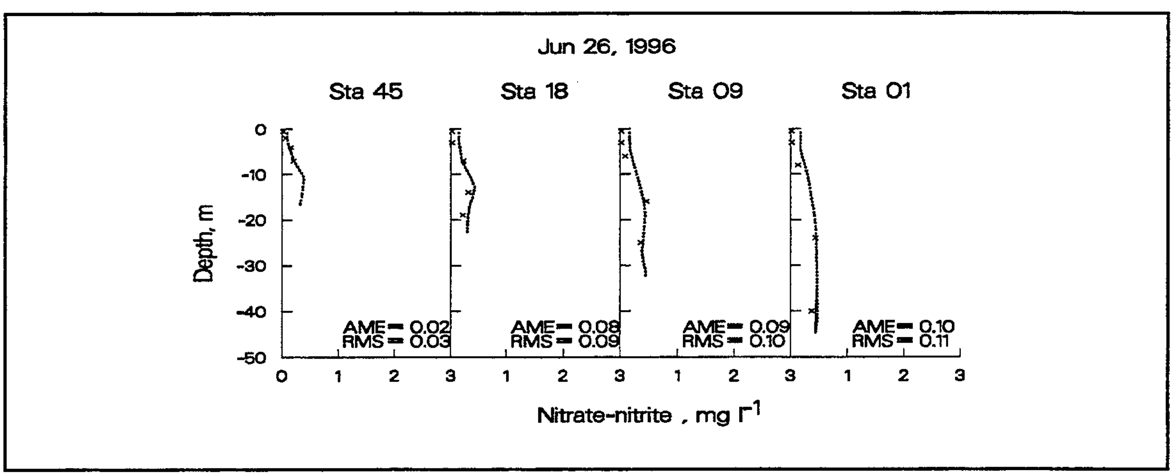

Figure A185. 1996 Allatoona Reservoir computed (...) versus observed (x) nitrate-nitrite for stations along mainstem, June 26

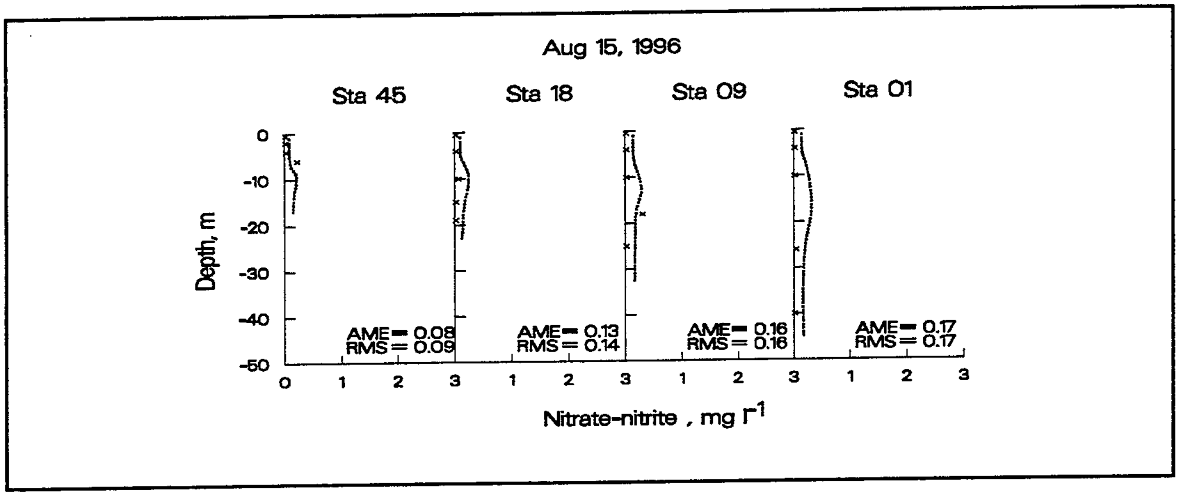

Figure A186. 1996 Allatoona Reservoir computed (...) versus observed (x) nitrate-nitrite for stations along mainstem, August 15

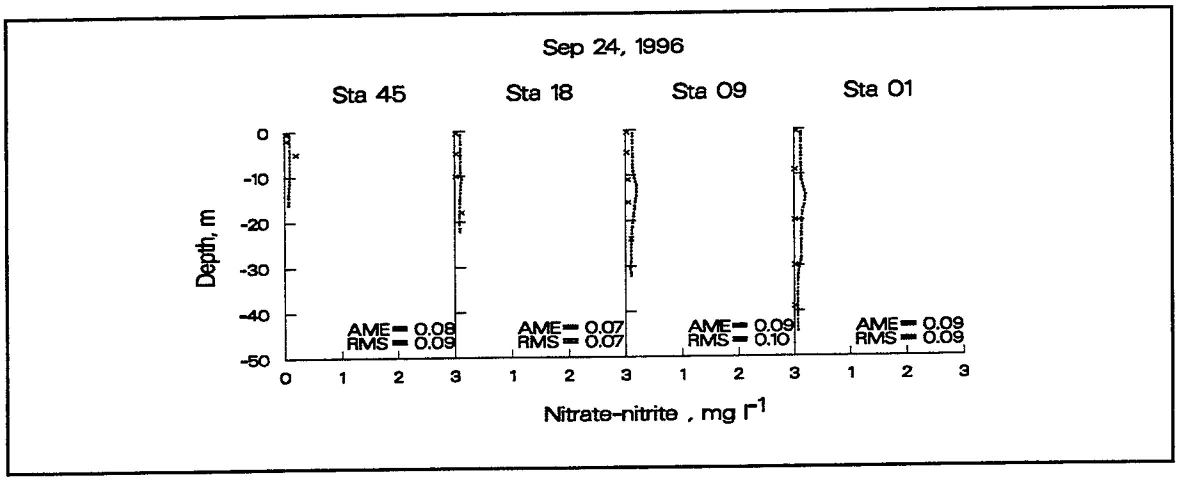

Figure A187. 1996 Allatoona Reservoir computed (...) versus observed (x) nitrate-nitrite for stations along mainstem, September 24

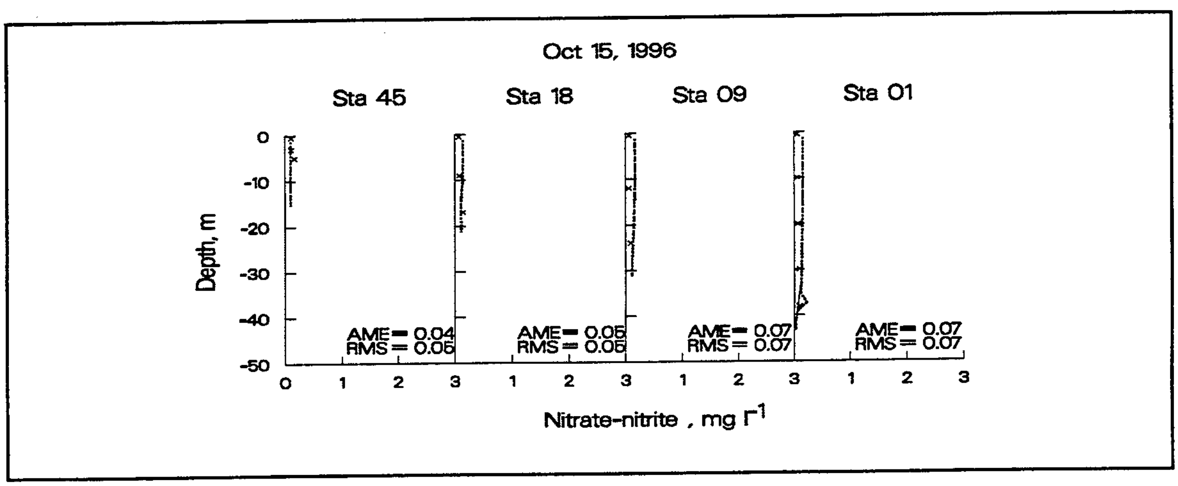

Figure A188. 1996 Allatoona Reservoir computed (...) versus observed (x) nitrate-nitrite for stations along mainstem. October 15

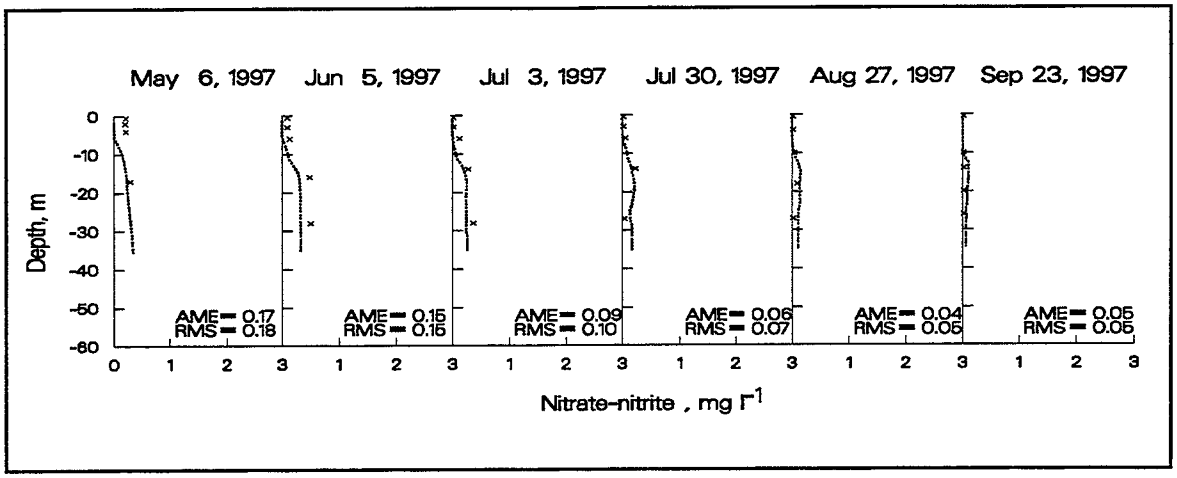

Figure A189. 1997 Allatoona Reservoir computed (...) versus observed (x) nitrate-nitrite for station 09

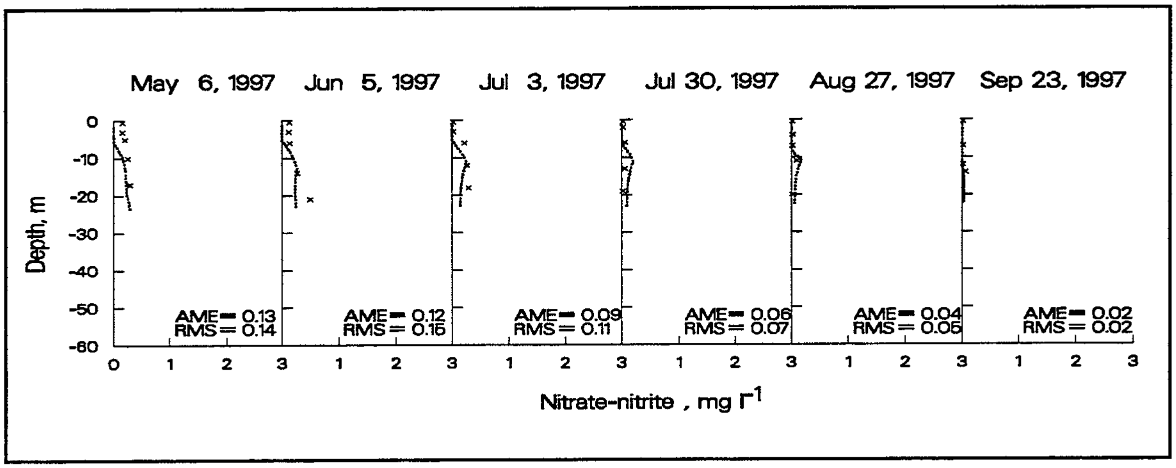

Figure A190. 1997 Allatoona Reservoir computed (...) versus observed (x) nitrate-nitrite for station 18

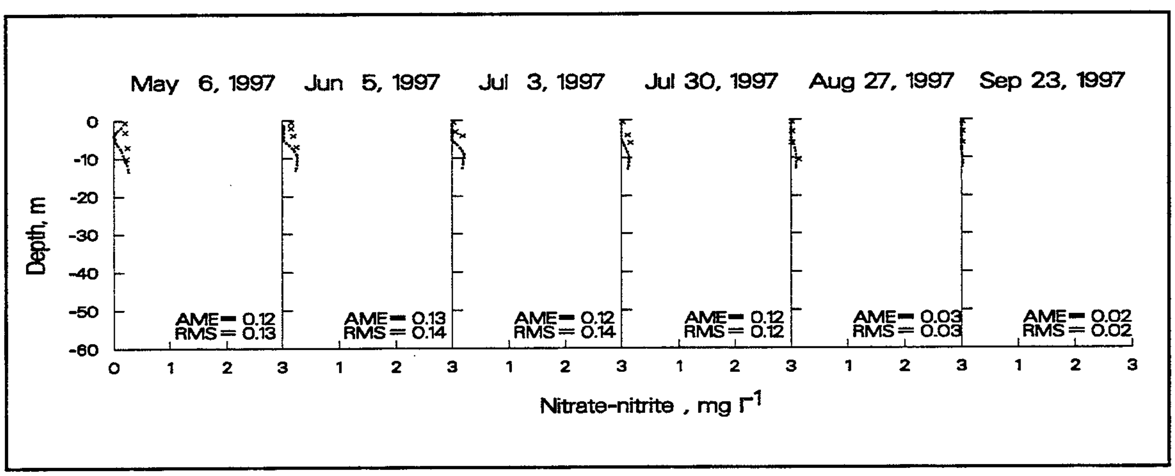

Figure A191. 1997 Allatoona Reservoir computed (...) versus observed (x) nitrate-nitrite for station 45

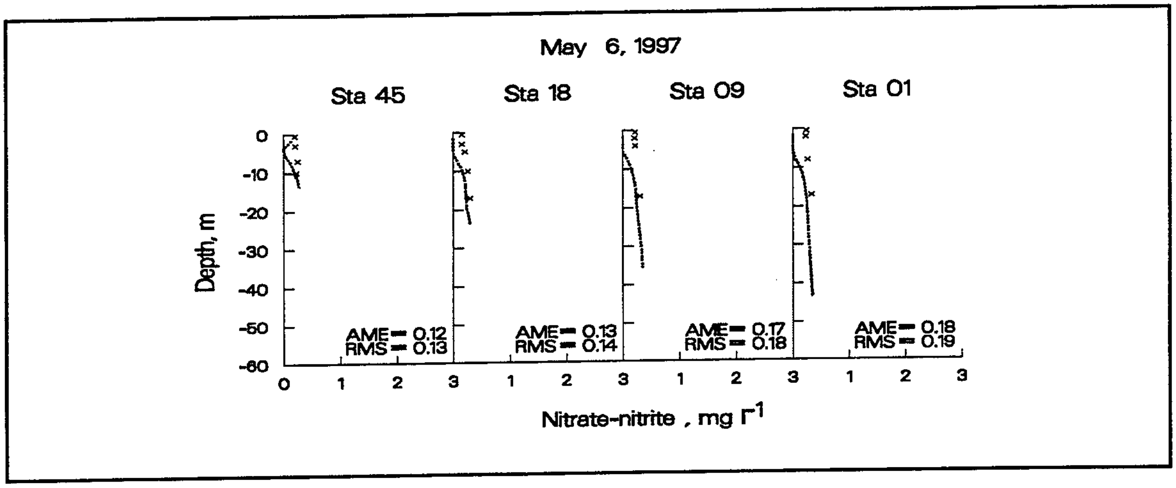

Figure A192. 1997 Allatoona Reservoir computed (...) versus observed (x) nitrate-nitrite for stations along mainstem, May 6

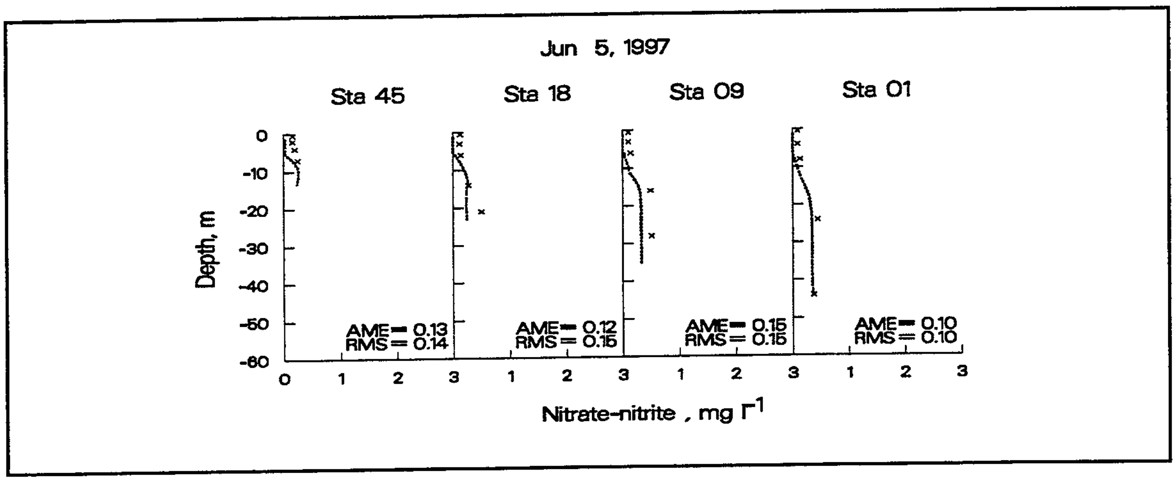

Figure A193. 1997 Allatoona Reservoir computed (...) versus observed (x) nitrate-nitrite for stations along mainstem, June 5

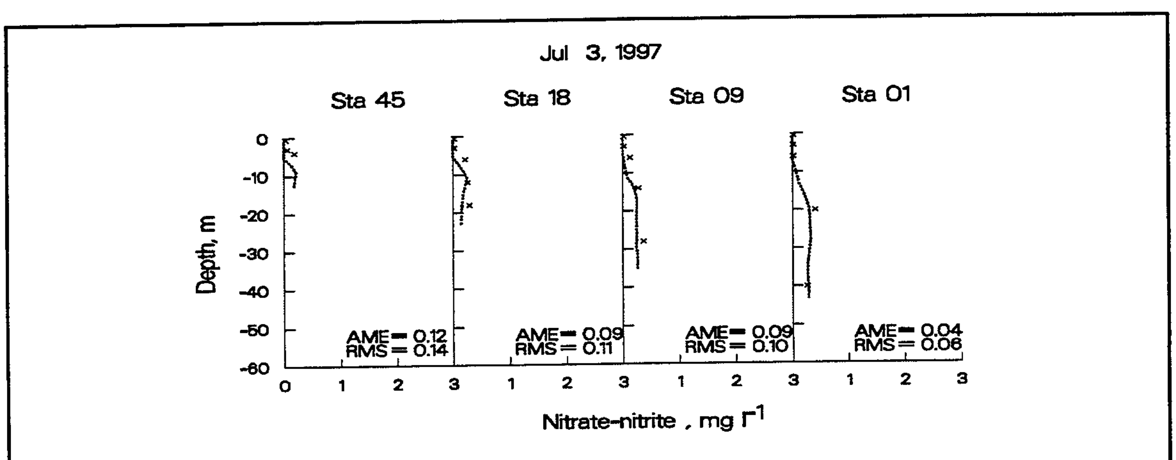

Figure A194. 1997 Allatoona Reservoir computed (...) versus observed (x) nitrate-nitrite for stations along mainstem, July 3

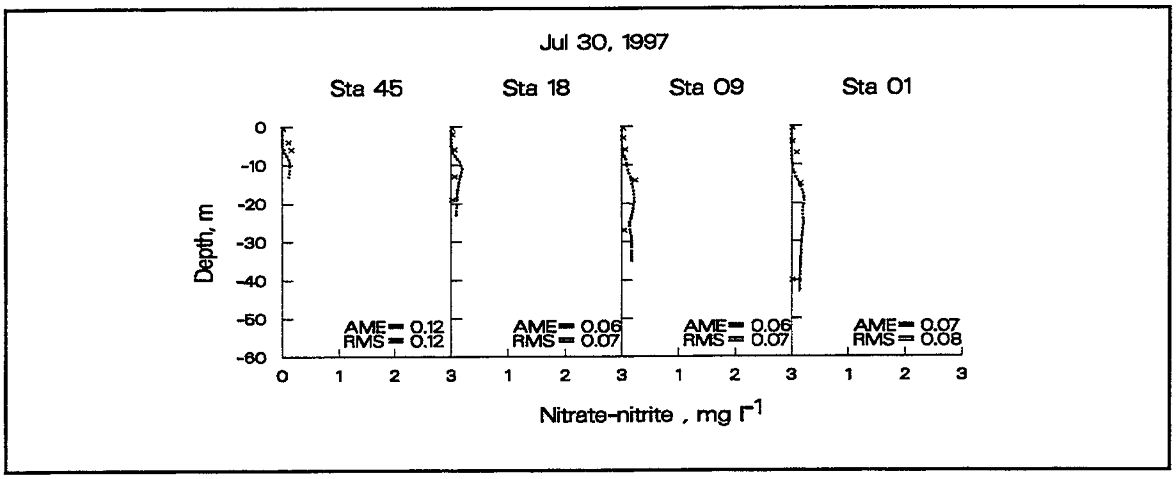

Figure A195. 1997 Allatoona Reservoir computed (...) versus observed (x) nitrate-nitrite for stations along mainstem, July 30

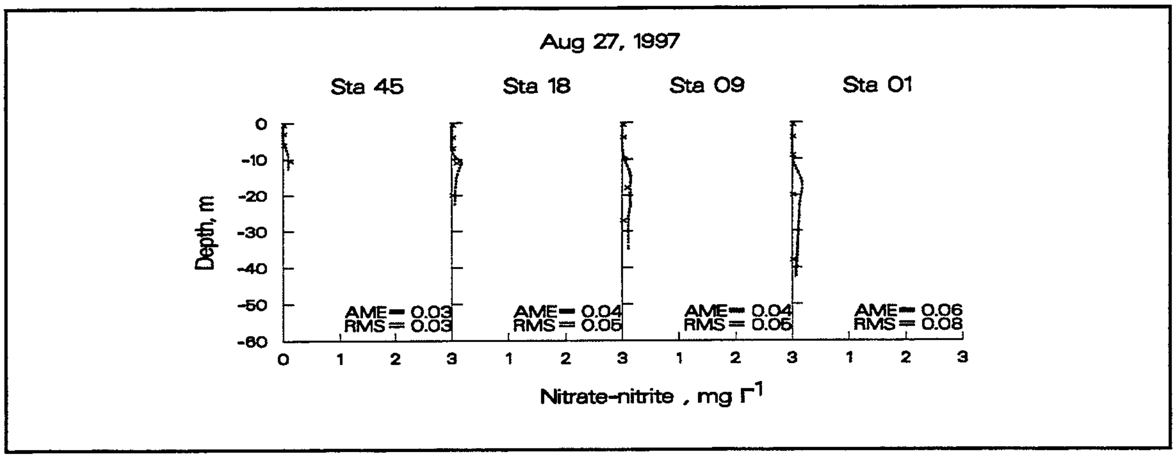

Figure A196. 1997 Allatoona Reservoir computed (...) versus observed (x) nitrate-nitrite for stations along mainstem, August 27

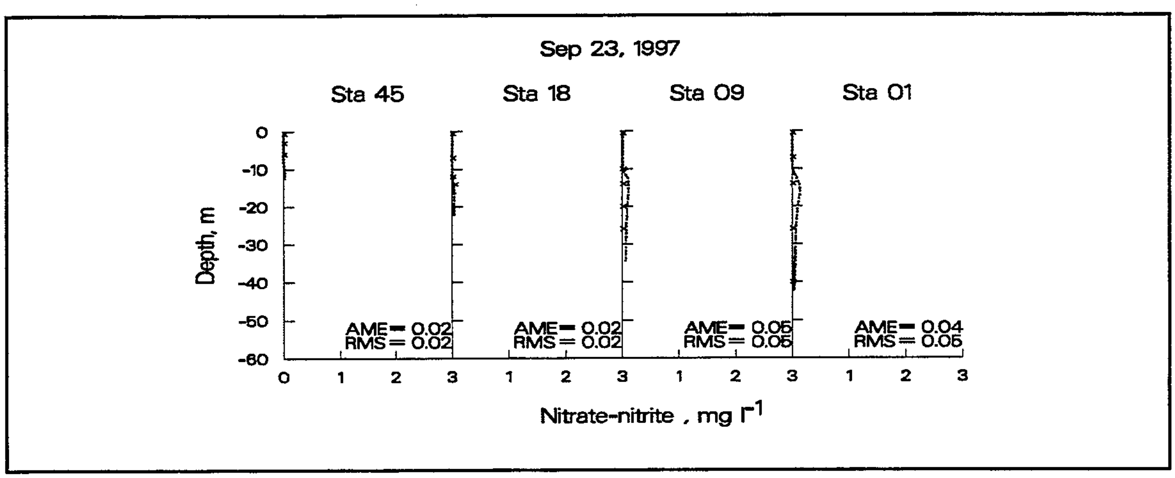

Figure A197. 1997 Allatoona Reservoir computed (...) versus observed (x) nitrate-nitrite for stations along mainstem, September 23

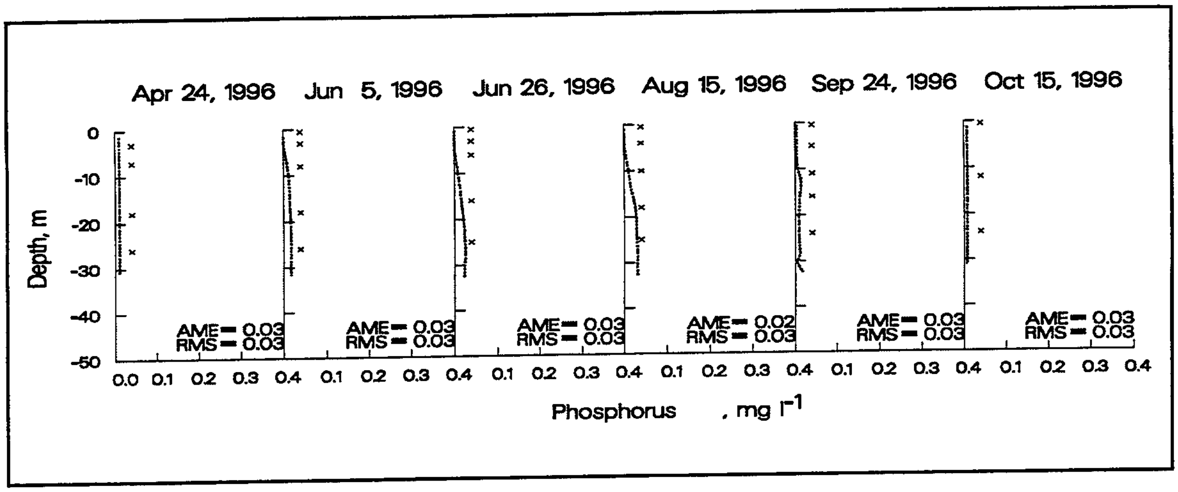

Figure A198. 1996 Allatoona Reservoir computed (...) versus observed (x) bioavailable phosphorus for station 09

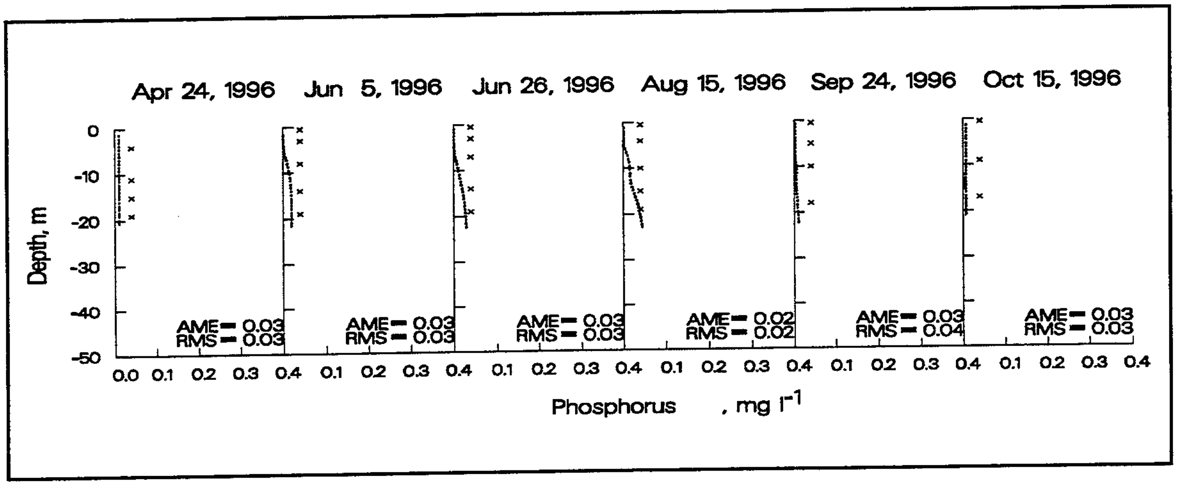

Figure A199. 1996 Allatoona Reservoir computed (...) versus observed (x) bioavailable phosphorus for station 18

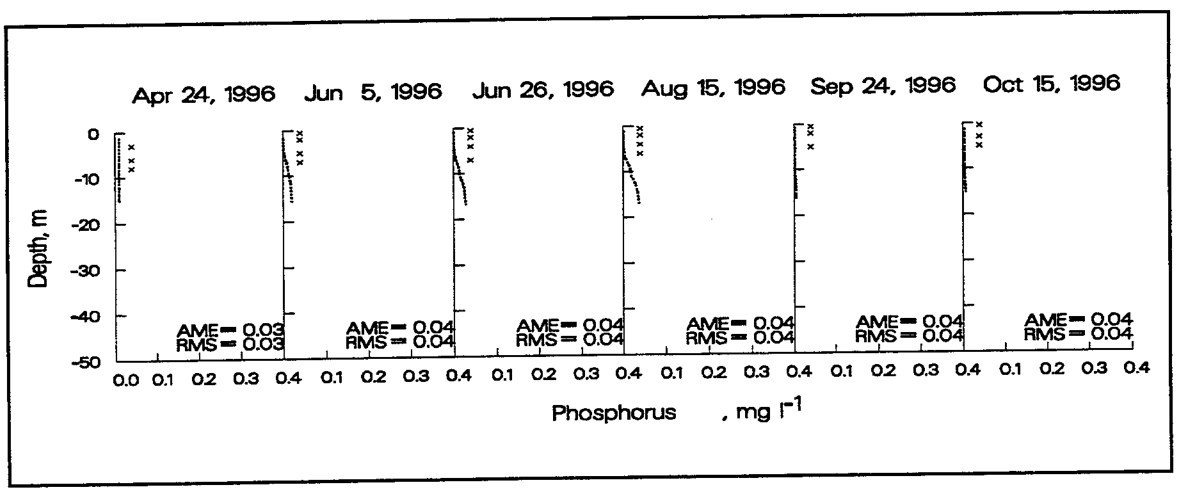

Figure A200. 1996 Allatoona Reservoir computed (...) versus observed (x) bioavailable phosphorus for station 45

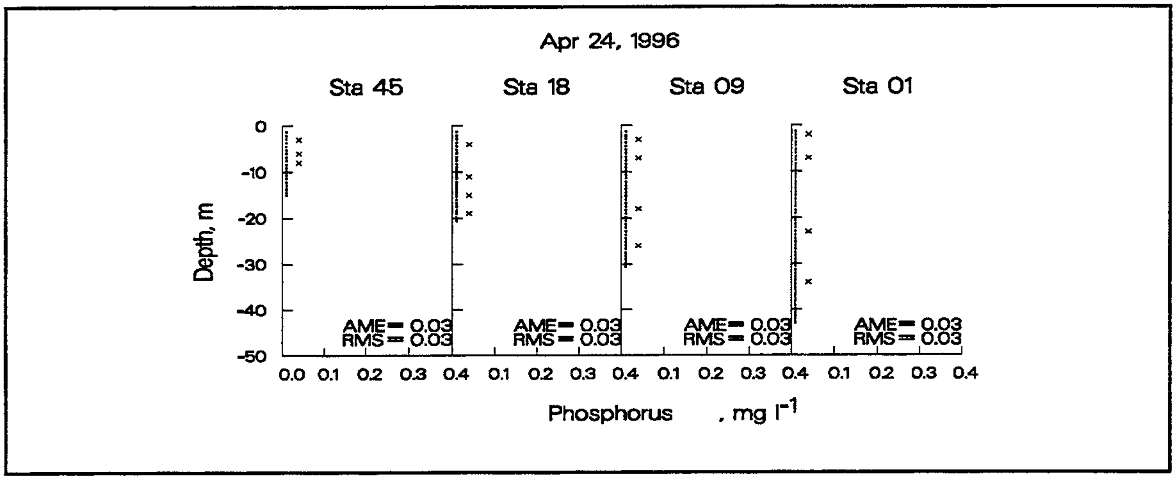

Figure A201. 1996 Allatoona Reservoir computed (...) versus observed (x) bioavailable phosphorus for stations along mainstem, April 24

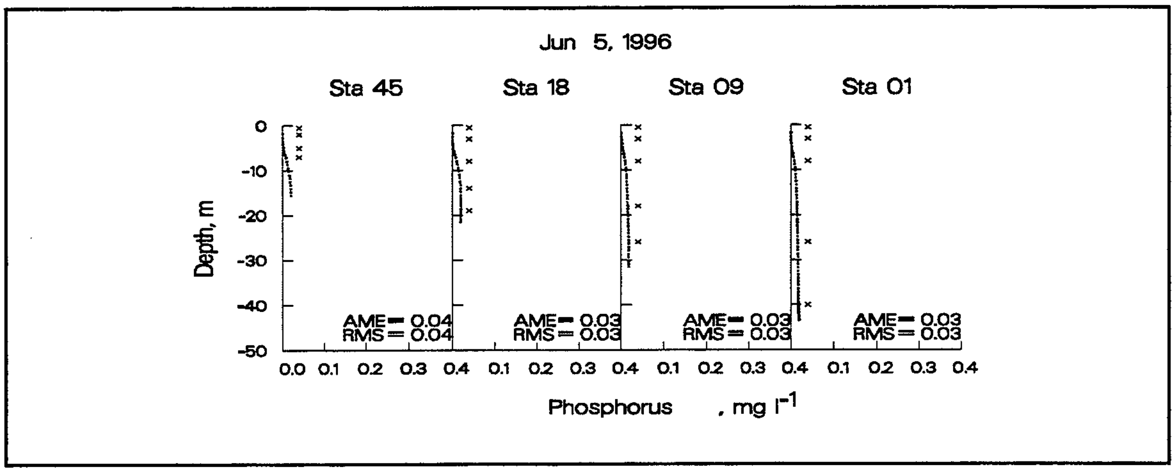

Figure A202. 1996 Allatoona Reservoir computed (...) versus observed (x) bioavailable phosphorus for stations along mainstem, June 5

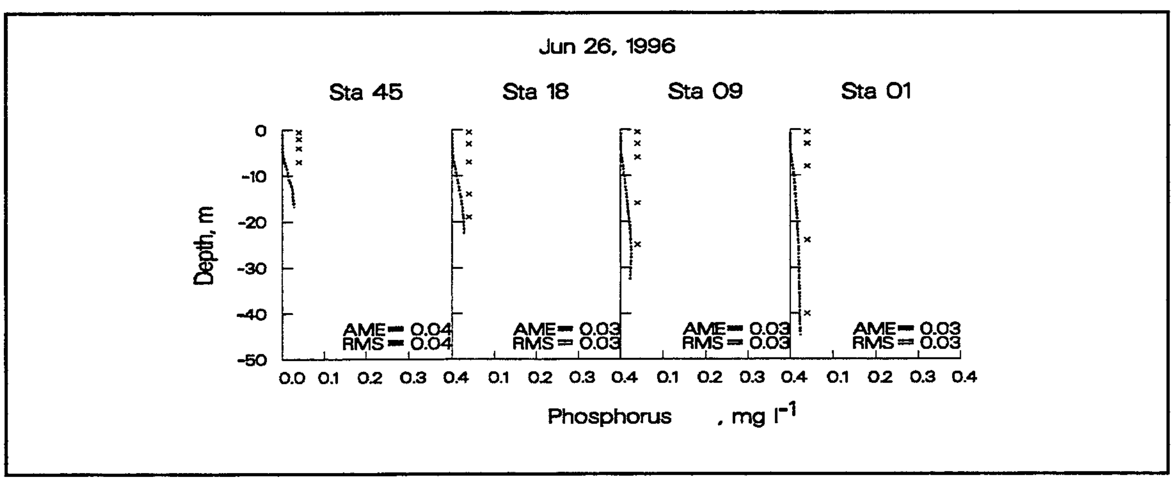

Figure A203. 1996 Allatoona Reservoir computed (...) versus observed (x) bioavailable phosphorus for stations along mainstem, June 26

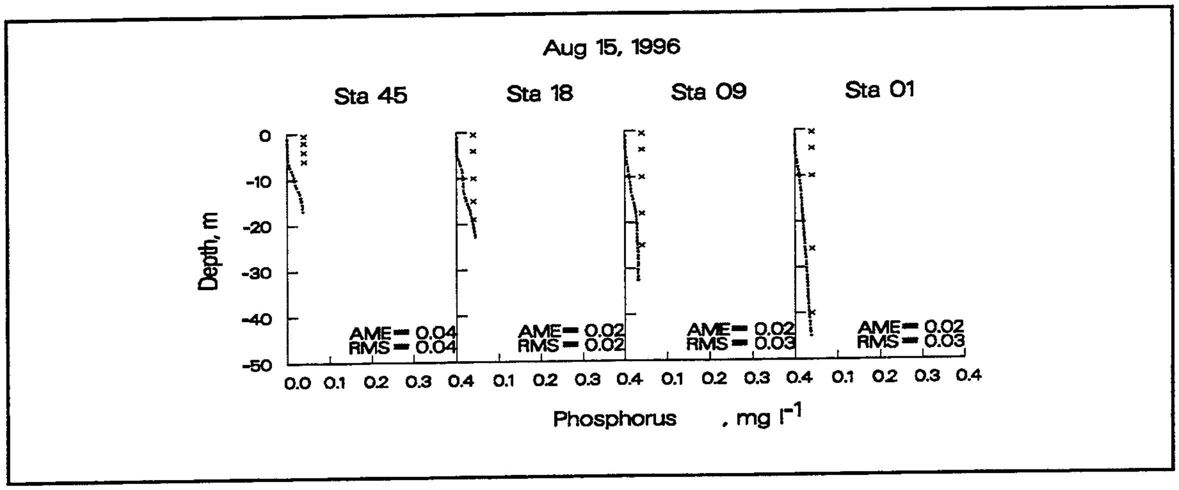

Figure A204. 1996 Allatoona Reservoir computed (...) versus observed (x) bioavailable phosphorus for stations along mainstem, August 15

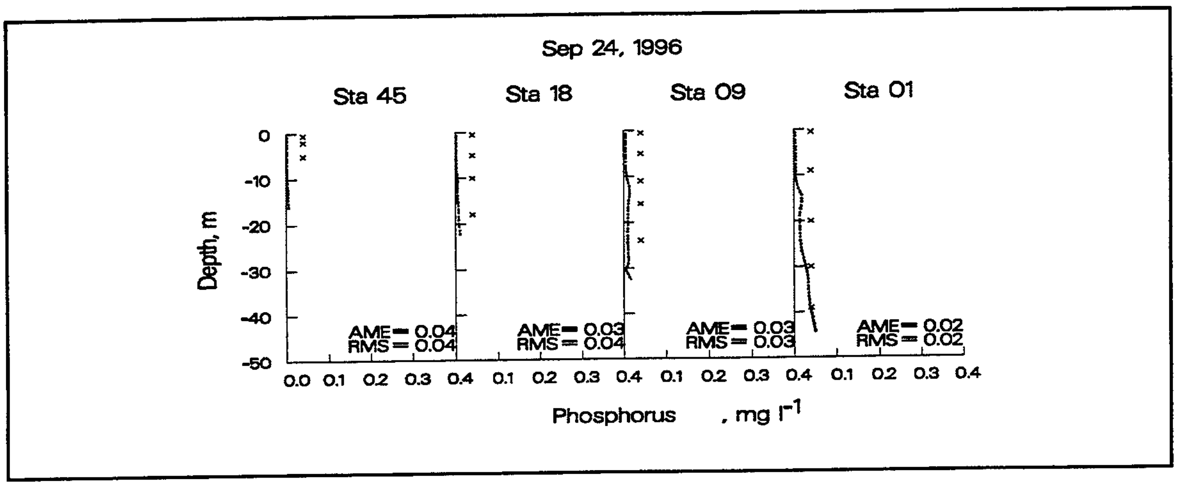

Figure A205. 1996 Allatoona Reservoir computed (...) versus observed (x) bioavailable phosphorus for stations along mainstem, September 24

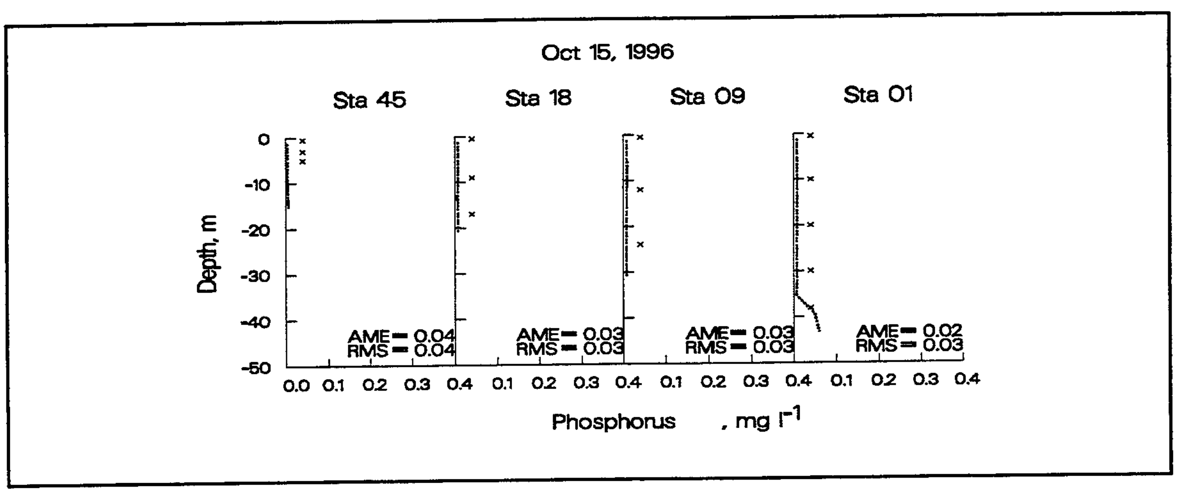

Figure A206. 1996 Allatoona Reservoir computed (...) versus observed (x) bioavailable phosphorus for stations along mainstem, October 15

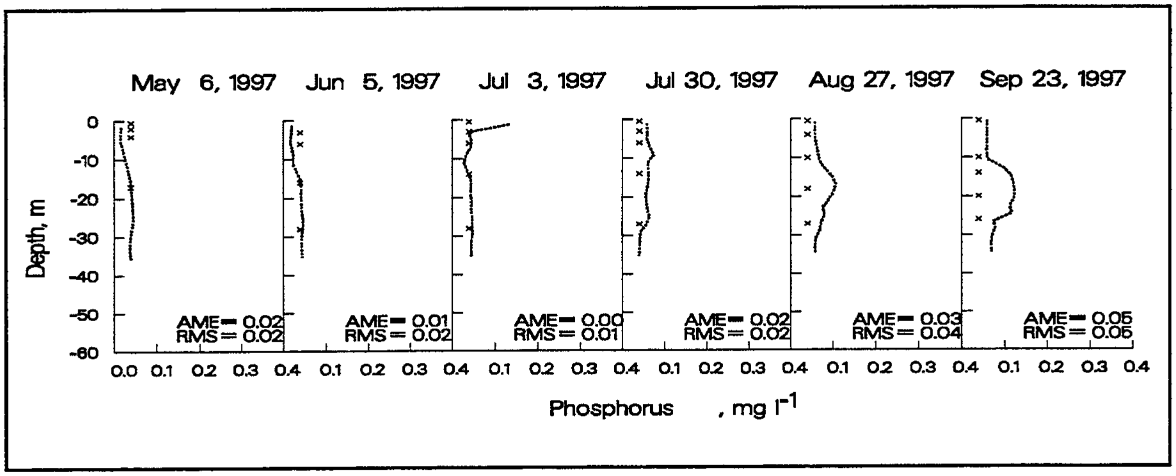

Figure A207. 1997 Allatoona Reservoir computed (...) versus observed (x) bioavailable phosphorus for station 09

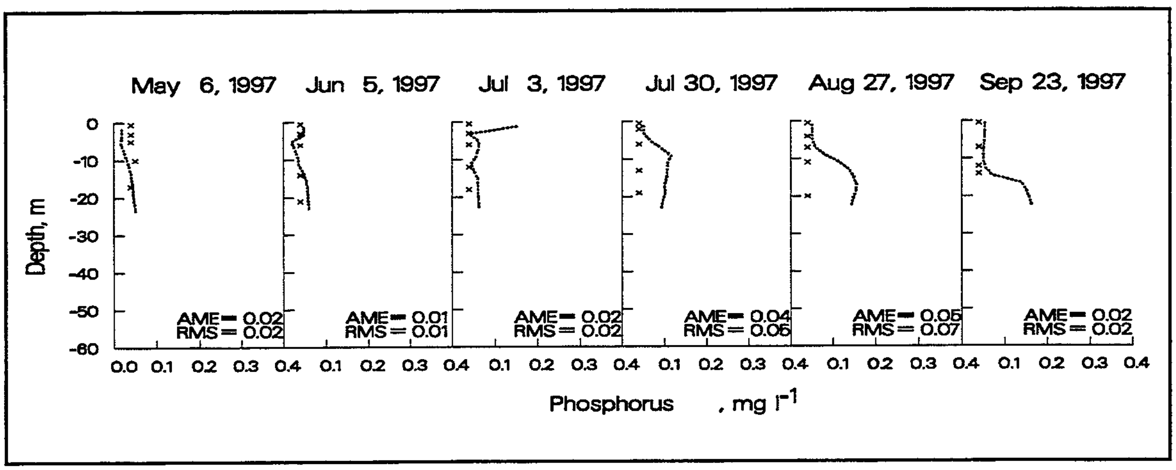

Figure A208. 1997 Allatoona Reservoir computed (...) versus observed (x) bioavailable phosphorus for station 18

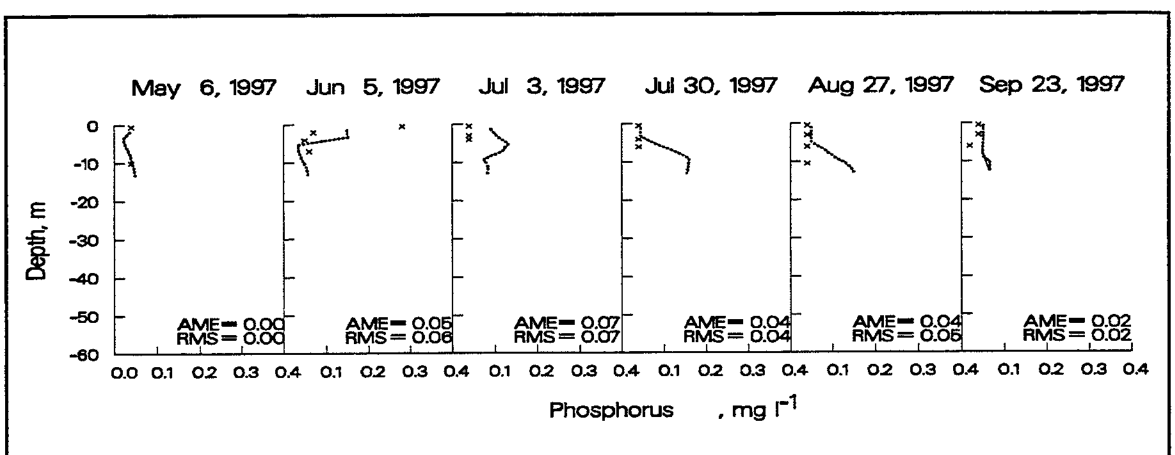

Figure A209. 1997 Allatoona Reservoir computed (...) versus observed (x) bioavailable phosphorus for station 45

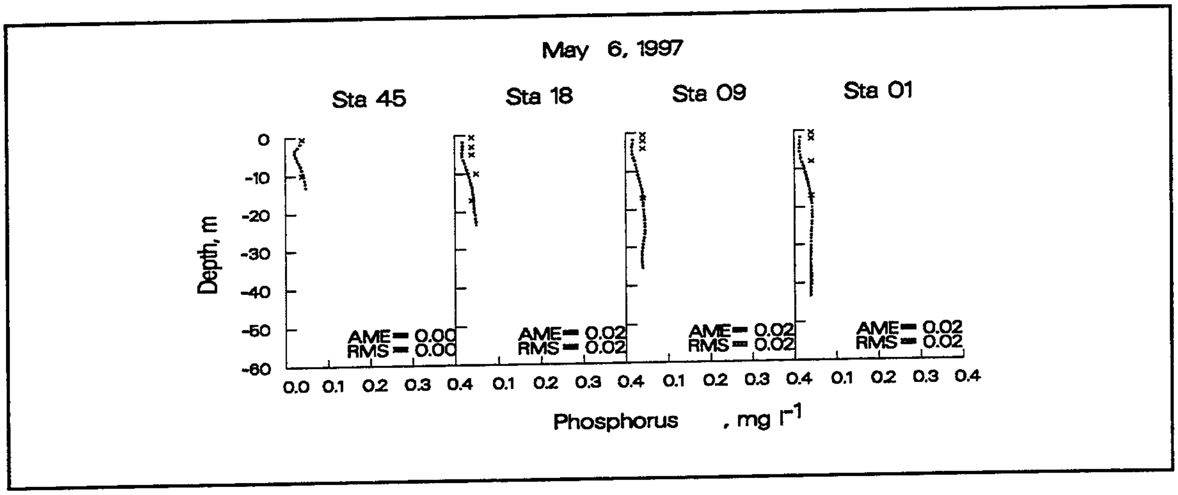

Figure A210. 1997 Allatoona Reservoir computed (...) versus observed (x) bioavailable phosphorus for stations along mainstem, May 6

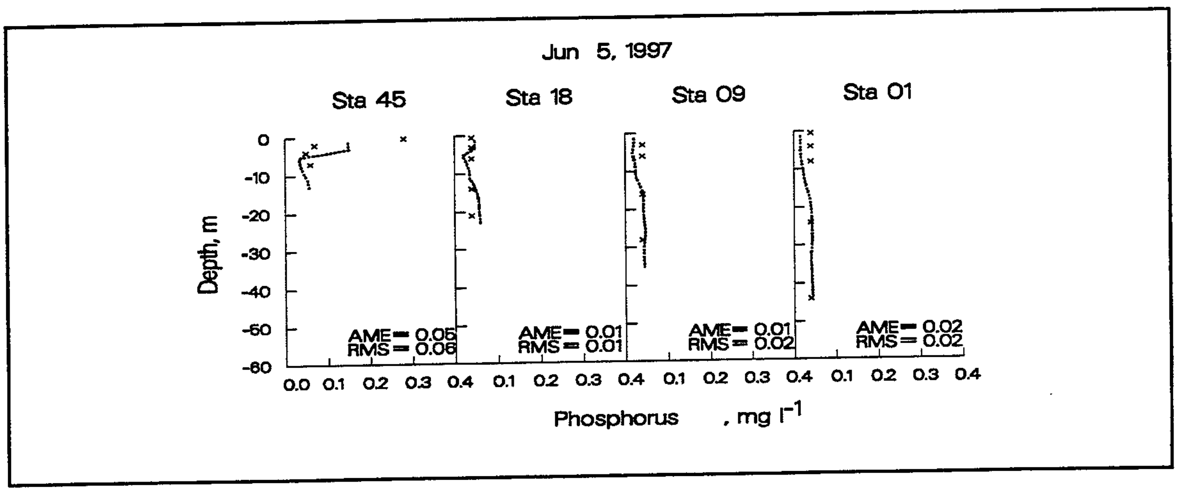

Figure A211. 1997 Allatoona Reservoir computed (...) versus observed (x) bioavailable phosphorus for stations along mainstem, June 5

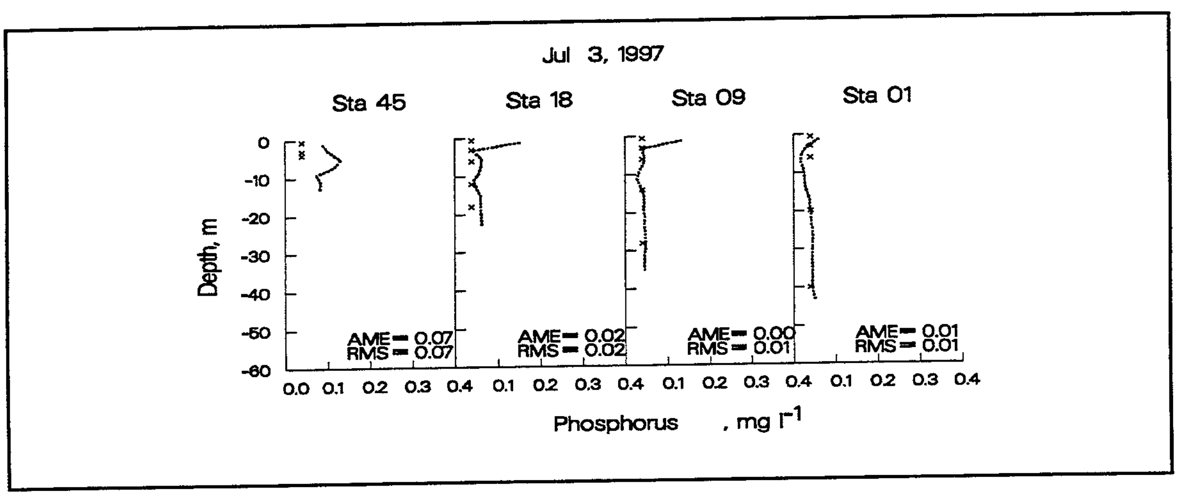

Figure A212. 1997 Allatoona Reservoir computed (...) versus observed (x) bioavailable phosphorus for stations along mainstem, July 3

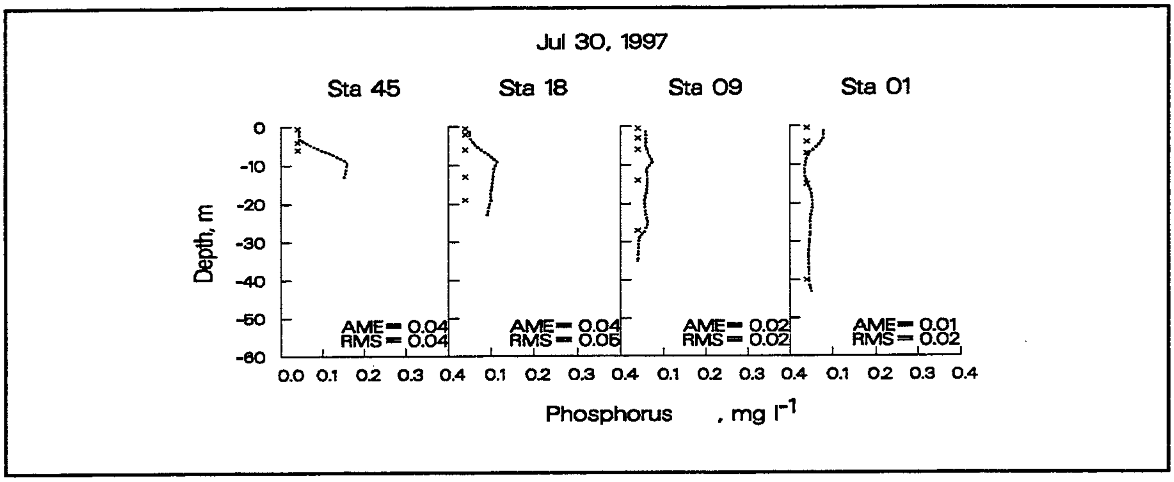

Figure A213. 1997 Allatoona Reservoir computed (...) versus observed (x) bioavailable phosphorus for stations along mainstem, July 30

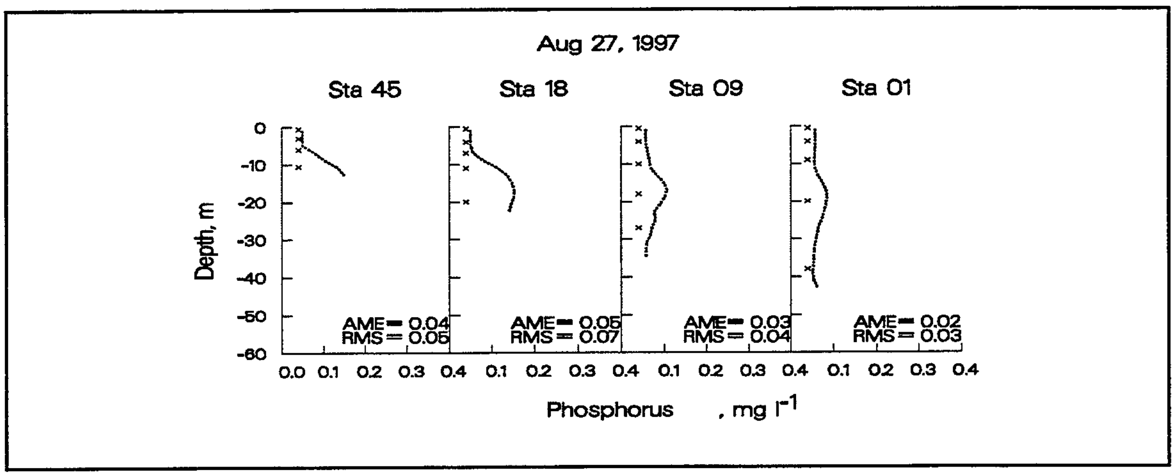

Figure A214. 1997 Allatoona Reservoir computed (...) versus observed (x) bioavailable phosphorus for stations along mainstem, August 27

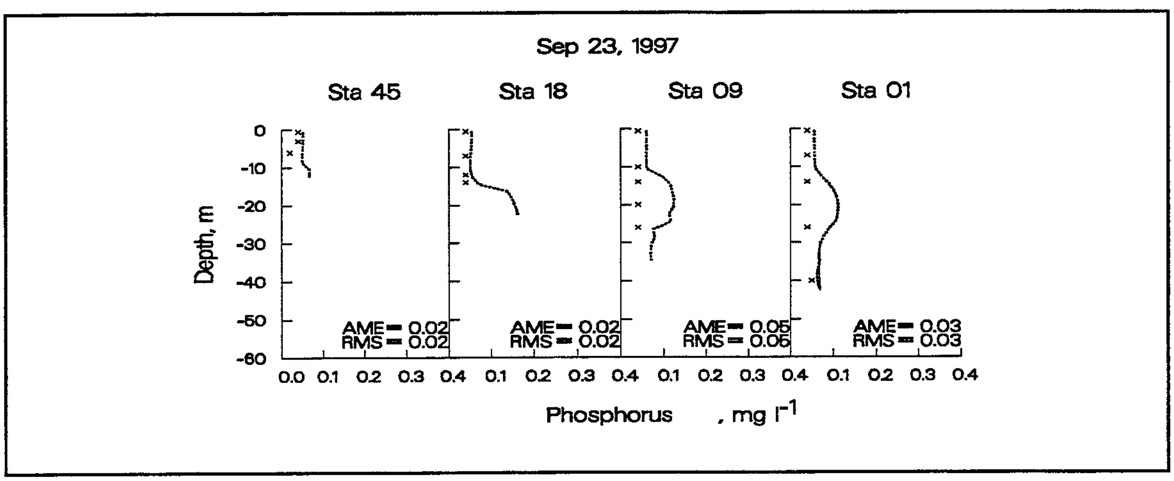

Figure A215. 1997 Allatoona Reservoir computed (...) versus observed (x) bioavailable phosphorus for stations along mainstem, September 23

West Point

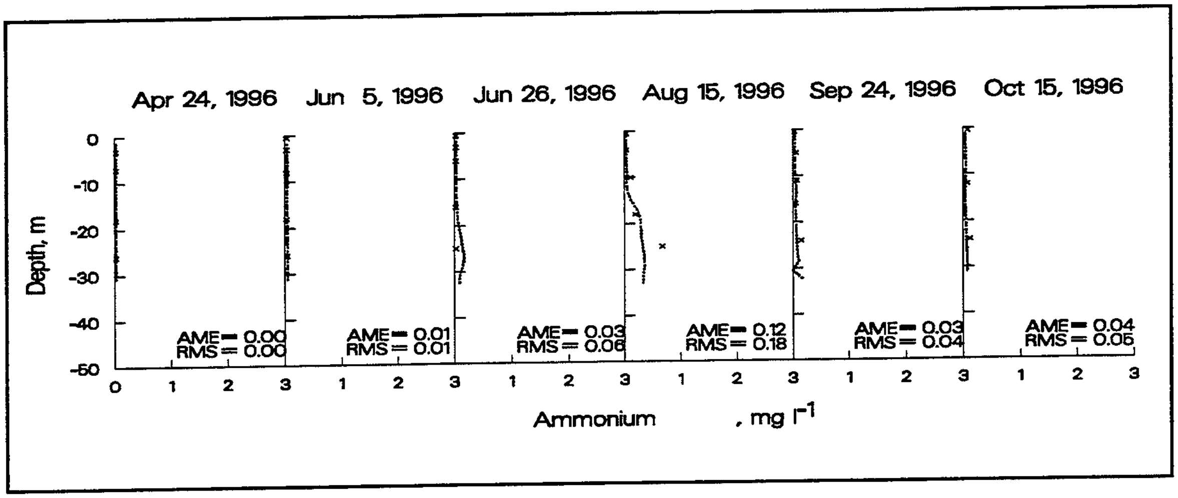

Figure A216. 1996 West Point Reservoir computed (...) versus observed (x) bioavailable phosphorus for station 09

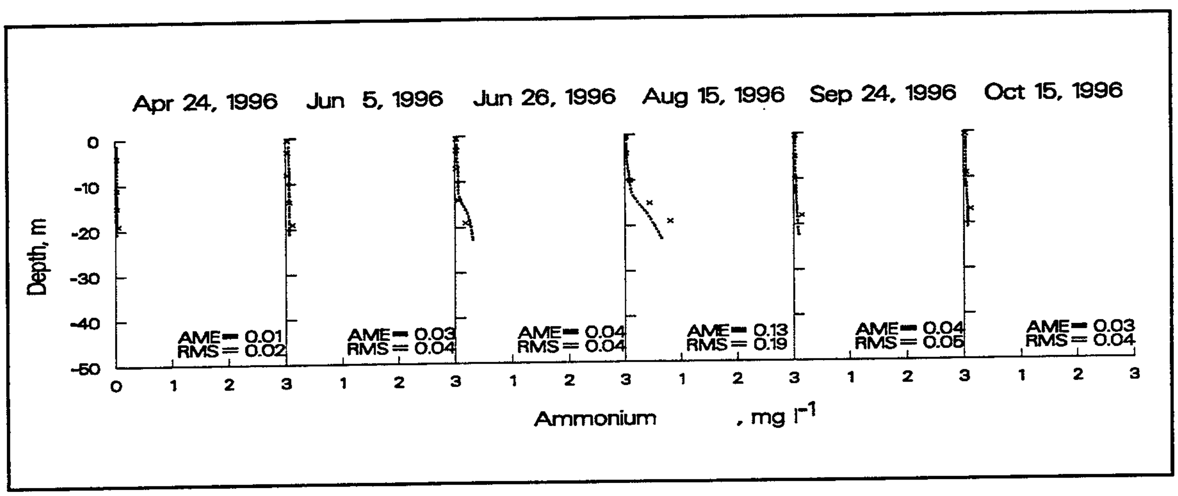

Figure A217. 1996 West Point Reservoir computed (...) versus observed (x) bioavailable phosphorus for station 18

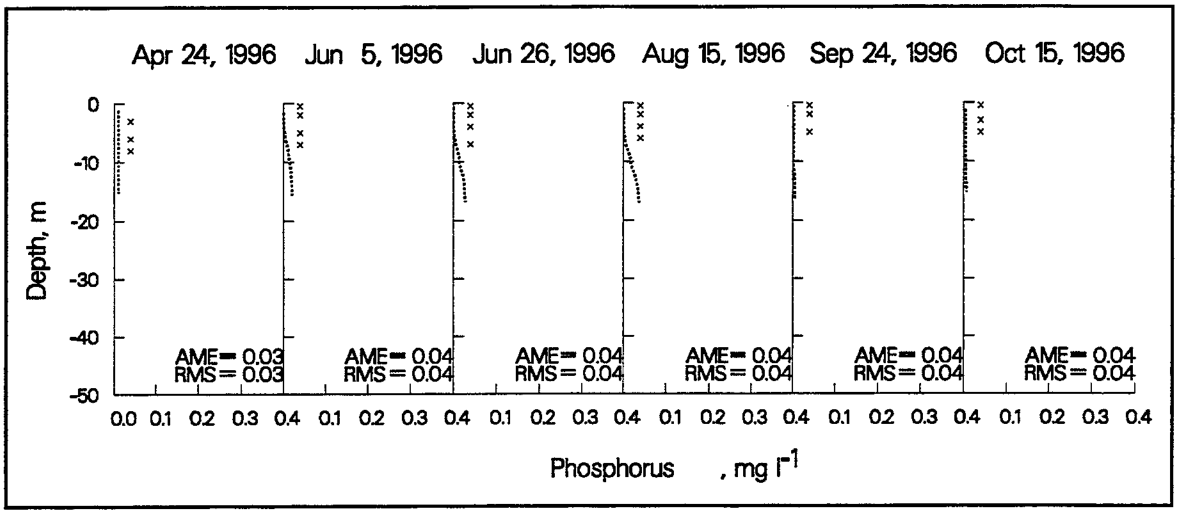

Figure A218. 1996 West Point Reservoir computed (...) versus observed (x) bioavailable phosphorus for station 45

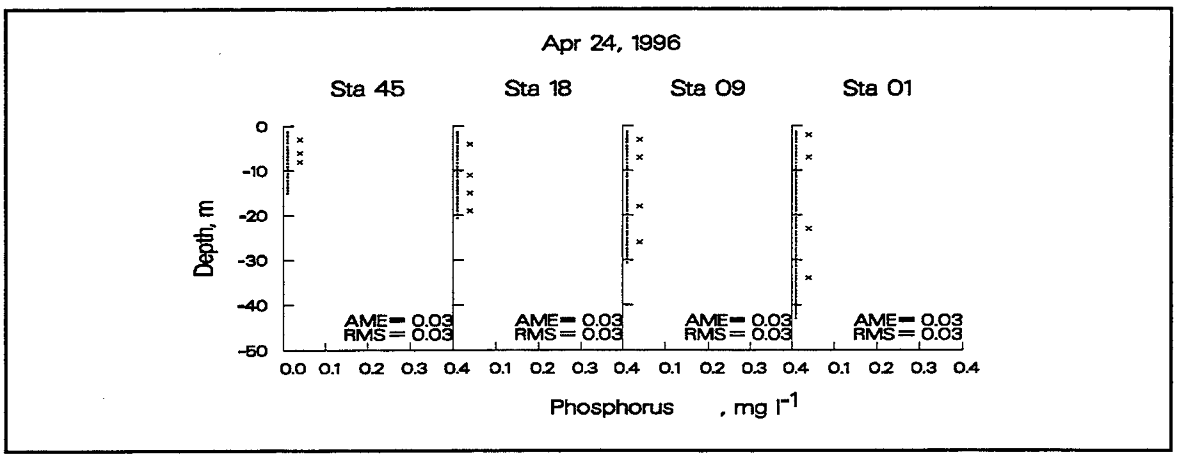

Figure A219. 1996 West Point Reservoir computed (...) versus observed (x) bioavailable phosphorus for stations along mainstem, April 24

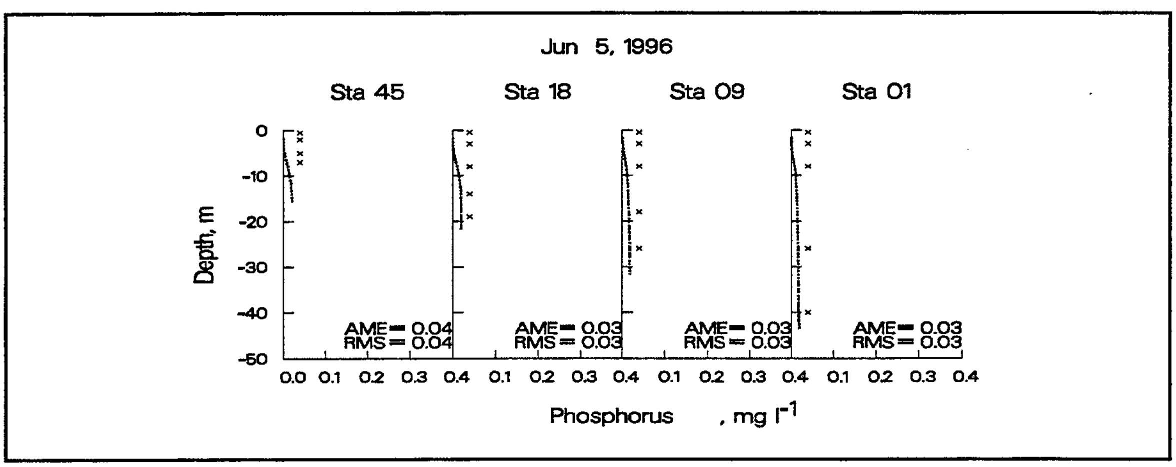

Figure A220. 1996 West Point Reservoir computed (...) versus observed (x) bioavailable phosphorus for stations along mainstem, June 5

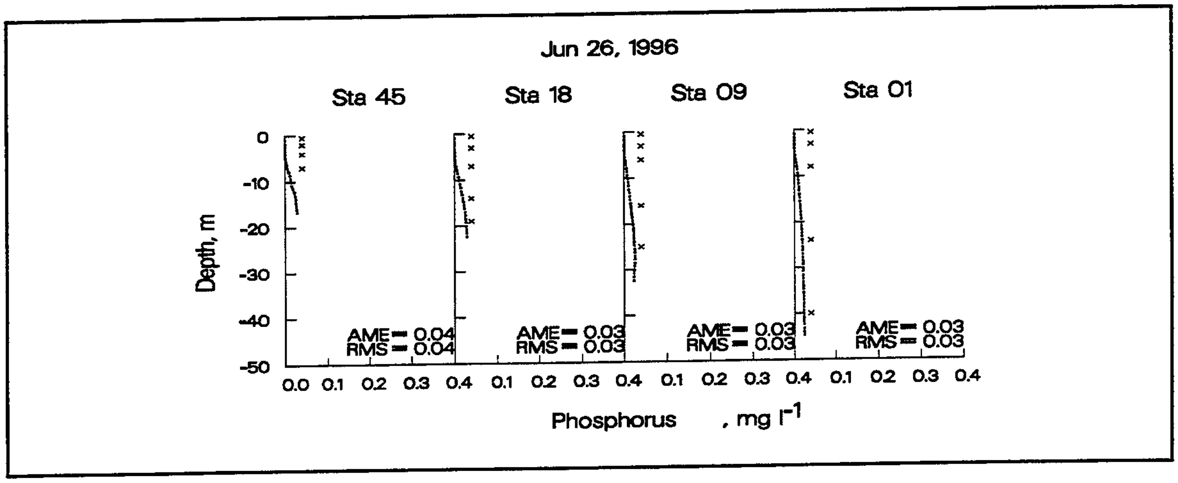

Figure A221. 1996 West Point Reservoir computed (...) versus observed (x) bioavailable phosphorus for stations along mainstem, June 26

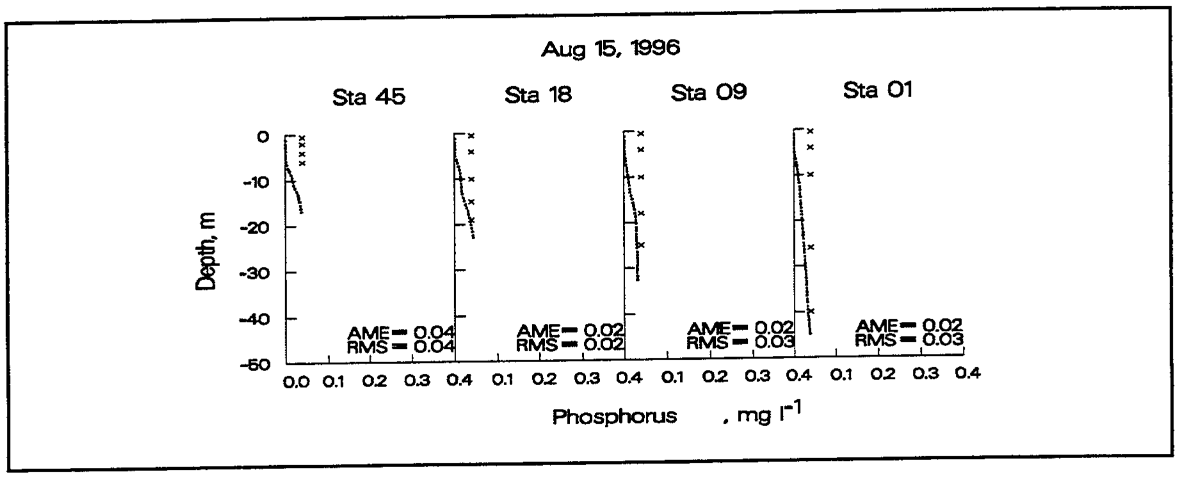

Figure A222. 1996 West Point Reservoir computed (...) versus observed (x) bioavailable phosphorus for stations along mainstem, August 15

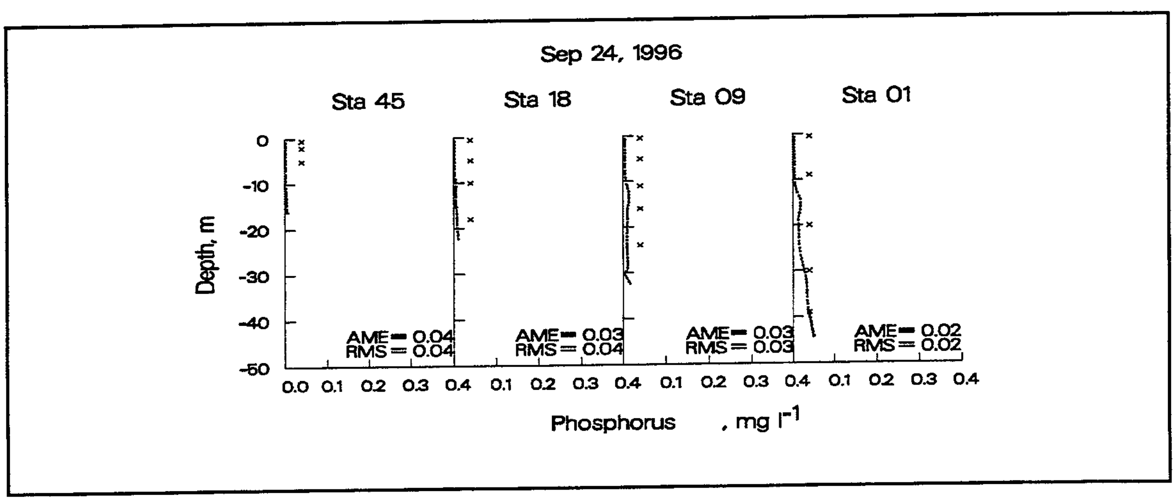

Figure A223. 1996 West Point Reservoir computed (...) versus observed (x) bioavailable phosphorus for stations along mainstem, September 24

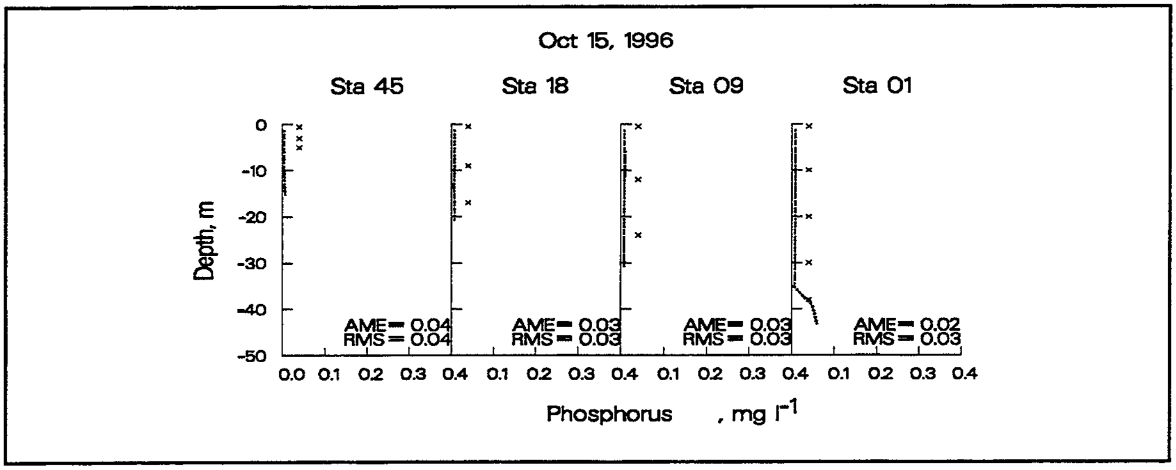

Figure A224. 1996 West Point Reservoir computed (...) versus observed (x) bioavailable phosphorus for stations along mainstem, October 15

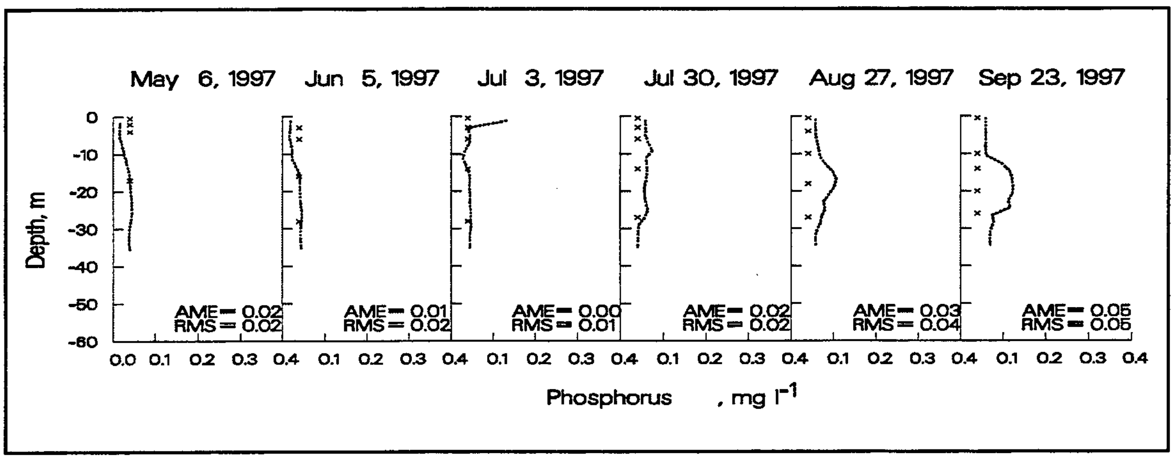

Figure A225. 1997 West Point Reservoir computed (...) versus observed (x) bioavailable phosphorus for station 09

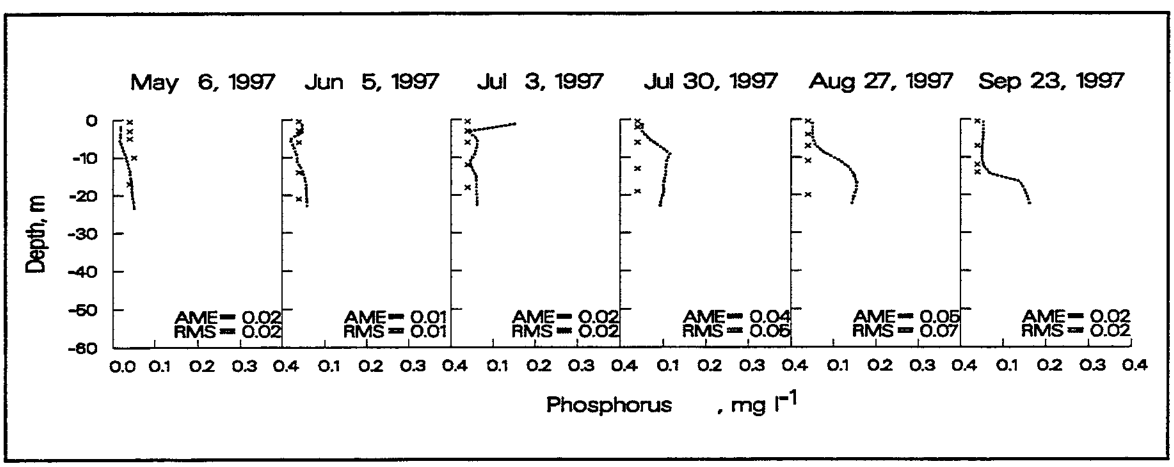

Figure A226. 1997 West Point Reservoir computed (...) versus observed (x) bioavailable phosphorus for station 18

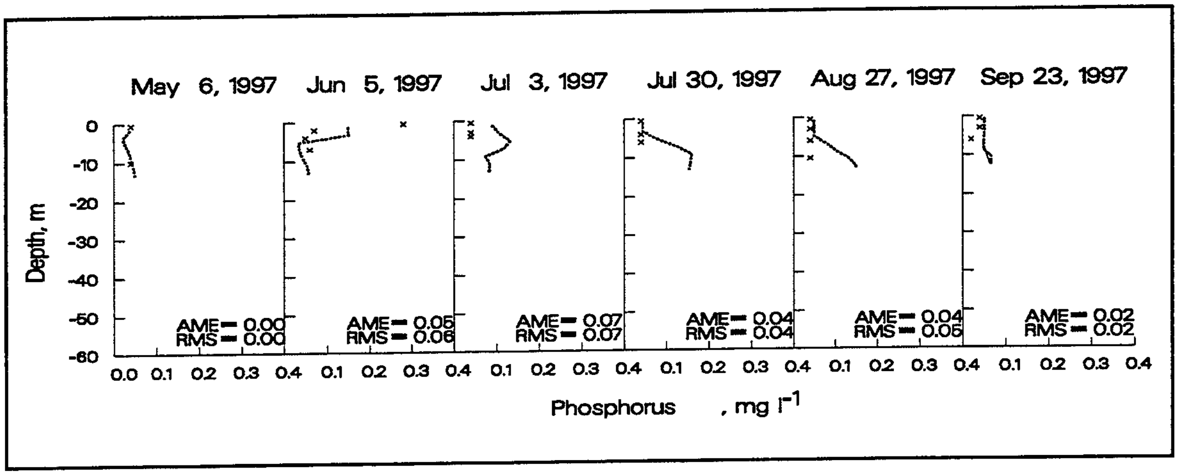

Figure A227. 1997 West Point Reservoir computed (...) versus observed (x) bioavailable phosphorus for station 45

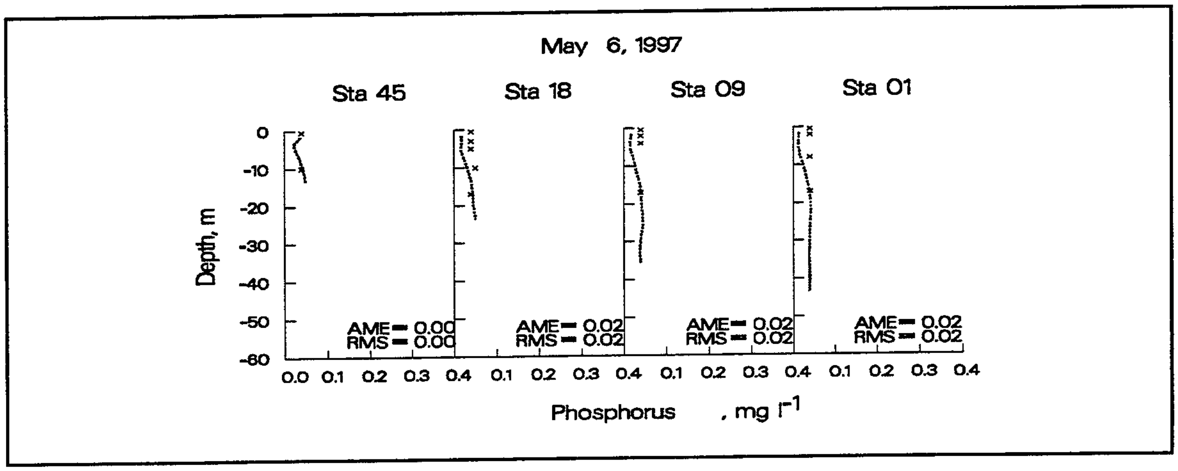

Figure A228. 1997 West Point Reservoir computed (...) versus observed (x) bioavailable phosphorus for stations along mainstem, May 6

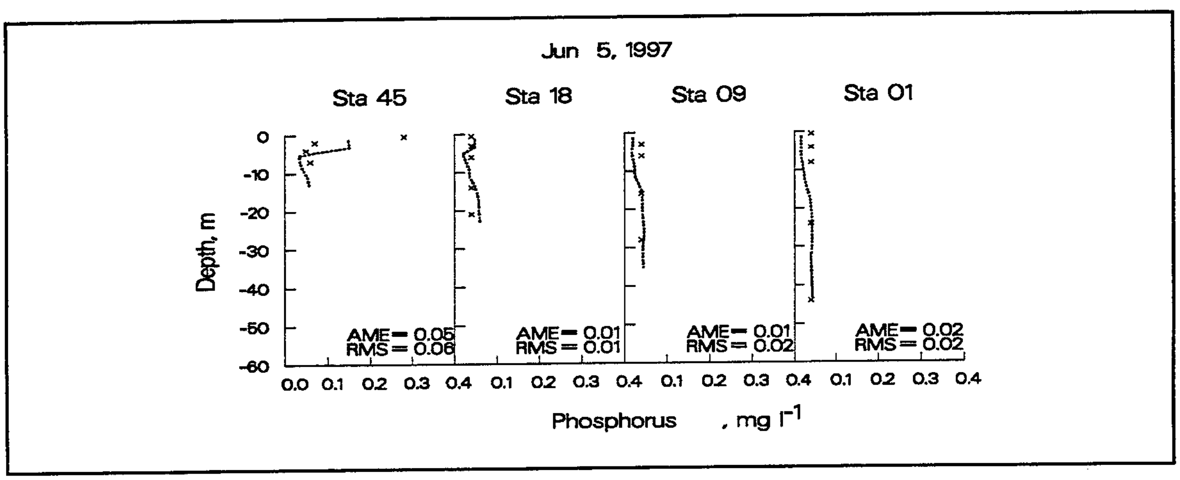

Figure A229. 1997 West Point Reservoir computed (...) versus observed (x) bioavailable phosphorus for stations along mainstem, June 5

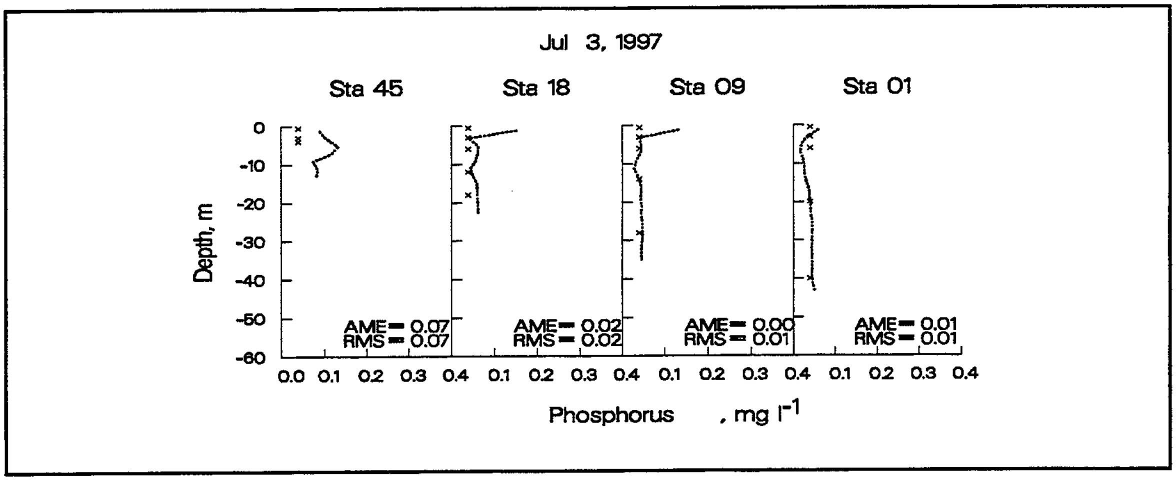

Figure A230. 1997 West Point Reservoir computed (...) versus observed (x) bioavailable phosphorus for stations along mainstem, July 3

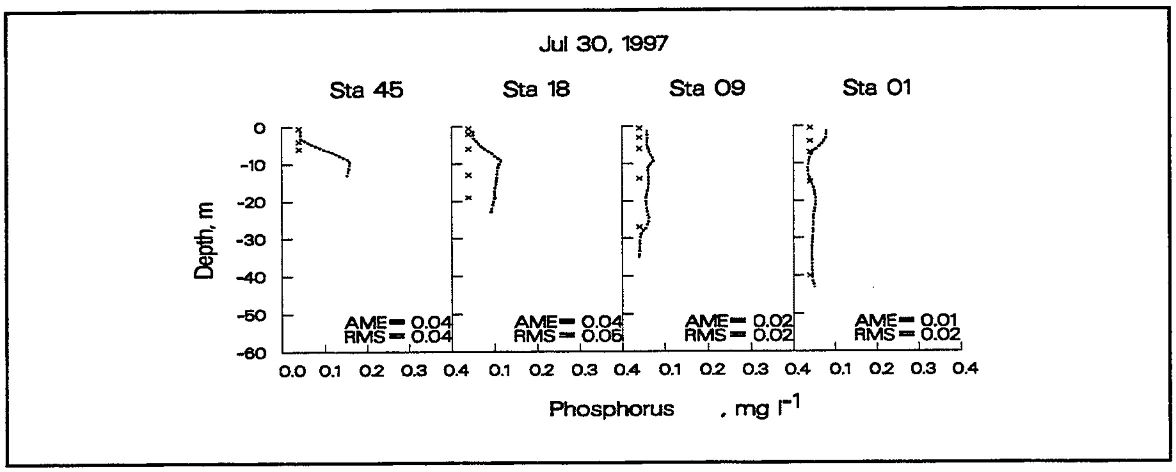

Figure A231. 1997 West Point Reservoir computed (...) versus observed (x) bioavailable phosphorus for stations along mainstem, July 30

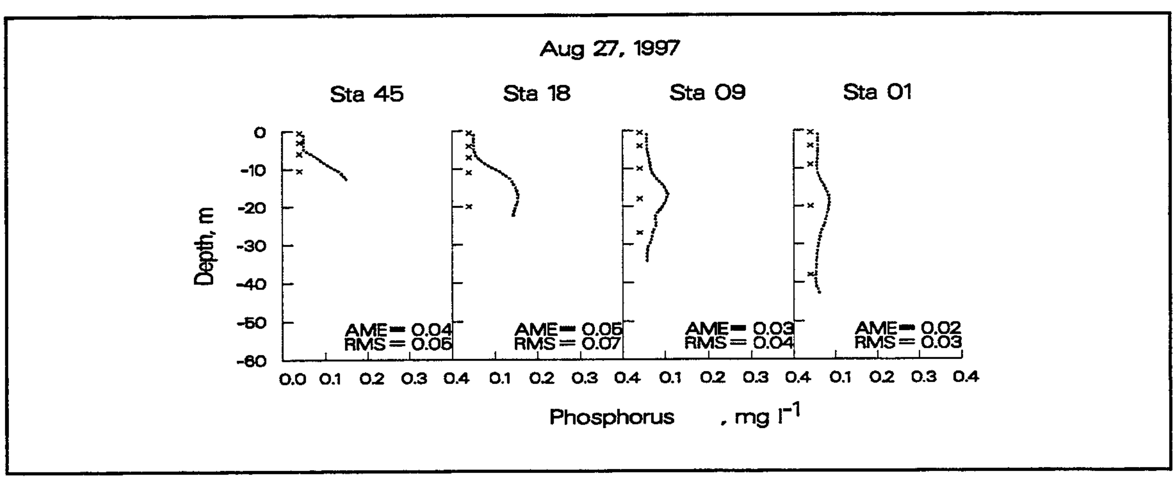

Figure A232. 1997 West Point Reservoir computed (...) versus observed (x) bioavailable phosphorus for stations along mainstem, August 27

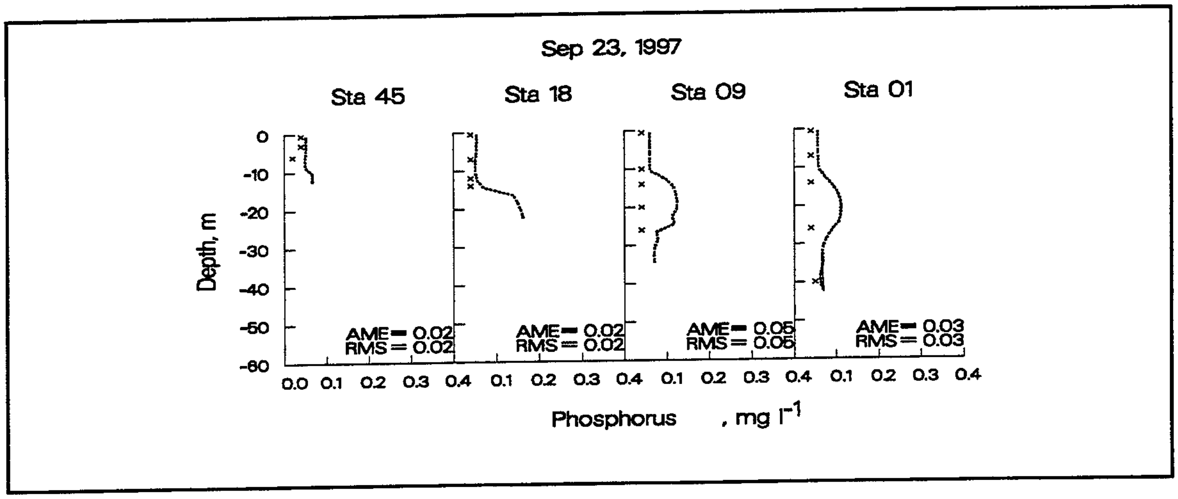

Figure A233. 1997 West Point Reservoir computed (...) versus observed (x) bioavailable phosphorus for stations along mainstem, September 23

REPORT DOCUMENTATION PAGE

Form Approved
OMB No. 0704-0188

1. REPORT DATE *(DD-MM-YYYY)*
July 2001

2. REPORT TYPE
Final Report

3. DATES COVERED *(From - To)*

4. TITLE AND SUBTITLE
Water Quality Modeling of Allatoona and West Point Reservoirs Using CE-QUAL-W2

5a. CONTRACT NUMBER

5b. GRANT NUMBER

5c. PROGRAM ELEMENT NUMBER

6. AUTHOR(S)
Thomas M. Cole, Dorothy H. Tillman

5d. PROJECT NUMBER

5e. TASK NUMBER

5f. WORK UNIT NUMBER

7. PERFORMING ORGANIZATION NAME(S) AND ADDRESS(ES)
U.S. Army Engineer Research and Development Center
Environmental Laboratory
3909 Halls Ferry Road
Vicksburg, MS 39180-6199

8. PERFORMING ORGANIZATION REPORT
ERDC/EL SR-01-3

9. SPONSORING / MONITORING AGENCY NAME(S) AND ADDRESS(ES)
U.S. Army Engineer District, Mobile
Mobile, AL 36628-0001;
Georgia Department of Environmental Resources
Atlanta, GA 30334

10. SPONSOR/MONITOR'S ACRONYM(S)

11. SPONSOR/MONITOR'S REPORT NUMBER(S)

12. DISTRIBUTION / AVAILABILITY STATEMENT
Approved for public release, distribution unlimited.

13. SUPPLEMENTARY NOTES

14. ABSTRACT
The Georgia Environmental Protection Division (GEPD) is concerned about the effects of increased nutrient loadings into Allatoona and West Point Lakes from point and nonpoint sources due to projected population growth in the region. Water demand and nutrient loading will most likely increase in the future. The ability to predict the effects of increased nutrient loading in West Point and Allatoona would allow GEDP to set waste load allocations and better manage the reservoirs for water quality in the future. To meet this goal, the GEPD requested the assistance of the Water Quality and Contaminant Modeling Branch at the U.S. Army Engineer Research and Development Center, Waterways Experiment Station, to develop a water quality model for Allatoona and West Point Lakes. CE-QUAL-W2, a two-dimensional, longitudinal and vertical hydrodynamic and water quality model, was chosen for the study. The objective of this study was to provide a calibrated water quality model for Allatoona and West Point Lakes capable of predicting future water quality conditions resulting from changes in water allocations, point/nonpoint nutrient loadings, and reservoir operations.

CE-QUAL-W2 was calibrated for temperature and algal/nutrient/dissolved oxygen interactions for Allatoona and West Point Reservoirs. The model quite accurately captures the physics of both reservoirs. Any alteration in the physics should be predicted with a high degree of accuracy.

15. SUBJECT TERMS
Dissolved oxygen, Hydrodynamic, Nutrients, Two dimensional, Water quality models

16. SECURITY CLASSIFICATION OF:			17. LIMITATION OF ABSTRACT	18. NUMBER OF PAGES	19a. NAME OF RESPONSIBLE PERSON
a. REPORT	b. ABSTRACT	c. THIS PAGE		153	19b. TELEPHONE NUMBER *(include area code)*
UNCLASSIFIED	UNCLASSIFIED	UNCLASSIFIED			